9-10-2024

DISSECTING THE INTERPLAY OF PROTEIN SYNTHESIS AND DEGRADATION PATHWAYS IN CELLULAR ADAPTATION TO STRESS

Brittany Friedson
Rowan University

DISSECTING THE INTERPLAY OF PROTEIN SYNTHESIS AND DEGRADATION PATHWAYS IN CELLULAR ADAPTATION TO STRESS

by
Brittany Friedson

A Dissertation

Submitted to the
Department of Molecular Cell Biology and Neuroscience
Rowan-Virtua School of Translational Biomedical Engineering & Sciences
In partial fulfillment of the requirement
For the degree of
Doctor of Philosophy
at
Rowan University
July 18, 2024

Mentor: Katrina Cooper, D. Phil, Associate Professor, Department of Molecular Biology

Dissertation Chair: Brian Weiser, Ph.D., Assistant Professor, Department of Molecular Biology

Committee Members:
Natalia Shcherbik, Ph.D., Associate Professor, Department of Cell Biology & Neuroscience
Jessica Loweth, Ph.D., Assistant Professor, Department of Cell Biology & Neuroscience
Kiran Madura, Ph.D., Professor, Department of Pharmacology, Rutgers University

Acknowledgements

I am extremely grateful for the wonderful support I've received throughout my PhD journey. First, I want to thank my mentor, Dr. Katrina Cooper, for believing in me and teaching me essential skills to grow as a scientist. Her support and encouragement to explore new research directions have been invaluable.

Thank you to Dr. Randy Strich and my committee members—Dr. Brian Weiser, Dr. Natalia Shcherbik, Dr. Jessica Loweth, and Dr. Kiran Madura—for their constructive feedback and guidance. Their insights and support have significantly shaped my projects and personal growth.

I am also grateful for my lab colleagues, including Tamaraty Robinson, Alicia Campbell, Dr. Steven Doyle, Dr. Sara Hanley, Dr. Stephen Willis, Mariam Onabanjo, Justin Bauer, and Dr. David Stieg, for helping to create a supportive and fun work environment, filled with laughter and great conversations. I am also inspired by all their intelligence and perseverance. Special thanks to Dr. Hanley and Dr. Willis for teaching me crucial lab techniques, and to the students I have been given the opportunity to help mentor.

I want to extend my gratitude to all my family and friends for believing in me and for helping to decrease my stress levels outside of work. I am also deeply grateful to Nathan Dawley for his unwavering love and support, which have been a constant source of motivation and comfort, and for the cherished memories we continue to create together. Last but not least, my heartfelt thanks to my mom and stepdad for their unconditional love and support throughout this journey.

Abstract

Brittany Friedson
DISSECTING THE INTERPLAY OF PROTEIN SYNTHESIS AND DEGRADATION PATHWAYS IN CELLULAR ADAPTATION TO STRESS
2024-2025
Mentor: Katrina Cooper, D. Phil
Doctor of Philosophy in Molecular Cell Biology and Neuroscience

Adaptation to stress requires cells to reprogram transcription, translation, and proteolytic pathways. Although much is known about the response of each program, it remains unclear how they coordinate following stress. My studies in *S. cerevisiae* identified the Cdk8 kinase module (CKM) of the Mediator complex as a new player in coordinating these processes. It is well established that the CKM consists of four highly conserved proteins (cyclin C, its cognate kinase Cdk8, and two structural proteins Med12 and Med13) and predominantly represses a subset of stress responsive genes in yeast. We demonstrated for the first time that the CKM also positively regulates the transcription of a subset of translation initiation factor (TIF) and ribosomal protein (RP) genes through an indirect mechanism. Consistent with this, we observed that the CKM is important for survival under conditions which alter or inhibit protein synthesis. Moreover, during nutrient deprivation, cells repress translation by degrading specific TIFs and storing mRNA in processing bodies (P-bodies). We found that nitrogen starvation causes Med13 to relocate to P-bodies, where it aids in the degradation of Edc3, showing a novel cytoplasmic role for Med13. Lastly, I demonstrated the degradation of the TIF eIF4G1 during nitrogen starvation involves K33 and K63-linked ubiquitination by the Cul3 E3 ligase complex and requires Atg8's ubiquitin (Ub) interacting motif (UIM), indicating a new role of Ub in selective autophagy. Given the conserved nature of all the players, these studies are highly relevant to the control of proteostasis in higher eukaryotes.

Table of Contents

Table of Contents (Continued)

Table of Contents (Continued)

Table of Contents (Continued)

Table of Contents (Continued)

Table of Contents (Continued)

Table of Contents (Continued)

List of Figures

List of Figures (Continued)

Figure Page

List of Figures (Continued)

Figure Page

List of Tables

Table Page

Chapter 1

Introduction

Disclaimer*:* A portion of this chapter is adapted from: Friedson B, Cooper KF. Cdk8 Kinase Module: A Mediator of Life and Death Decisions in Times of Stress. *Microorganisms*. 2021; 9(10):2152. *B Friedson wrote the original manuscript; KF Cooper edited the manuscript.

Protein Homeostasis and Disease

Transcription and translation of mRNA contribute to protein synthesis, while the ubiquitin proteasome system (UPS) and autophagy pathways contribute to degradation. Regulated synthesis and proteolysis of mRNA and proteins are important for homeostasis and for governing many cellular processes, such as cell growth and eliciting the appropriate response to stress (**Figure 1.1A**). Imbalances in these mechanisms are associated with conditions such as cancers, Alzheimer's Disease, heart defects, and intellectual disability [1-3]. For instance, enhanced protein synthesis can lead to uncontrolled cell growth and survival as seen in cancers, while defective degradation can lead to toxic protein aggregation and enhanced cell death as seen in neurodegenerative disease **(Figure 1.1B)**. Particularly in Alzheimer's disease, the insufficient removal of beta amyloid proteins can cause aggregation and eventual plaque formation, leading to neurodegeneration [4]. Thus, balanced protein homeostasis is important to avoid various diseases. However, the regulatory mechanisms and coordination of protein homeostasis pathways during stress remain unclear. My studies demonstrated throughout chapters 3, 4, 5, and 6 contribute to our understanding of these pathways.

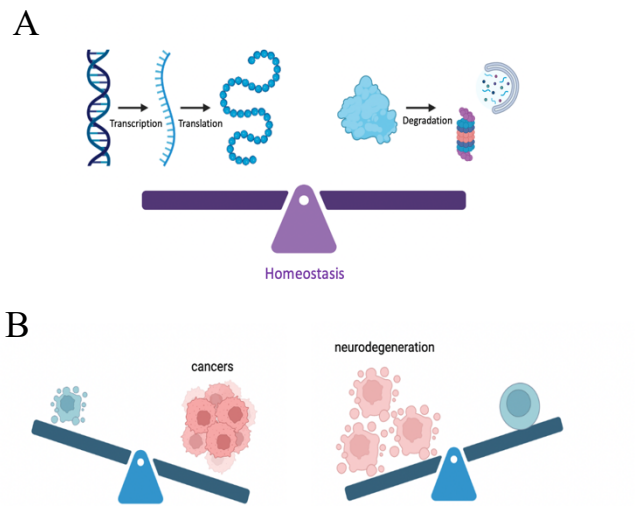

Figure 1.1. Balance of Protein Homeostasis Pathways. Regulated protein synthesis and degradation are important for controlling homeostasis and cellular outcomes. (A) Efficient regulation and activity of protein synthesis and degradation pathways are important for maintaining homeostasis. The major pathways involved in protein synthesis are transcription and translation, while degradation involves the ubiquitin proteasome system (UPS) and autophagy**.** (B) Dysregulated protein synthesis and degradation can lead to diseases associated with inappropriate cell survival or death, such as cancers and neurodegenerative diseases.

Cellular Stress Response Signaling

Cells experience a wide range of stresses due to environmental fluctuations, including changes in temperature, osmolarity, reactive oxygen species, and nutrient availability. To survive and thrive, cells must adapt to and mitigate these stresses as they occur. One key mechanism for adapting to stress involves altering the cellular proteome [5]. Coordinated regulation of protein synthesis and degradation pathways are thus necessary to promote survival or programmed cell death, depending on the type and severity of the stress [6, 7] (**Figure 1.2**). The molecular details of how cells execute cell death and cell survival pathways, however, are not fully understood. Significantly less clear is how protein synthesis and degradation pathways coordinate in response to different stressors. Chapters 3, 4, 5, and 6 will address these gaps in knowledge.

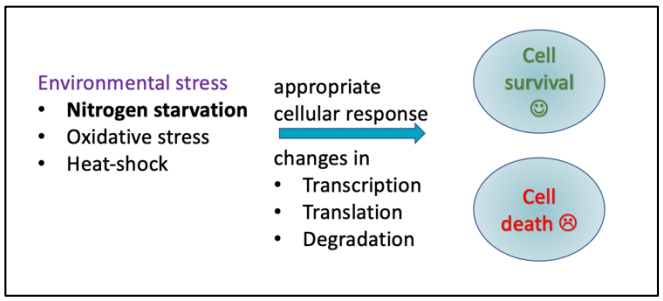

Figure 1.2. Cellular Responses to Environmental Stress. Types of environmental stressors a cell may be exposed to include nitrogen starvation, oxidative stress, and heat-shock. Coordinated and complex changes in transcription, translation, and degradation are necessary for appropriate stress adaptation.

Cell Survival

Several conserved key survival mechanisms outlined below are triggered following unfavorable environmental cues. Complex changes in protein synthesis and degradation pathways play key roles in promoting a cell survival response to stress. However, how protein synthesis machinery is regulated at the level of transcription and degradation to promote cell survival in stress is not well understood.

Signal Transduction Through TORC1 Inhibition. The conserved target of rapamycin kinase complex 1 (TORC1) positively controls protein biosynthesis to promote cell growth and metabolism in physiological conditions [8]. TORC1 activity couples environmental and nutritional cues to downstream effectors in eukaryotes by phosphorylating a wide range of targets that drive protein, lipid, and nucleotide synthesis [9]. Several cellular mechanisms are key to survival.

Nutrient deprivation is an environmental trigger that inhibits TORC1 and induces cellular survival. Inhibition of TORC1 triggers changes in multiple cellular programs, including transcription, translation, and protein degradation. This is best studied in yeast following nitrogen starvation, where cells promote a pro-survival response by inhibiting

general protein synthesis to conserve energy and arrest cell growth [10, 11]. Inhibition of global translation largely depends on phosphorylation of a translation initiation factor eIF2α [12], inhibition of translation-associated gene transcription, and degradation of translation-associated proteins [13, 14]. This response is also coordinated with cells upregulating genes that are translated into proteins needed to survive the stress response, notably those encoding autophagy.

Translational Reprogramming. Global inhibition of general translation occurs to help conserve energy required for promoting a cell survival response [15]. Translational machinery must also be fine-tuned to synthesize stress-response proteins (SRPs) necessary for survival [16-19]. To do so, environmental stressors trigger a shift from primarily cap-dependent to cap-independent translation to produce stress-specific mRNAs. These can occur by inhibiting transcription of genes encoding translation machinery as well as degrading specific proteins involved in translation [13]. However, the complete mechanisms involved in the reprogramming of translation machinery through both transcription and degradation pathways for survival are not fully understood. We elucidate new mechanisms involved in controlling translation machinery at the transcriptional level in Chapters 3 and 4, and at the degradative level in Chapters 4 and 5.

P-Body and Stress Granule Formation. Another crucial process for inhibiting mRNA translation involves the formation of processing bodies (P-bodies). The P-bodies are membrane-less conserved organelles which form following stress by liquid-liquid phase separation (LLPS) of translating mRNAs and RNA binding proteins (RBPs). Although they have been described as sites of mRNA degradation, their major role is to conserve translating RNA for future use once the stress is removed [20] [21]. Stress

granules similarly form through LLPS in response to specific stress. However, unlike P-bodies, stress granules contain translation initiation factors as well as unique RBPs [21].

Transcriptional Reprogramming. Many genes involved in translation are inhibited to suppress general translation machinery in stress. At the same time, the expression of SRP also depends on transcriptional changes to express stress response genes (SRG). Many of these SRPs are involved in autophagy, a catabolic process which becomes upregulated in adverse conditions such as nitrogen starvation to recycle proteins and organelles in the vacuole [17, 22, 23]. Enhanced degradation of transcription factors also serves an important role in transcriptional reprogramming.

Upregulation of Autophagy Pathways. Autophagy is a highly conserved catabolic process that is used to maintain homeostasis and becomes upregulated in adverse conditions such as nitrogen starvation to recycle proteins and organelles in the vacuole [17, 22, 23] (refer to "Protein Degradation Pathways" section below for more details on autophagy). Selective autophagy pathways can degrade specific targets such as damaged organelles (mitophagy, ER-phagy, ribophagy), or aggregated proteins (aggrephagy). This method of selective degradation is important for cellular quality control, with aberrant selective autophagy being a cause of many human diseases, including neurodegeneration [24]. However, how autophagy selectively degrades translation machinery following stress remains unclear.

Together, these demonstrate the importance in the coordination of different protein homeostasis pathways in responding appropriately to stress including nitrogen starvation (**Figure 1.3**), though how they coordinate remains unclear.

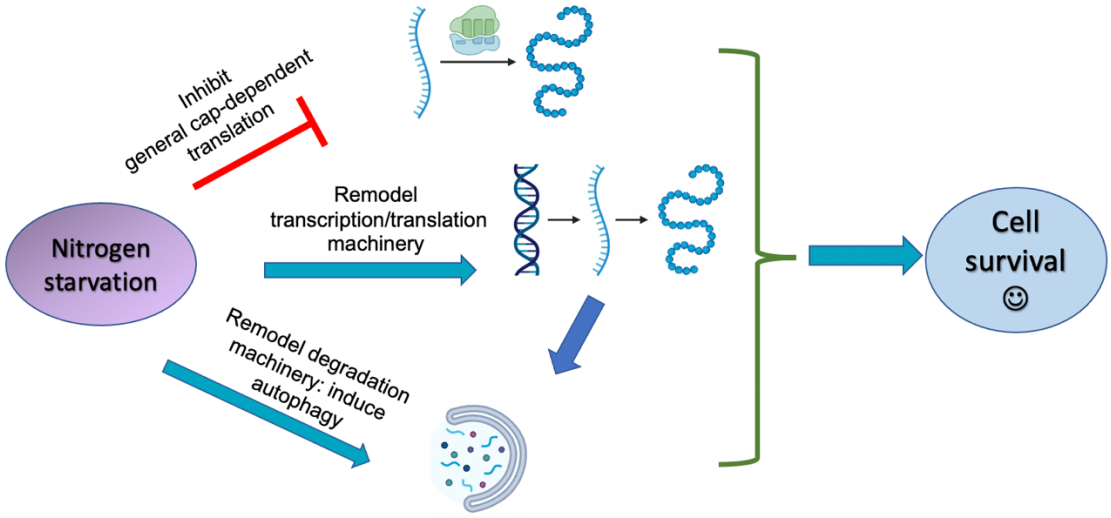

Figure 1.3. Protein Homeostasis Pathways in Nitrogen Starvation. Protein synthesis and degradation pathways must coordinate together to promote survival following nitrogen starvation. Following nitrogen starvation, general translation is inhibited, while transcription and translation machinery are remodeled to form stress response genes (SRG) and stress response proteins (SRP) necessary for cell survival. Many of these SRP are involved in the induction of a degradation process called autophagy, which can degrade proteins and organelles inside a lysosome (vacuole in yeast). The proteins degraded via autophagy also play a role in controlling transcription and translation, further demonstrating a close relationship between these protein homeostasis pathways in stress.

Cell Death

Stresses such as heat-shock and oxidative stress induce pro-death pathways. High reactive oxygen species (ROS) levels induce protein and organelle damage, stimulating regulated cell death (RCD) pathways in both yeast and mammals [25]. Oxidative stress stimulates transcription factor activity, upregulating many genes encoding antioxidants (catalases) and pro-survival chaperones [26] required to reinstate cellular homeostasis. Phosphorylation of translation initiation factor eIF2α suppresses global translation to arrest cell growth, while damaged proteins become degraded predominantly by the UPS, serving as important adaptive mechanisms [12] [27]. Failure to neutralize the toxic effects of

reactive oxygen triggers cells to switch to upregulating genes required for cell death pathways [25]. An important step in RCD induction involves disruption of mitochondrial integrity [28]. Mitochondrial outer membrane permeabilization (MOMP) leads to the release of various mitochondrial intermembrane space proteins that activate caspases which promote cell death [29].

Transcriptional Control During Stress

Brief Outline of Transcription

Proper regulation of gene expression is crucial for executing diverse cellular functions. In eukaryotic cells, RNA polymerase II, responsible for transcribing mRNA, requires transcription factors (TFs) to bind to promoters on DNA [30]. TFs are regulatory proteins whose primary function is to activate or inhibit transcription. Some transcription factors bind to specific DNA sequences located near the transcription start site within the promoter region, assisting in the formation of the transcription initiation complex. Alternatively, other transcription factors bind to upstream regulatory sequences (URS), such as enhancers, where they can either promote or inhibit the transcription of the associated gene [31]. Expression of genes can be broadly classified into two groups: constitutive or induced. Induced genes are upregulated or repressed following internal and external changes in the cellular environment and during development. Housekeeping genes, for example genes expressing ribosome components, are constitutively expressed. As such less is known about how these genes are controlled following stress. The research presented in Chapter 3 of this thesis has revealed that the CKM plays a role.

Cdk8 Kinase Module: a Major Player in Transcription Following Stress

The Cdk8 Kinase Module (CKM), a stress-responsive multi-subunit complex with several known functions in transcription. The CKM is a dissociable part of the Mediator complex and contains four subunits- Med12, Med13 (which serves as a tether for CKM binding to the Mediator), Cdk8 kinase, and cyclin C (**Figure 1.4A**). The core Mediator is a conserved multi-subunit coactivator complex [32] which communicates signals from transcription factors (TFs) to facilitate RNA pol II-directed DNA transcription [33] [34] [35]. In the budding yeast *S. cerevisiae,* CKM association with the Mediator is thought to prevent Pol II interaction with gene promoters [36] [37] [38] [39]. Cyclin C binding is also required for activation of the Cdk8 kinase, which plays a role in transcription by phosphorylating the C terminal domain of RNA polymerase II as well as several different regulatory factors [40] [41] [42].

Direct binding of the CKM with the Mediator in yeast represses transcription of early meiotic genes and stress response genes (SRG), which are induced by entry into meiosis and environmental stress, respectively [40] [43] [44] [45] [46] [47]. Cdk8 phosphorylates transcriptional activators to inhibit gene transcription [7], affecting Sip1 and Gal4 activity, Msn2 and Rim15 nuclear export, and promoting Gcn4 degradation in physiological conditions [40, 48-51]. In higher organisms, the CKM can act as both a transcriptional repressor and activator of genes indirectly and directly [52] [53]. Repression of SRG genes in yeast is relieved through the selective degradation of cyclin C and Med13 (**Figure 1.4A, right panel**) in different stresses, including nitrogen starvation and oxidative stress, to help elicit either cell survival or cell death [7]. For instance, cyclin C nuclear release in yeast following oxidative stress is required for full mRNA accumulation

of *DDR2* and *CTT1* [54], genes that encode a multi-stress response protein and catalase, respectively. In response to nitrogen starvation, autophagy (*ATG*) genes are upregulated to promote survival [55], and this is mediated by various transcriptional regulators including Med13 and cyclin C of the CKM [46, 56].

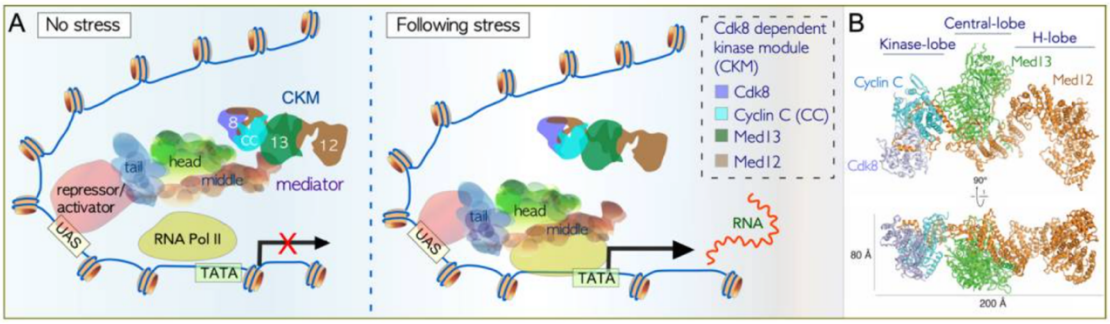

Figure 1.4. Model of the Interaction of the CKM with the Core Mediator Complex and RNA Pol II. (A). In unstressed cells, the CKM associates with the Mediator at UAS sites found in promotors, by the interaction of Med13 with the mediator hook. This inhibits the Mediator-RNA pol II interaction, preventing PIC formation and transcription of mRNA. Following stress, the CKM is released from the Mediator, permitting PIC assembly and transcription of mRNA. Additional repressors and/or activators also mediate transcription by binding to UAS motifs (Upstream Activating Sequence). Adapted from Cherji et al (2017). NAC. PMID:28575439. (B) Structure of the yeast CKM determined by cryo-EM and mass spectrometry. Reproduced with permission from Li et al (2021) Scientific Advances. PMID: 33390853. CKM—Cdk8 kinase module, RNA Pol II—RNA polymerase II, PIC—preinitiation complex, Å—Angstrom. Figure from Friedson and Cooper (2021) [7].

Class I Cyclins Control Transcription

Cyclins are key players in transcription and can help drive progression through the cell cycle [57]. Early research revealed that these proteins exhibit oscillating levels due to their synthesis and subsequent degradation [58]. Cyclins collaborate with cyclin-dependent serine/threonine protein kinases (Cdks), whose activity also fluctuates at specific stages of the cell cycle in response to cyclin binding. Active cyclin-Cdk complexes propel cell cycle

progression by phosphorylating proteins crucial for various cellular processes such as proliferation, differentiation, metabolism, and homeostasis [59]. Class I cyclins are the primary cell cycle regulators.

Role of Other CDKs and Cyclins in Transcription

As mentioned above, cyclin C/Cdk8 is a conserved transcriptional cyclin-Cdk complex. Like other Cdks, Cdk8 associates with cyclin C constitutively [60], and like other class II cyclins, cyclin C is constitutively expressed [61]. Initially, cyclin C-Cdk8, cyclin H-Cdk7 and cyclin K-Cdk9 were identified as Cdks involved with transcription, but more recently Cdk12 and 13 have been shown to have roles in transcription as well [62, 63]. In addition, cyclin C pairs with Cdk19, which controls a different subset of genes from cyclin C/Cdk8 [64]. These Cdks all have different roles in regulating transcription which has been summarized in a recent review: [65]. Lastly, cyclins and their Cdk partners serve numerous functions beyond cell cycle regulation and transcription, including roles in proteolytic degradation, programmed cell death, DNA damage repair, metabolism, and stem cell self-renewal [61].

Translational Control During Stress

Brief Outline of Major Steps and Components in Translation

Translational control also plays an important role in driving cell growth and progression through the cell cycle. Translation is a highly coordinated and complex process which synthesizes proteins according to the mRNA template, and this involves the coordination of transfer RNA (tRNA), ribosomes, and initiation factors (TIFs) [66]. Like transcription, the translation process can be divided into several steps: initiation, elongation, and termination, followed by recycling of the ribosome. In cap-dependent

translation, TIFs of the eukaryotic translation initiation factor 4F (eIF4F) complex recognize the mRNA 5' cap structure (which consists of guanosine with a methyl group on the 7-position, m7G) and mediate recruitment of the ribosome to mRNA (**Figure 1.5**). The ribosomes can then scan downstream of the 5′ cap until they encounter an AUG initiation codon. The yeast eIF4F complex comprises of the highly conserved cap-binding protein eIF4E, the DEAD box RNA helicase Ded1 [67], and the scaffolding protein eIF4G1. The scaffolding ability of eIF4G1 serves an important function in the rate-limiting step in cap-dependent translation [68] [69] [70] [67] [71]. Following initiation, the tRNA can function as an adaptor between mRNA and the growing chain of amino acids to form a protein.

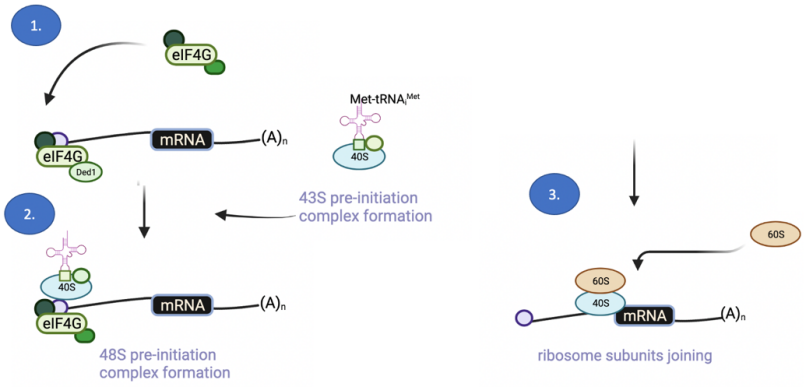

Figure 1.5. Cap-Dependent Eukaryotic Translation Initiation. (1) Translation initiation factors (TIFs) recognize the mRNA 5' cap structure and form the eukaryotic translation initiation factor 4F (eIF4F) complex to mediate recruitment of the 43S pre-initiation complex to mRNA. The eIF4F complex comprises of the cap-binding protein eIF4E, the DEAD box RNA helicase Ded1, and the scaffolding protein eIF4G1. (2) The charged tRNA then attaches to the start codon (AUG) and the small 40S subunit of ribosome binds to the mRNA, forming the 48S pre-initiation complex. (3) Finally, the large 60S ribosomal subunit binds to the 40S, enabling initiation of translation.

Ribosome and TIF Expression are Highly Regulated

The eukaryotic 80S ribosome further consists of the large 60S and small 40S subunit, and formation of each subunit requires the coordinated assembly of several ribosomal proteins (RPs), assembly factors, and ribosomal RNA (rRNA) [72]. Production of rRNA largely occurs through Pol I in the nucleolus [73], and gene expression of both RPs and TIFs occur via Pol II transcription through complex regulatory processes involving several transcriptional regulators [74] [75] [76] [77] [78]. For instance, in yeast, the DNA-binding transcriptional regulator Rap1 recruits the mediator and directly binds to ribosomal gene promoters to promote gene expression of many RP genes [76]. Enhanced expression of Gcn4, a known transcriptional activator of amino acid biosynthesis genes, can also repress specific genes encoding ribosomal proteins through direct binding with Rap1 [75] [79].

This controlled expression of specific RPs serves functions in translation to control cellular processes. For instance, the 60S RP Rpl22 is required to produce proteins which induce meiosis in yeast [80]. RPs and TIFs are thus highly regulated to carry out necessary cellular functions. Dysregulation of this machinery is associated with uncontrolled cell growth and cell cycle progression and has been implicated in several cancers [81] [82]. Thus, ribosomes can be an ideal target for drug development in cancer. However, the complete mechanisms which control RP and TIF expression require further investigation.

Translation Machinery Changes in Stress

In normal physiological conditions, eukaryotic mRNAs possess a 5' cap structure essential for efficient binding of TIFs like eIF4G1 [83]. Environmental stressors trigger a shift from primarily cap-dependent to cap-independent translation to produce stress-

specific mRNAs. This process involves the direct recruitment of the 40S ribosome to a specific internal ribosome entry site (IRES) element within the 5'UTR, bypassing the requirement for initiation factors such as eIF4G1 [84]. However, much remains unknown as to how this occurs in nitrogen starvation.

Under stress conditions, specific TIFs including eIF4G1 become degraded [13], contributing to the shut-down of general cap-dependent translation. However, the complete function and mechanism of eIF4G1 degradation is not fully understood. Enzymatic activity of Ded1, another DEAD box RNA helicase, is also required for translation repression following TORC1 inhibition [85], demonstrating a dual role of a TIF in enhancing and repressing translation in stress. A previous study also demonstrated that, following protein synthesis inhibition, cap-independent translation is important for TORC1 expression, enabling re-entry of cell-cycle progression [86]. Modulating translation initiation thus plays essential roles in fine-tuning gene expression and cell growth when global translation is inhibited in stress. However, the precise changes in translation machinery post-stress are complex and remain poorly understood. In Chapter 5, I address these gaps in knowledge by elucidating the autophagy mechanism involved in eIF4G1 degradation following nitrogen starvation.

Protein Degradation Pathways

Ubiquitin-Proteasome System

Maintaining the timely expression and proper functioning of proteins is essential for coordinating cellular processes and responding to stress. Thus, protein proteolysis via the ubiquitin proteasome system (UPS) ensures a rapid control of cellular mechanisms.

Ubiquitin (Ub) is a small molecule that covalently attaches to lysine residues of a target. Proteins and organelles can be tagged with Ub chains by a three-step enzymatic cascade utilizing E1 Ub-activating, E2 Ub–conjugating and a variety of E3 Ub-ligating enzymes [87] (**Figure 1.6A**). An E2 can directly transfer ubiquitin to the substrate or to an E3 ubiquitin ligase which then transfers the ubiquitin to the substrate [88]. There are at least 80 different E3 ligases in yeast [89], and over 1,000 known E3 ligases in mammalian systems, indicating that E3s are required for substrate specificity [90]. Deubiquitinating enzymes (DUBs) can further eliminate ubiquitin from substrates via proteolytic cleavage and can alter ubiquitin chains to regulate substrate signaling [91].

A unique feature of ubiquitin is its capacity to form various homo- and heterotypic linkage types facilitated specific E3 ligases and DUBs. Within homotypic ubiquitin chains, ubiquitin monomers are linked to one of seven lysine (K) residues or to the N-terminal methionine (M1) via the Gly76 carboxyl group of the previous Ub moiety [92] (**Figure 1.6B**). For instance, K48-linked chains are the most abundant signal for proteasomal degradation [93]. Ub chains can be recognized by intrinsic or extrinsic receptor proteins which help deliver the tagged substrates to the 19S cap of the proteasome as a part of the UPS [94-96]. Once substrates are directed into the proteasome for degradation, ubiquitin molecules are cleaved off for recycling by deubiquitinating proteins (**Figure 1.6C**). Upon entering the proteasome, a substrate is captured, unfolded, and aligned by ATPases. It is then guided through the central channel and hydrolyzed into small peptides within the proteolytic core of the proteasome [97]. Alternatively, Ub can form different proteolytic or non-proteolytic signals, such as protein trafficking, depending on the type of chain linkage that is produced on a substrate [98-100].

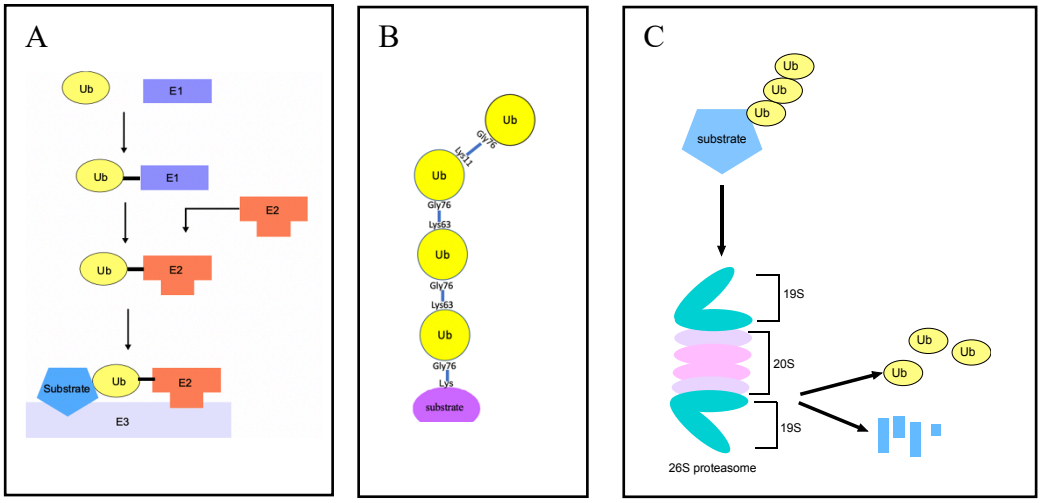

Figure 1.6. Mechanisms of Ubiquitination and the Ubiquitin Proteasome System (UPS). (A) Proteins and organelles can be tagged with ubiquitin (Ub) chains by a three-step enzymatic cascade. This occurs via E1 Ub-activating, E2 Ub–conjugating and E3 Ub-ligating enzymes. (B) Different Ub chain linkages can form between the Glycine76 (Gly76) on the previous Ub and a lysine of the next Ub moiety. This example demonstrates a mixed Ub chain linkage of Lys11 (K11) and Lys63 (K63), bound to a lysine on the substrate. (C) Ubiquitination directs substrates to the 26S proteasome for degradation. The proteasome consists of two 19S regulatory lids, which help recognize the ubiquitinated substrate. The 20S core contains proteolytic active sites which hydrolyze the protein.

Autophagy

Macroautophagy (hereafter referred to as autophagy) is a highly conserved catabolic process that is used to maintain homeostasis and becomes upregulated in adverse conditions such as nitrogen starvation to recycle proteins and organelles in the vacuole [17, 22, 23]. The pathways governing autophagy were first defined in yeast [101]. The significance of this discovery led to Yoshinori Ohsumi being awarded the Nobel Prize in Physiology or Medicine in 2006. Shortly thereafter, Daniel Klionsky also used genetics to define components of a yeast-specific pathway called cytoplasm-to-vacuole targeting (CVT) [102] [103]. Together, these studies laid the groundwork for many seminal discoveries on mechanisms governing autophagy both in yeast and higher eukaryotes

[104]. To date, over 43 autophagy-related genes have been identified, most of them with mammalian orthologs that regulate autophagy at different stages.

The process of autophagy is subdivided into 4 ordered steps: initiation/nucleation, elongation/closure, docking/fusion, and degradation/efflux [105]. It commences at the phagophore assembly site (PAS), where highly conserved autophagy related (Atg)-proteins and donor membranes are recruited [106, 107]. The phagophore then expands to sequester cargo from the cytoplasm, forming the double-membrane autophagosome upon membrane sealing, and the enclosed cargo is delivered to the vacuole (lysosome in metazoans) for degradation [108] (**Figure 1.7**). Today, macroautophagy, microautophagy, and chaperone-mediated autophagy (CMA) are the three major groups used to classify autophagy mechanisms. They are defined by the type of cargoes and the lysosomal delivery system employed. Macroautophagy and microautophagy are conserved from yeast to human, whereas and CMA is only found in mammals [109]. The similarities and differences between these pathways have been reviewed elsewhere, including their roles in human diseases [110] [111] [108].

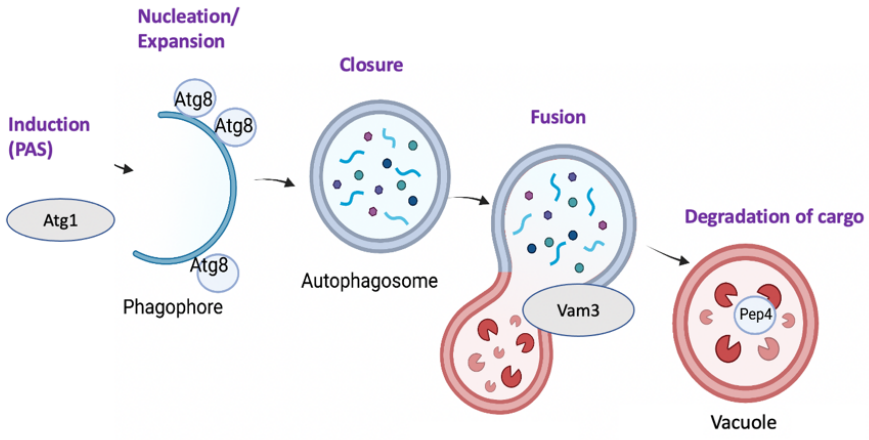

Figure 1.7. Major Players and Steps in General Autophagy. In yeast, highly conserved autophagy related (Atg)-proteins and donor membranes are recruited to induce expansion of a phagophore assembly site (PAS). The phagophore then sequesters cargo from the cytoplasm, and its membranes seal to form the double-membrane autophagosome. The enclosed cargo then fuses with the vacuole so that the cargo can be degraded by proteases. Atg1- protein kinase involved in autophagic vesicle formation; Atg8- ubiquitin-like protein with a role in membrane fusion and phagophore expansion during autophagosome formation; Vam3- aids fusion of autophagosome with vacuole; Pep4 - a vacuolar protease required for protein turnover.

Bulk Autophagy. In yeast, cargos destined for autophagic destruction are destroyed either by nonselective (bulk) or selective autophagy processes. Bulk autophagy is initiated by stress which inhibits the nutrient sensing complex TORC1 (target of rapamycin kinase complex) [112], including starvation stress, and can randomly degrade cytosolic proteins sequestered in the autophagosome [23, 113]. Formation of the phagophore assembly site (PAS) and Atg1 activation in bulk autophagy require the trimeric scaffolding complex that consists of Atg17, Atg29 and Atg31 (**Figure 1.8, left panel**).

Selective Autophagy. Selective autophagy, on the other hand, utilizes selective autophagy receptor proteins (SAR) to recognize and deliver cargo to growing phagophores. This process predominantly removes dysfunctional organelles and protein aggregates, and occurs to maintain homeostasis in normal conditions [114] and promote a cellular response to starvation or cytotoxic stress [115]. Here, the formation of the PAS and Atg1 activation is also dependent upon the singular scaffold protein Atg11, acting as a bridge between the SAR and PAS (**Figure 1.8, middle panel**)

Since its discovery, many selective autophagy pathways have been uncovered that degrade specific targets such as damaged organelles (mitophagy, ER-phagy, ribophagy), or aggregated proteins (aggrephagy). As such, selective pathways are involved in cellular

quality control, with aberrant selective autophagy being pathognomonic of many human diseases, prominently including neurodegeneration [24].

Sorting Nexins and Receptor Proteins in Selective Autophagy. In addition to using core autophagy proteins like nonselective autophagy, selective autophagy can be assisted by sorting nexins which help transport cargo to the vacuole [116]. For instance, the sorting nexin heterodimer Snx4-Atg20 promotes selective autophagy of various cellular components, including mitochondria (coined mitophagy), cytoplasm-to-vacuole targeting (CVT) pathway, ribosomes (coined ribophagy), and proteasomes (coined proteaphagy) [117-119]. Selective autophagy also utilizes receptor proteins, which tether specific damaged organelles and proteins to the core ubiquitin-like autophagy protein Atg8 (LC3 in mammals) at phagophores [120].

Cargo-Hitchhiking Autophagy. Recently, a third subclass of macroautophagy has recently been discovered in yeast by Ohsumi group [121] and our group [56]**.** This pathway utilizes receptor proteins, but instead of using the Atg11-built PAS, it requires the 17C scaffold for delivery of the cargos to vacuoles (**Figure 1.8, right panel)**. This hybrid macroautophagy mechanism also is assisted by the conserved sorting nexin Snx4-Atg20 heterodimer complex [56]. We called this pathway Snx4-assisted autophagy, whereas Ohsumi's group coined it cargo-hitchhiking autophagy [121].

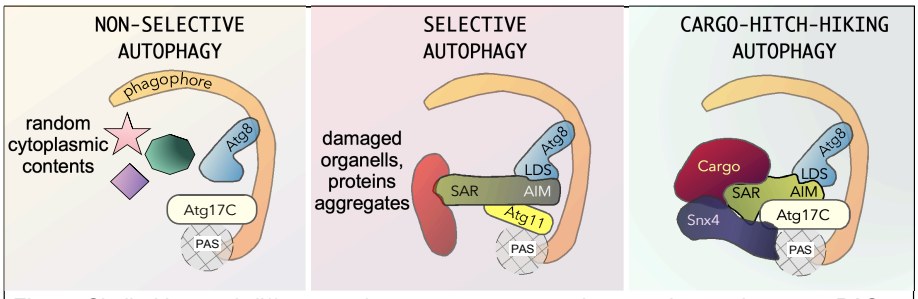

Fig. 1. Similarities and differences between macro-autophagy pathways in yeast. PAS - phagophore assembly site; SAR - selective autophagy receptor; AIM - Atg8 interacting motif; LDS - LIR (LC3 interacting region) docking site.

Figure 1.8. Three Major Types of Autophagy. (Left panel) Non-selective autophagy, also referred to as bulk autophagy, degrades random cytoplasmic contents in stress. This requires the scaffold complex at the phagophore assembly site (PAS) involving Atg17 complex (Atg17C). (Middle panel) Selective autophagy degrades specific damaged organelles, proteins and aggregates. This occurs through the use of a selective autophagy receptor (SAR) which binds to a specific domain of Atg8 and recognizes specific cargo. The scaffold complex at the PAS requires Atg11. (Right panel) Cargo-hitchhiking autophagy is a hybrid selective autophagy mechanism which requires the Atg17C, a SAR, and a sorting nexin (for example, Snx4).

Dual Nuclear and Cytoplasmic Functions of the CKM in Stress

In yeast, the CKM predominantly negatively regulates SRGs. Following stress, the CKM is dissolved, allowing for SRG expression. Work from our group has shown that CKM dissolution is mediated by degradation of cyclin C and Med13 of the CKM following different stresses to relieve repression of stress response genes [7]. Importantly, we determined that cell survival and cell death elicited different responses depending on the stress (outlined in **Figure 1.9**).

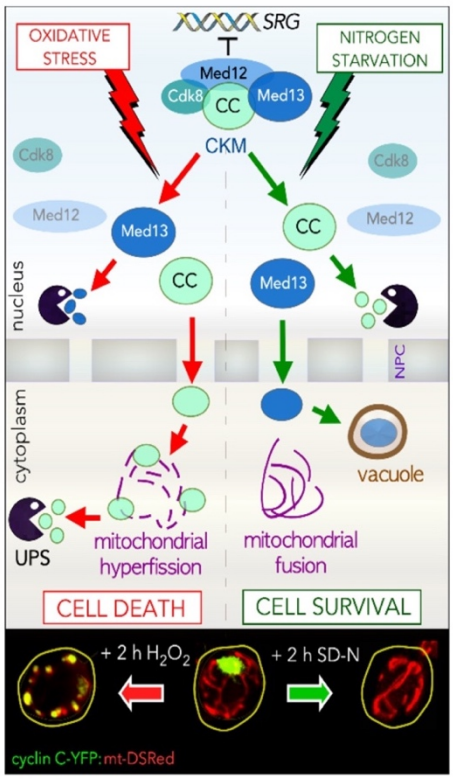

Figure 1.9. Subunits of the Cdk8 Kinase Module Serve Transcriptional and Cytoplasmic Functions in Stress. Top panel: Model outlining the different mechanisms used by the CKM to relieve repression on SRG's in response to either cell death (oxidative stress) or cell survival (nitrogen starvation) cues in yeast. Bottom panel: Live fluorescence images of cyclin C-YFP and DS-Red tagged mitochondria demonstrating the different phenotypes observed after 2 h treatment with H2O2 (left) or following nitrogen starvation (SD-N—right). CKM-Cdk8 kinase module, SRG's—stress response genes, YFP—yellow fluorescence protein.

CKM's Response to Cell Death Cues

Following cell death cues induced by oxidative stress, cyclin C, but not Cdk8, translocates to the cytoplasm, where it relocalizes with the outer mitochondrial membrane. Release of cyclin C from the CKM and nuclear exit is first dependent upon MAPK phosphorylation and degradation of Med13 [122]. Cytoplasmic cyclin C then interacts with the conserved mitochondrial fission machinery and is required for stress-induced

mitochondrial fission. It also promotes regulated cell death before being destroyed by the UPS. This secondary role of cyclin C is highly conserved from yeast to mammalian cells [53] [123]. Moreover, in mammalian cells, cyclin C has been identified as a tumor suppressor in solid cell tumors and blood cancers (reviewed in [124]).

CKM's Response to Cell Survival Cues

In yeast, survival cues triggered by nitrogen starvation elicit a different response. Cyclin C is instead degraded by the UPS in the nucleus. This preserves mitochondrial integrity, which is essential for survival [46]. Med13 is instead degraded by vacuolar proteolysis by a new selective cargo hitchhiking pathway. This allows the de-repression of autophagy-related (*ATG*) genes and promotes cell survival [46] [56]. Like other cargo-hitchiking routes, the autophagic degradation of Med13 requires the Atg17 trimeric scaffold complex and is promoted by the sorting nexin heterodimer Snx4-Atg20 [56]. Ksp1 is the selective autophagic receptor that associates with Atg8 and Med13. More recently, we have identified a role for Med13 in promoting P body assembly as well as the autophagic degradation of Edc3, a conserved B-body assembly factor (see Chapter 4).

Rationale

The balanced synthesis and degradation of mRNA and proteins are essential for cellular homeostasis, and in governing various processes like cell growth and stress response. Disruptions in these mechanisms are implicated in diseases such as cancers, Alzheimer's Disease, heart defects, and intellectual disability [1-3]. For instance, excessive protein synthesis can drive uncontrolled cell growth observed in cancers, while impaired protein degradation can lead to toxic protein aggregation and increased cell death,

characteristic of neurodegenerative diseases. Thus, maintaining protein homeostasis is crucial in preventing disease onset.

Despite the recognized importance of protein homeostasis, the regulatory mechanisms and interplay of protein homeostasis pathways remain poorly understood. For instance, coordinated control of RPs and TIFs is critical for cell growth and appropriate responses to stress [15] [15]. However, how RP and TIFs are regulated at the level of gene expression are not well understood. This is important to understand because dysregulated ribosome and TIF biogenesis are associated with aging, cancers, and neurodegenerative diseases [125] [126]. Thus, I investigated the transcriptional mechanisms which control translational machinery (See Chapter 3).

The highly conserved translation initiation factor eIF4G1 is critical for cap-dependent translation and controlling cellular growth. Dysregulation of eIF4G1 has emerged as a significant factor in various cancers, neurodegenerative disease, and impaired neurodevelopment such as Autism Spectrum disorder [81, 127, 128], [129] [130], highlighting the importance in investigating the mechanisms which control its expression. Previous studies demonstrate that eIF4G1 is degraded following TORC1 inhibition and that its depletion promotes autophagy in mammalian cells by impairing cell proliferation and mitochondrial activity [131, 132]. However, the mechanisms which control eIF4G1 degradation remains unknown. Furthermore, recent insights suggest a closer relationship between ubiquitin and autophagy than previously appreciated [133]. A recent study suggested that a de-ubiquitinase promotes eIF4G1 autophagy in yeast following nitrogen starvation [13], however the precise roles of ubiquitin in selective autophagy pathways are

still unclear. Thus, I aimed to investigate the ubiquitin-dependent autophagy mechanism required for eIF4G1 proteolysis (see Chapter 5).

The Cdk8 kinase module (CKM) is a highly conserved complex with regulatory functions in both the nucleus and cytoplasm [7], controlling cell fate under different stress conditions. Dysregulation of the CKM has been linked to developmental diseases and numerous human cancers [134-137]. However, we still do not have a comprehensive understanding of the CKM's functional roles and mechanisms in the cellular stress response. For instance, our lab recently found that Med13 is the only CKM subunit which re-localizes to the cytoplasm for autophagic degradation following nitrogen starvation [56], but Med13's function in the cytoplasm required more investigation. Therefore, we aimed to elucidate the nuclear and cytoplasmic roles of CKM in cellular responses to translation-limiting stresses, including nitrogen starvation (see Chapter 4) and antibiotic exposure (see Chapter 3).

Here, I use the baker's yeast *S. cerevisiae* as a model organism to address these aims due to the easy ability to manipulate multiple genes and to better understand these complex molecular pathways. Yeast is a useful model organism to test the transcriptional roles of a multi-subunit complex such as the CKM because of the easy ability to knockout each subunit. Additionally, the CKM is known to have highly conserved transcriptional and non-transcriptional stress-response roles from yeast to man [7]. Taken together, this thesis focuses on understanding the molecular mechanisms involved in protein synthesis, and how these also coordinate with degradation pathways to elicit an appropriate response to stress.

Chapter 2

Materials and Methods

Yeast Strains and Plasmids

Experiments were primarily performed with endogenously labeled proteins in the *S. cerevisiae* W303 background [138] and are listed in Supplemental Tables for each chapter. Most strains were constructed using replacement methodology, including C-terminus tagging of eIF4G1 with 3xMYC [139]**.**

Strains containing endogenously C terminally tagged eIF4G1-5xMYC were constructed using integrating plasmids HB0535 or HB0536. HB0535/HB0536 were made in a pRS303 backbone [140] and gifted by Won-Ki Huh from Seoul National University [141]. HB0535/HB0536 were integrated by cutting the PRS303 backbone derived from. Strains containing KXR ubiquitin chain mutants were a gift from Daniel Finley from Harvard Medical School as made as described in [142]. Strains used for NUbiCA assays were a gift from Gwenaël Rabut from Institute of Genetics and Development of Rennes [143]. Other strains used were from the Research Genetics yeast knockout collection and are derived from BY4741 strain background. In accordance with the Saccharomyces Genome Database, the TIF4631 gene will be designated as its protein name eIF4G1. Members of the CDK8 module-ySSN8/CNC1/UME3/SRB11, SSN3/CDK8/UME5/SRB10, SRB8/MED12/ SSN5 and SSN2/MED13/UME2/SRB9- will use SSN8/CNC1, SSN3/CDK8, SRB8/MED12, and SSN2/MED13 gene designations, respectively. Throughout the manuscript we use RPL and RPS designations for RP 60S and 40S encoded genes, respectively.

Yeast strains formed with CRISPR/Cas9 gene editing technology using a Cas9-1-step plasmid pJR3428 [144]. CRISPR method was carried out using a protocol adapted from Michael Law lab at Stockton University and Jasper Rine lab at University of California Berkley, with our additional protocol modifications available upon request. CRISPR-mediated deletion of potential Cul3 binding site on eIF4G1 (residues 932-936) in RSY2955 was formed using the primers as indicated in Table S1.

Plasmids used in this study are listed in Table S2 of each chapter. Details of their construction, as well as the plasmids themselves, are available upon request. The wild-type epitope-tagged Vph1-mCherry plasmid has been previously described [46]. The galactose inducible dominant-negative Rsp5 WW1 mutant plasmid pRsp5Δcis was a gift from Natalia Shcherbik at Rowan University [145]. The Cas9 guide RNA plasmid pJR3428 to form CRISPR strains was a gift from Michael Law at Stockton University and originally derived from [144]. GFP tagged Rpl25 and Rps2 were gifts from D. Strauss at Biochemie-Zentrum Heidelberg [146, 147].

Cell Growth

Yeast cells were grown in either grown in either rich, non-selective medium (YPD 2% [wt/vol] glucose, 2% (w/v) Bacto peptone, 1% (w/v) yeast extract) or synthetic minimal dextrose medium (SD: 0.17% w:v yeast nitrogen base without amino acids and ammonium sulfate, 0.5% w:v ammonium sulfate, 1x supplement mixture of amino acids, 2% w:v glucose) allowing plasmid selection as previously described [45]. For all experiments, the cells were grown to mid-log phase (~6×10^6 cells/ml) in YPD or 2% glucose media, selecting for plasmids when appropriate. For Cycloheximide and Hygromycin protein chase experiments, 150 μg/ml Cycloheximide or 2 mg/ml Hygromycin was added to mid-log

phase cells. *E. coli* cells for isolating plasmids were grown in LB medium with selective antibiotics as previously described [45].

For nitrogen-starvation experiments, cells were grown to mid-log (between ~$5x10^6$ and $6x10^6$) in SD medium, spun down, washed in 2x volume of water, and resuspended in SD-N media for indicated time points [148]. For experiments with cells containing plasmids expressed from a Gal1 promoter, yeast cells were grown overnight in selective synthetic minimal medium containing galactose (SD: 0.17% w:v yeast nitrogen base without amino acids and ammonium sulfate, 0.5% w:v ammonium sulfate, 1x supplement mixture of amino acids, 2% w:v galactose), followed by resuspension in SD-N medium for the indicated time points. All protein extracts were prepared from 25-ml culture samples per timepoint and washed in H_2O, and the pellet was flash frozen in liquid nitrogen.

Yeast Cellular Assays

For yeast growth plating assays, cells were grown to mid-log, diluted to ~$3x10^6$ cells/mL, and spotted in 10-fold serial dilutions (4 μl for each dilution) onto YPD plates containing translation inhibitors at the indicated concentrations. Specific concentrations of antibiotics were used to allow sufficient growth of wild-type cells while observing potential changes in the growth of CKM mutants. For growth plating assays with canavanine, cells were spotted in 10-fold serial dilutions onto SD medium plates without arginine and containing L-canavanine at the indicated concentration. To determine recovery, cells were grown to mid-log and then switched to liquid medium containing translation inhibitors for the indicated number of days, followed by serial dilutions 10-fold onto YPD plates. The plates were imaged using an iBright FL1500 imaging system (Thermo) following an incubation of 2 days at 30°C. To measure cell proliferation, strains were grown overnight

in biological triplicates to mid-log in selective SD medium. They were then diluted to OD=0.1 in selective SD medium containing the indicated concentrations of drugs. Technical duplicates of 200 µl total of each sample were pipetted into a 96-well plate. Using a Synergy plate reader, OD_{600} of each well was collected every 3 or 5 minutes on continuous orbital at 30°C. T=0 values were normalized to 1, and Log_{10} measurements were plotted at 2 h intervals with a line of best-fit.

The Y2H assays were performed exactly as described [149]. In short, three biological replicates containing a Gal4-binding domain construct (pAS2 backbone) and a Gal4-activating domain construct (Gal4-AD-T7) were plated on medium selecting for plasmid maintenance (-LEU, -TRP). Interaction between proteins was monitored by selection on -LEU, -TRP -ADE, -HIS plates for 3 days at 30°C. Activation of the two other reporter genes, AUR1-C and MEL1, was monitored by the addition of 200 ng/mL Aureobasidin A (Takara Cat# 630466) and 40ug/mL of X-alpha-Gal (GoldBio Cat# 484 XA250) respectively. The nitrogen starvation viability assays were executed in biological triplicate as described (Willis et al., 2020). Following staining with phloxine B (Millipore Sigma, P2759), 30,000 cells were counted per timepoint using fluorescence-activated cell analysis (FACs). P values were determined using the unpaired Student's t-test. Data are mean ± standard deviation

RT-qPCR Analysis

RT-qPCR analyses in yeast grown to mid-log in physiological conditions were executed as previously described [54]. RNA was then extracted using the NEB Total RNA Miniprep Kit (NEB T2010S) using both the genomic DNA removal columns and 5 µl DNase (NEB T2004) to remove contaminating DNA. The resulting RNA was quantified,

and 1µg of RNA was converted to cDNA using the cDNA maxima kit following manufacturer directions (Thermo K1641). The resulting cDNA was diluted 1/100 in dH2O and 5µl added to a reaction containing 7.5µl Power SYBR master mix (Thermo 4367659), 0.5µl of 10µM of each primer, and 1.5µl dH2O. The reactions were then loaded onto the Applied Biosystem StepOne thermocycler using the standard cycle (40 cycles,95°C denature 15 seconds, 60°C anneal and extension 1 minute).

Quantitation of mRNA was achieved using Actin (*ACT1*) as an internal reference standard for yeast cells. The delta-delta-CT (ΔΔCT) method was used to determine transcript levels of each gene [150]. Each condition was performed in biological triplicates and technical duplicates. Statistical significance was determined via Student's *t* test analysis, with data as mean ± standard deviation. Oligonucleotides used during these studies are available upon request.

ChIP Assays

Protocol adapted from Wal et al., 2012 [151]. Briefly, cells were grown to mid-log phase, pelleted, and stored at -80°C until needed. Thawed cells were resuspended in FA lysis buffer (50 mM HEPES pH 8.0, 150 mM NaCl, 2 mM EDTA, 1% w/v Triton) with 50 mg/mL protease inhibitor cocktail. Zymolyase (USBiological CAS# 37340-57-1) and incubated at 37°C for 10 min, inverting occasionally. Cells were pelleted 3500 RPM, 5m RT and checked for spheroplasts. The pellet was resuspended in NP-S buffer (0.5 mM Spermidine, 0.075% Triton, 50 mM NaCl, 10 mM Tris-HCl pH 7.5, 5 mM $MgCl_2$, 1 mM $CaCl_2$), vortexed, respun, and the pellet resuspended in NP-S buffer containing 1mM B-ME. (VWR, CAS# 60-24-2). Optimized concentrations of MNase (NEB MO247S) were

added, and reaction was incubated at 37°C with inversion every 2 min, for 10m. The reaction was quenched with 10 mM EDTA, and samples placed on ice for 10 min. Cell debris was pelleted, 10 m, max speed and supernatant collected. The pellet was washed with NP-S containing 0.2% SDS, sonicated briefly (4 cycles, 10s pulse, medium speed). Samples were centrifuged once more for debris removal, 15 min, max speed, and the supernatant added to previous step. A portion of the sample was run on 2% agarose gel to verify efficient cleavage of chromatin into mononucleosomes. A percentage of the chromatin was retained as input control (2-5%) and stored at -80°C until further use. An additional portion was used as a non-specific control for immunoprecipitation. 1 mg of appropriate antibody was added to chromatin preps and incubated at 4°C overnight rotating (anti-MYC UpState/EMD Millipore Corp, 05-724, anti-HA Abcam ab9110, anti-GFP Wako Pure Chemical Corp, 012-20,461).

For immunoprecipitation, protein beads were equilibrated in NP-S buffer, and added to samples. After incubation, beads were washed with the following steps: 1X FA lysis buffer supplemented with 0.025% SDS and protease inhibitor, 1X FA lysis buffer, 1X FA high-salt buffer with protease inhibitor (50 mM HEPES pH 7.5, 1 M NaCl, 1% Triton, 2 mM EDTA), 2X Wash buffer 3 with protease inhibitor (10 mM Tris-HCl pH 8, 20 mM LiCl, 1% IGEPAL, 2 mM EDTA, 1% Triton). Beads were resuspended in FA wash buffer 3 and treated with both RNase A and proteinase K. Input samples were thawed and treated with RNase A and proteinase K. Chromatin was purified using 1:1 volumes of PCI (25:24:1 phenol, chloroform, isoamyl alcohol). The aqueous layer was precipitated with 100% EtOH and the pellet washed with 70% EtOH, dried and resuspended in dH_2O, and quantified. Purified DNA was used in qPCR amplification using ThermoFisher

PowerSYBR Green PCR MasterMix and StepOne real-time PCR system. Primers were designed for individual gene promoter regions and quantified using percentage input. Assays were conducted in triplicate, with three independent biologicals.

Western Blot Analysis

Yeast extracts for western blot analysis of comparing unstressed mutants were prepared using glass bead lysis as previously described [122]. In short, 50 ml of mid-log cells were lysed with glass beads in RIPA V buffer (50 mM Tris pH 8, 150 mM NaCl, 0.158% Sodium deoxylcholate, 1% NP-40) supplemented with 1 mM PMSF, 14 mM ß-mercaptoethanol, 1 µg/ml pepstatin, 1 µg/ml leupeptin, and 1x protease inhibitor (GoldBio, GB-333). 30-40 µg of total protein was subject to western analysis.

Protein extracts for western blot studies of protein degradation in stress were prepared using a NaOH lysis procedure exactly as described in [152]. In short, protein extracts were prepared from 25 ml per timepoint. For visualizing endogenous eIF4G1 degradation, ~2-6 µl of protein extract for each sample was loaded onto a gel due to the high abundance of eIF4G1 in the cell. For visualizing all other proteins, ~8-10 µl was loaded onto the gel. Proteins were separated on 10% SDS polyacrylamide gels and transferred for 1 h 15 minutes in running buffer containing 20% methanol. To visualize Med13, proteins were specifically separated on 6% SDS polyacrylamide gels and transferred for 1 h 15 minutes in running buffer containing 10% methanol.

To detect proteins, 1:5000 dilutions of anti-MYC (UpState/EMD Millipore Corp.,05–724), 1:2500 anti-GFP (Wako, 012-22541), 1:2500 anti-HA (Abcam, ab9110), or 1:1000 anti-Pgk1 (Abcam) antibodies were used. The anti-eIF4G1 antibodies (used in 1:2000) were kindly provided by P. Rajyaguru from Indian Institute of Science; anti-Rpl3

(ScRPL3) antibodies were from the Developmental Studies Hybridoma Bank, University of Iowa; anti-Ded1 antibodies were gifted by T. Bolger lab from The University of Georgia. Western blot signals were detected using 1:5000 dilutions of either goat anti-mouse (Abcam, ab97027) or goat anti-rabbit (Abcam, ab97061) secondary antibodies conjugated to alkaline phos-phatase and CDP-Star chemiluminescence kit (Invitrogen, T2307).

All protein degradation assays were performed in triplicate unless otherwise stated. For quantification of degradation kinetics, band intensities (Local Bg. Corr. Volume) of each time point were measured with saved G2i files of western blot images using iBright CL1500 Imaging system and iBright Analysis software (ThermoFisher). The band intensity value at each time point was first divided by unstressed T=0 band intensity. These values were then divided by Pgk1 loading band intensity values, which were also normalized to their T=0 intensities. All the normalized values were then multiplied by 100 to calculate a percentage decrease in band intensity relative to T=0, with T=0 band intensity representing 100% protein. These percentage values were then converted to Log10, with the value of Log10 at T=0 as 2. This information was used to determine the line of best fit that was calculated by simple linear regression analysis in GraphPad Prism 7. Protein half-life was extrapolated using the linear regression analysis, where 1.7 (log of 50, half of 100%) was used as the y value in the slope-intercept form equation. P values shown are relative to wild-type final time points and were generated from GraphPad Prism 7 using unpaired parametric T tests; NS $P \geq 0.05$; *$P \leq 0.05$, **$P \leq 0.005$; ***$P \leq 0.001$; ****$P \leq 0.0001$. All error bars indicate mean ± SD.

A. Equations to compare protein levels in T_x (time point of X h) relative to T_0 (time point of 0 h) using Microsoft Excel:

1. (Protein band intensity value at T_x) / (protein band intensity value at T_0) = protein value normalized to T_0
2. (Loading control band intensity value at T_x) / (loading control band intensity value at T_0) = loading control value normalized to T_0
3. (Protein value normalized to T_0) / (loading control value normalized to T_0) = normalized protein value
4. (Normalized protein value)*(100) = percent protein relative to T_0
5. Log10(percent protein relative to T_0) = Log% protein value, where value at T_0 is equal to 2
6. Enter Log% protein value in GraphPad Prism and use simple linear regression analysis for line of best fit (with the line constrained to go through Y=2)

To further calculate half-life:

1. Linear regression analysis on GraphPad prism will demonstrate m and b values in a slope-intercept form equation (y=mx+b), where Y= 1.7 (log of 50, half of 100%)
2. Solve for x to calculate $T_{1/2}$

B. Equations to compare protein levels in mutant relative to WT from western blot analyses:

    1. (Protein band intensity value in mutant) / (protein band intensity value in WT) = protein value normalized to WT

2. (Loading control band intensity value in mutant) / (loading control band intensity value in WT) = loading control value normalized to WT
3. (Protein value normalized to WT) / (loading control value normalized to WT) = normalized protein value
4. Enter Log_2 of normalized protein values into GraphPad Prism for visualizing protein expression relative to WT as bar graphs

eIF4G1-GFP Cleavage Assays

Strains harboring eIF4G1-GFP fusion protein were grown to mid-log in SD, washed, and resuspended in SD-N. Protein extracts were prepared using NaOH as described above (25 mL/time- point). Due to the large size of eIF4G1-GFP, proteins were separated using Invitrogen Blot^{TM} 4–12% Bis-Tris Plus gradient gels with 1X MOPS SDS running buffer (NW04122BOX). Proteins were transferred to PVDF membranes in 1X Blot^{TM} transfer buffer for 1 h 30 min (BT00061). GFP-tagged proteins were detected using 1:5000 dilution of anti-GFP (FUJIFILM Wako Pure Chemical Corp., 012–20,461) antibodies and goat anti-mouse secondary antibodies conjugated to alkaline phosphatase.

Immunoprecipitation to Detect Ubiquitination with VU1 Antibody

For immunoprecipitation experiments, 1 L of cells were grown to mid-log, washed, and resuspended in SD-N media (250 mL/timepoint). Protein extracts were prepared using a glass bead lysis method exactly as described in [122], except protein A beads (GoldBio, P-400-5) were pre-washed with IP wash solution (500 mM NaCl, 25 mM Tris, pH 7.4). 500 μg of total protein was immunoprecipitated per timepoint. Anti- GFP antibodies (Invitrogen,A11122) was used for immunoprecipitations. To visualize ubiquitin and the

large eIF4G1-GFP fusion protein, proteins were separated using Invitrogen Blot^{TM} 4–12% Bis-Tris Plus gradient gels with 1X MOPS SDS running buffer (NW04122BOX). Proteins were transferred to PVDF membranes in 1X Blot^{TM} transfer buffer for 1 h 30 min (BT00061). The blot was pretreated with 0.5% glutaraldehyde according to the VU-1 antibody protocol outlined by LifeSensors (VU101), and probed with 1:2000 dilution of VU-1 anti-ubiquitin antibodies (LifeSensors, VU101). For input control, the blot was re-probed with 1:5000 dilution of anti-GFP antibodies (Invitrogen, A11122).

Fluorescence Microscopy

Cells were grown to mid-log (~6 × 10^6 cells/ml) in selective SD medium then analyzed by fluorescence microscopy before and after the stress condition. Single plane images were obtained using a Keyence BZ-X710 fluorescence microscope with a ×100 objective with ×1.0 camera magnification (PlanApoλ Oil, NA 1.45) and a CCD camera. Data were collected using BZ-X Analyzer software. All images of individual cells were optically sectioned (0.2-μM spacing), deconvolved and slices were collapsed to visualize the entire fluorescent signal within the cell.

Quantification of Ssn2/Med13-mNeongreen fluorescence within the vacuole was obtained using the Hybrid cell count function within the analyzer software (at least 200 cells were counted per sample). For analysis, single extraction settings were used. Red (vacuole, Vph1-mCherry) was set as the extraction area and green (Ssn2/Med13-mNeongreen) was set as the target area. The percentage of cells with vacuolar Ssn2/Med13- mNeongreen was calculated using Area ratio (1st) (ratio of the total area of the target area to the extraction area) for at least 200 cells.

NanoBiT-Based Ubiquitin Conjugation Assay (NUbiCA)

NUbiCA was performed as previously described [143] with modifications. Protein extracts for western blot studies in whole cell lysate were prepared using a NaOH lysis procedure exactly as described in [152]. In short, protein extracts were prepared from 200 ml per timepoint. To visualize the large eIF4G1-LgBiT/His fusion protein, proteins were separated using Invitrogen Blot^{TM} 4–12% Bis-Tris Plus gradient gels with 1X MOPS SDS running buffer (NW04122BOX). Proteins were transferred to PVDF membranes in 1X Blot^{TM} transfer buffer for 1 h 30 min (BT00061). To allow LgBiT fragment renaturation after transfer, the membranes were washed in TBS-T (50 mM Tris pH 7.5, 150 mM NaCl, 0.05% Tween 20) for at least 1 h. To visualize the NanoBiT signal produced by the conjugation of SmBiT-ubiquitin to LgBiT/His-tagged proteins, the membranes were incubated in TBS-T supplemented with 1% NanoLuc substrate furimazine (Nano-Glo Luciferase Assay Substrate from Promega REFN113A) for 15 minutes. The luminescence signals were then recorded for up to 20 min using using iBright CL1500 Imaging system. For a loading control of eIF4G1-LgBiT/His levels, 1:1000 dilutions of anti-HIS (Sigma, H1029) antibodies were used. For loading control of whole cell lysate, 1:1000 anti-Pgk1 (Abcam) antibodies were used. Western blot signals were detected using 1:5000 dilutions of either goat anti- mouse (Abcam, ab97027) or goat anti-rabbit (Abcam, ab97061) secondary antibodies conjugated to alkaline phos-phatase and CDP-Star chemiluminescence kit (Invitrogen, T2307).

Western blot studies of immunoprecipitated eIF4G1-LgBiT/His was completed similarly except protein extracts were prepared using a glass bead lysis method exactly as described in [122]. Protein A beads (GoldBio, P-400-5) were pre-washed with IP wash

solution (500 mM NaCl, 25 mM Tris, pH 7.4). 500 µg of total protein was immunoprecipitated per timepoint. Anti-HIS (Sigma, H1029) antibodies were used for immunoprecipitations. Samples were then loaded onto Invitrogen Blot^{TM} 4–12% Bis-Tris Plus gradient gels and the blot was incubated with furimazine substrate using the same method as described above. The luminescence signals were then recorded for up to 20 min using using iBright CL1500 Imaging system. To visualize eIF4G1-LgBiT/His as a loading control, the blot was then incubated with 1 µM HiBiT (Biosynth, CRB1001507) added to 1% furimazine and TBS-T for 15 minutes. HiBiT binds to LgBiT and releases a luminescent signal in the presence of the furimazine substrate.

To detect a NanoBiT signal on eIF4G1-LgBit/His using a plate reader, protein extracts were prepared using a glass bead lysis method exactly as described in [122]. 100 µg of total protein for each sample was diluted 1:10 in RIPA V glass bead lysis buffer up to 30 µl total volume. The diluted sample was then added to 1% furimazine (Nano-Glo Luciferase Assay Substrate from Promega REFN113A) with or without 1 µM HiBiT (Biosynth, CRB1001507) to control for eIF4G1-LgBiT/His expression. Nano-Glo luciferase assay buffer (Promega REFN113A) was then added up to a total volume of 200 µl for all samples. The samples were added to a clear 96-well plate (skipping a well between each sample to avoid cross-talk of luminescence). Luminescence signal was read using a Synergy H1 plate reader with an integration time of 1 second and full light emission.

TUBE-Based Mass Spectrometry Proteomics

WT cells expressing endogenously tagged eIF4G1-3xMYC were grown to mid-log in SD complete medium and resuspended in SD-N. Samples were saved at 0 and 3 h SD-

N, 250 ml per timepoint. Protein extracts were prepared using a glass bead lysis method exactly as described in [122]. Protein G beads (GoldBio, P-400-5) were pre-washed with IP wash solution (500 mM NaCl, 25 mM Tris, pH 7.4). 400 µg of total protein was immunoprecipitated per timepoint. Samples were incubated with Anti-MYC (UpState/EMD Millipore Corp.,05–724) antibodies overnight for immunoprecipitations. The next day, samples were washed with IP wash solution x4, and incubated with Protein G beads for 1 hour at 4°C. Samples were then boiled for 5 minutes in 2X SDS loading buffer. To identify potential ubiquitination and proteins bound to eIF4G1-3xMYC, the eluents were sent to LifeSensors for Tandem Ubiquitin Binding Entities (TUBEs) and mass spectrometry analysis as described: https://lifesensors.com/tube-based-mass-spectrometry/ .

^{35}S-Radiolabeled Methionine Incorporation to Determine Translation Rate

Yeast cells were grown to mid-log phase in SD medium, washed with dH_2O, and resuspended with methionine-depleted SD minimal medium (SD-Met) for 1 hour. After 1 hour incubation of the cells at 30 °C, final concentration of 50 µM unlabeled-methionine and 1 µCi/ml of ^{35}S-Methionine and ^{35}S-Cysteine mixture (11 mCi/mL, PerkinElmer) was added at time 0 (T0). At 10-min intervals of incubation in 30 °C, 200 µl of ice-cold 50% TCA was added to 1 mL aliquots of the cultures for protein precipitation. Proteins were then washed and collected on Whatman 25-mm glass microfiber filters for CPM measurement in a scintillation counter Beckman LS6500. Translation rate was determined by the rate of incorporation (CPM/cells per mLx10^3), plotted as a function of time. All measurements were conducted in biological triplicates.

Proteasome Activity Assay

Cells were lysed with glass beads using lysis buffer A (25 mM Tris, pH 7.4, 10 mM MgCl2, 10% glycerol) supplemented with fresh 1mM ATP, 1 mM DTT, and 5 µL (for 500 µL of buffer) of protease inhibitor and phosphatase inhibitor. Cells were spun at full speed for 4 minutes at 4º C and lysates were transferred to a new tube. Bradford protein assays were used to determine protein concentrations. Each reaction required 50 µg of protein which was brought up to a total volume of 50 µL using lysis buffer and pipetted into one well a 96-well dish. To monitor proteasomal-independent fluorescence as a control, 72.5 µM of proteasomal inhibitor MG132 was added to each control well. Finally, the substrate buffer (lysis buffer A, 200 µM SUC-LLVY-AMC, 1 mM DTT, and 1 mM ATP) was added to each well. SUC-LLVY-AMC was used as a fluorescent substrate to determine chymotrypsin-like proteasome activity. Fluorescence was immediately monitored via the plate reader. Fluorescent readings (excitation = 360, emission = 400) were taken every 5 minutes for 90 minutes at 30º C with gentle shaking.

RNA Gel and Northern Blot Analysis

All yeast strains were grown in SD medium and frozen at the same concentration during mid-log phase (25 mL each) to ensure loading from equal number of cells per sample. Total RNA was isolated from cells using formamide-EDTA one-step extraction as previously described [153]. Total RNA was then separated on 1% agarose gels [154], transferred to nylon membranes (Hybond N; GE Biosciences), and first visualized by methylene blue staining. Individual rRNA species were then detected by Northern hybridizations using ^{32}P-labeled oligonucleotide probes as described [155]. We used the following probes: y500 against 18S rRNA (5′-AGAATTTCACCTCTGACAATTG), y540

against 25S rRNA (5′-TCCTACCTGATTTGAGGTCAAAC), and a probe against $tRNA^{Val}$. All hybridizations were analyzed using a Typhoon 9200 PhosphorImager and ImageQuant software (GE Biosciences). For quantification, volume for each fragment was converted to phosphorimaging units and subtracted from the average background signal. To correct for unequal loading between lanes, the 18S or 25S rRNA of each sample was then normalized to the tRNA signal in the same samples. Normalized 18S or 25S rRNA levels were then quantified as Log_2 fold change relative to WT.

Sucrose Gradient Analysis

Sucrose gradient centrifugation analysis was done as described before [156]. Briefly, cells were grown in YPD medium to mid-log phase (OD_{600} ~ 0.7 - 0.8), and were harvested after treatment with cycloheximide (CHX, 100 µg/ml) for 2 mins. Cells were lysed by bead beating (30" vortexing: 30" on ice per one cycle; 12 cycles) in lysis buffer containing 100 mM NaCl, 3 mM $MgCl_2$, 10 mM Tris-HCL pH-7.4, 0.2 mg/ml of heparin and 100 µg/ml of CHX. Lysates were clarified by centrifugation at 21,000 x g for 10 min, RNA concentration was measured spectrophotometrically. Extracts equivalent to 150 µg of RNA were loaded onto 15-45% (wt/vol) sucrose gradients prepared in 70 mM NH_4Cl, 4 mM $MgCl_2$, and 10 mM Tris–HCl (pH 7.4) buffer. Gradients were centrifuged at 188 000 × g at 4°C for 4 h 15 min (Beckman SW41Ti rotor, 36,000 rpm) at 4°C and analyzed by fractionation with continuous monitoring of absorbance at λ=254 nm (A_{254}) using EM-1 UV monitor.

Statistical Analysis

All presented results included at least two independent biological experiments. The figure legends indicate the actual number. Prism-GraphPad was used to generate *p* values

using unpaired Student's *t*-tests; NS $p \geq 0.05$; *$p \leq 0.05$; **$p \leq 0.01$; ***$p \leq 0.005$; ****$p \leq 0.001$. All error bars indicate mean ± SD.

Chapter 3

The Cdk8 Kinase Module (CKM) Maintains Constitutive Expression of a Subset of Translation Genes and Controls Survival in Translation-Limiting Stress

Disclaimer: A large portion of this chapter is adapted from: Friedson B, Willis SD, Shcherbik N, Campbell A, Cooper KF. The CDK8 kinase module: a novel player in the transcription of translation initiation and ribosomal genes. *Under revision, MBoC. 2024**

*Author contributions: B Friedson devised the project, performed yeast experiments, wrote and revised the manuscript; SD Willis performed mammalian experiments and provided ideas/edits; N Shcherbik helped with yeast experiments and provided ideas/edits; A Campbell carried out ChIP analyses; KF Cooper supervised and provided ideas/edits.

Abstract

Survival following stress is dependent upon reprogramming transcription and translation. Communication between these programs following stress is critical for adaptation but is not clearly understood. The Cdk8 kinase module (CKM) of the Mediator complex modulates the transcriptional response to various stresses. Its involvement in passing a signal to translational machinery has yet to be elucidated, highlighting an existing gap in knowledge. Here, we report that the CKM positively regulates a subset of ribosomal protein (RP) and translation initiation factor-encoding (TIF) genes under normal physiological conditions in *Saccharomyces cerevisiae*. In mamalian cells, the CKM regulates unique sets of RP and TIF genes, demonstrating a limited conservation of function across species. In yeast, this is mediated by Cdk8 phosphorylation of one or more transcription factors which control RP and TIF expression. Conversely, the CKM is disassembled following nutrition stress, permitting repression of RP and TIF genes. The

CKM also plays a transcriptional role important for promoting cell survival, particularly during translational machinery stress triggered by ribosome-targeting antibiotics. Furthermore, the activity of Cdk8 promotes cell survival following ribosome inhibition. These results provide mechanistic insights into the CKM's role in regulating the expression of a subset of genes associated with translation. Together, these emphasize the importance of the CKM as a central hub in controlling cellular responses to stress.

Introduction

The reprogramming of transcription and translation is critical for adaptation to environmental cues and physiological stresses. The molecular mechanisms that control both processes are well understood, but less is known about how the programs are coordinated to control cellular outcomes.

The conserved Cdk8 Kinase Module (CKM) is a dissociable component of the 26-subunit Mediator complex, which regulates gene expression by RNA polymerase II (RNA Pol II) [157, 158]. As such, the Mediator complex exists as two distinct entities, depending on whether it is bound to the CKM, forming a larger CKM-Mediator complex. In addition, the CKM exists as a stable entity in cells and likely functions independently of the Mediator [159-161]. The CKM consists of cyclin C, its cognate kinase Cdk8, and two structural proteins, Med12 and Med13, which interact with the Mediator [159, 162, 163]. In mammals, the CKM contains paralogues of all components except cyclin C, namely MED12L, MED13L, and CDK19 [164]. The biological roles of these paralogues remain poorly understood, but they appear to be functionally distinct [165].

The basic functions of the CKM–Mediator are to activate or block RNA Pol II transcription initiation. Additional roles for CKM-Mediator in regulating RNA Pol II

elongation rate have been described [166, 167] but it remains unclear if this function is mediated by the CKM-Mediator complex or the CKM acting as an independent entity [166-168]. In yeast and mammalian cells alike, the CKM both positively and negatively regulates gene transcription, predominantly in response to unfavorable environmental cues and during developmental programs [7, 36, 53, 64, 169-171]. The precise mechanism of how the CKM-Mediator regulates translational gene expression is poorly understood [36]. Structural and biochemical studies identified the CKM–Mediator association as reversible, leading to the model that the CKM sterically inhibits the mediator from interacting with RNA Pol II at promoters [39, 41, 158, 159, 162, 172-176].

As a kinase that associates with the Mediator, the CKM regulates transcription by phosphorylation of various targets, including RNA Pol II C-terminal repeat domain (CTD) [177, 178] and other regulatory factors including Mediator components [49, 179-189]. Key among these targets are many transcription factors (TF), as Cdk8-mediated phosphorylation can repress and activate TF activity [49, 50, 183, 187, 190-192]. In addition, phosphorylation of TFs by the CKM-Mediator may be transmitted directly through enhancer regulatory elements to either repress or activate transcription [168, 193]. In addition, mediator-free CKM can phosphorylate histone H3 [159]. Thus, CKM impacts key transcriptional outputs that affect cellular and developmental homeostasis.

Deciphering the contribution of the CKM to diverse biological outputs is important as the dysfunction of any of its members is linked to a multitude of human diseases, including cancer [134-137]. Furthermore, genetic variations in paralogues CDK19, MED12L, and MED13L of the mammalian CKM are linked to a large spectrum of neurological disorders [194, 195]. In yeast, the CKM acts predominantly as a repressor of

stress response genes, including those that encode for antioxidants and molecular chaperones, though a role in gene activation following stress has been reported [43, 45, 47, 49, 157, 160, 196-200]. Repression is relieved by disassociating the CKM from the mediator and disassembling the CKM [201]. The molecular mechanisms controlling these processes are not well understood. Our studies have shown that the translocation of cyclin C or Med13 to the cytoplasm contributes to stress-induced transcriptional reprogramming [22-24]. Intriguingly, cyclin C and Med13 have secondary roles in the cytoplasm, whereby, in response to cell death-inducing insults, cytoplasmic cyclin C is required for mitochondrial fission and mediates intrinsic cell death pathways [123, 201]. Med13 is released into the cytoplasm following cell survival cues, where it promotes the assembly of a subset of ribonucleoproteins into processing bodies (P-bodies) [202]. Thereafter, in yeast, Med13 is destroyed by a hybrid autophagy/lysosomal pathway called Snx4-assisted autophagy [149, 203].

Restricting the biosynthesis of the translation machinery, including ribosomes, is a universal phenomenon that enables cells to survive with limited intracellular resources, as ribosome biogenesis consumes over 60% of cellular energy and assets [204]. Most genes that encode for translational machinery proteins are actively transcribed, substantially devoting intracellular resources to ribosome synthesis alone [205]. Moreover, under normal growth conditions, cells generate ribosomal proteins (RPs) in wide excess to meet supply and demand for efficient production of new ribosomes, further spending cellular resources [206]. Therefore, when the cells encounter nutrient depletion, it is crucial for cell survival to reduce intracellular energy consumption by reprogramming ribosome biosynthesis [207]. In yeast, in addition to reprogramming the ~ 90 ribosomal genes, cells

must alter the transcription of ~ 200 non-ribosomal factors that are required for the assembly of the small and large ribosomal subunits [208, 209].

Control of genes encoding RPs is complicated [74]. In yeast, the conserved activator (Rap1) is required for Mediator recruitment and expression of most RP genes [48, 210-213]. In stress conditions, Gcn4 is rapidly translated and transported to the nucleus, where it simultaneously represses most RP genes and activates many stress response genes [214, 215]. This provides cells with a mechanism to quickly adapt to environmental cues.

The CKM responds to a variety of translation-limiting stresses, but the contribution the CKM plays in ribosome gene expression remains unknown. However, it has been shown that the direct phosphorylation of Gcn4 by Cdk8 triggers its degradation in physiological conditions, suggesting a link between the CKM and RP gene expression [216]. In this study, we show that under normal physiological conditions, the CKM promotes the expression of a subset of genes encoding translation machinery components, including ribosomes, in yeast. Additional work done by others in our lab further demonstrated a similar observation in mouse and human cells. Unlike the Mediator, the CKM is not found at the promoter of some of these genes, suggesting that the role of the CKM is indirect. This role of CKM-mediated control of RP gene expression is important as it promotes survival in translation stress. These studies, therefore, reveal an unanticipated role of the CKM in translation machinery gene expression and in promoting survival in stresses that block translation.

Results

The CKM Positively Regulates the Transcription of a Subset of Ribosomal Genes and Translation Initiation Factors

When nutrient supply decreases, ribosome biosynthesis must be repressed to avoid the consumption of intracellular resources. As CKM-regulated gene transcription is linked to environmental cues, I asked if it regulates genes encoding RPs in the budding yeast model system. Using RT-qPCR in wild-type (WT) and *med13*Δ cells, I monitored the expression of genes encoding for 40S (*RPS6A, RPS9A, RPS20,* and *RPS24A*) and 60S RPs (*RPL3* and *RPL25*) in normal physiological conditions. I observed that *RPL3,* but not the other RP genes we tested, decreases in *med13*Δ cells **(Figure 3.1A).** These results show that the CKM is required for maintaining constitutive gene expression of *RPL3*.

Next, we asked if the CKM positively regulates the expression of genes encoding for TIFs in physiological conditions. I analyzed the expression of DEAD-Box RNA helicase Ded1, the large scaffolding protein eIF4G1 (eukaryotic Translation Initiation Factor 4G1 encoded by *TIF4631*), its paralog eIF4G2 (encoded by *TIF4632*), eIF4E (encoded by *CDC33*), and eIF6 (encoded by *TIF6*). Proteins encoded by these genes, outlined in **Figure 3.1B**, mediate the recruitment of the ribosome to mRNA and serve as a rate-limiting step in cap-dependent translation initiation [67-71]. RT-qPCR analysis revealed decreased expression of these genes except eIF4E in *med13*Δ **(Figure 3.1C).** Similar results were also obtained for *TIF4631, DED1*, and *RPL3* expression in *cdk8*Δ cells **(Figure 3.1D).** This suggests a model in which the CKM positively regulates the transcription of a subset of TIFs in physiological conditions. This result was unanticipated as the yeast CKM has been known to predominantly negatively regulate genes in

physiological conditions, including a subset of stress response genes (SRGs) [45, 160, 196-198].

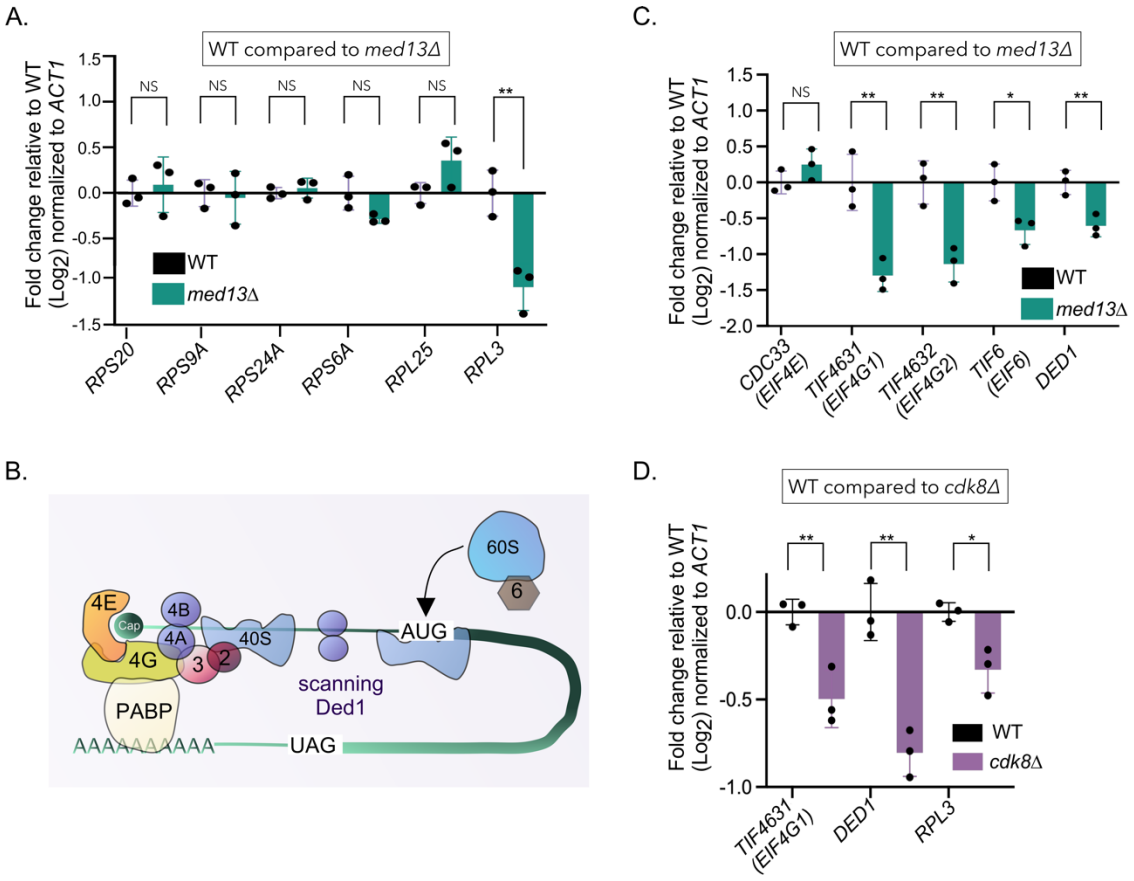

Figure 3.1. The CKM maintains constitutive expression of several translation-associated genes in *S. cerevisiae*. (A) RT-qPCR analysis of the 40S (*RSP20, RSP9A, RSP24A,* and *RSP6A*) and 60S (*RPL25* and *RPL3*) ribosomal protein-encoding genes in wild-type (WT, RSY10) and *med13*Δ (RSY2444) cells in unstressed conditions. ΔΔCt results for relative fold change (Log2) values using WT unstressed cells as a control. Transcript levels are given relative to the internal *ACT1* mRNA control. (B) Schematic of the translation initiation factors members, Ded1, and ribosomal subunits. 4E: eIF4E, 4G: eIF4G1, 2: eIF2, 3: eIF3, 4A: eIF4A, 4B: eIF4B, 6: eIG6. (C) As in A, except that translation initiation factors and *DED1* were examined. (D) As in A and C, except that *cdk8*Δ (RSY2176) was analyzed. For all RT-qPCR assays, the error bars indicate the SD from the mean of two technical replicates from three independent cultures (N=3). For all assays: *p $\leq$ 0.05, **p $\leq$ 0.01; NS: Non Significant.

The CKM Maintains Steady-State Levels of Specific Translation-Related Proteins

It is well known that protein levels can be modulated by various mechanisms, including alterations in the rate of synthesis or stability of mRNA, or the synthesis or stability of the protein itself [217]. To assess whether the decrease in gene expression observed in CKM mutants correlated with reduced protein levels, quantitative Western blot analyses was used. I prepared protein extracts from mid-log cells, and analyzed the levels of endogenous eIF4G1, Rpl3, and Ded1. I detected decreased amounts of eIF4G1, Rpl3, and Ded1 in both *med13*Δ and *cdk8*Δ relative to WT (**Figure 3.2A, quantified in 3.2B**). A similar decrease in eIF4G1 was also observed in $cdk8^{D290A}$, the kinase-dead Cdk8 mutant (**Figure 3.2C, quantified in 3.2D**), suggesting that Cdk8 kinase activity fine-tunes the expression of translation-related transcripts. Cycloheximide chase assays also revealed that deletion of the CKM subunits does not affect the protein stability of eIF4G1, with a half-life of ~6.2 h in WT and ~5.5 h in *med13*Δ (**Supplemental Figure A1A**, quantified in **Figure A1B**). Together, these findings illustrate that the reduction in mRNA levels **(Figure 3.1)** is associated with decreased levels of the corresponding proteins in CKM mutants. This further supports the conclusion that CKM plays a positive role in regulating the expression of a specific subset of genes involved in translation.

Loss of a CKM Subunit Results in Decreased rRNA Levels in Yeast

Several ribosome proteins have roles in the maturation of small and large subunit ribosomal rRNA (rRNA) and pre-rRNA processing. Ribosomal RNA is a major structural component of ribosomes required for protein synthesis. Thus, we next asked whether altered ribosome protein expression in CKM mutants is associated with changes in 18S rRNA (component of the yeast 40S ribosome subunit) and 25S rRNA (component of the

yeast 60S ribosomal subunit) expression. Northern blot analyses of samples (with equal numbers of cells used as a loading control) suggest a decrease in overall 18S rRNA (**Figure 3.3A, quantified in 3.3B**) and 25S rRNA (**Figure 3.3A, quantified in 3.3C**) in exponentially growing CKM mutants relative to WT. This further supports a model that ribosome expression is altered in CKM mutants through changes in ribosome subunits as well as rRNA.

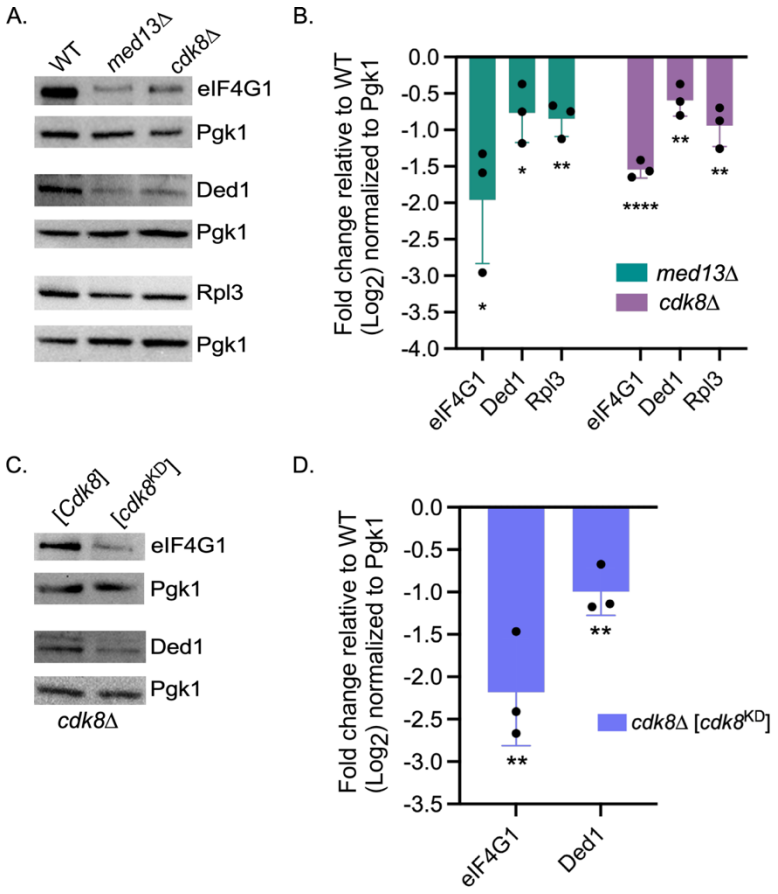

Figure 3.2. Protein levels of eIF4G1, Ded1, and Rpl3 in CKM mutants are decreased compared to WT in *S. cerevisiae*. (A) Western blot analysis of endogenous eIF4G1, Ded1, and Rpl3 in WT (RSY10), *med13*Δ (RSY2444), and *cdk8*Δ (RSY2176) cells. Pgk1 was used as a normalization control protein. Protein extracts were made from cells growing in physiological conditions until mid-log phase. (B) Quantification of protein levels obtained in A. The bars indicate fold change (Log2) protein expression relative to WT. Error bars

indicate S.D., N = 3 of biologically independent experiments. (C) As in A except that endogenous eIF4G1 and Ded1 were analyzed in extracts made from *cdk8*Δ (RSY2176) cells expressing wild-type Cdk8 or Cdk8 kinase-dead mutant from a plasmid, pUM511 or pUM516, respectively. (D) Quantification of protein levels detected in C using the same strategy as described in B. *p ≤ 0.05, **$p \leq 0.01$, ****$p \leq 0.001$.

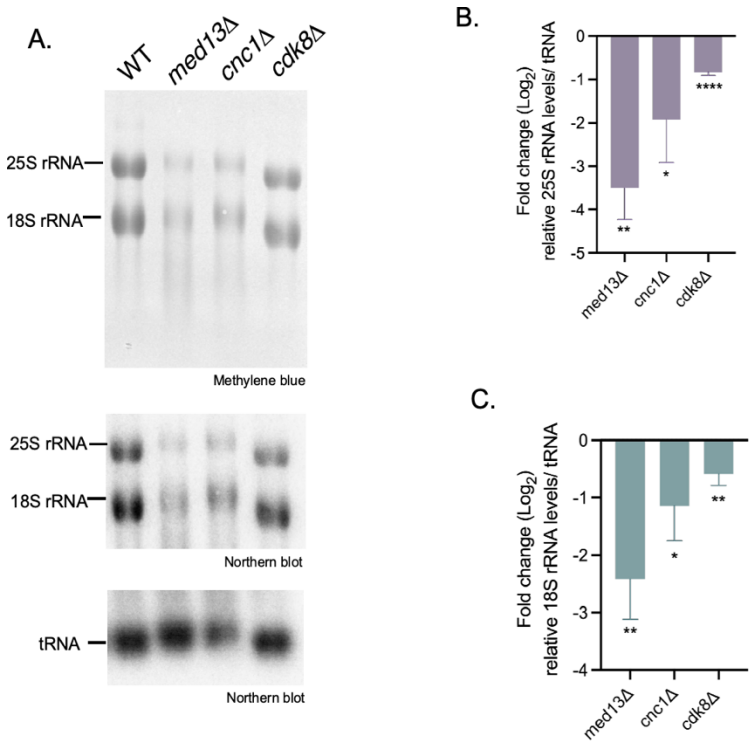

Figure 3.3. 25S and 18S ribosomal RNA (rRNA) decrease in CKM knockout mutants in *Saccharomyces cerevisiae*. (A) Northern blot analysis of 25S and 18S rRNA levels in in wild-type (RSY10), *med13*Δ (RSY2444), *cnc1*Δ (RSY391) and *cdk8*Δ (RSY2176) cells in unstressed conditions. All samples were loaded using an equal volume of cells. For all blots, tRNA levels were used as loading controls. (B) Quantification of 25S rRNA levels obtained in A. (C) Quantification of 18S rRNA levels obtained in A. Quantification in B-C indicate fold change (Log_2) rRNA expression relative to wild-type control. Error bars indicate S.D., N = 2 of biologically independent experiments. *p ≤ 0.05, **p ≤ 0.01, ***p ≤ 0.001, ****p ≤ 0.0001.

The CKM Does Not Directly Regulate RPL3 or EIF4G1 Expression

Having established that the CKM regulates the expression of a subset of translation-associated genes in yeast and mammals, we switched back to the yeast model system to address whether this control is direct or indirect. Using chromatin immunoprecipitation (ChIP) analysis, we examined whether the CKM was recruited to *TIF4631* and *RPL3* promoters. We used *ATG8* as a technical control, as the CKM strongly represses the expression of this conserved autophagy-related gene [46, 203]. As anticipated, endogenous cyclin C was found at the promoter of *ATG8*. In contrast, we did not observe cyclin C at *RPL3* or *EIF4G1* promoters in physiological conditions (**Figure 3.4A**). This suggests that the yeast CKM indirectly regulates *RPL3* or *EIF4G1* expression at the level of transcription. Using RT-qPCR, we determined that the CKM also does not regulate *RAP1*, a transcriptional activator of most RP genes [213] **(Supplemental Figure A2)**. Binding of the yeast CKM to the Mediator in physiological conditions prevents interaction of RNA Pol II at gene promoters [36] [37] [38] [39], suggesting the possibility that the CKM inhibits the transcription of a repressor of a subset of RP and TIF genes (**Figure 3.4B, top panel**). As cyclin C/Cdk8 kinase is active under normal physiological conditions, an additional explanation for these results is that this kinase is required to phosphorylate one or more factors to control a subset of RP and TIF genes (**Figure 3.4B, bottom panel**). Phosphorylation by Cdk8 likely inactivates a repressor or activates an activator of these genes, though these possibilities are not mutually exclusive.

To determine which TFs Cdk8 potentially interacts with to positively regulate these genes, we used YEASTRACT (**Y**east **S**earch for **T**ranscriptional **R**egulators **A**nd **C**onsensus **T**racking) which demonstrates regulatory associations between target

genes and transcription factors in *Saccharomyces cerevisiae.* Using this curated repository, regulatory associations of yeast transcription factors were extracted for the genes we analyzed in **Figure 3.1** (listed in **Supplemental Table A3A**). This analysis revealed 14 transcription factors which can potentially bind to the regulatory regions of genes regulated by the CKM, including the genes *DED1*, *RPL3*, *TIF6*, *TIF4631* (*EIF4G1)*, and *TIF4632* (*EIF4G2).* A list of all the transcription factors and their enrichment scores are shown in **Figure A3B**. Among these TFs include Tup1, which was previously found to repress several RP genes in stress [218] and interacts with Cdk8 in physiological conditions [219] [220]. These results suggest the possibility that the CKM phosphorylation is important for the binding of one or more of these TFs to a subset of RP and TIF genes. Nevertheless, given that the CKM disassembles following stress [46, 201, 203], the hypothetical functionality of CKM could offer a cell the capability to effectively reduce ribosomal protein expression as needed in the aftermath of stress.

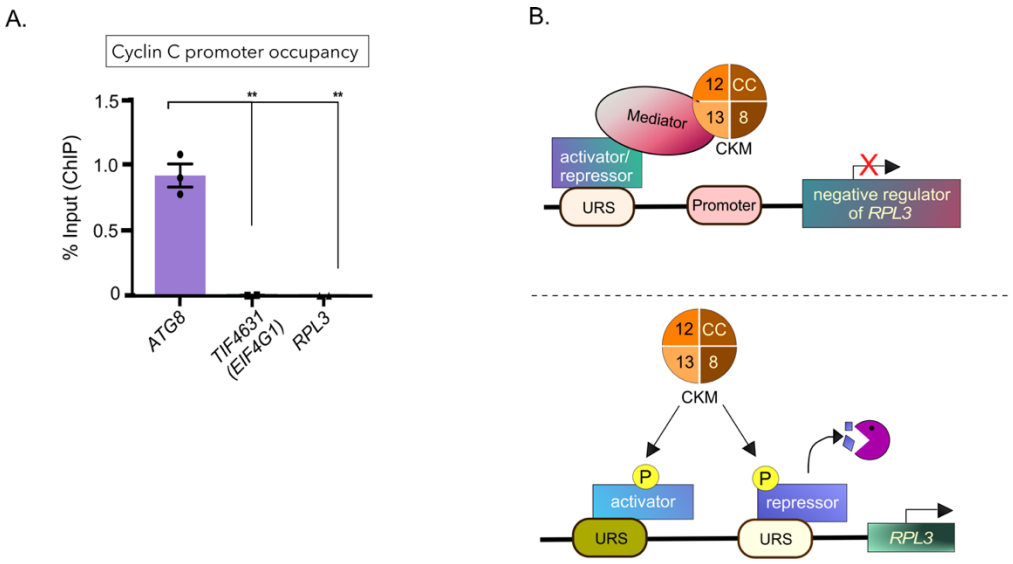

Figure 3.4. The CKM does not directly control RP and TIF gene expression. (A) ChIP analysis performed in yeast for endogenous cyclin C-TAP fusion (RSY1775) promoter occupancy of *ATG8, TIF4631,* and *RPL3* genes. Error bars indicate S.D., N = 3 of biologically independent experiments. $^{**}p \leq 0.01$. (B) Schematic outlying a model in which the CKM indirectly upregulates a subset of RP-encoding gene expression in physiological conditions. See text for details. 8: Cdk8; CC: cyclin C; 12: Med12; 13: Med13. URS: Upstream regulatory sequence.

Loss of Med13 Does Not Significantly Hinder Polysomes or Translation Rate in Physiological Conditions

Defects in the expression of translation machinery can reduce the efficiency of translation, and this reduction in translation can cause slower or inhibited cell growth in physiological conditions [221, 222]. My in vivo 35S-Radiolabeled methionine incorporation analyses suggested there is no difference in the rates of translation in exponentially dividing *med13*Δ yeast mutants relative to WT (**Figure 3.5A**). Thus, CKM mutants do not have a defect in general translation or cell growth in physiological conditions, despite our findings that several translation-related proteins decrease in CKM mutants.

To test whether populations of ribosome complexes are altered in a CKM mutant, I carried out sucrose density centrifugation with the help of Dr. Natalia Shcherbik. Monosomes are individual 80S ribosomal subunits with low overall translational efficiency, while polysomes are an assembly of multiple ribosomes at the mRNA which promotes efficient translation of mRNA. Each of these groups of ribosomes separate due to differences in densities and can be visualized by peaks following centrifugation. To confirm the presence of ribosomal subunits in the correct fraction, we carried out western analysis of all fractions using an antibody for Rpl3, a subunit within the 60S ribosome. We found that the ribosome peaks from exponentially growing *med13*Δ cells are not

significantly altered relative to WT (**Figure 3.5B).** The presence of several polysome peaks in a Med13 knockout (**Figure 3.5B**) is indicative of sufficient translation, consistent with our observation of a normal translation rate. However, we observed small extra peaks in 80S and the first polysome peak. These small peaks, known as half-mers, are commonly associated with the presence of mRNA bound to free 40S ribosome subunits due to a deficit in 60S ribosomes [223]. Depletion of Rpl3 results in impairments in 60S ribosomal subunit assembly and the appearance of half-mer polysomes [224]. The small half-mers in Figure 3.5B thus support our observation that expression of the 60S RP Rpl3 slightly decreases in Med13 mutants, though more studies would be required to understand the complete effects of Med13 on overall ribosome assembly. Consistent with this, northern blot analyses carried out by Dr. Natalia Shcherbik revealed that mature 25S rRNA, an important component in 60S ribosome biogenesis, decreases in *med13*Δ mutants (not shown here; included in: Friedson et al., *manuscript under revision,* 2024).

Nevertheless, these data demonstrate that the decreased expression of a sub-set of translational proteins in a CKM mutant does not significantly hinder polysome assembly or general translation efficiency in physiological conditions. These data further imply the existence of a mechanism that compensates for the reduced expression of selective translation-related genes, such as *RPL3*, in CKM-defective cells. This model is consistent with one proposed by Mittal *et al*. [215], who observed that yeast cells could compensate for the lack of individual RP genes.

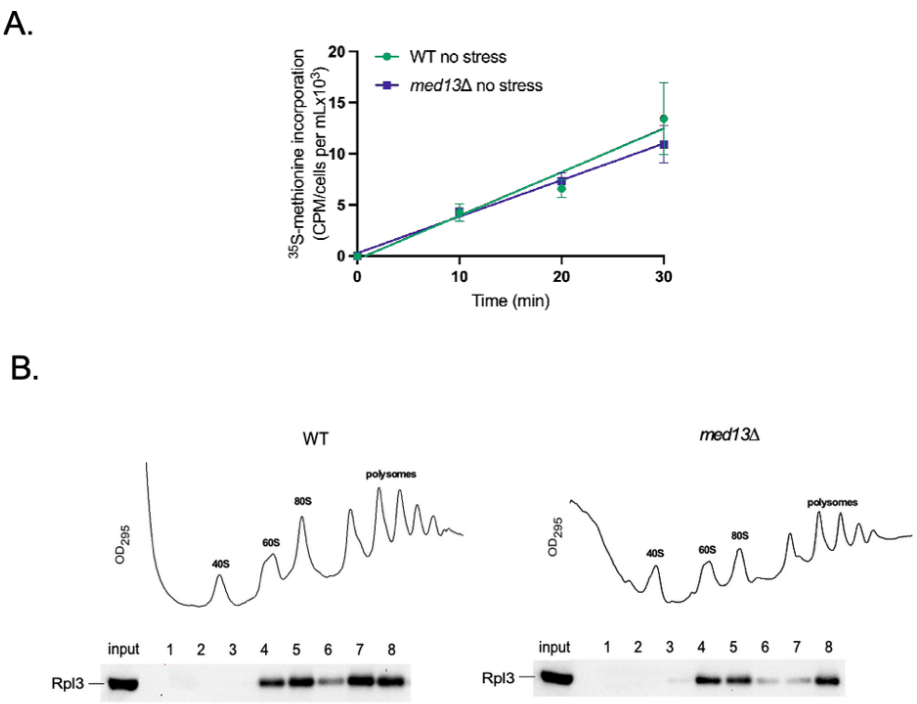

Figure 3.5. Med13 is not required for translation under normal physiological conditions. (A) [^{35}S]-radiolabeled methionine incorporation in WT (RSY10) and *med13*Δ (RSY2444) cells grown under physiological conditions. Error bars indicate S.D., N = 3 of biologically independent experiments; NS: Non-Significant. (B) Sucrose density centrifugation to observe the presence of 40S, 60S, and 80S ribosomes, as well as polysomes in WT (RSY10) and *med13*Δ (RSY2444) cells. To detect the presence of 60S ribosomal protein Rpl3 in each subfraction as a control, endogenous Rpl3 was observed using western blot analysis.

Loss of a CKM Subunit Causes Nuclear Accumulation of a 60S Ribosomal Protein

RPL3 and *EIF6* levels decrease in a CKM mutant, while another 60S ribosome component *RPL25* was not altered at the level of mRNA. Previous studies have shown that depletion of Rpl3 or eIF6 causes a deficit in 60S ribosomal subunits and the appearance of half-mer polysomes, likely due to defects in pre-RNA processing [225] [226] [224]. Furthermore, depletion of Rpl3 and eIF6 impairs the nuclear export of Rpl25 of pre-60S

ribosomal particles, which has been observed using fluorescence microscopy [224] [227]. This led us to ask whether Rpl25 nuclear accumulation was also affected in an unstressed CKM mutant. Rpl25 is a protein of the cytoplasmic 60S ribosomal subunit and component of pre-ribosomal processing. Though we observed no significant changes of RPL25 mRNA expression in a *med13*Δ mutant (refer to Figure 1A), abnormal nuclear accumulation of Rpl25-GFP can also be visualized in fluorescence microscopy. Rpl25-GFP is more present throughout the cytoplasm than in the nucleolus in WT cells as expected, but instead accumulates more within the nucleolus in *med13*Δ (**Supplemental Figure A3A**). There were no obvious defects in nucleolar morphology, suggesting that the nuclear accumulation of ribosomal protein in CKM mutants is not due to a defect of the nucleolus itself. Accumulation of Rpl25-GFP is visualized up to the nuclear pore in *med13*Δ and *cdk8*Δ (**Figure A3B)**, and nuclear localization of the ribosomes in a *med13*Δ mutant was further confirmed with intensity profiles (**Figure A3C)**. However, we did not observe nucleolar accumulation of 40S ribosomal protein Rps9a-GFP (**Figure A3D**). These data indicate that mutations of the CKM can cause nucleolar accumulation for some, but not all, ribosomal proteins. More studies would be required, however, to understand why nuclear accumulation of Rpl25 occurs in CKM mutants.

The CKM Promotes Survival Following Treatments with Translation Inhibitors

It is known that decreased expression of specific translation components such as eIF4G1 confers hypersensitivity to specific translation-inhibiting antibiotics [228, 229]. Therefore, we asked if the cells could compensate for CKM defects following stress caused by impaired translation. To test this, I used cell survival assays with sub-lethal

concentrations of five antibiotics that interfere with different stages of protein synthesis **(outlined in Table 1).**

Table 1

List of the Classes of Antibiotics and Drugs Used to Inhibit or Alter Protein Synthesis

Name	Class	Mechanism	Ref.
Hygromycin B (Hyg B) and Geneticin (G418)	Aminoglycoside	Induces error-prone protein translation causing aberrant protein production through miscoding errors, induces premature translation termination, and stop codon readthrough. Inhibits subunits dissociation and formation of translation initiation complexes at high concentrations. Also known to affect ribosome translocation during translation elongation.	[230-234]
Cycloheximide	Glutarimide	Specifically interacts with the E site of the 60S ribosomal subunit, and reduces the translation rate by inhibiting the translocation step of the elongation.	[82, 235].
Bleomycin	Glycopeptide	Cleaves tRNA.	[82, 236]
Anisomycin	Pyrrolidine	Interacts with the A site of the 60S ribosomal subunit and inhibits peptidyl transferase activity during elongation.	[82, 236]
Paromomycin	Aminoglycoside	Interacts with the A-site of 60S subunit. Inhibits dissociation of ribosomes after termination. Affinity for cytoplasmic ribosomes and mitoribosomes. Interferes with mitochondrial activity and reduces mitochondrial membrane potential.	[237, 238]
Chloramphenicol	Phenicol	Inhibits mitochondrial protein synthesis in eukaryotic cells.	[239]

Cells were grown to mid-log and then assayed for survival after plating serial dilutions onto media containing the different classes of antibiotics. Consistent with previous reports [45-47], no differences in the growth of WT and CKM mutants were observed on solid YPD medium **(Figure 3.6A, left)**. However, all the CKM mutants exhibited significantly reduced growth when on media containing the aminoglycosides Hygromycin B (Hyg. B) or 25 μg/ml Geneticin (G418). A similar but less dramatic effect was observed in the presence of translation-elongation inhibitors (Cycloheximide, and Anisomycin), and the tRNA-depleting drug Bleomycin Anisomycin (**Figure 3.6A** and see **Figure 3.6B** for a schematic of their mechanism of action). These findings uncover a new role for CKM in cell adaptation to the stress conditions caused by inhibition of various stages of protein translation (i.e., translational stress). Consistent with the described survival analyses, null CKM mutants also grew significantly slower than WT in liquid medium containing Hyg B (**Figure 3.6C**). In addition, they were less able to recover from Hyg B stress (induced by treating the cells for 4 h in 2mg/ml Hyg B, a concentration sufficient to arrest cell growth) (**Figure 3.6D).** Similar results were obtained using the Cdk8 kinase-dead allele **(Supplemental Figure A4)**, demonstrating that the Cdk8 kinase activity is important for survival following translation stress. Together, these results support a model in which the CKM serves a transcriptional role in promoting the survival response to drug-induced translation stress.

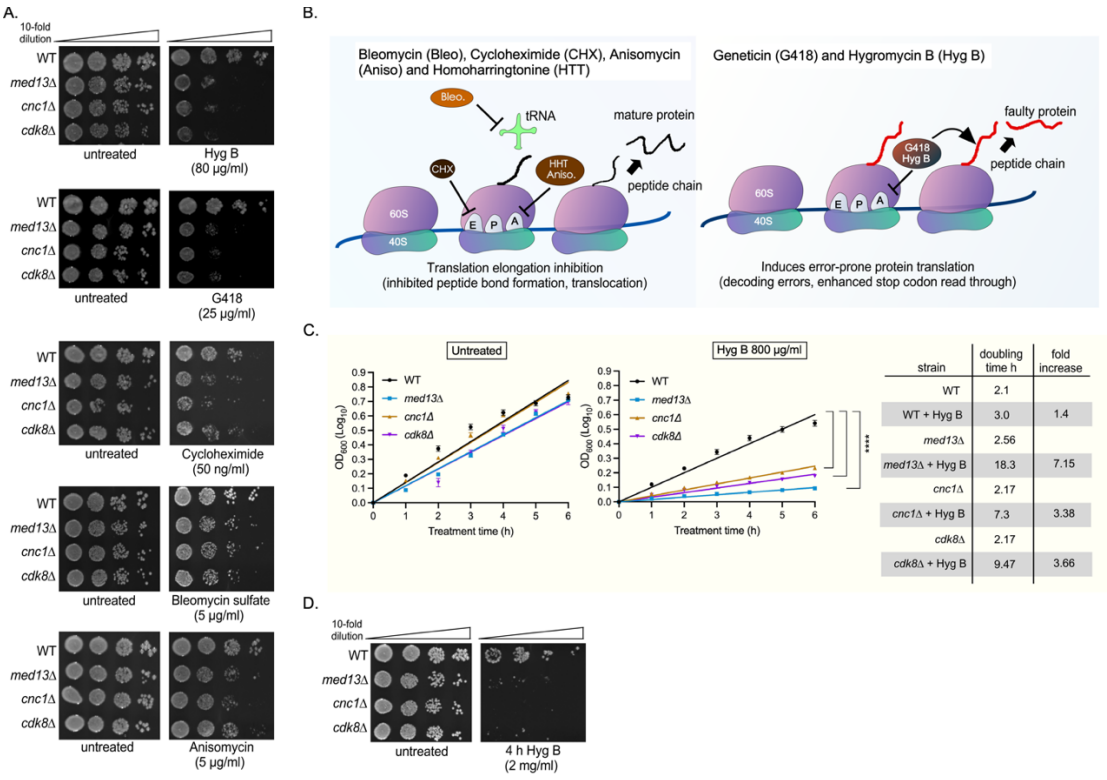

Figure 3.6. CKM mutants are sensitive to various translational inhibitors in *S. cerevisiae*. (A) WT (RSY10), *med13*Δ (RSY2444), *cnc1*Δ (RSY391) and *cdk8*Δ (RSY2176) cells were grown to mid-log phase in Synthetic complete Dextrose medium (SD-complete), adjusted to the same cell density, and 10-fold dilutions were plated on the plain YPD agar medium and YPD medium supplemented with the drugs indicated on the Figure. Drugs concentrations are shown. Hyg B - hygromycin B, G418 - Geneticin. (B) Schematic representation illustrating the effects of the drugs utilized in A on the distinct phases of protein synthesis. (C) Left-hand and middle panels: the liquid culture cell growth assays of the strains indicated in A. Cultures were grown in SD-complete medium and supplemented or not with 800 μg/ml Hyg B for 6 hours at a temperature of 30°C. Error bars indicate S.D., N = 3 of biologically independent experiments. Right-hand panel: Summary of the doubling times of the strains shown with and without treatment with 800 μg/ml Hyg B. (D) As in A, except the strains were treated for 4 h with 2 mg/ml Hyg B before 10-fold dilutions were plated onto YPD medium. ****$p \leq 0.001$.

CKM Subunits Remain Predominantly Nuclear Following Exposure to Hygromycin B

Our previous studies have established that the CKM disassembles following cell death and survival cues [7, 45, 46, 54, 122, 201, 203, 240, 241], whereby either cyclin C

or Med13 translocate to the cytoplasm before their degradation, following cell death or survival, respectively [54, 203]. Next, we asked if the CKM remains intact following 2 mg/ml Hyg B treatment. I found that the cyclin C decay was similar to its natural turnover [45] (2.5 h and 3 h, respectively; **Figure 3.7A**, quantified in **Figure 3.7B**). Considering that the half-life of cyclin C following heat shock was 2.5 mins, oxidative stress was 30 mins, and nitrogen starvation was 45 min [45, 46, 240], detection of an unaltered cyclin C half-life following Hyg B treatment strongly argued that this protein is not actively degraded upon Hyg B treatment. Furthermore, I did not observe cyclin C-mCherry fusion cytoplasmic foci following Hyg B treatment, suggesting that cyclin C does not exit the nucleus in this stress (**Figure 3.7C**). Similar results were obtained with Med13 **(Figures 3.7D, 3.7E, and 3.7F)**, although I did observe a slight decrease in Med13 half-life in response to Hyg B (half-life of 4 h compared to 6 h observed in cycloheximide-treated cultures) [241]. However, it is important to mention that following a different type of stress, i.e., nitrogen starvation, the half-life of Med13 was significantly shortened down to 2.6 h [203]. We previously found that Med13 Is degraded within the vacuole in nutrient stress [56], so I observed Med13-mNeongreen localization in Hyg B treatment using mutants of the vacuolar proteases Pep4/Prb1. Mutating these proteases inhibits vacuolar degradation and can thus be useful for visualizing proteins within the vacuole. Similarly to cyclin C-mCherry, no Med13- mNeongreen cytoplasmic foci were detected **(Figure 3.7F)**. Taken together, these data demonstrate that the CKM stays intact following Hyg B treatment.

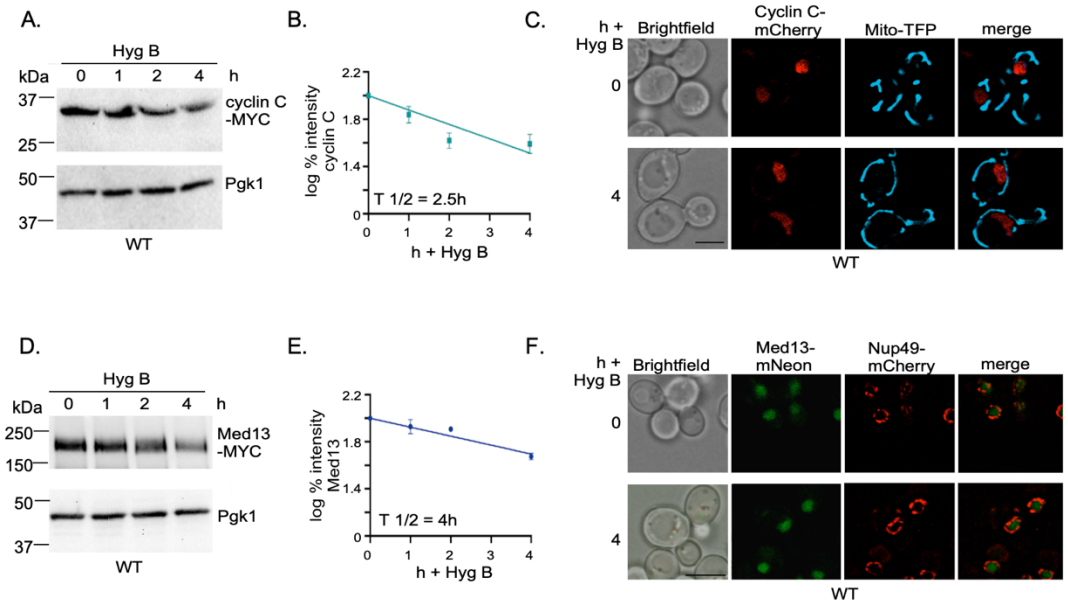

Figure 3.7. The CKM remains in the nucleus following exposure to Hygromycin B. (A) Western blot analysis of extracts prepared from mid-log WT (RSY10) cultures expressing cyclin C-MYC (pKC337) treated with 2 mg/ml Hygromycin B in SD-complete medium for the indicated times. Pgk1 was used a normalization control protein. (B) Quantification of the results obtained in A to demonstrate degradation kinetics. The linear regression line indicates Log% (Log10) protein expression at 1 h, 2h, and 4 h of 2 mg/ml Hyg B treatment relative to 0 h. Error bars indicate S.D., N = 3 of biologically independent experiments. (C) Fluorescence microscopy of cyclin C-mCherry localization in WT (RSY10) cells expressing the mitochondria marker Mito-TFP. Cells were visualized before (0 h) and after 4 h of 2 mg/ml Hyg B treatment. Representative single-plane images are shown. Scale: 5 µm. (D and E). As in A, except that Med13-MYC was examined. (F) Fluorescence microscopy of Med13-mNeongreen localization in *pep4*Δ *prb1-*Δ*1.6R* (RSY2305) cells expressing the nuclear marker Nup49-mCherry. Cells were visualized before (0 h) and after 4 h of 2 mg/ml Hyg B treatment. Representative single-plane images are shown. Scale: 5 µm.

Dissecting the CKM's Role in Resistance to Translation Inhibition Stress: Does the CKM Control Proteasome Activity?

Efficient proteasome activity is necessary for maintaining protein homeostasis in physiological conditions and eliciting the correct response to stress. As Hygromycin B treatment can lead to an accumulation of aggregates, proteasome activity is necessary to

prevent or remove these aggregates. These suggest the possibility that the role of the CKM in promoting survival following Hygromycin B treatment may also be attributed to a potential function in regulating proteasomes. However, much remains unclear as to how the assembly and specific activities of proteasomes are regulated both before and after stress.

I accumulated some findings from the beginning of my time in the lab which suggest that cyclin C may play a role in proteasome activity in yeast, which can be an additional role of the CKM in a cell's response to stress. With thanks to Dr. Kiran Madura and Dr. Weiser for their contributions of resources and ideas, I utilized a proteasome activity assay which allows us to detect the activity of proteasomes in vitro. The protocol for proteasome activity measurement and antibodies against proteasome subunits were kindly provided by Dr. Kiran Madura.

Rpn4 is a transcription factor involved in the normal transcriptional upregulation of proteasome subunit protein levels, with similarities to the role of Nrf1 in mammals. Moreover, a reduction of Rpn4 levels sensitizes the cell to a variety of stresses [242]. Utilizing SUC-LLVY-AMC as a substrate to determine chymotrypsin-like activity of the proteasome, I found that chymotrypsin-like proteasome activity in yeast is not significantly lower in both *cnc1Δ* cells relative to WT. However, a mutant lacking Rpn4 demonstrates lower proteasome activity as expected, and a double mutant lacking both cyclin C and Rpn4 reveal an even more significant decrease in proteasome activity (**Supplemental Figure A5A,** quantified in **Figure A5B**). The growth of a *cnc1Δrpn4Δ* mutant is much slower than an Rpn4 mutant as well (not shown in this report). These data suggest that cyclin C-Cdk8 and Rpn4 may have synergistic roles for upregulating proteasome activity,

though the exact role of cyclin C with proteasomes remains unknown. Moreover, decreased proteasome activity is associated with inefficient removal of misfolded proteins, suggesting another possibility that the CKM aids in preventing or removing misfolded proteins. As aminoglycosides antibiotics induce protein misfolding [243], this suggests an additional explanation for the decreased survival observed in CKM mutants in the presence of aminoglycoside antibiotics.

Western analysis of *cdk8Δ* and *cnc1Δ* cells that there is no significant change in the protein expression of proteasome subunits due to the CKM (**Figure A5C**). However, observation of the Rpn12 subunit revealed an additional band present in *cdk8Δ* and *cnc1Δ* cells, and the band is more prominent in double mutants lacking both Rpn4 and either Cdk8 or cyclin C. Rpn12 is a non-ATPase component of the 19S regulatory lid of the proteasome, where proteins are recognized and unfolded. This subunit is essential for proteasome integrity and for incorporation of the substrate receptor subunit Rpn10 into the proteasome [244]. Modifications of proteasome subunits which regulate proteasome activity include methylation, ubiquitination, acetylation, phosphorylation, and myristylation [245], though the effects of Rpn10 modification are not clear**.** Nevertheless, more experiments are required to determine the relationship between cyclin C-Cdk8 and proteasome integrity/activity in yeast.

Additional Observations: Cyclin C Promotes Cell Death in Stressors Which Inhibit Both Translation and Mitochondrial Activity/Permeability

Paromomycin sulfate is an aminoglycoside antibiotic with similarities to the aminoglycoside Hygromycin B by binding to rRNA, inhibiting translocation, and inducing misreading of mRNA [246]. Utilizing plating assays on solid YPD medium containing

Paromomycin, I observed that *med13*Δ and *cdk8*Δ are hypersensitized while *cnc1*Δ is resistant (**Figure 3.8A**). Similarly, *cnc1*Δ mutants continue to grow in a high concentration of this inhibitor in liquid medium, compared to WT cells which arrest cell growth following at least 10 h of treatment (**Figure 3.8B**). This suggests that cyclin C plays a specific role in promoting inhibited growth with this drug, distinct from the transcriptional role of the CKM in promoting resistance. Moreover, I observed that all CKM mutants are more resistant and recover better than WT following recovery from 24 h Paromomycin treatment (**Figure 3.8C**). This indicates that the transcriptional role of the CKM in slowing growth in the presence of this inhibitor may help to mediate a long-term survival response.

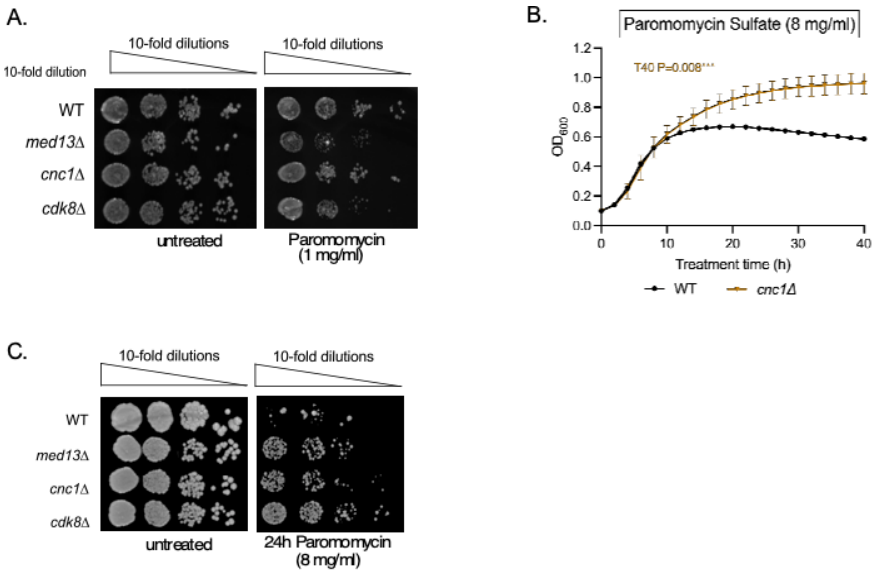

Figure 3.8. Cyclin C has a transcriptional and cytoplasmic response to Paromomycin. Paromomycin is an aminoglycoside antibiotic which interferes with both protein synthesis and the mitochondria. (A) Wild-type (RSY10), *med13*Δ (RSY2444), *cnc1*Δ (RSY391) and *cdk8*Δ (RSY2176) cells were grown to mid log in SD-complete medium and 10-fold dilutions plated on untreated YPD medium and YPD medium treated with 1 mg/ml Paromomycin (an aminoglycoside which causes mitochondrial membrane permeability). (B) Doubling times of wild-type (RSY10) and *cnc1*Δ (RSY391) cells in SD complete medium with and without 8 mg/ml Paromomycin. (C) Wild-type (RSY10), *med13*Δ (RSY2444), *cnc1*Δ (RSY391) and *cdk8*Δ (RSY2176) were treated with 8mg/ml Paromomycin and plated in 10-fold dilutions on YPD medium to observe recovery.

Paromomycin has been found to interfere with mitochondrial membrane potential in addition to its ribosome binding function [237]. We previously found that cyclin C plays a secondary cytoplasmic role in promoting mitochondrial fission following ROS stress [247], so I tested whether the resistance of cyclin C is due to a secondary role at the mitochondria. I found that mitochondria remained predominantly reticular in *cnc1*Δ relative to WT following 20h of Paromomycin treatment (**Figure 3.9A,** quantified in **Figure 3.9B**)**,** suggesting that cyclin C is important for mitochondrial fission following Paromomycin treatment. Fluorescence microscopy reveals that, following 20 h of 8 mg/ml Paromomycin treatment, the mitochondria undergo fission and cyclin C colocalizes near mito-TFP, a mitochondrial marker (**Figure 3.9C**, cytoplasmic cyclin C quantified in **Figure 3.9D**). We expected that mitochondria fission and the response of cyclin C would occur much later than 4 h of treatment because Paromomycin sulfate is known to have a slow rate of uptake in yeast [237]. Furthermore, following 20 h of treatment with both Paromomycin and 30 mM NAC (an inhibitor of ROS), no changes in cyclin C localization were observed (**Figure 3.9E**), suggesting that cyclin C re-localization from the nucleus to the mitochondria is due to increased ROS production. Taken together, these data suggest that the cyclin C elicits a dual cytoplasmic and transcriptional response to defects in translation when mitochondrial activity is simultaneously inhibited. Moreover, my observation that all CKM mutants demonstrate enhanced recovery/survival following 24 h Paromomycin treatment (refer to Figure 3.8C) is consistent with our previous observations of increased survival of CKM mutants following sublethal concentrations of oxidative stress [247]. As the CKM degrades to upregulate pro-survival stress response genes (SRG) following minimal oxidative stress, this suggests the possibility that the CKM disassembles

to also enhance SRG and survive following ROS-induced Paromomycin treatment. More studies are needed, however, to test this model.

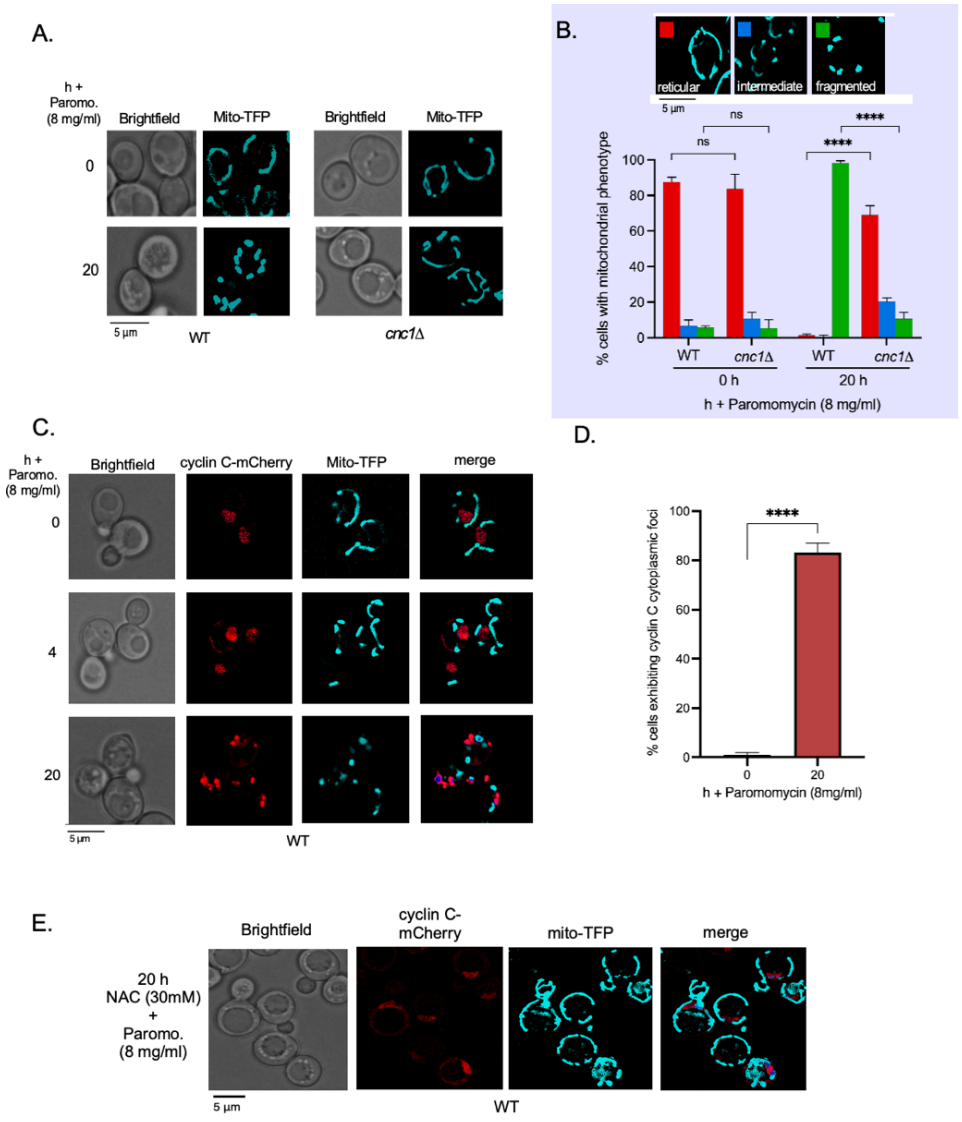

Figure 3.9. Cyclin C re-localizes to the mitochondria and promotes mitochondrial fission following Paromomycin treatment. Fluorescence microscopy of WT (RSY10) and *cnc1*Δ (RSY391) cells expressing the mitochondria marker Mito-TFP. Cells were visualized before (0 h) and after 20 h of 8 mg/ml Paromomycin treatment. Representative single-plane images are shown. Scale: 5 µm. (B) Quantification of A. Bar graph indicates % cells with reticular, intermediate, or fission mitochondrial phenotypes (see key of mitochondrial phenotype examples shown above) relative to WT. Error bars indicate S.D., N = 3 of

biologically independent experiments. (C) Fluorescence microscopy of cyclin C-mCherry (pSW205) localization in WT (RSY10) cells expressing the mitochondria marker Mito-TFP. Cells were visualized before (0 h) and after 4 h and 20 h of 8 mg/ml Paromomycin treatment. Representative single-plane images are shown. Scale: 5 μm. (D) As in C, except WT (RSY10) cells were pre-treated with both 8 mg/ml Paromomycin and 30 mM NAC and visualized at 20 h of treatment.

I next wanted to ask whether cyclin C responds to defective mitochondria induced by direct mitochondrial translation inhibition. So, I tested CKM growth in the presence of mitochondrial translation inhibitor Chloramphenicol and observed that *cnc1*Δ mutants are more resistant to this inhibitor while *med13*Δ and *cdk8*Δ are hypersensitized (**Figure 3.10)**. This further suggests that cyclin C can specifically inhibit growth when mitochondrial translation is inhibited, whereas the CKM simultaneously serves a transcriptional role in promoting survival in this stress.

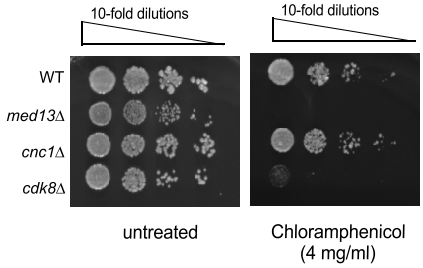

Figure 3.10. Cyclin C mutants are more resistant than Med13 or Cdk8 mutants following direct mitochondrial translation inhibition. A. Wild-type (RSY10), *med13*Δ (RSY2444), *cnc1*Δ (RSY391) and *cdk8*Δ (RSY2176) cells were grown to mid log in SD-complete medium and 10-fold dilutions plated on untreated YPD medium and YPD medium treated with 4 mg/ml Chloramphenicol.

Discussion

Transcription and translation are important for the synthesis of proteins necessary for cellular processes. However, much remains unknown as to how these processes are coordinated. In this study, we demonstrate a novel role of the CKM in maintaining constitutive expression of several translation-associated genes in unstressed conditions from yeast. In short, in physiological conditions, Cdk8 kinase activity of the CKM helps maintain constitutive expression of a subset of TIF and RP genes (**Figure 3.11**, left hand panel). However, we observe some differences in CKM's control of translation-related gene expression between yeast, mouse, and human cell lines, suggesting that the specificity of RP and TIF genes regulated by the CKM varies between species. Following stress which causes inhibited or altered protein synthesis, such as Hygromycin B treatment, the CKM remains assembled and promotes cell survival (**Figure 3.11**, middle panel**)**. The CKM plays a transcriptional role in this stress, likely due to its role in positively regulating RP and TIF genes. Following nutrition stress, RP and TIF gene expression is predominantly repressed and cyclin C and Med13 are destroyed [46, 202, 203]. These suggest a model that CKM disassembly following nutrition stress contributes to the repression of RP and TIF gene expression [215] (**Figure 3.11,** right-hand panel). Further experimentation is required, however, to understand the role of the CKM in RP expression following nutrition and direct ribosomal stress.

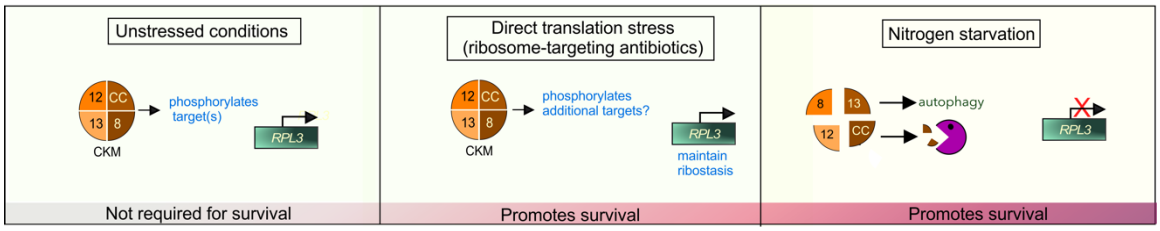

Figure 3.11. Model of outlining the role of the CKM in controlling RP-encoding gene expression. Left-hand panel: The CKM positively regulates a subset of RP and TIF genes in physiological conditions through either Mediator dependent or independent mechanisms. One possibility is that CKM interaction with the Mediator inhibits the transcription of a repressor of a subset of RP and TIF genes. Alternatively, Cdk8 of the CKM may also phosphorylate one or more additional transcription factors which can bind to the upstream regulatory sequence (URS) of *RPL3* and a subset of other RP and TIF genes. This allows the CKM to repress a repressor (such as by triggering its degradation) or activate an activator of these genes. This role of the CKM is not essential for survival. Middle panel: CKM activity promotes survival in translation stress, including errors in translation elongation (inhibited peptide bond formation and translocation) and mistranslation. This may result from RP and TIF genes being upregulated to maintain ribostasis. Cdk8 also may be required to phosphorylate other targets that regulate RP and TIF expression. Alternatively, the CKM may also serve functions distinct from RP and TIF gene expression to promote survival following translation stress (see discussion for details). Right-hand panel: following nutrition stress, the translation machinery is predominantly repressed and autophagy is induced to conserve energy for survival [15]. The CKM is disassembled, and Med13 and cyclin C are degraded by autophagy and the proteasome, respectively. This disassembly may permit the accumulation of a repressor which in turn represses RP genes [215]. Future studies would be required to test this model in nitrogen starvation. 8: Cdk8; CC: cyclin C; 12: Med12; 13: Med13.

Binding of the yeast CKM to the Mediator in physiological conditions prevents interaction of RNA Pol II at gene promoters [36] [37] [38] [39]. Cdk8 of the CKM also phosphorylates transcriptional activators to inhibit gene transcription [7], affecting Sip1 and Gal4 activity, Msn2 and Rim15 nuclear export, and promoting Gcn4 degradation in physiological conditions [40, 48-51]. These suggest that the CKM's mechanism in maintaining constitutive expression of specific RPs and TIFs like *RPL3, EIF4G1*, *EIF6,* and *DED1* can be either dependent or independent of the CKM's interaction with the

Mediator. We observed that the CKM positively regulates *RPL3* and *EIF4G1* but does not directly bind to their promoters, consistent with the established model that the yeast CKM directly represses specific genes at their promoters. This suggests the possibility that CKM interaction with the Mediator inhibits the transcription of a repressor of a subset of RP and TIF genes. We also found that several TFs, including stress-responsive TFs Tup1, Cst6, and Hsf1, can form regulatory associations with the subset of RP and TIF genes positively regulated by the CKM. Tup1 and Hsf1 repress RP genes during stress [218] [114], suggesting that Cdk8 phosphorylation may negatively regulate a repressor of RP and TIF genes. However, this does not exclude the possibility that the CKM may also upregulate an activator of these genes. Nevertheless, the interaction of these TFs with specific RP or TIF genes and the CKM requires further investigation.

Previous studies have shown that depletion of Rpl3 or TIF6 causes a deficit in 60S ribosomal subunits and the appearance of half-mer polysomes, likely due to defects in pre-RNA processing [225] [226] [224]. Furthermore, depletion of Rpl3 and TIF6 impairs the nuclear export of Rpl25 pre-60S ribosomal particles [224] [227]. These findings are consistent with the small half-mers and nuclear retention of Rpl25 we observe in CKM mutants. These data strongly suggest that the slight decreases in RPL3 and TIF6 expression in CKM-depleted cells causes a deficit in 60S ribosomal subunits. Consistent with this, in collaboration with Dr. Natalia Shcherbik's lab, we observed that mature 25S rRNA, an important component in 60S ribosome biogenesis, decreases in *med13*Δ mutants (not shown here; included in: Friedson et al., *manuscript under revision,* 2024). We propose that lack of CKM activity leads to downregulation of a subset of TIFs and RPs, thus initiating the rRNA/RP co-regulation feedback loop that eventually mediates suppression

of 25S rRNA maturation. Further experimentation is required to address these two alternative models.

As the CKM controls a subset of RP and TIF-encoding genes involved with translational processes, we were surprised to observe that the CKM does not affect general translation rates in physiological conditions. This suggests that cells can compensate for the slight reduction of a subset of RP and TIF proteins. This model is consistent with the results of others that discovered that the downregulation of RP genes can be compensated for by the cell [215]. In addition, translation can also still occur with slight decreases of eIF4G1 levels in yeast and mammalian cells, while complete depletion of eIF4G1 significantly inhibits translation [248, 249].

The CKM may regulate RP and TIF genes due to their secondary roles in stress responses. For instance, eIF4G1 forms stress granules to suppress translation during stress [250]. Mammalian RPL3 induces mitochondrial apoptotic pathways, inhibiting cell migration and invasion [251]. Cyclin C/Cdk8 control cell survival under oxidative and nutrient stress [7], suggesting CKM's potential role in modulating RP and TIF expression to manage stress responses. However, differences in cell death mechanisms between yeast and mammals imply these roles may be non-conserved. Further experiments would be needed to confirm this potential mechanism.

The sensitivity of CKM mutants to antibiotics which inhibit or alter protein synthesis is consistent with previous yeast competitive fitness screens which demonstrated decreased competitive growth of CKM knockout mutants compared with WT [252, 253], as well as our previous observations that the CKM promotes survival in prolonged nitrogen starvation [56] [46]. These suggest a role of the CKM in promoting growth or survival

when resources are limited. One possible explanation is that this is due to a decrease in several RP and TIFs. For instance, depletion of eIF4G1 causes enhanced sensitivity to Hyg B in yeast [254] [255].

Alternatively, factors distinct from RP and TIF expression could also serve a role in the CKM's response to ribosome-targeting antibiotics. For instance, previous findings have found that proteasome assembly defects and changes in ubiquitin have a role in Hyg B sensitivity [256, 257]. We recently observed in our lab that the CKM may also play a role in promoting proteasome activity in specific cell lines, suggesting the possibility that defects in proteasome activity or assembly may also contribute to the sensitivity of CKM mutants to translation inhibitors. Thus, more studies are required to determine how translation machinery and other potential processes regulated by the CKM, including SRG, could be contributing to how the CKM responds to translation inhibitors. Moreover, it has been reported that Cdk8 activity is required for glycolysis, possibly by phosphorylating a Rap1 cofactor [258]. These roles would most likely not be mutually exclusive, and further studies are needed to precisely define the contribution the CKM plays in surviving translation stress.

Moreover, further comparisons with other translation inhibitors in yeast suggest that response of the CKM to translation inhibition is specific to a translation inhibitor's mechanism of action. For instance, we observed that cyclin C promotes mitochondrial fission-induced cell death following treatment with a translation inhibitor Paromomycin, which is known to induce oxidative stress and mitochondrial membrane permeability [237]. Our lab previously found that cyclin C also promotes mitochondrial fission following hydrogen peroxide treatment, which directly induces oxidative stress [124].

Thus, since we observed that cyclin C remains nuclear after removing oxidants with NAC, the secondary response of cyclin C following Paromomycin treatment is likely due to enhanced oxidative stress. This demonstrates that, while cyclin C serves a transcriptional function to promote survival in direct translation inhibition stress, the secondary mitochondrial response of cyclin C can overcome its transcriptional role to induce cell death when oxidative stress is present or when mitochondria translation is directly inhibited with Chloramphenicol (**Figure 3.12**, bottom panel).

Lastly, the CKM's positive regulation of eIF4G1 expression is significant because eIF4G1 is crucial for cap-dependent translation [259] and is frequently overexpressed in cancers, promoting cancer progression and metastasis [260-262]. Thus, eIF4G1 and ribosomes are a favorable target for inducing cell death during cancer treatments [263]. Cyclin C, MED12, and CDK8/19 expression are linked to a wide range of cancers [124, 264], and may contribute to eIF4G1 amplification. Our studies suggest that targeting the CKM may be useful for sensitizing cells to treatment with clinically approved ribosomal inhibitors [263]. Conversely, eIF4G1 overexpression can alleviate α-synuclein-related toxicity linked to Parkinson's disease [265, 266]. Further research is needed to elucidate CKM's role in regulating eIF4G1 expression. Nevertheless, our work reveals a new link between CKM and translation-associated pathways, offering insights into potential cancer therapies.

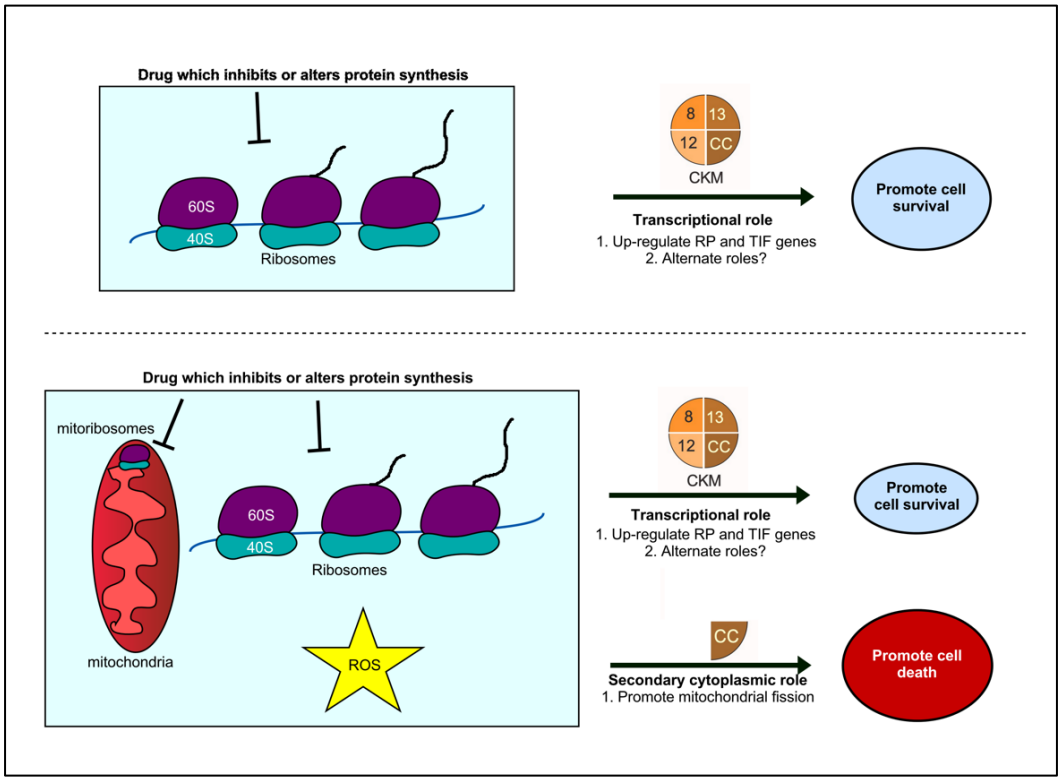

Figure 3.12. Model of the CKM's response to translation stress. (Top panel) Assembly of the CKM serves a transcriptional role in promoting survival following treatment with several ribosome-targeting antibiotics which inhibit or alter protein synthesis. However, the exact transcriptional role requires investigation. One possible explanation is that the CKM promotes the upregulation of RP and TIF genes, and/or the CKM serves alternative transcriptional roles for promoting survival. (Bottom panel) The CKM serves a dual transcriptional and cytoplasmic role following treatment with antibiotics which directly inhibit mitochondrial translation (Chloramphenicol) or antibiotics which both repress translation and induce ROS (Paromomycin). The secondary role of cyclin C with these drugs is sufficient to override its transcriptional role and promote cell death. For instance, cyclin C promotes mitochondrial fission following treatment with Paromomycin, which helps promote cell death.

Chapter 4

Dissecting Transcriptional and Cytoplasmic Roles of the CKM with Translation Machinery Following Nitrogen Starvation

Disclaimer: A large portion of this chapter is adapted from: Hanley S*, Willis SD*, Friedson B*, Cooper KF. Med13 is required for efficient P-body recruitment and autophagic degradation of Edc3 following nitrogen starvation. *Under revision with MBoC.*

*These authors contributed equally to the manuscript.

Author contributions: S Hanley devised the project, wrote the original manuscript, and carried out experiments/prepared figures; SD Willis carried out experiments/prepared figures and provided ideas/edits for the manuscript; B Friedson carried out experiments/prepared figures, provided ideas/edits for the manuscript, and performed rebuttal experiments; KF Cooper supervised, carried out experiments/prepared figures, provided ideas and edits for the manuscript, and performed rebuttal experiments.

Abstract

The Cdk8 kinase module (CKM), a conserved, detachable unit of the Mediator complex, plays a vital role in regulating transcription and communicating stress signals from the nucleus to other organelles. Here, we describe a new transcription-independent role for Med13, a CKM scaffold protein, following nitrogen starvation. In *S. cerevisiae*, nitrogen starvation triggers Med13 to translocate to the cytoplasm. This stress also induces the assembly of processing bodies (P-bodies) to attenuate translation. Here, we report that cytosolic Med13 co-localizes with P-bodies, where it helps recruit Edc3, a highly conserved mRNA decapping activator and P-body assembly factor, into these conserved ribonucleoprotein granules. Moreover, Med13 orchestrates the autophagic degradation of

Edc3 through a selective autophagy pathway that utilizes Ksp1 as its autophagic receptor protein. In contrast, the autophagic degradation of Xrn1, another conserved P-body assemble factor, is Med13 independent. These results place Med13 as a new player in P-body assembly and regulation following nitrogen starvation. They support a model in which Med13 acts as a conduit between P-bodies and phagophores, two condensates that use liquid-liquid phase separation in their assembly. Here, we also describe a new transcriptional role of the CKM in controlling the expression of several translation-associated genes following nitrogen starvation. These new findings are important, as defective autophagy, translation machinery expression, and P-body function contribute to the pathobiology of age-linked degenerative neuropathies.

Introduction

When cells face environmental stress like nutrient deprivation, they must fine-tune protein synthesis machinery to ensure survival or programmed cell death. Following nitrogen starvation, which inhibits the nutrient sensing complex TORC1 (target of rapamycin kinase complex) [112], cells inhibit protein synthesis to conserve energy and halt growth for cellular survival [10, 11]. Despite overall translation repression, cells must fine-tune translational machinery to also synthesize stress-response proteins essential for survival, many of which are involved in autophagy—a process upregulated during adverse conditions like nitrogen starvation to recycle proteins and organelles in the vacuole [17, 22, 23]. However, the mechanisms which control protein synthesis machinery following nitrogen starvation remain unclear. This is important to understand because dysregulation

of protein homeostasis pathways is linked to various conditions including cancer, Alzheimer's, heart defects, and intellectual disability [1-3].

The fine-tuning of protein synthesis following nitrogen starvation involves transcriptional repression of translation-associated genes, aggregation of cytoplasmic mRNA-protein (mRNP) granules referred to as processing bodies (P-bodies), and degradation of translation machinery components [13, 14]. However, the ways in which these processes coordinate together are regulated remain understudied. P-bodies emerge through liquid-liquid phase separation (LLPS), resulting in the formation of distinct liquid droplets separate from the cytoplasm [267]. These liquid condensates can be formed to store or degrade non-translating mRNA-protein complexes [21]. In yeast, key constituents of P-bodies encompass mRNA decapping enzymes such as Dcp1/Dcp2, Edc3, Dhh1, the Pat–Lsm1–7 complex, and Xrn1 [21]. Edc3 plays a pivotal role as a scaffold for P-body formation, facilitated by its multivalent interactions [268]. The intricate molecular mechanisms governing P-body formation and dissolution remain elusive but are crucial as their dysregulation is implicated in various degenerative proteinopathies, such as ALS and Alzheimer's disease. This suggests that RNA-binding protein (RBP) aggregates may undergo pathological transitions with age, potentially driving age-associated neurodegenerative diseases [269]. Supporting this notion, heightened P-body presence correlates negatively with lifespan in aging yeast cells [270].

The Mediator complex's conserved Cdk8 kinase module (CKM) serves as a pivotal transcriptional repressor for numerous stress response genes, including those vital for autophagy [46, 56]. Comprising cyclin C, Cdk8, and the scaffold proteins Med13 and Med12, the CKM is integral to this regulatory function [7]. While primarily recognized for

its transcriptional repression in yeast [43, 160, 271], instances of positive modulation have also been documented [272, 273]. For instance, we recently discovered that the CKM has a conserved transcriptional role in maintaining constitutive expression of several translation-associated proteins, including ribosomal protein and translation initiation factors (Chapter 3). However, how the CKM controls transcription of translation-associated genes following stress remains to be explored.

Under stress conditions like starvation or oxidative damage, the CKM disassembles, with the fate of its components contingent upon the stressor [54, 56]. Nitrogen starvation prompts nuclear degradation of cyclin C while Med13 shifts to the cytoplasm, where it undergoes degradation via Snx4-assisted autophagy (SAA-Med13) [7]. In yeast, autophagy depends on expansion of phagophores to sequester cargo from the cytoplasm and eventual delivery to the vacuole for degradation [108]. Selective autophagy also utilizes receptor proteins, which tether specific cargo, including damaged organelles and specific proteins, to the core autophagy protein Atg8 at phagophores [120]. The selective autophagy of Med13 employs the receptor protein Ksp1 to transport Med13 to phagophores, facilitated by the trimeric 17C scaffold complex, commonly utilized in bulk (non-selective) pathways [149].

In this study, we unveil a novel role of the CKM in mediating repression of several translation-associated genes following nitrogen starvation in *S. cerevisiae*. Recently, our lab found that Med13 also localizes to P-bodies and helps recruit Edc3 to P-bodies following nitrogen starvation (Hanley et al., *manuscript under revision,* 2024). We further demonstrate a role of Med13 in promoting the autophagic degradation of Edc3. Likewise, we observe that Edc3 also mediates autophagic degradation of Med13, and this is

dependent on a direct interaction between these two proteins. These findings demonstrate new roles of Med13 in controlling P-body dynamics and mRNA expression in the cellular response to nitrogen starvation. Together, these underscore a dual nuclear and cytoplasmic function of the CKM in promoting survival following nutrient stress.

Results

Edc3 Facilitates the Autophagic Degradation of Med13 Following Nitrogen Starvation

Med13 re-localizes to the cytoplasm for autophagic degradation following nitrogen starvation and is required to promote survival in prolonged periods of starvation [56] (Hanley et al., *manuscript under revision,* 2024). Our lab also previously observed that Med13 associates with P-bodies following nitrogen starvation (Hanley et al., *manuscript under revision,* 2024), so we wanted to investigate whether Med13's autophagic degradation depended on P body formation.

Previous research demonstrated Edc3's necessity for P-body formation under glucose deprivation stress [274]. Dcp2 is an established P-body protein [275]. So, to assess if Edc3 played a similar role during nitrogen starvation, cells expressing Dcp2-GFP were examined for P-body formation in an *edc3*Δ mutant strain. Sara Hanley previously showed with fluorescence microscopy that Dcp2-GFP foci were depleted in *edc3*Δ mutants (Sara Hanley Thesis, 2023). To confirm this, I repeated this experiment in more replicates and quantified the number of cells with Dcp2-GFP foci. We observed that Dcp2-GFP foci are significantly reduced in *edc3*Δ compared to WT, confirming that Edc3 is essential for P-body formation in nitrogen-depleted cells (**Figure 4.1A, quantified in Figure 4.1B**).

Next, we investigated whether Med13's autophagic degradation depended on Edc3. Using fluorescence microscopy, I monitored Med13-mNeon in *edc3*Δ cells expressing the vacuole marker Vph1-mCherry. To visualize vacuolar Med13-mNeon, we utilized the vacuolar protease deficient *pep4*Δ mutant and observed Med13-mNeon appearance in vacuoles in live cells after 4 hours in SD-N, as previously described [56]. While Med13-mNeonGreen appeared nuclear in mid-log cells grown in SD in both strains, there was a decrease in vacuoles positive for Med13-mNeonGreen signal in *edc3*Δ *pep4*Δ cells compared to *pep4*Δ single mutants (**Figure 4.1C**). The percentage of cells with vacuolar Med13 is shown in **Figure 4.1D**. These findings strongly suggest that Edc3 promotes Med13's entry into the vacuole.

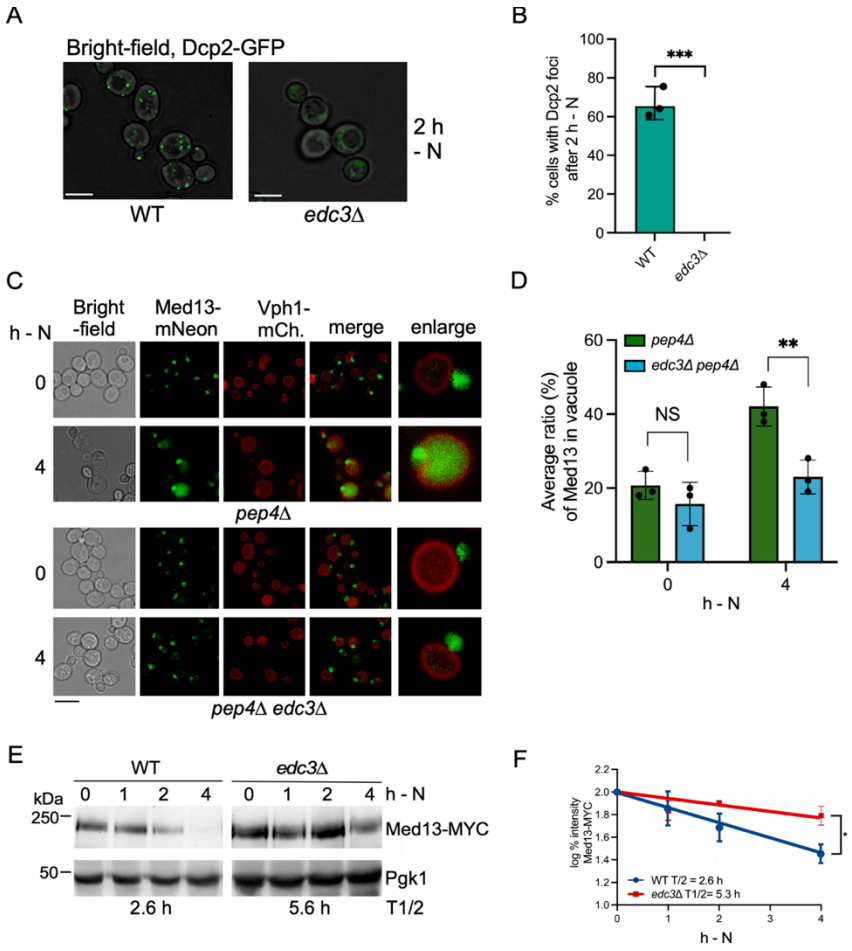

Figure 4.1. Edc3 is required for P body formation following SD-N and promotes the autophagic degradation of Med13. (A) Fluorescence microscopy of endogenous Dcp2-GFP following 2 h in SD-N in WT and *edc3*Δ mutants. (B) Quantification of A demonstrating % cells with Dcp2 foci after 2 h SD-N. (C) Fluorescence microscopy of endogenous Med13-mNeon in *pep4*Δ and *edc3*Δ*pep4*Δ strains before and following 4 h SD-N. Vph1-mCherry was used to mark the vacuoles. (D) Quantification of Ssn2/Med13-mNeongreen fluorescence within the vacuole was also obtained using the Hybrid cell count function within the analyzer software (at least 200 cells were counted per sample). For analysis, single extraction settings were used. Red (vacuole, Vph1-mCherry) was set as the extraction area and green (Ssn2/Med13-mNeongreen) was set as the target area. The percentage of cells with vacuolar Ssn2/Med13- mNeongreen was calculated using Area ratio (1st) (ratio of the total area of the target area to the extraction area) for at least 200 cells. Scale bar = 5 µm. NS – not significant, **P ≤ 0.005; N=3 of biological replicates. (E) Representative western blot image of endogenous Med13- 9MYC following SD-N in the strains shown. Due to its large IDR domain Med13, Med13-9MYC resolves just below 250 kDa on a 6% SDS-PAGE gel (Hanley et al., 2021). Pgk1 was used as a loading control, and the half-lives are indicated. Scale bar = 5 µm.

Our previous studies have determined that Med13 is actively degraded by autophagy in SD-N with its half-life decreasing from >6 h in unstressed cultures [241] to 2.6 h [56]. Using quantitative western blot analysis, Stephen Willis observed that Med13 was partially stabilized in *edc3*Δ compared to wild-type cells, with its half-life increasing from 2.6 to 3.5 h after nitrogen depletion (**Figure 4.1E, quantified in Figure 4.1F**). As EDC3 deletion reduces P body formation [276], these results suggest that autophagic degradation of Med13 requires efficient P-body assembly.

Med13 and Edc3 Can Interact

Given that Med13 co-localized with known P-body proteins, we investigated this result further. Edc3 is predominantly located in the cytoplasm, suggesting a model in which cytosolic Med13 interacts with Edc3 only after nutrition stress. Consistent with this, using co-immunoprecipitation analysis, Dr. Katrina Cooper in our lab observed increased FLAG-Edc3 binding to Med13-HA following 2 h in SD-N (**Figure 4.2A**). Next, colleagues in my lab used yeast two-hybrid (Y2H) analysis to ask which domain of Edc3 interacts with Med13. Edc3 protein structure is highly conserved throughout eukaryotes and is composed of three domains (**Figure 4.2B**, upper panel) : i) an N-terminal Lsm domain (Like-Sm) [277] that binds to Dcp1 and Dcp2 [276], ii) a central unstructured domain (Intrinsically Disordered Region, IDR) that contains an FDF motif that interacts with the RNA helicase and decapping activator Dhh1 [276], and iii) a C-terminal YjeF-N domain [278] which self-interacts and promotes Edc3 dimerization and P-body formation [276]. The results (**Figure 4.2B lower panel, and Figure 4.2C**) revealed an interaction between the central domain of Edc3 with the polyQ/N containing Med13 construct. Together these results show that the IDR domain of Edc3 interacts with the polyQ/N domain of Med13.

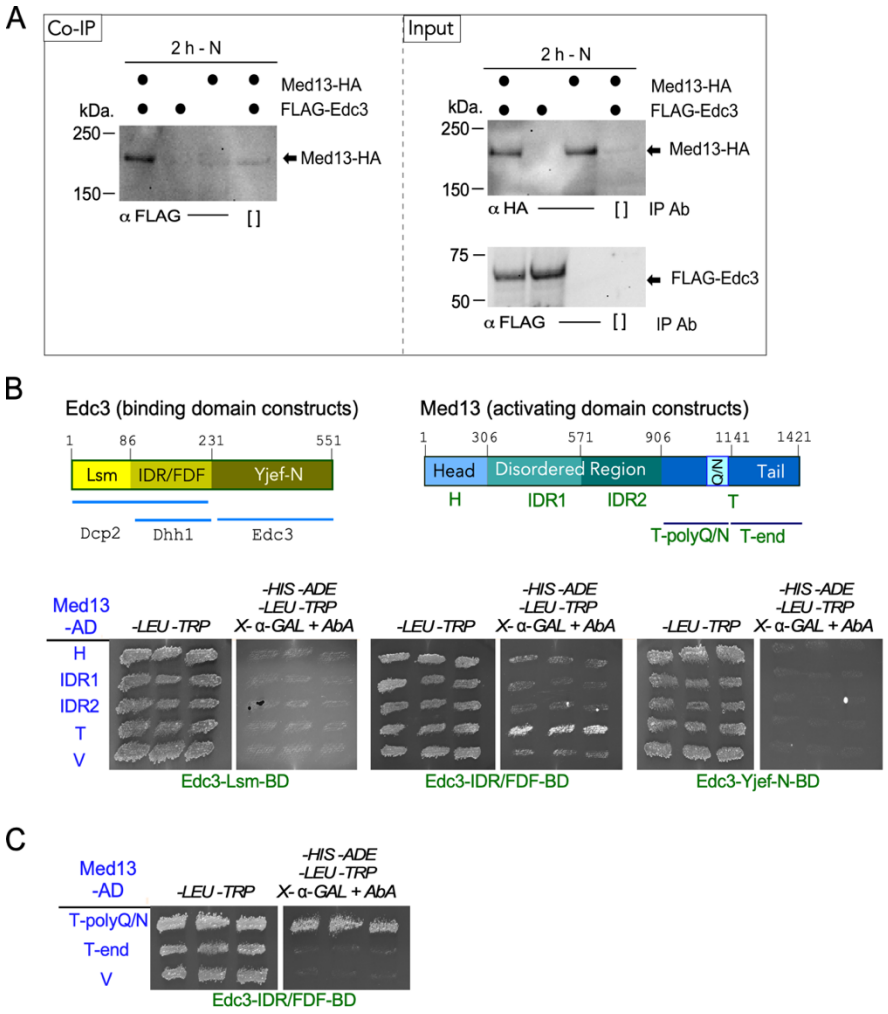

Figure 4.2. Med13 interacts with the IDR/FDF domain of Edc3. (A) Co immunoprecipitation analysis of Med13 and the Edc3 before and after nitrogen starvation. Cells harboring Med13-HA and FLAG-Edc3, or respective vector controls, were immunoprecipitated from whole cell lysates obtained from *pep4*Δ *prb1*-Δ.1 cells following 2 h in SD-N. For input controls, Med13 and Edc3 were immunoprecipitated from lysates using the indicated antibodies. [] - no antibody control; * - heavy chain. (B) Upper panels. Schematic of the Med13 and Edc3 Y2H constructs used. Known RNP interactors of Edc3 are indicated as described in (Decker et al., 2007) (B). Lower panels. Y2H analysis of Med13 and Edc3. Schematics of Med13 (Stieg et al., 2018) and Edc3 (Decker et al., 2007) structural domains used are shown in the top panels. In the bottom panel, Y2H Gold cells expressing the indicated Gal4-BD-Edc3 and the Gal4-AD-Med13 subclones were plated onto medium, selecting for plasmid maintenance (left panel, -LEU -TRP) or interaction by induction of all four reporter genes, ADE2, HIS3, MEL1, and AUR1-C, as described in the material and methods section. (C) As in B, except that the two Med13 tail clones (Hanley et al., 2021) were used.

The PolyQ/N Prion-Like Domain of Med13 is Required for Edc3 Recruitment to P-Bodies

Decker et al. (2007) demonstrated that *edc3*Δ cells exhibit impaired P-body assembly in the absence of the C-terminal Q/N-rich prion-like motif of Lsm4 [276]. Given that Med13 interacts with Edc3 through its polyQ/N domain (Sara Hanley Thesis, 2023), we investigated whether Med13 plays a role in recruiting Edc3 to P-bodies following nitrogen starvation. Given that the the polyQ/N domain of Med13 interacts with Edc3, we investigated the potential contribution of the polyQ/N domain of Med13 to P-body formation. The polyQ/N region was deleted from the chromosomal MED13 allele to generate med13-Q/NΔ (strain created by Stephen Willis). Dr. Katrina Cooper monitored Dcp2-GFP and Edc3-mCherry localization in SD-N and observed a reduction in Edc3-mcherry and Dcp2-GFP foci in both *med13*Δ and med13-Q/NΔ cells compared to wild-type (**Figure 4.3A and 4.3D, respectively**). I repeated these experiments to quantify the number of cells with Dcp2-GFP and Edc3-mCherry foci (**Figure 4.3B-C and 4.3E-F**). Together, these data demonstrate a requirement of the Q/N domain for Med13-mediated P-body formation. The underlying cause for this reduction in Dcp2 foci in the med13-Q/NΔ allele as opposed to the null variant remains presently unknown. Collectively, these findings suggest that the Q/N-rich domain of Med13 enhances Edc3 condensate formation in SD-N.

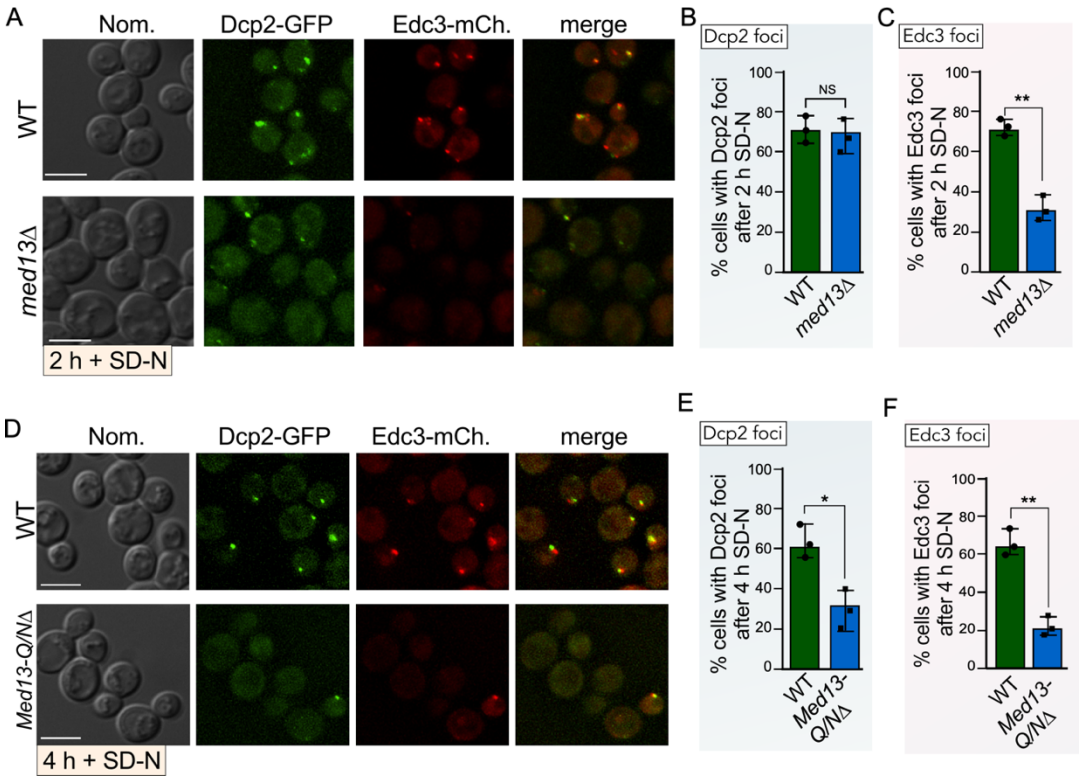

Figure 4.3. Med13 Q/N domain is required for the efficient recruitment of Edc3 to P bodies following SD-N. (A) Fluorescence microscopy of endogenous Dcp2-GFP in WT and *med13*Δ harboring Edc3-mCherry following 2 h in SD-N. (B-C) Quantification of % cells with Dcp2 and Edc3 foci relative to WT. (D) Fluorescence microscopy of endogenous Dcp2-GFP in WT and *Med13-Q/N*Δ harboring Edc3-mCherry following 4 h in SD-N. (E-F) Quantification of % cells with Dcp2 and Edc3 foci relative to WT. N = 3. NS= Not significant. Scale bar = 5 µm.

Med13-Dependent Degradation of Edc3 Occurs via Autophagy During Nitrogen Starvation

Previous research has shown that a subset of translation and mRNA metabolism factors undergo reduced abundance via autophagy in response to nitrogen starvation [13, 132]. We aimed to investigate whether Edc3 follows a similar regulatory pattern upon nitrogen starvation. Monitoring Edc3-MYC levels in an *atg8*Δ mutant and its isogenic control revealed a shortened half-life of ~3.0 hours for Edc3-MYC following nitrogen

starvation in the WT strain, while it remained substantially stabilized in the *atg8*Δ mutant (**Figure 4.4A, quantified in Figure 4.4B**). We then investigated whether Med13 is necessary for the autophagic degradation of Edc3. Stephen Willis then repeated this assay in *med13*Δ cells and found that Edc3-MYC was protected from degradation in the mutant (**Figure 4.4A, quantified in Figure 4.4B**). These findings suggest a model where Med13 facilitates efficient autophagic degradation of Edc3. I then conducted RT-PCR analysis and observed no changes in EDC3 mRNA levels in *med13*Δ cells compared to WT (**Figure 4.4C**). This contributes to the model that Med13 regulates Edc3 protein expression, but not its gene expression.

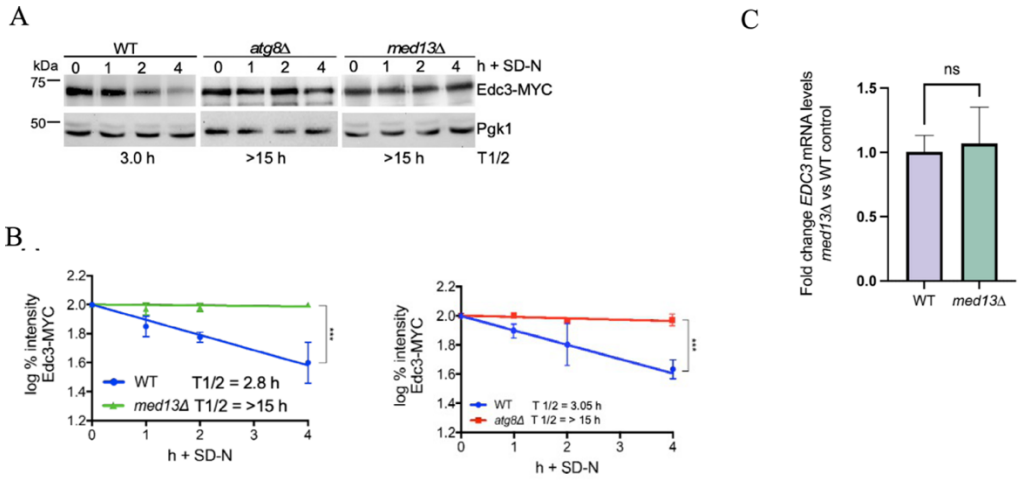

Figure 4.4. Med13-dependent degradation of Edc3 occurs via autophagy during nitrogen starvation. (A) Western blot analysis of endogenous Edc3-MYC in the strains shown. Pgk1 was used as a loading control. The half-lives, calculated from 3 independent experiments, are given. (B) Linear regression analysis and half-life of endogenous Edc3-MYC following nitrogen depletion in WT and *med13*Δ (left) or *atg8*Δ (right) strains N=3. ***P ≤ 0.001. (C) RT-qPCR assays probing for EDC3 mRNA expression in the WT and med13Δ in mid-log unstressed cells. Transcript levels are given relative to the internal ACT1 mRNA control. Three biological replicates and technical duplicates were analyzed. NS- not significant.

The Autophagic Degradation of Ribosomes and Translation Initiation Factor eIF4G1 Following Nitrogen Starvation is Med13 Independent

To determine if Med13 selectively degrades other proteins involved in translational control, I monitored the autophagic degradation of eIF4G1 [279]. eIF4G1 (also referred to as TIF4631) is an essential initiation factor required for mRNA translation via the 5' cap structure [280]. It is also turned over following TORC1 inhibition by rapamycin by autophagy [13, 132] (Refer to chapter 5 for a detailed analysis of eIF4G1 autophagy). Using quantitative western blot analysis, I also observed eIF4G1 degradation following TORC1 inhibition triggered this time by nitrogen starvation. As anticipated from previous studies, autophagy protein Atg8 is important for eIF4G1 degradation (**Figure 4.5A,** quantified in **Figure 4.5B**). Unlike Edc3, however, the autophagic degradation of eIF4G1 is independent of Med13 (**Figure 4.5C and quantified in 4.5B**). This indicates that both proteins are actively targeted for degradation following nitrogen starvation, but only Edc3 requires Med13 for its destruction.

Moreover, ribosomes are selectively degraded following nitrogen starvation [14]. However, I observed no differences following nitrogen starvation in the accumulation of free GFP from Rpl25-GFP and Rps2-GFP, conserved 60S and 40S ribosome subunits, respectively (**Figure 4.5D**). This indicates that Med13 is not required for ribophagy as the compact fold of GFP renders it resistant to vacuolar hydrolases [281].

The Autophagic Degradation of Xrn1 Following Nitrogen Starvation is Med13 Independent

To further determine if Med13 selectively degrades Edc3, we monitored the autophagic degradation of Xrn1, another conserved P-body assembly factor [279, 282].

Using quantitative western blot analysis, we observed Xrn1 degradation following TORC1 inhibition triggered by nitrogen starvation. The half-life was calculated to be 4.2 h compared to its turnover value of 11 h [283]. Deletion of *ATG8* significantly stabilized Xrn1 to more than 15 h (middle panel of **Figure 4.5E**, quantified in **4.5F**), indicating that autophagy is used to actively degrade Xrn1 following nitrogen starvation. However, the autophagic degradation of Xrn1 is independent of Med13 (right panel of **Figure 4.5E,** quantified in **4.5F**). This indicates that Edc3 and Xrn1 are actively targeted for degradation following nitrogen starvation, but only Edc3 requires Med13 for its destruction.

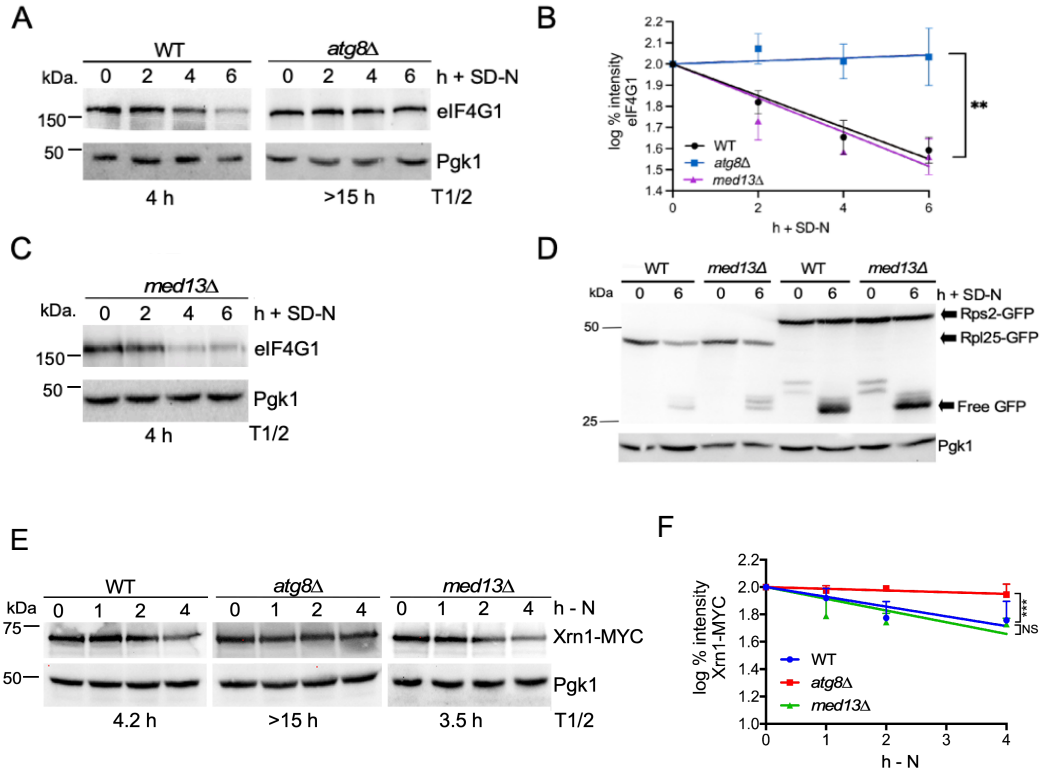

Figure 4.5. Autophagic degradation of eIF4G1, ribosomes, and Xrn1 are Med13 independent. (A) Western blot analysis of endogenous eIF4G1 in *atg8*Δ. The blots were probed with anti EIF4G1. (B) Linear regression analysis and half-life of eIF4G1 in the strains shown. N=3 biological replicates. **P ≤ 0.005. (C) Western blot analysis of endogenous eIF4G1 in *med13*Δ. For all blots, Pgk1 was used as a loading control. (D) Western blot analysis of GFP vacuolar cleavage of ribosomal proteins Rps2 and Rpl25 in

*med13*Δ for the indicated time points. (E-F) Western blot analysis of endogenous Xrn1-MYC following nitrogen starvation (- N) in the strains shown. Pgk1 was used as a loading control. The half-lives, calculated from 3 independent experiments, are given. ***P ≤ 0.001.

Med13 Acts as a Conduit for Edc3 Between P-Bodies and Developing Phagophores

The selective autophagic breakdown of Med13 necessitates Ksp1 as its receptor protein, which is subsequently recognized by the LC3-Docking Site (LDS) of Atg8 [149, 284]. According to this model, one would predict that the autophagic degradation of Edc3 relies on both Ksp1 and the LDS site in Atg8. To examine this hypothesis, protein levels of endogenous Edc3-9MYC were tracked in *atg8*Δ cells expressing either the wild-type or LDS mutant allele of ATG8 on a plasmid. The results phenocopied the *atg8*Δ degradation kinetics and demonstrated that Edc3 was stabilized in both *atg8*^{LDS} mutants (**Figure 4.6A, quantified in 4.6B**). Consistent with this model, the destruction of Edc3 also required Ksp1 (**Figures 4.6C, quantified in 4.6D**). These results suggest that Med13 and Edc3 utilize the same selective autophagic degradation pathway, whereas Xrn1 destruction is Med13 independent.

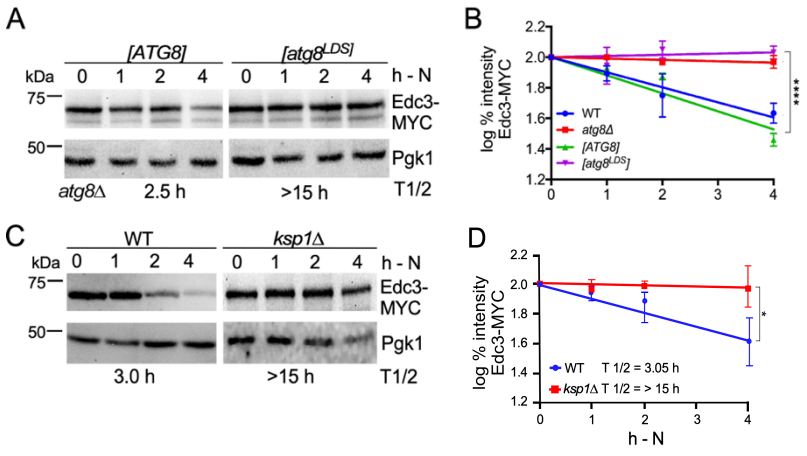

Figure 4.6. The LDS region of Atg8 and the receptor protein Ksp1 are required for the autophagic degradation of Edc3. (A) Western blot analysis of endogenous Edc3-MYC in the strains shown following nitrogen starvation (- N). Pgk1 was used as a loading control. The half-lives, calculated from 3 independent experiments, are given (B) Linear regression analysis of the decay kinetics of Edc3-MYC in the strains shown following nitrogen starvation. The kinetics of Edc3 degradation from Figure 6 in WT and *atg8*Δ cells was drawn on the graph to demonstrate that the *atg8*^{LDS} mutant phenocopies *atg8*Δ ****P ≤ 0.0001. (C) Western blot analysis of endogenous Edc3-MYC in the strains shown following nitrogen starvation (- N). The half-lives, calculated from 3 independent experiments, are given. Pgk1 was used as a loading control.

The CKM Plays a Transcriptional Role in Controlling Ribosomal Protein and Translation Initiation Factor mRNA Expression Following Nitrogen Starvation

Our lab recently found that assembly of the CKM at the mediator helps maintain constitutive expression of a subset of translation genes in physiological conditions, including 60S ribosomal protein (RP) *RPL3* and translation initiation factors (TIFs) such as *EIF4G1* (Chapter 3). On the other hand, we observed that other ribosomal protein genes, such as *RPS9A*, were unaltered in CKM mutants in physiological conditions.

Many translation-associated genes are repressed following nitrogen starvation to mediate inhibition of protein synthesis and quiescence entry [79]. Our lab observed that the CKM disassembles in nitrogen starvation and relieves repression of ATG stress responsive genes [46, 56]. So, to test whether the CKM also plays a role in controlling translation-associated genes in this stress, we carried out RT-qPCR analysis to measure mRNA expression levels of *EIF4G1* (yeast gene name TIF4631), *RPL3,* and *RPS9A* before after 1 h nitrogen starvation (SD-N). I observed in both *med13Δ* and *cdk8Δ* mutants in physiological conditions that *EIF4G1* **(Figure 4.7A)** and *RPL3* **(Figure 4.7B)** mRNA levels decrease relative to WT, while *RPS9A* mRNA levels remain the same, as previously observed (**Figure 4.7C**). Moreover, we observe a significant decrease in expression of all

these genes following 1 h SD-N in WT cells, as expected. In *med13Δ* and *cdk8Δ* cells, however, mRNA expression levels of *EIF4G1, RPL3, and RPS9A* do not decrease as efficiently as in WT cells following 1 h SD-N **(Figure 4.7A-C)**. These data suggest that assembly of the CKM before stress plays an additional transcriptional role in mediating the downregulation of RP and TIF genes following nitrogen starvation stress. Alternatively, the decreased mRNA levels in the CKM mutants could be due to inefficient degradation of these mRNA following stress. Thus, more studies are required to determine the mechanism of how this occurs.

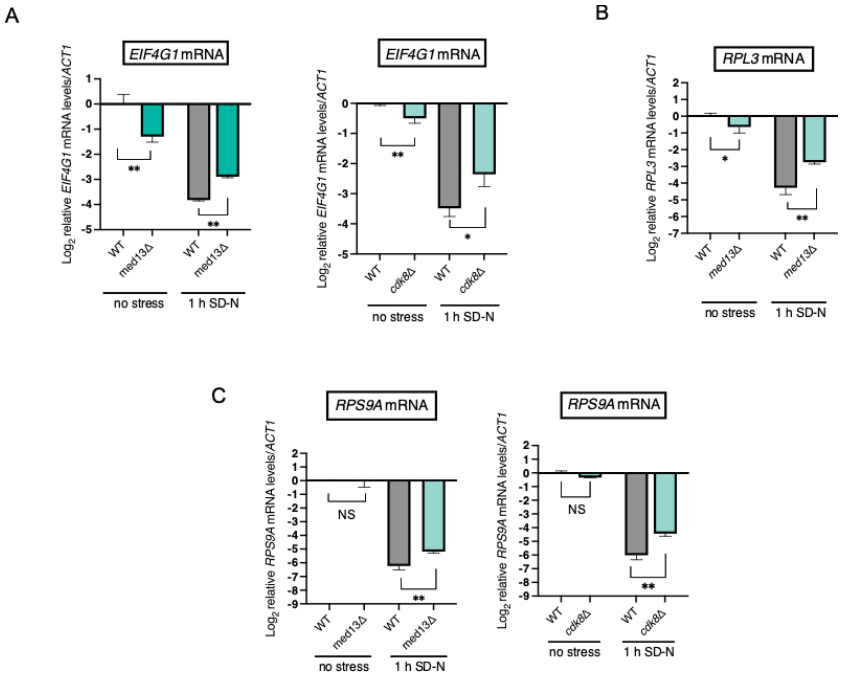

Figure 4.7. Ribosomal protein (RP) and translation initiation factor (TIF) mRNA do not efficiently decrease in CKM mutants following nitrogen starvation. (A) RT-qPCR analysis of the TIF *EIF4G1* in wild-type (WT, RSY10) and *med13*Δ (RSY2444) (left graph) or *cdk8*Δ (RSY2176) (right graph) cells before and after 1 h nitrogen starvation (SD-N). ΔΔCt results for relative fold change (Log2) values using WT unstressed cells as a control. Transcript levels are given relative to the internal *ACT1* mRNA control. (B) As in A, except mRNA levels of the 60S RP *RPL3* was measured. (B) As in A, except mRNA levels of the 40S RP *RPS9A* was measured.

Discussion

The Cdk8 kinase module serves important and diverse roles in the cellular response to stress. In this study, we uncovered a new transcriptional and secondary cytoplasmic role for Med13 induced by nutritional stress. Under unstressed conditions, the CKM acts as a negative regulator of ATG transcription [7], and this repression is relieved upon nitrogen depletion following degradation of cyclin C and Med13 of the CKM [46]. Moreover, we recently uncovered that the CKM maintains constitutive expression of a subset of translation-associated genes in physiological conditions (Chapter 3). The repression of ribosomal protein (RP) genes and translation initiation factor (TIF) genes, as well as the degradation of their mRNA, is important for inhibiting translation following nitrogen starvation [79]. In this study, we observe that mRNA expression levels of RPs and TIFs are not efficiently decreased in CKM mutants. One explanation for this is the possibility that these mRNA are not efficiently degraded in CKM mutants. Another possibility is that the CKM serves a role in efficient down-regulation of these genes following nitrogen starvation. However, as we found that the CKM does not directly regulate translation genes in unstressed conditions (Chapter 3), more studies would be required to determine how the CKM contributes to reduced expression of these genes in stress.

Following nitrogen starvation, Med13 is the only CKM component which is targeted to the cytoplasm for degradation. Its degradation occurs via Snx4-assisted autophagy, with Ksp1 serving as its receptor protein [149]. Our current study sheds light on the secondary cytoplasmic role of Med13 following starvation before its autophagic degradation. Specifically, Med13 localizes to P-bodies, and this interaction, mediated by the polyQ/N domain of Med13, is essential for efficiently recruiting Edc3 to P-bodies.

Additionally, Med13 is crucial for the autophagic degradation of Edc3. These findings support a model (outlined in **Figure 4.8**) wherein, following nitrogen depletion, Med13 facilitates the delivery of Edc3 from P-bodies to the pre-autophagosomal structure (PAS) for degradation. Moreover, this degradation pathway is specific as it targets Edc3, but not Xrn1, another P-body assembly factor. This degradation pathway also does not involve alternative translational proteins, including ribosomes or eIF4G1, which undergo autophagic degradation following TORC1 inhibition [132, 279].

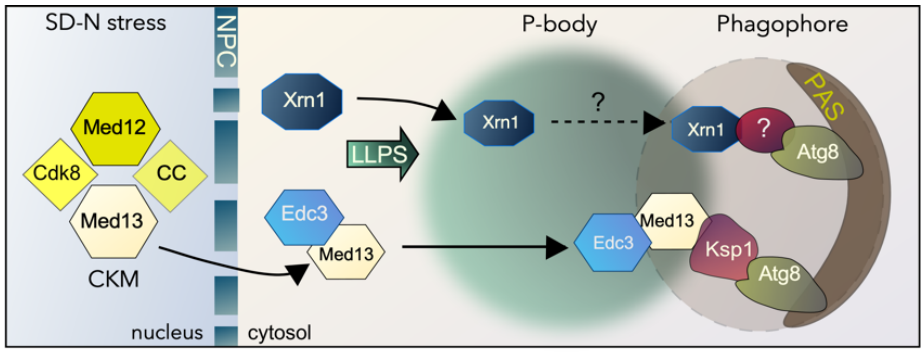

Figure 4.8. Schematic of the role of Med13 in Edc3-biology following nutrient depletion. See text for details. NPC -nuclear pore complex, CKM – Cdk8 kinase module, LLPS – liquid-liquid phase separation, PAS – phagophore assembly site.

Ribophagy and granulophagy represent two other selective autophagy mechanisms responsible for delivering ribonucleoprotein (RNP) granules to the vacuole [14, 285]. The Med13-dependent autophagic degradation of Edc3 describes a third mechanism that does not overlap with these pathways. Unlike granulophagy, where P-bodies are encapsulated within autophagosomes, Med13-mediated degradation selectively targets a subset of P-body proteins. Granulophagy also employs the selective autophagy Atg11 scaffold for

forming the PAS [285], whereas Med13-directed autophagy relies on the trimeric 17C scaffold normally used by bulk autophagy [56]. These differences underscore that Med13-mediated autophagy of Edc3 represents an alternative fate for Edc3 post P-body formation.

Taken together, efficient control of protein synthesis machinery is important for maintaining survival in translation-limiting stresses. We have observed that the CKM promotes survival in a variety of stresses associated with translation repression, including prolonged nitrogen starvation (Hanley et al., *manuscript under revision,* 2024) and ribosome-targeting antibiotics (Friedson et al., *manuscript under revision,* 2024; see Chapter 3). Moreover, in *S. cerevisiae*, the ability to survive nutrient deprivation depends upon correctly entering and exiting quiescence [286], and we demonstrated that Med13 is important for maintaining efficient quiescence entry (Hanley et al., *manuscript under revision,* 2024). Our studies strongly suggest that these phenotypes are associated with the nuclear and cytoplasmic roles of the CKM in controlling P body protein and translation machinery expression, though more studies would be needed to test this model.

The persistence and dysregulation of RNP granules are closely associated with neurodegenerative diseases, including ALS, dementia, and myopathies [287]. While underlying mechanisms remain unclear, many proteinopathies are characterized by persistent aberrant RNA granules that fail to disassemble [15]. The findings demonstrated in this study can thus help us potentially understand a variety of diseases.

Chapter 5

Ubiquitin and Autophagy Pathways Coordinate to Degrade Translation Initiation Factor eIF4G1 Following Nitrogen Starvation

Disclaimer: A large portion of this chapter is adapted from: Friedson B, Cooper KF. The Cul3-RING E3 ubiquitin ligase complex promotes Snx4-assisted autophagy of eIF4G1. *In preparation 2024.* * Author contributions: B Friedson devised the project, wrote the original manuscript, and carried out experiments/prepared figures. KF Cooper supervised and provided ideas for the manuscript.

Abstract

Following nutrient deprivation stress, attenuated protein synthesis and degradation are critical for cellular survival. Energy and nutrient limitations suppress global protein synthesis, whilst upregulating stress response proteins required for appropriate adaptation. This includes downregulating the synthesis and turnover of cap-dependent translation machinery components while simultaneously upregulating cap-dependent translation pathways. The mechanisms used to downregulate cap-dependent translation following nutrition stress remain unclear. Previous studies revealed that the autophagic degradation of eIF4G1, conserved cap-dependent translation initiation factor is assisted by the deubiquitinase Ubp3. Here, I discovered that the conserved translation initiation factor eIF4G1 is degraded by the Snx4-dependent autophagy pathway following nitrogen starvation *in S. cerevisiae*. Previous studies revealed that the autophagic degradation of eIF4G1, is assisted by the deubiquitinase Ubp3. Here, I demonstrate that eIF4G1 is degraded by a Snx4-assisted selective autophagy pathway that requires the ubiquitin-

interacting motif (UIM)-UIM-docking site (UDS) in Atg8 following nitrogen starvation. Furthermore,the autophagic degradation of eIF4G1 requires the ubiquitin conjugating enzymes Ubc4/Ubc5, K33 and K63 ubiquitin chains, and the E3 ligase complex scaffold protein Cul3 Moreover, eIF4G1 does not require the proteasome for degradation, exhibiting a new role for ubiquitination in promoting selective autophagy of a translation initiation protein. This is important because dysregulation of eIF4G1 and ubiquitin pathways are associated with a wide range of cancers and neurodegenerative disease. Together, these data demonstrate the crosstalk of ubiquitin and autophagy in modulating the expression of regulators in protein synthesis.

Introduction

Protein synthesis and degradation are important for governing many cellular processes such as cell growth, protein homeostasis, and eliciting the appropriate response to stress. Imbalances in protein synthesis or degradation pathways are thus associated with conditions such as cancers, Alzheimer's Disease, heart defects, and intellectual disability [1-3]. However, the regulation and coordination of protein homeostasis pathways during stress are still largely unclear.

Upon encountering adverse environmental stimuli such as nutrient deprivation, cells mount a coordinated response, which includes changes in protein translation and degradation pathways [6, 7]. Nutrient deprivation triggers cells to mount pro-survival responses which are triggered by inhibiting TORC1 kinase activity. This results in the inhibition of general cap-dependent protein synthesis to conserve energy and arrest cell growth [10, 11]. Inhibition of translation machinery is also mediated by the autophagic degradation of translation machinery components, including ribosomal proteins and

specific initiation factors [13, 14]. This is coordinated with the upregulation of the transcription and translation of autophagy pathways, which are needed for survival.

Another crucial process for inhibiting mRNA translation involves the formation of processing bodies (P-bodies). P-bodies are conserved membrane-less organelles that form by liquid-liqud phase separation in the cytoplasm following stress. They contain non-translating mRNA-protein complexes (mRNPs) [20] which both inhibits mRNA translation but also stores the mRNA future use upon removal of the stress [21]. The formation of P-bodies therefore represents another mechanism for regulating general translation following stress.

The model organism *S. cerevisiae* represent a strong genetic system to study the cellular response to stress. In yeast, macroautophagy (hereafter autophagy) depends on highly conserved autophagy related (Atg)-proteins and donor membranes to form the phagophore assembly site (PAS), which encloses cargo in a double membraned autophagosome for delivery to the vacuole [106-108]. Cargos are degraded by using either selective or non-selective (bulk) pathways [114, 288]. Bulk autophagy is induced during starvation stress and growing phagophores randomly engulf cytoplasmic contents. The pre-autophagosomal site (PAS) is dependent upon Atg1 autophosphorylation mediated by its interaction with the Atg17 scaffold complex (Atg17, Atg29 and Atg21). Atg1 activation during selective autophagy is dependent upon the cargo interacting with a receptor protein, which is brought to the PAS by interaction with the singular Atg11 scaffold [289, 290].

Recently, we and others have discovered a hybrid autophagy pathway that uses a receptor protein with the 17C scaffold [56, 121]. Cargo degradation is aided by the heterodimeric sorting nexin Snx4-Atg20, which helps transport cargo to the vacuole [116].

This mechanism has been coined Snx4-assisted autophagy and cargo-hitchhiking autophagy and is used to degraded Med13, Rim15, and Msn2, and other large transcriptional regulators. The sorting nexin heterodimer Snx4-Atg20 also promotes selective autophagy of various cellular components, including mitochondria (coined mitophagy), cytoplasm-to-vacuole targeting (CVT) pathway, ribosomes (coined ribophagy), and proteasomes (coined proteaphagy) [117-119]. It remains to be determined if these pathways also require an autophagy receptor protein.

The autophagic degradation of selective cargos also requires receptor proteins to interact with the core autophagy protein Atg8 (LC3 in mammals) at phagophores [120]. Atg8 is a ubiquitin-like protein which contains conserved hydrophobic pockets known as the Atg8-family interacting motif (AIM) docking site (LDS) and the ubiquitin-interacting motif (UIM)-UIM-docking site (UDS). These domains of Atg8 can interact with binding sites of receptor proteins to allow sequestration of specific cargo in the autophagosome [291-293]. For instance, we discovered that the autophagic degradation of Med13 requires its receptor protein, Ksp1, to interact with the LDS site on Atg8 [149].

In mammalian cells, studies have revealed that many selective autophagy pathways require ubiquitin (Ub) [294], a small molecule that covalently attaches to lysine residues of a target. In a K63-linked ubiquitin chain, each ubiquitin monomer is bound to lysine 63 of the recipient [295], and this can signal the delivery of cargo to the vacuole for the selective autophagy of substrates [296, 297]. For example, defective mitochondria are directly ubiquitylated with K63-linked chains mediated by the E3 ubiquitin ligase Parkin for sequestration to the vacuole and subsequent recognition by specific autophagy receptors (through a process coined as mitophagy) [298, 299]. Thus, ubiquitination of cargo is

important for recognition by autophagic adaptors or receptors in mammalian cells [300]. K33-linked ubiquitination can also function in protein trafficking [301, 302], though its roles in autophagy and stress are unclear. Taken together, ubiquitin and autophagy are more intricately linked than previously thought [303].

Much less is known about the role of Ub in autophagy in yeast [294]. For instance, previous studies have revealed that mitophagy in yeast also requires ubiquitin, but unlike in mammalian cells, the mitochondria are not directly ubiquitinated. Although no direct evidence has shown that Atg32 is a ubiquitin-binding receptor, a recent study reported that Atg32 is ubiquitinated at K282 [304], allowing a precise control of mitophagy. Moreover, it is becoming more clear that Ub in yeast can also function as a bridge between a ubiquitin-binding receptor and the LDS site of Atg8 [305]. However, the precise mechanisms and functions of Ub in yeast autophagy pathways require further investigation.

Ribophagy requires the E3 ligase Rsp5 and deubiquitinase (DUB) Ubp3 and its associated cofactor Bre5 [13, 14, 306]. Limited findings demonstrate that the DUB Ubp3 and its cofactor Bre5 also assist autophagic degradation of the highly conserved translation initiation factor eIF4G1 following nitrogen starvation in yeast [13, 132]. EIF4G1 serves as a scaffold for the assembly of other initiation factors to form the eIF4F complex, which recruits the 40S ribosome to mRNA in physiological conditions [307]. Thus, eIF4G1 is required for the rate-limiting step of translation, and its expression is important for controlling cap-dependent translation and cell growth. However, the detailed mechanisms of eIF4G1 autophagic degradation, including the roles of ubiquitin, have not been elucidated.

Reduced eIF4G1 expression is important for stimulating the appropriate cellular response to stress. Adverse nutrient conditions inhibit translation of cap-dependent mRNA, while many stress-specific mRNA require cap independent translation [27, 308], highlighting that a cell needs to alter how eIF4G1 can bind to mRNA in stress. EIF4G1 depletion in mammalian cells is also linked to inhibited translation of mRNAs involved in cell growth and proliferation, thereby inhibiting cell proliferation and mitochondrial activity. The effects of eIF4G1 depletion thus mimics nutrient starvation or inhibition of mTOR and promotes autophagy in mammalian cells [16, 131, 249]. These further indicate that the expression levels of eIF4G1 significantly impacts how a cell responds to stress. Moreover, dysregulated eIF4G1 expression is associated with various diseases. EIF4G1 overexpression stimulates cancer cell proliferation and survival across several cancers [81, 127] and can remove toxic alpha-synuclein aggregation associated with Parkinson's Disease in a yeast model [309].

So, to better understand how its expression is controlled in stress, we further investigated the mechanism of ubiquitin-dependent autophagic degradation of eIF4G1 following nitrogen starvation. To examine this, we used the yeast model *Saccharomyces cerevisiae* due to the easy ability to manipulate genes for understanding complex processes. Moreover, protein synthesis and degradation pathways are highly conserved from yeast to mammalian cells, including translation and autophagy. Here, we demonstrate that eIF4G1 undergoes degradation through a Snx4-assisted selective autophagy pathway upon nitrogen starvation, indicating a new role of Snx4 in promoting autophagy of a translation initiation factor. Our study further reveals that eIF4G1 degradation necessitates the ubiquitin conjugating enzymes Ubc4/Ubc5, K33 and K63 ubiquitin chains, and the E3 ligase

complex scaffold protein Cul3 (cullin 3) as well as the E3 ligase Rsp5. Moreover, this involvement of Cul3 in promoting selective autophagy of a substrate is distinct from other known autophagy pathways. These highlight a novel role for ubiquitin, particularly in K33 ubiquitin chains and Cul3, in facilitating selective autophagy of a translation initiation protein. These data further hold significance because dysregulation of both eIF4G1 and ubiquitination are implicated in various cancers and neurodegenerative diseases [128, 310-313].

Results

eIF4G1 is Degraded via Vacuolar Proteolysis Following Nitrogen Starvation

Previous findings suggest that eIF4G1 is degraded by the autophagy following TORC1 inhibition in yeast [13, 132]. Here, we set out to determine the molecular mechanisms used to deliver eIF4G1 to the vacuole. To first confirm that eIF4G1 is actively destroyed following nitrogen starvation, I starved wild-type cells of nitrogen (SD-N medium) and used quantitative western blot analysis to determine endogenous eIF4G1 protein degradation kinetics. I observed that endogenous eIF4G1 levels significantly decreased following 6 h of SD-N, with a half-life of 4 h (**Figure 5.1A and quantified in 5.1B**). Cycloheximide chase assays revealed that the half-life of eIF4G1 is 5.8 h in the unstressed cultures in the W303 yeast strain background (**Supplemental Figure C1A**), indicating that eIF4G1 is actively degraded following nitrogen starvation. These initial studies were performed using an antibody to eiF4G1. I also obtained similar results measuring the stability of eIF4G1 endogenously tagged with MYC at the C terminus (**Supplemental Figure C1B-C and quantified in C1D** and see **Figure 5.2G and 5.3A**). These demonstrate that tagging eIF4G1 with MYC did not significantly alter its protein

stability in physiological conditions and that eIF4G1-MYC can also be actively degraded following nitrogen starvation. Furthermore, eIF4G1-MYC protein levels remain reduced when WT cells are starved of nitrogen for up to 24 h SD-N (**Supplemental Figure C1E**).

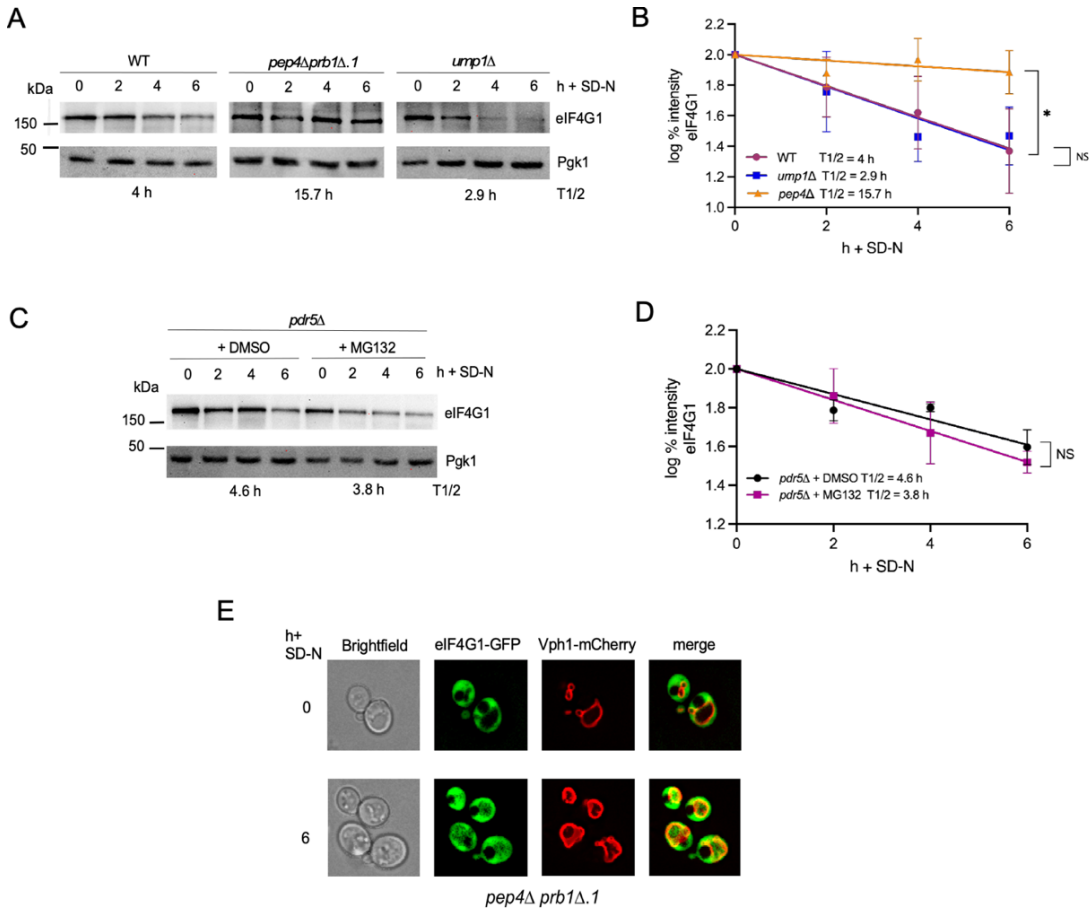

Figure 5.1. eIF4G1 is degraded via vacuolar proteolysis following nitrogen starvation. (A) Western blot analysis of extracts prepared from WT (RSY10), *ump1*Δ (RSY2160), and *pep4*Δ *prb1*Δ*.1* (RSY449) cells at mid-log in SD complete medium then resuspended in SD-N medium for the indicated times. Endogenous eIF4G1 was examined using anti-eIF4G1 antibody and Pgk1 was used a normalization control protein. (B) Quantification of the results obtained in A to demonstrate degradation kinetics. The linear regression line indicates Log% (Log10) protein expression at 2 h, 4 h, and 6 h of SD-N relative to 0 h. T1/2 indicates half-life of protein and error bars indicate S.D., N = 3 of biologically independent experiments. (C-D) As in A and B, except extracts were prepared from *pdr5*Δ (RSY1858) cells grown to low mid-log in SD complete medium then pre-treated with 100 μM of proteasome inhibitor MG132 for 2 h (or with DMSO alone as a control), then

resuspended in SD-N medium for the indicated times. Mutation of the multidrug transporter Pdr5 allows yeast cell membrane permeability of MG132. (E) Fluorescence microscopy of eIF4G1-GFP localization in *pep4*Δ *prb1*Δ*.1* (RSY2653) cells expressing the vacuolar marker Vph1-mCherry (pSW221). Cells were visualized before (growing in SD) and after 6 h of SD-N. Representative single-plane images are shown. Scale: 5 μm.

To further confirm whether eIF4G1 is targeted specifically to the vacuole for degradation in nitrogen starvation, I observed eIF4G1 stability in *pep4*Δ *prb1*Δ.1, two vacuolar endopeptidases [101]. Quantitative western blot analysis coupled with linear regression analysis of endogenous eIF4G1 revealed that the half-life of eIF4G1 is 15.7 h in *pep4*Δ *prb1*Δ*.1* cells compared to the 4 h half-life observed in wild-type cells (**Figure 5.1A and quantified in 5.1B**). This indicates that eIF4G1 degradation in SD-N is mediated by vacuolar proteolysis. In contrast, eIF4G1 was degraded in a mutant of the 20S proteasome maturation factor Ump1 [314] (Right panel of **Figure 5.1A and quantified in 5.1B**) and following treatment with the proteasome inhibitor MG132 (**Figure 5.1C and 5.1D**), These results suggest that eIF4G1 does not require the proteasome for degradation following nitrogen starvation.

To confirm this model, I used autophagic eIF4G1-GFP cleavage assays [315]. This mechanism takes advantage of the observation that the fold of the GFP protein resists fast vacuolar degradation resulting in the accumulation of free GFP [316]. I observed free GFP after 6 h in SD-N (**Supplemental Figure C1F**), confirming our initial results that that eIF4G1 is degraded in the vacuole. Consistent with this, using live cell imaging I observed the accumulation of endogenous eIF4G1-GFP in in *pep4*Δ *prb1*Δ*.1* cells following 6 h in SD-N (**Figure 5.1E**). These results are consistent with a model that eIF4G1 proteolysis following nitrogen starvation occurs in the vacuole but not the proteasome.

The Sorting Nexin Snx4 Assists eIF4G1 Autophagic Degradation Following Nitrogen Starvation

A previous study revealed that eIF4G1 degradation following nitrogen starvation requires Atg7, a protein involved in autophagosome formation which promotes the early step of autophagy [13]. To confirm that autophagy is required to degrade eIF4G1, I analyzed its degradation kinetics and tested more core autophagy mutants. Quantitative western blot analysis revealed that eIF4G1 also requires phagophore assembly proteins Atg1 and Atg8, as well as autophagosome fusion protein Vam3 (**Figure 5.2A and quantified in Figure 5.2B**), further supporting a model that eIF4G1 requires core autophagy machinery for vacuolar proteolysis.

Next, I asked if eIF4G1 is degraded by bulk autophagy or by a selective autophagy pathway. In normal conditions, the scaffold protein Atg11 is necessary for selective autophagy, facilitating phagophore formation at the cargo site [289]. However, under nitrogen starvation, Atg11 is degraded by the UPS [317], and Atg17 anchors Atg1 and other Atg proteins to the pre-autophagosomal structure (PAS) near the vacuole [318, 319]. Analysis of endogenous eIF4G1 degradation revealed that Atg17 but not Atg11 is required for eIF4G1 destruction (**Figure 5.2C and quantified in Figure 5.2D**). These data suggest that, similar to bulk and cargo-hitchhiking pathways, 17C built phagophores mediate eIF4G1 autophagic degradation.

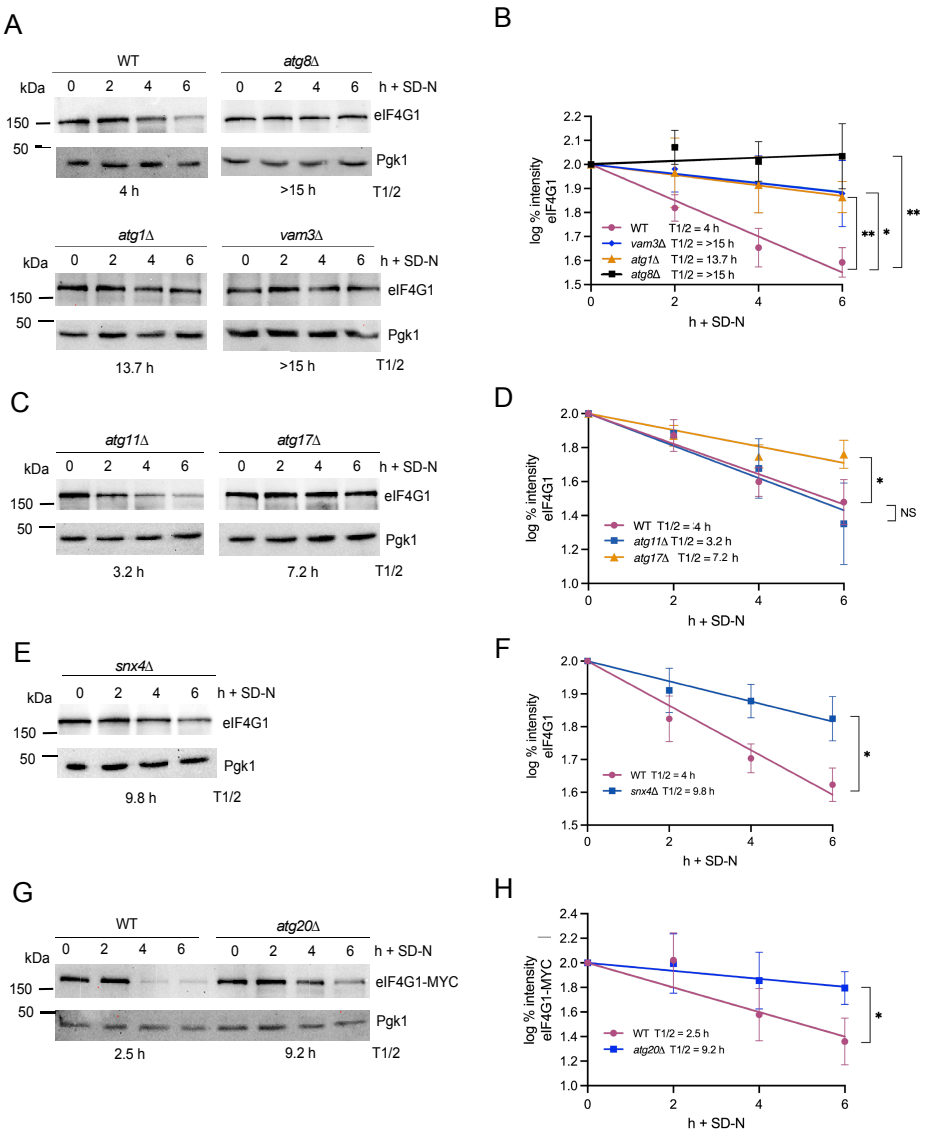

Figure 5.2. The sorting nexin Snx4 promotes eIF4G1 autophagic degradation following nitrogen starvation. (A) Western blot analysis of extracts prepared from WT (RSY10), *atg1*Δ (RSY2094), *atg8*Δ, and *vam3*Δ (RSY2551) cells at mid-log in SD complete medium then resuspended in SD-N medium for the indicated times. Endogenous eIF4G1 was examined using anti-eIF4G1 antibody and Pgk1 was used a normalization control protein. (B) Quantification of the results obtained in A to demonstrate degradation kinetics. The linear regression line indicates Log% (Log10) protein expression at 2 h, 4 h, and 6 h of SD-N relative to 0 h. T1/2 indicates half-life of protein and error bars indicate S.D., N = 3 of biologically independent experiments. (C-D) As in A and B, except extracts were prepared from WT (RSY10), *atg11*Δ (RSY2248), *atg17*Δ (RSY2104) cells. (E-F) As in A and B, except extracts were prepared from WT (RSY10) and *snx4*Δ (RSY2272) cells. (G-H) As in A and B, except extracts were prepared from WT (RSY2909) and *atg20*Δ (RSY2934) cells expressing endogenous eIF4G1-3xMYC.

The sorting nexin heterodimer Snx4-Atg20 binds to the scaffold protein Atg17 [118] to promote Atg1 kinase binding to the PAS [320]. Snx4-Atg20 also promotes selective autophagy of mitochondria, peroxisomes, ribosomes, and proteasomes [117, 118, 321-324]. More recently, we found that Snx4 and Atg17 additionally mediate autophagic degradation of the transcription factor Med13 [56]. As we observed Atg17 assists in eIF4G1 degradation, I tested whether Snx4 assists eIF4G1 degradation similarly to Med13. Here we report that both Snx4 (**Figure 5.2E and quantified in 5.2F**) and its binding partner Atg20 (**Figure 5.2G and quantified in 5.2H**) assist eIF4G1 degradation. These suggest a model in which eIF4G1 autophagy occurs through phagophores tethered to the vacuole and is assisted by Snx4-Atg20. The half-life of eIF4G1 in Snx4 and Atg17 mutants are 9.8 h and 7.2 h, respectively, compared to >13 h in core autophagic mutants. These indicate that Snx4 and Atg17 promote efficient eIF4G1 degradation, though eIF4G1 autophagic degradation can still occur in their absence. Nevertheless, these findings demonstrate a new role of Snx4 in promoting the selective autophagy of a translation initiation factor.

eIF4G1 Requires a Ubiquitin-Binding Adaptor for Autophagic Degradation

Next, I set out to test if the autophagic degradation of eIF4G1 is mediated by selective autophagy pathways. Atg8 contains conserved hydrophobic pockets known as the Atg8-family interacting motif (AIM) docking site (LDS) and the ubiquitin-interacting motif (UIM)-UIM-docking site (UDS), which interact with a receptor's AIM or UIM, respectively [291-293]. To ask if eIF4G1 requires an LDS- or UDS-binding receptor protein for autophagic degradation, I monitored its degradation in *atg8*Δ harboring mutations in the LDS (Y49A and L50A mutations) or UDS (I76A, F77A, and I78A

mutations*)* Atg8 sites. The Atg8^{UDS} but not the Atg8^{LDS} mutant significantly stabilized endogenous eIF4G1-5xMYC (**Figure 5.3A and quantified in 5.3B**) compared to the WT allele, with a similar stabilization seen in *atg8*Δ. These demonstrate that the Atg8 UDS is required for eIF4G1 degradation. Furthermore, as the Atg8 UDS binds to proteins with a ubiquitin binding domain (UBD) [292], this suggests that eIF4G1 requires a ubiquitin-binding receptor or adaptor with a for its selective degradation.

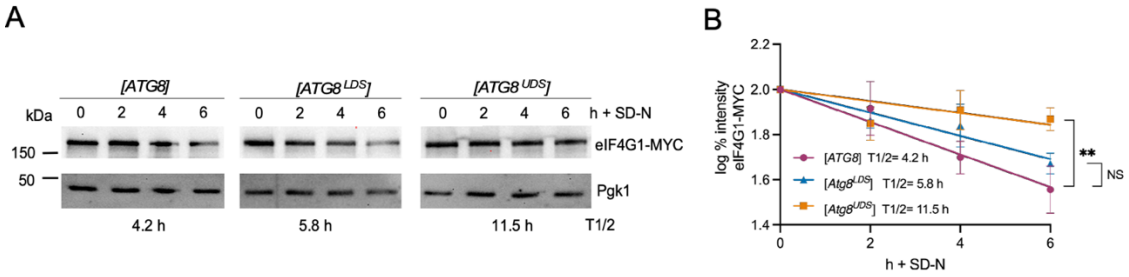

Figure 5.3. eIF4G1 requires a ubiquitin-binding adaptor for autophagic degradation. (A) Western blot analysis of extracts prepared from *atg8*Δ cells expressing endogenous eIF4G1-5xMYC (RSY2948) and plasmids of either WT, LDS, or UDS alleles of GFP-Atg8 (named pSW337, pSH36, pSW557, respectively). Cells were grown in SD-TRP selective medium and resuspended in SD-N medium for the indicated times. Pgk1 was used a normalization control protein. (B) Quantification of the results obtained in A to demonstrate degradation kinetics. The linear regression line indicates Log% (Log10) protein expression at 2 h, 4 h, and 6 h of SD-N relative to 0 h. T1/2 indicates half-life of protein and error bars indicate S.D., N = 3 of biologically independent experiments.

We next asked which receptor/adaptor is required for eIF4G1 autophagic degradation. Ubiquitin can tag substrates for recognition by a selective autophagy receptor (SAR). The most well understood Ub binding SAR in yeast is Cue5, which can remove ubiquitinated protein aggregates and proteasomes [325, 326]. However, I found that

endogenous eIF4G1-MYC is still degraded in a *cue5*Δ mutant (middle panel of **Supplemental Figure C2A and quantified in C2B**), suggesting that it requires a different SAR. More recently, it has been found that 65 alternative Ub binding proteins can also physically interact with both ubiquitin and Atg8 [327]. Among these include the Ub binding shuttle factor Dsk2 [327] and the Ub-regulatory protein Ubx5 which interacts specifically with the Atg8 UDS domain [291]. However endogenous eIF4G1 is still degraded in Ubx5 or Dsk2 mutants (I used a triple mutant of Dsk2, Rad23 and Ddi1 because these receptor proteins are functionally redundant) (**Supplemental Figure C2A-C**). Furthermore, mutants in the redundant receptors Atg19 and Atg34 involved in the cytoplasm-to-vacuolar targeting (CVT) selective autophagy pathway did not influence the degradation of eIF4G1 (**Supplemental Figure C2C**, middle panel), suggesting that eIF4G1 is not targeted through the CVT pathway. Together, these data demonstrate that eIF4G1 is independent of several known yeast receptor proteins. Further studies are needed to identify which of the 65 UIM containing proteins will fulfill this role [305]. Nevertheless, the requirement of a functional UDS site in Atg8 strongly suggests that eIF4G1 utilizes a UIM containing receptor protein which can recognize the UDS site.

Ubiquitin Mediated Signaling is Required for the Autophagic Degradation of eIF4G1

The observation that eIF4G1 requires an UIM containing adaptor protein strongly suggest a role of ubiquitin in eIF4G1 proteolysis following nitrogen starvation. To test this, I used quantitative western blot analysis of eIF4G1 in mutants defective in various stages of ubiquitination pathway. I first confirmed previous studies that Ubp3, a de-ubiquitinating enzyme signalling [91] assists in eIF4G1 autophagy [14] [13] (**Figure 5.4A and quantified in 5.4B**). Next, I discovered that the autophagy degedration of eIF4G1 requires

the conserved E2 ubiquitin conjugating enzymes Ubc4 and paralog Ubc5 (Ubc4/5) which loclaize trhoughout the cell [88]. I found that eIF4G1 is significantly stabilized in a Ubc4/5 mutant with a half-life of 18.7 h compared to 4.6 h in WT (**Figure 5.4C and quantified in 5.4D**). This demonstrates that the transfer of ubiquitin mediated by E2's Ubc4/5 is necessary for eIF4G1 autophagic degradation.

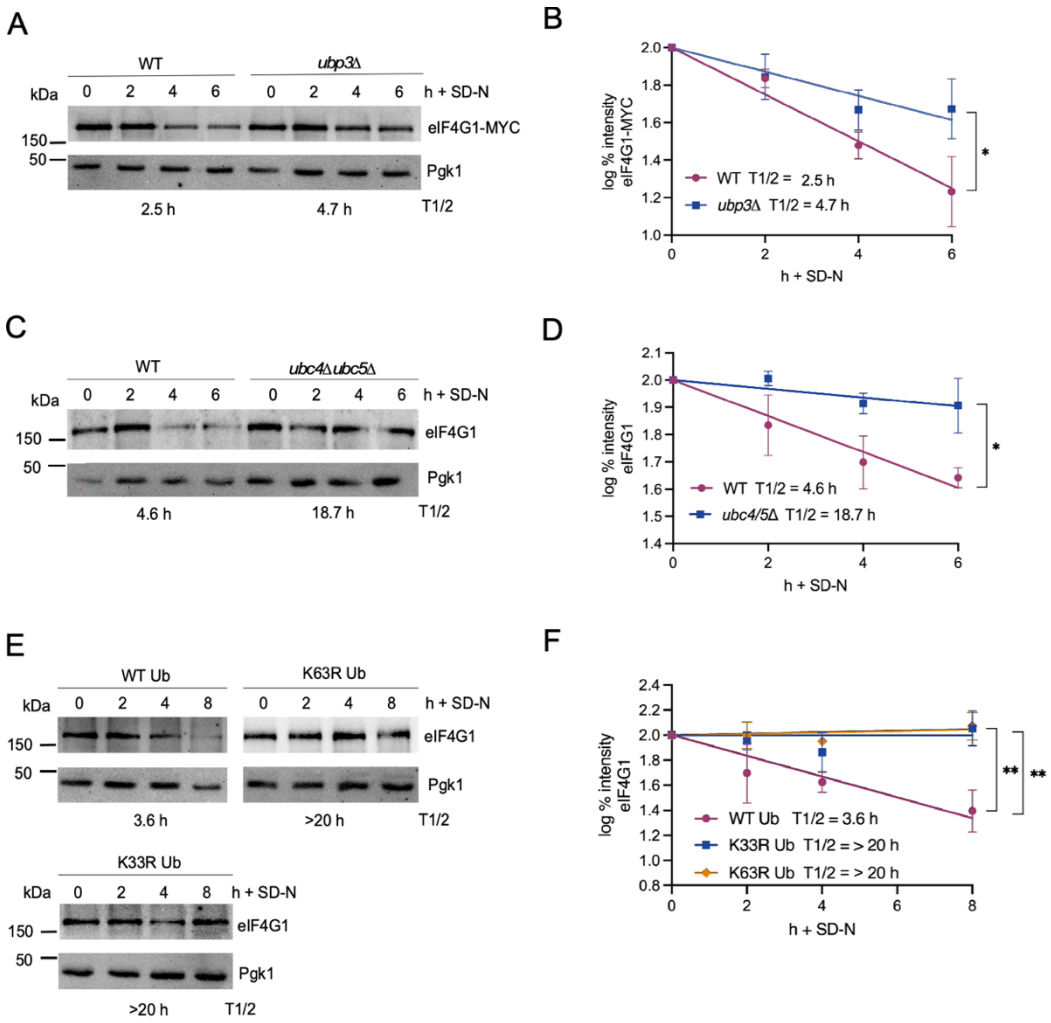

Figure 5.4. The deubiquitylating enzyme Ubp3, ubiquitin conjugating enzymes Ubc4/5, and ubiquitin chains K33 and K63 signal eIF4G1 for autophagic degradation. (A) Western blot analysis of extracts prepared from mid-log WT (RSY2909) and *ubp3*Δ (RSY2935)

cells expressing endogenous eIF4G1-3xMYC resuspended in SD-N medium for the indicated times. Pgk1 was used a normalization control protein. (B) Quantification of the results obtained in A to demonstrate degradation kinetics. The linear regression line indicates Log% (Log10) protein expression at 2 h, 4 h, and 6 or 8 h of SD-N relative to 0 h. T1/2 indicates half-life of protein and error bars indicate S.D., N = 3 of biologically independent experiments. (C-D) As in A and B, except extracts were prepared from WT (RSY414) and *ubc4*Δ*ubc5*Δ (RSY415) cells. Endogenous eIF4G1 was examined using anti-eIF4G1 antibody. (E) As in C-D, except extracts were prepared from strains expressing WT ubiquitin (Ub) (RSY2770/SUB280), K63R Ub (RSY2771), and K33R Ub (RSY2776). Ub mutant strains were created and gifted by Daniel Finley at Harvard University.

I next tested whether Ubc5 expression can promote eIF4G1 degradation independently from Ubc4 because nitrogen starvation causes a cell to enter stationary phase [328] and Ubc5 (but not Ubc4) expression increases in stationary phase [329]. I observed that Ubc5 alone is sufficient to promote eIF4G1 degradation following nitrogen starvation (**Supplemental Figure C3**), suggesting that the E2 ubiquitin conjugating step mediating eIF4G1 degradation is induced following stress. However, the *ubc4/5Δ* double mutant caused more significant stability of eIF4G1 than *ubc5Δ* alone, suggesting that both Ubc4 and its paralog Ubc5 are required to mediate efficient autophagic degradation of eIF4G1. Together, these demonstrate that eIF4G1 autophagy requires a ubiquitin signal modified by the E2's Ubc4/5 followed by the DUB Ubp3.

The Ubiquitin Chains K33 and K63 Signal eIF4G1 for Autophagic Degradation

A unique feature of ubiquitin is its capacity to form various homo- and heterotypic linkage types facilitated specific E3 ligases and DUBs. These linkages create unique proteolytic and non-proteolytic intracellular signals that can be specifically recognized by proteins containing ubiquitin binding domains (UBDs) [98-100]. Thus, to understand the

signaling function of Ub in eIF4G1 autophagic degradation, we aimed to identify the specific Ub-linked chains involved.

Within homotypic ubiquitin chains, ubiquitin monomers are linked to one of seven lysine (K) residues or to the N-terminal methionine (M1). For instance, in a K63-linked ubiquitin chain, each ubiquitin monomer is bound to lysine 63 of the recipient [295], and this can signal the delivery of cargo to the vacuole for the selective autophagy of substrates [296, 297]. K33-linked ubiquitination can also function in protein trafficking [301, 302], though its roles in autophagy are not well known. I utilized strains with mutants in different polyubiquitination linkages [142] (strains were gifted by Daniel Finley at Harvard Medical School) and found that endogenous eIF4G1 significantly stabilized in K63R and K33R Ub chain mutants with a half-life of >20 h in both mutants compared to a half-life of 3.6 h in the WT strain (**Figure 5.4E and quantified in 5.4F**). These data demonstrate that K63 and K33-linked polyubiquitination chains both help signal eIF4G1 through autophagic degradation. The known roles of K63-linked chains and K33-linked chains in intracellular protein trafficking suggest the possibility that these specific Ub chains are necessary for the re-localization of eIF4G1 to selective autophagy machinery.

The Cul3 E3 Ubiquitin Ligase Complex Promotes eIF4G1 Autophagic Degradation

E3 ligases serve a crucial role in assembling ubiquitin chains on a specific substrate [330]. There are at least 80 different E3 ligases in yeast, many of which are redundant [89]. However, one of these, the conserved Cul3 ubiquitin ligase complex (CRL3), promotes the formation of K33-linked ubiquitination [301]. Deletion of Cul3 resulted in endogenous eIF4G1 being significantly stabilized in *cul3*Δ mutants with a half-life of 11.7 h compared to a half-life of 4 h in WT (**Figure 5.5A and quantified in 5.5B**). This suggests a new

model in which Cul3 promotes eIF4G1 autophagic degradation, consistent with our observation that eIF4G1 also requires K33-linked ubiquitination.

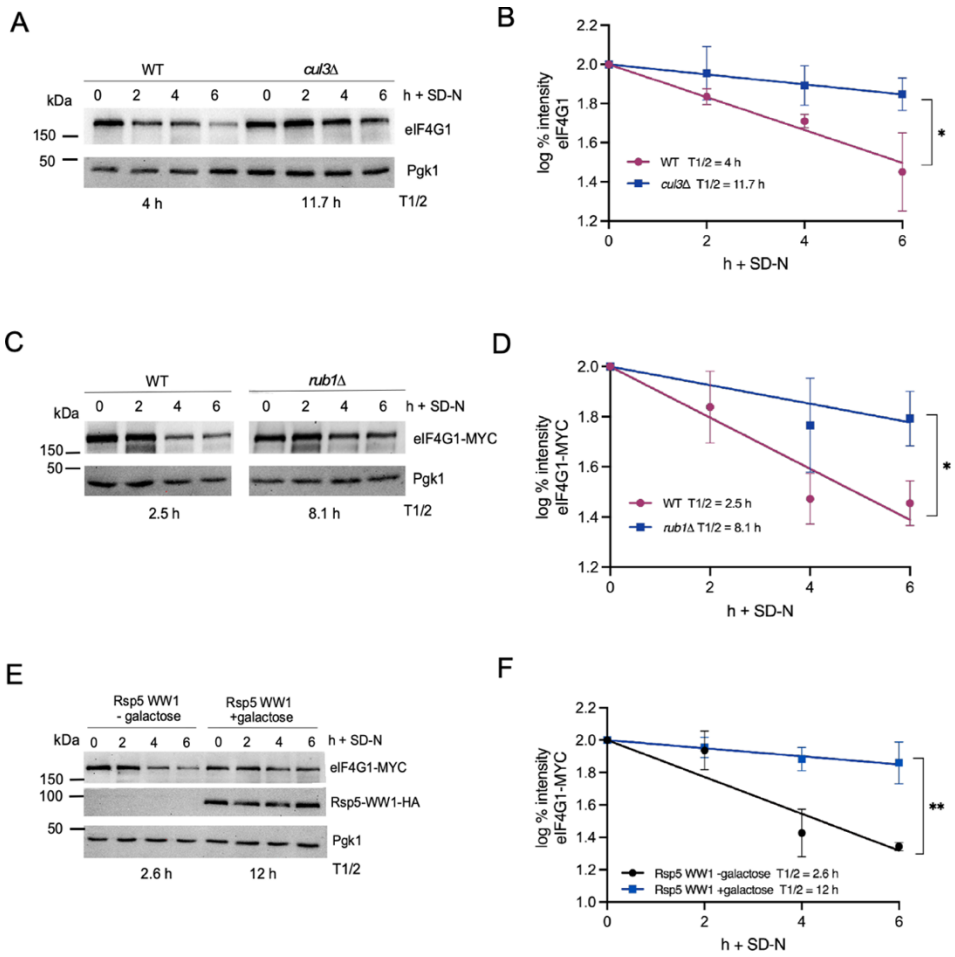

Figure 5.5. The Cul3 ubiquitin ligase complex, along with E3 ligase Rsp5, promote eIF4G1 autophagic degradation following SD-N. (A) Western blot analysis of extracts prepared from mid-log WT (RSY10) and *cul3*Δ (RSY2813) cells resuspended in SD-N medium for the indicated times. Endogenous eIF4G1 was examined using anti-eIF4G1 antibody and Pgk1 was used a normalization control protein. (B) Quantification of the results obtained in A to demonstrate degradation kinetics. The linear regression line indicates Log% (Log10) protein expression at 2 h, 4 h, and 6 h of SD-N relative to 0 h. T1/2 indicates half-life of protein and error bars indicate S.D., N = 3 of biologically independent experiments. (C-D) As in A and B, except extracts were prepared from WT (RSY2924) and *rub1*Δ (RSY2913) cells expressing endogenous eIF4G1-5xMYC. (E-F) As in A and B, except extracts were prepared from WT (RSY2909) cells expressing endogenous eIF4G1-3xMYC and a galactose-inducible plasmid (pRsp5Δ*cis*) which produces a dominant-negative

mutant of the Rsp5 WW1 substrate binding domain. Cells were grown with (+) or without (-) 2% galactose overnight to mid-log in -URA selective medium and resuspended in SD-N medium for the indicated times. Induction of Rps5-WW1-HA mutant plasmid in galactose was observed with antibodies to HA. Pgk1 was used a normalization control protein.

Cul3 is a conserved scaffolding protein within the Cullin-RING E3 ligase (CRL) complex, where RING stands for really interesting new gene [331], and are involved in diverse cellular processes [332]. CRL's mediate the direct transfer of Ub from E2 to the substrate and consists of the following major components: Cullin scaffold protein, RING-box protein which recruits the E2 Ub enzyme, a Bric-a-brac/Tramtrack/Broad (BTB) adaptor protein, and a substrate recognition subunit [333]. Importantly, dimerization and activation of CRL activity highly depends on a covalent post-translational modification by the ubiquitin-like protein Nedd8 (yeast ortholog is Rub1) [334, 335], which specifically targets Cullins through a process called neddylation [336]. So, to test whether efficient Cul3 activity is required to promote eIF4G1 autophagic degradation, I tested eIF4G1 stability in a Rub1 mutant. We found that endogenous eIF4G1-5xMYC was partially stabilized in *rub1*Δ mutants with a half-life of 8.1 h compared to 2.5 h in WT cells (**Figure 5.5C and quantified in 5.5D**), further supporting a model that efficient Cul3 activity promotes eIF4G1 degradation following nitrogen starvation. Our observation that *rub1*Δ mutants do not completely stabilize eIF4G1 in yeast is not surprising because Rub1 modification is not essential for cell viability or cullin functions in budding yeast but is essential in other organisms [335, 337, 338]. Thus, these data indicate that Cul3 activation by Rub1 in yeast helps promote but is not required for eIF4G1 autophagic degradation to occur.

Moreover, quantification of western blot analyses described in Figure 5A and 5C revealed that eIF4G1 protein expression slightly decreases in both *rub1*Δ and *cul3*Δ mutants relative to WT at T=0 h before stress (quantifications shown in **Supplemental Figure C4A-B**). This further demonstrates new roles of the Cul3 RING ubiquitin ligase complex in not only promoting autophagic degradation of a substrate following nutrient deprivation stress, but also in maintaining constitutive levels of eIF4G1 in physiological conditions. Our observation that eIF4G1 also requires K63 and K33 Ub linkages, which are both associated with signaling protein trafficking, further suggests the possibility that Cul3 promotes the intracellular trafficking of eIF4G1 through the autophagy pathway.

An Additional E3 Ligase, Rsp5, Promotes eIF4G1 Autophagic Degradation

It has been previously demonstrated that the autophagic degradation of ribosomes (coined ribophagy) requires the E3 ligase Rsp5 in addition to the DUB Ubp3 [14, 339]. As eIF4G1 autophagic degradation is assisted by Ubp3, we asked whether eIF4G1 follows an analogous degradative pathway which utilizes Rsp5. Our observations that eIF4G1 also requires Ubc4/5 E2 enzymes and K63 Ub linkage chains further supported this possibility because Ubc4/5 are the primary E2's used for Rsp5 in yeast [340, 341] and Rsp5 can catalyze K63 Ub linkages [342, 343].

Rsp5 is essential, so I utilized a plasmid on a *GAL1* promoter (gifted from the Natalia Shcherbik lab at Rowan University), which expresses a dominant-negative mutation of its substrate-binding domain WW1 (RSP5-WW1) [145]). Rsp5-WW1 was induced overnight in SD medium with 2% galactose as the only carbon source. As a control, cells containing the plasmid were grown overnight to mid-log in SD medium with 2% glucose. The cells were washed and switched to nitrogen starvation medium made

using 2% galactose as the sugar source, or with 2% glucose as a control. The results revealed that endogenous eIF4G1-MYC also requires Rsp5 for autophagic degradation with a half-life of 12 h in the Rsp5 WW1 mutant relative to 2.6 h in cells with normal Rsp5 (**Figure 5.5E-F**). This is consistent with observations that both eIF4G1 and ribosomes require Ubp3 for autophagic degradation, demonstrating that eIF4G1 requires similar ubiquitin players as ribosomes for autophagy. Furthermore, quantification of western blot analyses described in Figure 5E revealed that endogenous eIF4G1-MYC protein expression slightly decreases in the Rsp5 mutant relative to WT at T=0 h before stress (quantifications shown in **Supplemental Figure C4C**), as we similarly observed in Cul3 mutants. These data suggest new roles of Rsp5 in promoting autophagic degradation of a translation initiation factor following nutrient deprivation stress and in maintaining constitutive levels of eIF4G1 in a nutrient rich environment. One possible role of Rsp5 in mediating eIF4G1 autophagic degradation could be due to the role of Rsp5 in intracellular trafficking of proteins [344], consistent with our observation that eIF4G1 requires K33 and K63 Ub linkages which are both associated with protein trafficking [302]. However, it is important to note that Rsp5 targets a multitude of substrates for polyubiquitination to mediate various cellular processes [345], including facilitating the stability of cytoplasmic ribosomes in optimal growth conditions [346]. The importance of Rsp5 in various cellular processes suggests an alternative possibility that Rsp5 controls eIF4G1 protein expression through multiple indirect mechanisms.

Cul3 Mediates Autophagy of Specific Substrates Involved in Protein Synthesis

The role of the Cul3 E3 ligase complex in promoting autophagic degradation of a substrate has not previously been described. Therefore, we asked whether Cul3 is required

for general autophagy by monitoring the autophagic cleavage of GFP-Atg8. The results show the accumulation of free GFP does not change between WT and *cul3*Δ cells (**Figure 5.6A**), illustrating that Cul3 is not needed for general autophagy.

Furthermore, like eIF4G1 autophagy, ribophagy requires the sorting nexin Snx4 [117] and ubiquitination enzymes Ubp3 and Rsp5 [14, 339]. This suggested the possibility that ribophagy may also require Cul3. Ribophagy has been previously established using GFP cleavage assays, so we asked whether Rpl25-GFP (a protein of the 60S ribosomal subunit) or Rps2-GFP (a protein of the 40S ribosomal subunit) are cleaved in a Cul3 mutant. I found that neither Rps2 nor Rpl25 required this E3 scaffold protein for vacuolar proteolysis (**Figure 5.6B-C**), further suggesting that Cul3 mediates autophagic degradation of specific substrates.

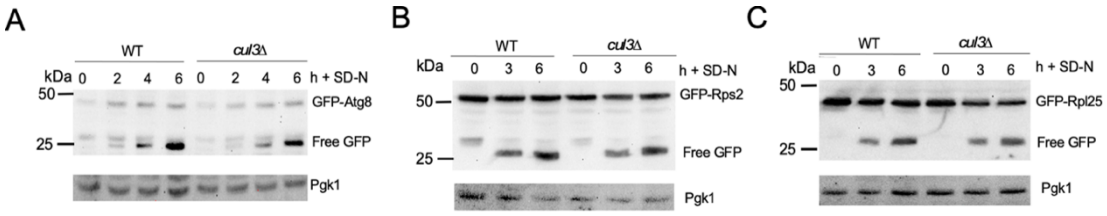

Figure 5.6. Cul3 mediates autophagy of specific substrates involved in protein synthesis. (A) Western blot analysis of GFP-Atg8 (pSW337) cleavage assays in WT (RSY10) and *cul3*Δ (RSY2813) cells at the indicated time points following nitrogen starvation. Free GFP indicates vacuolar proteolysis of full length GFP-Atg8. Pgk1 was used a normalization control protein. (B-C) As in A, except extracts were prepared from cells expressing GFP-Rps2 and GFP-Rpl25 plasmids, respectively.

Cul3 Does Not Directly Ubiquitinate eIF4G1

Next, we asked whether ubiquitination occurs directly on eIF4G1 to signal it through the autophagy pathway. Using the *pep4*Δ *pbr1*Δ1 mutant, eIF4G1-GFP was

immunoprecipitated before and after nitrogen starvation and the immunoprecipitates analyzed by western blot, probed with antibodies to ubiquitin. However, no ubiquitination of endogenous eIF4G1-GFP was observed (**Figure 5.7A**). One possible explanation for this was that ubiquitination of eIF4G1 may be transient and therefore may not be detected at the timepoints I tested.

To confirm this negative result, I used a NanoBiT-based ubiquitin conjugation assay (NUbiCA), a sensitive method for detecting both mono- and polyubiquitin signals on endogenously expressed proteins [143]. This method is beneficial for detecting transient ubiquitination of a substrate because, if ubiquitin binds to a protein, the SmBiT tag fused to ubiquitin can irreversibly conjugate to the LgBiT/His tag on the protein of interest. If ubiquitin and the protein of interest bind, then a luminescent reporter signal (referred as NanoBiT) is observed in the presence of the furimazine substrate. For a loading control of eIF4G1-LgBiT/His levels, I used HiBiT, a small peptide which binds with high affinity to LgBiT and which releases a luminescent signal in the presence of the furimazine substrate. The protein Htb2 requires Bre1 to be ubiquitinated in normal conditions in yeast [347]. So, as a positive control and to confirm that this assay works, I tested Htb2 ubiquitination in WT versus Bre1 mutant and observed a Htb2-LgBiT/His NanoBiT signal in WT unstressed conditions on a western blot as previously reported [143] (**Figure 5.7B**, last two lanes). However, I could not visualize a significant NanoBiT signal of eIF4G1-LgBiT/His before or after SD-N in whole cell lysate (**Figure 5.7B**, first 4 lanes) compared to the Htb2-LgBiT control. I similarly could not observe a NanoBiT signal following direct IP of 500 μg of the eIF4G1-LgBiT/His protein (not shown). I also could not detect a NanoBiT signal using a luminescence plate reader, which can read luminescent signals with higher sensitivity

(**Supplemental Figure C5**). Taken together, these data strongly suggest that eIF4G1 is not directly ubiquitinated before or after SD-N.

Consistent with these results is the observation that eIF4G1 was still degraded in a cis-mutant deleted for the single potential Cul3 recognition site (**Supplemental Figure C6B-C6C**). This site, APTST at residues 932-936 (see **Supplemental Figure C6A** for map of eIF4G1 residues), was identified using The Eukaryotic Linear Motif resource for Functional Sites in Proteins (ELM, an online database) [348] and deleted using CRISPR technologies [144]. However, our observation that eIF4G1-MYC still degrades in this mutant demonstrates that this residue alone is not required for promoting its autophagic degradation. This does not exclude the possibility that alternative or multiple residues within eIF4G1 are necessary to direct it through the autophagy pathway. More cis mutations of eIF4G1 would be required to test this.

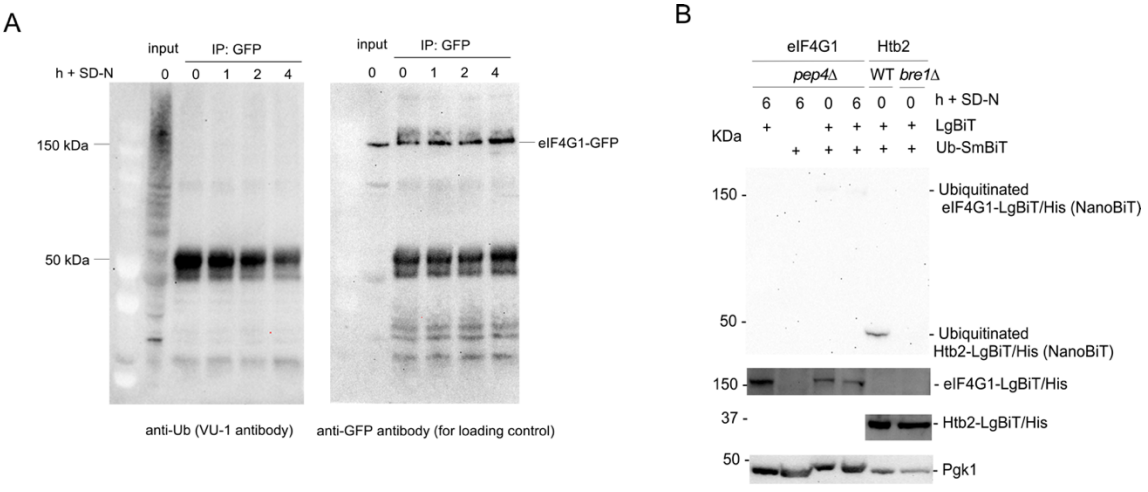

Figure 5.7. Ubiquitination does not occur directly on eIF4G1. A. Western blot analysis of extracts prepared from mid-log *pep4*Δ *prb1*Δ*.1* (RSY2653) cells expressing endogenously tagged eIF4G1-GFP and resuspended in SD-N medium for the indicated times. eIF4G1-GFP was immunoprecipitated with anti-GFP antibodies and the blot was incubated with anti-Ub antibodies (VU-1) to detect ubiquitination on eIF4G1-GFP. Input of whole cell lysate was used to detect ubiquitination as a positive control, and anti-GFP to detect

eIF4G1-GFP was used as a loading control. Experiment was repeated at least 3 times. B. Western blot analysis of extracts prepared from mid-log *pep4*Δ *prb1*Δ*.1* (RSY2653) cells expressing endogenously tagged eIF4G1-GFP and resuspended in SD-N medium for the indicated times. eIF4G1-GFP was immunoprecipitated with anti-GFP antibodies and the blot was incubated with anti-Ub antibodies (VU-1) to detect ubiquitination on eIF4G1-GFP. Input of whole cell lysate was used to detect ubiquitination as a positive control, and anti-GFP to detect eIF4G1-GFP was used as a loading control. Experiment was repeated at least 3 times. B. Western blot analysis using the NuBiCA assay to detect binding of endogenously expressed Ub-SmBiT with eIF4G1-LgBiT/His in a *pep4*Δ mutant (RSY2911). Cells expressing either just eIF4G1-LgBiT (RSY2912) or Ub-SmBiT (RSY2883) were used as a negative control. To validate that the assay works, cells expressing Ub-SmBiT and Htb2-LgBiT in a WT (RSY2897) and *bre1*Δ mutant (RSY2898) were used as a positive and negative control, respectively. The indicated strains were grown to mid-log (~6×10^6 cells), and whole cell lysate was separated by SDS-PAGE and transferred onto a PVDF membrane. The NanoBiT signal (demonstrating binding of Ub-SmBiT with LgBiT tagged protein) was visualized following incubation of the membrane with the NanoLuc substrate furimazine (NanoBiT). To control for the amount of Htb2-LgBiT/His or eIF4G1-LgBiT from the different strains, the same membrane was subsequently reprobed with anti-His antibody. The same membrane was then reprobed with anti-Pgk1 antibody with Pgk1 as a loading control for whole cell lysate. Images are representative of three independent experiments.

The Autophagic Degradation of eIF4G1 is Independent of Ksp1 and the MAPK Slt2

Phosphorylation by a kinase on serine or threonine sites often can serve as a marker to initiate ubiquitination [349] or promote protein-protein binding [350]. Several kinases are known to regulate phosphorylation of eIF4G in mammalian cells [351, 352], but the kinases for eIF4G1 in yeast are not well known. A previous study observed that eIF4G1 is directly phosphorylated by the kinase Ksp1 at 24 different serine sites in glucose deprivation [141]. However, I found that eIF4G1 degradation in nitrogen starvation does not require Ksp1 (**Supplemental Figure C7A and quantified in C7B**). I also observed that endogenous eIF4G1-MYC is only partially stabilized when all 24 serine sites phosphorylated by Ksp1 are mutated to alanine (refer to [141] for details on the site mutations), with a half-life of 5.7 h compared to 2.5 h in WT (**Supplemental Figure C7C**

and quantified in C7D). This suggests that recognition or modification of these specific serine sites can help promote degradation of eIF4G1, though it is not required.

Previous studies have shown that the Cell Wall Integrity (CWI) MAPK kinase pathway plays a role in selective autophagy [353]. Here, the MAPK kinase Slt2 promotes mitophagy by affecting mitochondrial recruitment to the PAS, and regulates pexophagy without affecting nonselective autophagy [354, 355] [356]. Therefore, we addressed if this mitogen activated pathway is required for the autophagic degradation of eIF4G1. Using a kinase dead Slt2 mutant *slt2*^{K54R} I found that eIF4G1 autophagic degradation does not require Slt2 kinase activity (**Supplemental Figure C7E and quantified in C5F**) following nitrogen starvation.

Mass Spectrometry (MS) Analysis of eIF4G1 Before and After Nitrogen Starvation

To better understand the proteins and potential modifications which promote eIF4G1 autophagic degradation, we next carried out mass spectrometry analysis of endogenous eIF4G1-MYC before and after 3h of nitrogen starvation (Disclaimer: This experiment needs to be repeated with more biological replicates and controls before we can confirm these results). I immunoprecipitated 1mg of eIF4G1-MYC from each of these conditions (**Supplemental Figure C8A** shows confirmation that IP worked) and sent the eluted samples to LifeSensors. Mass spectrometry proteomics analysis was performed on the two immunoprecipitation samples (eIf4G1-3xMYC (0h) and eIf4G1-3xMYC (3h)) to understand proteins pulled down, lysine modification, and ubiquitin signature. Peptides for a total of 839 proteins were detected for the eIf4G1-3xMYC (0h) sample, and peptides for a total of 1302 proteins were detected for the eIf4G1-3xMYC (3h) sample. Of these proteins, 756 were common between the two conditions, 76 unique proteins were found in

the eIf4G1-3xmyc(0h) sample, and 534 unique proteins were found in the eIf4G1-3xmyc(3h) sample (**Supplemental Figure C8B**). Nevertheless, a comprehensive list of the associated yeast proteins can be found in the following Excel file: https://docs.google.com/spreadsheets/d/112X3aSZ8Q0gqHvS5Ck2SQbSwsZCmWkug/edit#gid=937181191).

Among the peptides of proteins detected with eIF4G1-3xMYC, we noticed several ubiquitin-related proteins, including Ubp3, Bre5, CDC48 and Rsp5 detected at both 0h and 3h. These are consistent with observations that eIF4G1 autophagy is promoted by the E3 ligase Rsp5, the DUB Ubp3 (refer to Figure 4), and Bre5 of the Cdc48 complex [13]. Several autophagy-related proteins were detected in 3h of nitrogen starvation, including the vacuolar protease Prb1 and vacuole assembly protein Vac8, consistent with the role of autophagy in eIF4G1 degradation. Moreover, Snx41 is a sorting nexin which can interact with Snx4 to promote selective autophagy such as autophagy of proteasomes [117]. This is consistent with our observation that Snx4 assists eIF4G1 autophagy and suggests the possibility that Snx4 serves as a scaffold to bring eIF4G1 towards autophagy machinery. However, further studies would be required to verify these interactions and to understand why these proteins interact with eIF4G1.

Furthermore, we noticed that several proteins which interact specifically with the UDS domain of Atg8 [305] were detected in the MS analysis following 3h of nitrogen starvation, including Pil1, Ypt7, Coy1, Apm1, Did2, and Sec17 (See excel file link shown above). As we observed that eIF4G1 requires the UDS domain of Atg8 for autophagic degradation, these results suggest the possibility that one of these proteins may serve as the

receptor protein which mediates its degradation. Thus, more experiments are required to test the role of these proteins in eIF4G1 degradation following nitrogen starvation.

Discussion

The findings presented in this research shed light on the intricate interplay between protein synthesis and degradation pathways in the cellular stress response. Here, I uncovered the molecular mechanisms underlying the ubiquitin-dependendent autophagic degradation of the translation initiation factor eIF4G1 following nitrogen starvation (**Figure 5.8**). As eIF4G1 serves as a scaffold for the assembly of the cap-dependent translation initiation complex and controls cell growth in TORC1 inhibition stress [16, 131, 307], this degradation mechanism has potential implications for understanding diseases with impaired proteostasis and stress responses like cancer and neurodegenerative disorders.

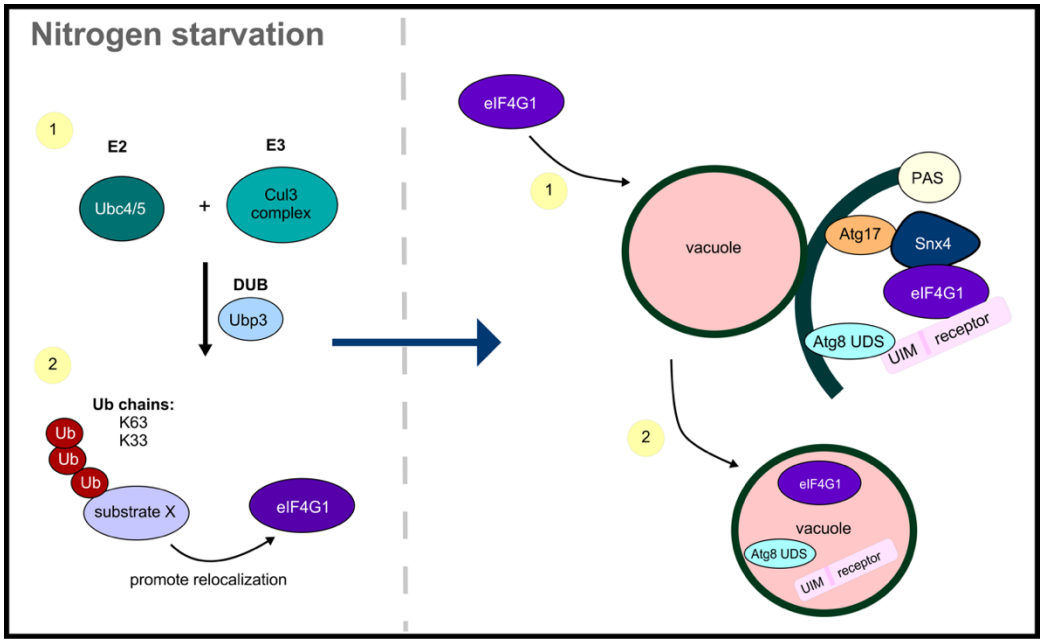

Figure 5.8. Model of ubiquitin-dependent and Snx4-assisted autophagic degradation of eIF4G1 following nitrogen starvation. Following nitrogen starvation, the E2 ubiquitin (Ub) conjugating enzymes Ubc4/Ubc5, and the Cul3 E3 RING scaffold complex mediate vacuolar degradation of eIF4G1. Formation of K63 and K33 Ub chain linkages, along with modification via the de-ubiquitinase (DUB) Ubp3, occur on an unknown substrate. Whether K63 and K33 Ub linkages form mixed or distinct chains remains unknown. Ubiquitination of the unknown substrate likely serves as a signal to trigger re-localization of eIF4G1 through the autophagy pathway. The sorting nexin heterodimer Snx4-Atg20 and autophagy-related protein Atg17 further mediate vacuolar proteolysis of eIF4G1 by serving as a scaffold to the phagophore assembly site (PAS) at the vacuole.

Our data confirm previous indications that eIF4G1 is actively degraded through autophagy and is assisted by the DUB Ubp3 following nitrogen starvation. We further observed that the autophagy protein Atg17 as well as the sorting nexin Snx4 and its cofactor Atg20, facilitate the targeting of eIF4G1 to phagophores tethered to the vacuole following nitrogen starvation. As Snx4 is involved in selective autophagy [324], this suggests that eIF4G1 is selectively degraded. Our observation that Snx4 promotes eIF4G1 autophagy contributes to our understanding of the sorting nexin's role in assisting the selective degradation of various substrates involved in protein homeostasis, including ribosomes, proteasomes, and the transcription factor Med13 [56, 117-119]. Moreover, the requirement of the Atg8 UDS in eIF4G1 degradation further supports a model in which eIF4G1 is degraded via a selective autophagy pathway. The Atg8 UDS binds to receptor proteins with a ubiquitin binding domain (UBD) [292], suggesting that eIF4G1 requires a ubiquitin-binding receptor or adaptor for its selective degradation. However, we could not observe stabilization of eIF4G1 in mutants of several known yeast receptor proteins, particularly those which bind to the Atg8 UDS and ubiquitin. Thus, more studies would be required to determine the receptor involved in eIF4G1 degradation.

Furthermore, this study elucidates the role of ubiquitination in eIF4G1 degradation. Ubiquitin, known primarily for its role in targeting proteins for proteasomal degradation, is shown here to play a crucial role in promoting selective autophagy of eIF4G1. Notably, we demonstrate that eIF4G1 degradation occurs predominantly through vacuolar proteolysis, rather than the proteasome, highlighting the specificity of a ubiquitin-dependent degradation pathway. The involvement of ubiquitin-conjugating enzymes (Ubc4/Ubc5) suggested many possibilities for the role of ubiquitination in eIF4G1 autophagy because Ubc4/Ubc5 can be localize in various cellular compartments and interact with several different E3 ligases for different cellular outcomes [357, 358]. Moreover, nitrogen starvation induces cellular entry into stationary phase [328], and Ubc5 (but not Ubc4) expression increases in stationary phase [329]. We observed that Ubc5 alone is sufficient to promote eIF4G1 degradation following nitrogen starvation, suggesting a likelihood that the E2 ubiquitin conjugating step responsible for promoting eIF4G1 degradation occurs following stress. However, we observed a more significant effect of both Ubc4/5 in eliciting its degradation, which supports the possibility that a ubiquitination mechanism can also occur in unstressed conditions to prime eIF4G1 for proteolysis following stress. Nevertheless, the involvement of the DUB Ubp3 in this pathway indicates that a ubiquitin chain is removed or modified to elicit a specific signal for promoting eIF4G1 autophagy.

To better understand the signaling roles of ubiquitin, we determined the Ub chain linkages involved in eIF4G1 autophagy and found that it requires both K33 and K63 Ub linkages. K63-linked chains are the second most abundant linkage type involved in endocytic trafficking and localization of cargo to the vacuole for selective autophagy [297,

302], consistent with the observation that K63 Ub linkages promote selective autophagy of eIF4G1. K33-linked ubiquitination, however, remains the least studied Ub linkage types. Some known roles of this Ub linkage type include protein trafficking [301], suggesting the possibility that K33 promotes re-localization of eIF4G1 to autophagy machinery. Furthermore, though the precise roles of this linkage in autophagy have not yet been elucidated, K33-linked ubiquitination has also been found to colocalize with Ub-binding autophagy adaptors [302, 359]. This suggests another potential role of K33 Ub linkages in helping eIF4G1 bind to a ubiquitin-binding adaptor for selective autophagy. Furthermore, it is unclear if eIF4G1 necessitates branched chains of multiple linkage types or if different Ub linkages are required at specific steps in signaling its autophagic degradation. Though K63 and K33 can each form both heterotypic and homotypic chains, there is not enough evidence of mixed K63/K33 chains, suggesting the likely possibility that these Ub linkages occur on distinct targets. More studies would be necessary to further understand the complete conformation of ubiquitin chains involved in eIF4G1 degradation.

Cul3, a conserved scaffold of the E3 CRL complex, is well known for promoting proteasomal degradation and trafficking of proteins [332]. Our study demonstrates a new role of Cul3 in promoting eIF4G1 autophagic degradation. Consistent with this, the ubiquitin-like protein Rub1 (mammalian ortholog is NEDD8) [334, 335], which specifically activates Cullins through a process called neddylation [336], also promotes eIF4G1 autophagy. Our observation that *rub1*Δ mutants do not completely stabilize eIF4G1 in yeast is not surprising because Rub1 neddylation activity is not essential for cell viability or Cullin functions in budding yeast but is essential in other organisms [335, 337, 338]. Thus, our data indicate that the Cul3 RING E3 ligase complex is important for

eIF4G1 autophagy, and Cul3 activation via Neddylation can help enhance this process. Moreover, Cul3 can promote both K33 and K63 Ub linkages [301, 360], consistent with our observation that K33 and K63 Ub linkages also promoting eIF4G1 autophagy. We further observed a slight decrease in eIF4G1 protein expression in both Cul3 and Rub1 mutants relative to WT in physiological conditions. This suggests that the Cul3 RING complex normally helps maintain stability or constitutive levels of eIF4G1 in yeast, though more studies would be required to further understand the roles of Cul3 before stress.

Mutations in Cul3 are risk factors for neurological disorders associated with autophagy deficiency, including schizophrenia, Parkinson's Disease, and Autism Spectrum Disorder [361, 362]. However, little is known about the pathogenic mechanisms associated with Cul3. A recent study observed that Cul3 deficiency in mice caused an abnormal increase in brain eIF4G1 protein expression as well as an increase in overall cap-dependent translation [363], demonstrating a conserved link between Cul3 activity and subsequent eIF4G1 expression. Another recent study found that, in breast cancer cell lines aberrant Cul3 overexpression, Cul3 degrades the autophagy regulator beclin 1 (BECN1) via the UPS to decrease autophagy and to promote tumor progression [364]. This further indicates that the functions of Cul3 in controlling eIF4G1 expression and autophagy pathways depend on cell type and cellular stress. Thus, more comprehensive studies are required to understand the complex roles of Cul3.

Rsp5 is a versatile E3 ligase which targets many substrates to control diverse cellular pathways [345, 365], so our observation that eIF4G1 autophagic degradation also requires Rsp5 could be attributed to several possibilities. For instance, Rsp5 may target an upstream substrate which indirectly controls eIF4G1 autophagic degradation. Rsp5 is also

involved in ribosome stability [346], suggesting the possibility that eIF4G1 degradation requires sufficient ribosome stability to be targeted for degradation. This E3 ligase also regulates several autophagic pathways, including aggrephagy, proteaphagy, and mitophagy [325, 366, 367], and can bind to Atg8 adaptors [325] including the common yeast autophagy receptor Cue5 [365]. However, as eIF4G1 does not require Cue5 for degradation, the mechanism by which Rsp5 promotes its degradation remains unclear. Nevertheless, like Cul3, Rsp5 can also promote intracellular trafficking [344]. Rsp5 can also recognize the E2's Ubc4/5 and promote K63 Ub linkages [340, 368], suggesting the possibility that Rsp5 helps produce K63 Ub linkages to promote intracellular trafficking of eIF4G1 following SD-N.

How specific is the pathway which targets eIF4G1 for degradation following nitrogen starvation? Proteolysis of eIF4G1 is specific for nitrogen starvation because glucose starvation does not induce eIF4G1 degradation [369]. Furthermore, only a subset of translation factors are degraded by autophagy following TORC1 inhibition. For instance, mRNA decapping protein Dcp2 is degraded by the proteasome, while other translation factors such as eIF4A and eIF3 do not get degraded [13, 132], implicating an important function for selectively degradating the initiation factor eIF4G1 via autophagy in nitrogen starvation. EIF4G1 can be found in various locations in the cytoplasm, including association with translating ribosomes and P-bodies [67, 279], also suggesting the possibility that eIF4G1 localization may play a role in its proteolysis. Our finding that eIF4G1 still degrades in a mutant of Slt2, which is essential for the increase of P-bodies in cell wall stress, indicates that eIF4G1 does not need to be sequestered to P-bodies to be targeted for degradation following nitrogen starvation. The selective autophagy of

ribosomal proteins and eIF4G1 occur similarly because they require the sorting nexin Snx4 and ubiquitin pathway components Ubp3 and Rsp5 (Kraft et al., 2008, Buchan et al., 2013). However, unlike ribosomal proteins, eIF4G1 also requires Cul3, which highlights a specific function of Cul3 in ubiquitin-mediated proteolysis of eIF4G1. These further suggest that the cues which trigger eIF4G1 degradation might differ from the signals which target P body-associated proteins and ribosomal proteins for degradation.

The precise PTM signals which occur directly on eIF4G1 to promote its autophagic degradation remain to be uncovered. We were unable to detect direct ubiquitination on eIF4G1 through various assays, suggesting a strong possibility that ubiquitin does not need to directly target eIF4G1 to trigger its proteolysis. Thus, more studies would be required to determine the substrate which becomes ubiquitinated to subsequently promote eIF4G1 autophagy. However, understanding the sites on eIF4G1 which direct its autophagic degradation would be beneficial for the development of CIS mutants which stabilize eIF4G1. We observed slight stability of eIF4G1 in a mutant of 24 phosphorylatable serine sites on eIF4G1, suggesting that recognition of these specific sites can help signal but are not required for eIF4G1 autophagy.

Taken together, ubiquitin and autophagy are more intricately linked than previously thought [303], and these data present a new crosstalk of autophagy and ubiquitination pathways in promoting the degradation of a translation initiation factor. The consistent functions of K33 and K63 ubiquitin linkages, as well as Cul3 and Rsp5, in intracellular protein trafficking suggests that ubiquitination likely serves as a signal to help eIF4G1 translocate to the autophagy machinery for degradation. However, more studies would be required to test this model and to determine the exact mechanism by which this occurs.

Moreover, more studies would be required to investigate the exact Ub linkages and to understand whether more E3 ligases are involved. Nevertheless, these data collectively demonstrate the crosstalk of ubiquitin and autophagy in fine-tuning the degradation of an important player in protein synthesis.

Dysregulation of eIF4G1 has emerged as a significant factor in various cancers and neurodegenerative diseases, underscoring its potential as a therapeutic target. Notably, serine mutations in eIF4G1 have been linked to Parkinson's Disease [128, 312], and overexpression of eIF4G1 can remove toxic alpha-synuclein aggregates in yeast [309]. The functions of eIF4G1 are highly conserved from yeast to humans, with slight differences in its functional domains [370]. Utilizing yeast to understand eIF4G1 autophagic degradation and the domains required for its proteolysis thus holds promise for the development of targeted therapeutic interventions. For instance, pharmaceutical agents targeting Neddylation can modulate Cullin ligase complexes to regulate cell growth in cancers [371]. Our discovery that Cul3 controls eIF4G1 autophagy offers potential avenues for stabilizing eIF4G1 expression and mitigating alpha-synuclein aggregation in neurodegenerative disorders. Shedding light on the mechanisms underlying eIF4G1 degradation can thus lay the groundwork for understanding and treating various medical conditions.

Chapter 6

Ubiquitin and Autophagy Pathways Coordinate to Degrade Transcription Factor Med13 Following Nitrogen Starvation

Abstract

The Cdk8 Kinase Module (CKM) is a highly conserved dissociable member of Mediator complex. It consists of 4 conserved proteins, Cyclin C, and its kinase Cdk8, Med12, and Med13, two structural proteins that connect them to the mediator. Together with RNA polymerase II, the CKM controls the transcription of a subset of stress response genes. In the budding yeast, the CKM predominantly regulates SRGs, including autophagy-related genes (ATGs) that encode core autophagy proteins. De-repression of *ATGs* occurs following nitrogen starvation. This is partly mediated by the CKM's dissolution, mediated by the degradation of cyclin C in the nucleus by the UPS. In addition, nitrogen starvation triggers the nuclear release of Med13 into the cytoplasm, where it promotes processing body (P-body) assembly before its degradation by Snx4-assisted cargo hitchhiking, a new autophagy pathway. Here, we show that ubiquitination is required for the autophagic degradation of Med13. As Med13 nuclear release is not dependent upon the degradation of cyclin C, this suggests a model in which a cytoplasmic ubiquitination event is required for Snx4-assisted cargo hitchhiking of Med13. This is exciting as it shows that ubiquitination and autophagy work hand in hand to mediate the selective degradation of a target.

Introduction

The ubiquitin-proteasome system (UPS) and macroautophagy (hereafter autophagy) are two degradation systems used by eukaryotic cells to selectively destroy key proteins. In general, short-lived and soluble misfolded/unfolded proteins, including transcription factors, are targeted by UPS. Autophagy is reserved for the selective degradation of faulty organelles and insoluble protein aggregates (selective autophagy) or random cytoplasmic content during starvation (non-selective – aka bulk autophagy) [104]. Ubiquitin and autophagy were initially thought to be two separate degradation systems. However, many recent studies have shown that ubiquitin is used as a signaling molecule in selective and non-selective autophagy pathways (reviewed in [100]). Understanding their cross-talk between these two mechanisms is important as dysregulation of ubiquitin-mediated autophagy pathways is associated with a number of human diseases [133].

In mammalian cells, ubiquitin-tagged proteins/organelles account for over 50% of autophagic cargos [303]. However, in *S. cerevisiae,* a notorious model system for identifying autophagic components, very few ubiquitinated events have been described. The selective autophagy of mitochondria (mitophagy) is best studied where the ubiquitination of the selective autophagic receptor protein Atg32 promotes mitophagy [304]. Recently, I have shown that the autophagic degradation of the transaction initiation factor eIF4G1 requires the Cul3 ring ligase complex (CRL3) and K33 mediated ubiquitination (Chapter 5 of this thesis). eIF4G1 itself is not directly ubiquitinated, suggesting that an unknown protein is the recipient molecule. As eIF4G1 ubiquitination requires the UDS domain of Atg8, this suggests that a UIM-containing receptor protein is most likely the target recipient in this pathway.

Here, we report that the autophagic degradation of Med13 also requires K33 mediated ubiquitination by CRL3. Med13 degradation is assisted by the conserved sorting-nexin heterodimer, Snx4-Atg20. It uses Ksp1 as a receptor protein that recognizes the LDS region of Atg8 [149]. Ksp1 does not contain any ubiquitin recognition sequences, making it unlikely to be the target of this ubiquitination. This suggests the possibility that Med13 itself may be the target, though more studies would be required to test this.

Results

Med13 Requires Ubiquitin Activity for Autophagic Degradation Following Nitrogen Starvation

The CKM subunit Med13 [56] is degraded by a new hybrid autophagy mechanism coined cargo hitchhiking that utilizes components of both selective and bulk autophagy pathways. We previously observed that Med13 also does not require the proteasome maturation factor Ump1 for degradation in nitrogen starvation, thereby discounting the requirement for a proteasome in its degradation [56]. However, using quantitative western blot analysis, I determined that Med13 requires the E2 Ub conjugating enzymes Ubc4/5 for its autophagic degradation following nitrogen starvation (**Figure 6.1A,** quantified in **6.1B**). This suggests that the ubiquitination of either Med13 or a protein needed for its degradation is required for the autophagic degradation of Med13.

To probe this model, I asked if the autophagic degradation of Med13 requires Ub-binding shuttle factors (Dsk2, Rad23, and Ddi1), which promote shuttling of substrates to the proteasome. However, after 6 h in nitrogen starvation media, Med13 was not observed in *dsk2*Δ *rad23*Δ *ddi1*Δ cells, suggesting that shuttle factors do not play a role (**Figure 6.1C**).

The Ub Mechanism that Promotes Med13 Degradation Depends on the Environmental Stress

Next, we wanted to identify the E3 ligase which is required for the autophagic degradation of med13. I first asked if SCF^{Grr} was required, as this multi-subunit E3 ligase conjugates ubiquitin to Med13 following oxidative stress [122]. Western blot analysis revealed that Med13 was still degraded in a *grr1*Δ mutant following 4 h in SD-N **(Figure 6.1D**), suggesting that this E3 ligase does not play a role. This suggests a model in which the ubiquitin machinery used to degrade Med13 in oxidative stress and nitrogen starvation are different. Consistent with this, the Ubc4/5 Ub enzymes are not required for Med13 proteasomal degradation following oxidative stress (**Figure 6.1E**). These data suggest that the Ub-dependent mechanism which mediates Med13 autophagy in nutrient deprivation is distinct from the mechanism which promotes its proteasomal degradation following oxidative stress.

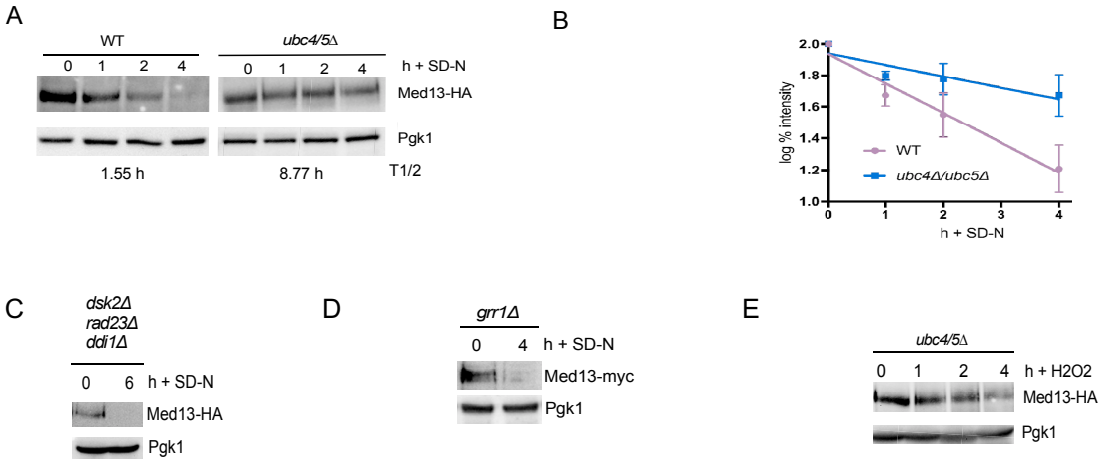

Figure 6.1. Ubiquitin-dependent autophagy of Med13 occurs specifically in nitrogen starvation**.** (A) Western blot analysis of extracts prepared from mid-log WT (RSY414) cells and *ubc4/5*Δ (RSY415) mutants resuspended in SD-N medium for the indicated times. Med13-HA was observed using an overexpression plasmid (PKC801) and Pgk1 was used a normalization control protein. (B) Quantification of the results obtained in A to

demonstrate degradation kinetics. The linear regression line indicates Log% (Log10) protein expression at 1 h, 2 h, and 4 h of SD-N relative to 0 h. T1/2 indicates half-life of protein and error bars indicate S.D., N = 3 of biologically independent experiments. (C) As in A, except Med13-HA levels were observed in *dsk2*Δ *rad23*Δ *ddi1*Δ mutants (RSY2196). (D) As in A, except endogenous Med13-MYC levels were observed in *grr1*Δ (RSY1771). (E) As in A, except Med13-HA levels were observed in *ubc4/5*Δ (RSY415) mutants incubated with Hydrogen Peroxide (H2O2) for the indicated times.

Med13 Requires K33 Ub Chain Linkages for Autophagic Degradation

Next, we set about identifying the E3 ligase that mediates the autophagic degradation of Med13. Over 100 E3 ligases have been identified in the budding yeast [89]. To narrow down the playing field, we first determined which type of Ub chain linkage mediates Med13 degradation, as different linkages are associated with specific E3 ligases [372]. The autophagic degradation of Med13 was therefore measured in ubiquitin mutants that harbor mutations in either K63 or K33 linkages [373]. The results show that Med13 was significantly stabilized in mutants that don't form K33 linkages (**Figure 6.2A-B,** quantified in **6.2C**). As K33 Ub chains are implicated in protein trafficking [302], this suggests the possibility that Ub may play a role in the re-localization of Med13 to autophagy machinery.

The Autophagic Degradation of Med13 Requires the RING E3 Ligase Scaffolding Protein Cul3

K33-linked ubiquitination is used by two conserved E3 ligases, Rsp5 and the Cul3 E3 Ring ligase complex (CRL3). Therefore, using quantitative western blot analysis I monitored Med13 degradation following nitrogen starvation in Rsp5 and Cul3 mutants. As Rsp5 is essential, so we utilized a plasmid on a *GAL1* promoter (gifted from the Natalia Shcherbik lab at Rowan University), which expresses a dominant-negative mutation (of its substrate-binding domain WW1 (RSP5-WW1 [145]). Rsp5-WW1 was induced overnight

in SD medium containing 2% galactose until cells were at mid-log. As a control, cells containing the plasmid were grown to mid-log in SD medium containing 2% glucose. At mid-log, cells were washed and switched to nitrogen starvation medium made using 2% galactose as the sugar source. The results revealed that endogenous Med13-MYC does not require Rsp5 for its autophagic degradation (**Figure 6.2D** and quantified in **6.2E**).

Using a similar approach, I asked if Cul3 is the E3 ligase used for the autophagic degradation of Med13. The results show that Med13-HA was significantly stabilized in *cul3*Δ cells in SD-N. This strongly suggests that Cul3 is required for the autophagic degradation of Med13 (**Figure 6.2F**, quantified in **6.2G**). A caveat to this interpretation is that these experiments were performed using Med13-HA on a centromeric plasmid under the control of the *ADH1* promotor. In addition, the BY4742 genetic background was used whereas other experiments were performed in the W303a strain. Thus, this experiment needs to be repeated using endogenously tagged Med13 in the W303a background. However, the results strongly suggest that the autophagic degradation of Med13 requires K33-linked ubiquitination and the CRL3 E3 ligase.

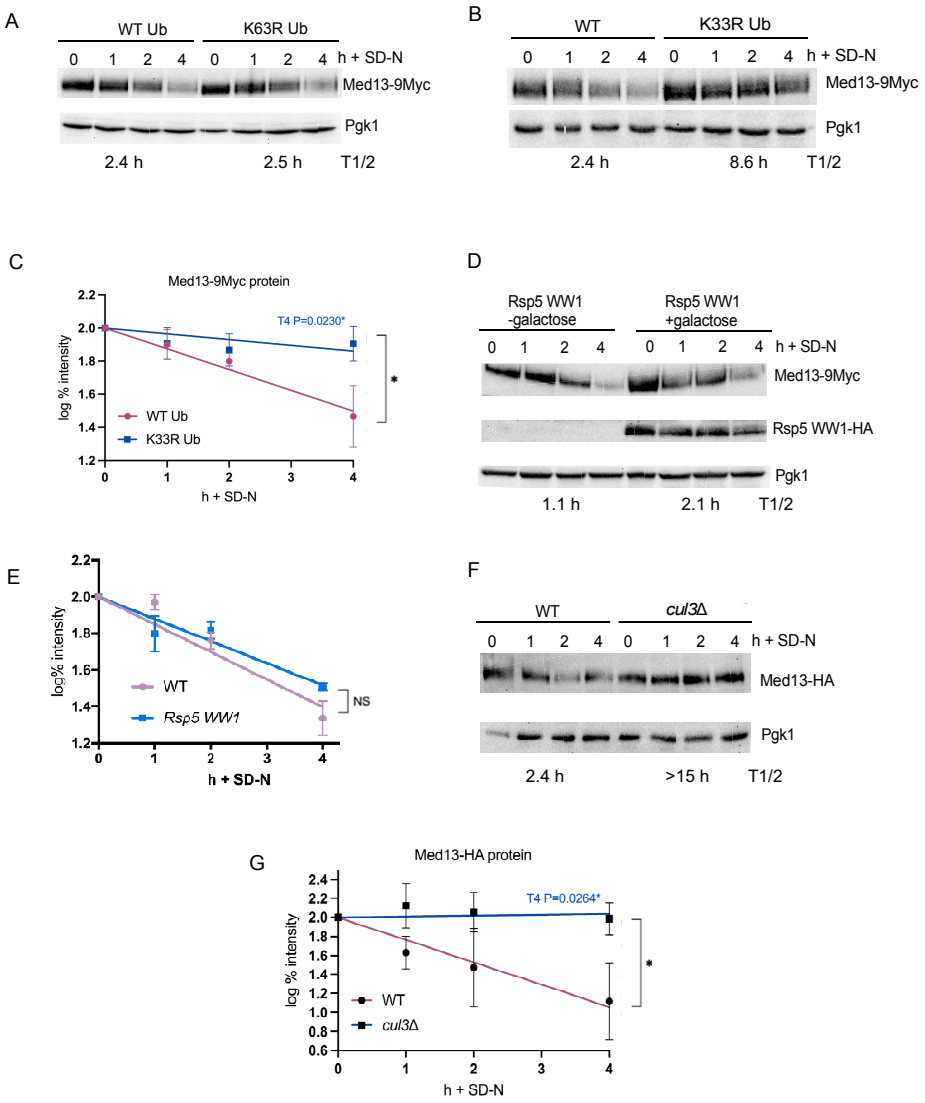

Figure 6.2. Med13 requires K33 Ub chain linkages and may require the RING E3 ligase scaffold Cul3. (A) Western blot analysis of extracts prepared from mid-log WT (RSY2720) and K63R Ub chain linkage mutants (RSY2721) expressing Med13 endogenously tagged with 9xMYC. Cells were resuspended in SD-N medium for the indicated times. Pgk1 was used a normalization control protein. (A) As in A, except extracts were prepared from from mid-log WT (RSY2720) and K33R Ub chain linkage mutants (RSY2801). (C) Quantification of the results obtained in B to demonstrate degradation kinetics. The linear regression line indicates Log% (Log10) protein expression at 1 h, 2 h, and 4 h of SD-N relative to 0 h. N = 3 of biologically independent experiments. (D) As in A, except extracts were prepared from WT (RSY2211) cells expressing endogenous Med13-9xMYC and a galactose-inducible plasmid (pRsp5Δ*cis*) which produces a dominant-negative mutant of the Rsp5 WW1 substrate binding domain. Cells were grown with (+) or without (-) 2% galactose overnight to mid-log in -URA selective medium and resuspended in SD-N medium for the indicated times. Induction of Rps5-WW1-HA mutant plasmid in galactose was observed with antibodies to HA. Pgk1 was used a normalization control protein. (E) Quantification of results obtained in D. (F) As in A, except Med13-HA levels were

observed using an overexpression plasmid (PKC801) in WT (RSY703) and *cul3*Δ mutants in BY4742 strain background. (G) Quantification of results obtained in F.

Med13 and eIF4G1 Require Slightly Different Ub-Dependent Mechanisms for Autophagic Degradation in Nitrogen Starvation

Following nitrogen starvation, eIF4G1 autophagic degradation requires the DUB Ubp3 and its binding partner Bre5, which are cofactors of CDC48 [13]. CDC48 is a complex ubiquitin-binding ATPase complex associated with proteolysis, including serving a role in the crosstalk between ubiquitin and autophagy pathways [374, 375]. Thus, since I observed that Med13 and eIF4G1 are both assisted by similar autophagy and ubiquitin-associated proteins for degradation (**Figure 6.3**), I determined whether Med13 also requires CDC48. As CDC48 is essential for many cellular processes, we had difficulty in utilizing and creating a mutant which effectively depleted this complex. So, we screened through mutants of several cofactors known to interact with CDC48, including Ubp3, but did not observe stabilization of Med13 (**Supplemental Figure D1A-B)**. These suggest that Med13 does not require these cofactors for CDC48. However, more studies would be required to determine the potential role of CDC48 in Med13 autophagy.

Discussion

The autophagic degradation of Med13 defines a new hybrid autophagy pathway that couples using a selective autophagy receptor protein with phagophores built from bulk-autophagy pathways. Now, we have discovered that K33 linked ubiquitination of Med13 by the Cul3 ring E3 ligase may also be required (**Figure 6.3**). However, it remains to be determined which step in the pathway requires Ub. One strong possibility is that the ubiquitination of Med13 itself triggers its autophagic degradation. Using Eukaryotic Linear

Motif resource for Functional Sites in Proteins (ELM, an online database), [348] we determined that Med13 does have a conserved CRL3 ligase site, which would need to be deleted to confirm this. In addition, NuBiCA assays could be used to determine if ubiquitination is direct. Nevertheless, both K33 ubiquitin linkages and Cul3 have been implicated in intracellular protein trafficking [302, 376], suggesting that ubiquitination likely transports Med13 to autophagy machinery. However, more studies would be required to test this model.

We recently observed that Med13 serves a secondary role in the cytoplasm following nitrogen starvation by promoting autophagic degradation of a P-body protein Edc3 (see Chapter 4). This suggests one possibility that this Ub-dependent autophagy pathway selectively targets Med13 to control P-body dynamics in nitrogen starvation. We also recently observed that Med13 positively regulates RP and TIF gene expression, including *EIF4G1* (see Chapter 3), in physiological conditions. These suggest an additional possibility that this ubiquitin dependent autophagy pathway targets Med13 to further control eIF4G1 levels, in addition to *ATG8* levels, following stress. Nevertheless, more studies are required to investigate why Ub targets Med13 to autophagy machinery.

I recently discovered that translation initiation factor eIF4G1 similarly requires Atg17, Snx4, K33, and Cul3 for autophagic degradation following nitrogen starvation (see Chapter 5). However, unlike Med13, eIF4G1 also requires the DUB Ubp3, the E3 ligase Rsp5, as well as the K63 Ub Chain linkage, but does not require the receptor protein Ksp1. These suggest that Cul3 and K33 Ub chain linkages are important for targeting both eIF4G1 and Med13 through autophagy, albeit through unique mechanisms **(Figure 6.3**). This is not surprising because these proteins serve unique functions and localize in

distinctive areas of the cell. For instance, the abundant eIF4G1 can normally be found at ribosomes in the cytoplasm to promote cap-dependent translation, while Med13 normally localizes to the nucleus to control transcription. Nevertheless, these data collectively demonstrate the crosstalk of ubiquitin and autophagy in fine-tuning the degradation of two important players in protein synthesis.

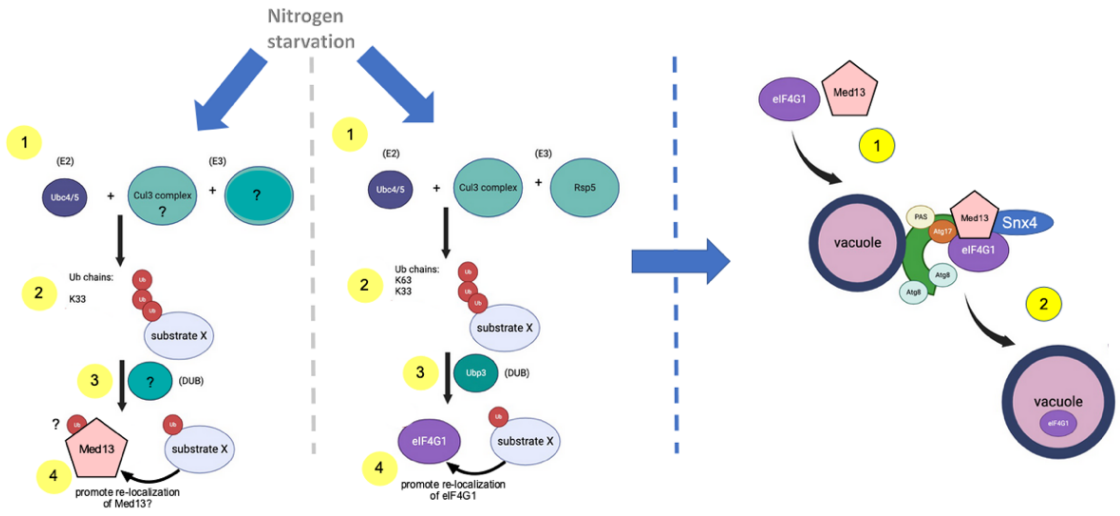

Figure 6.3. Model comparing ubiquitin-dependent autophagy of Med13 and eIF4G1 following nitrogen starvation. (Middle panel) Following nitrogen starvation, the E2 ubiquitin (Ub) conjugating enzymes Ubc4/Ubc5, along with the Cul3 E3 RING scaffold complex, and the E3 ligase Rsp5 mediate vacuolar degradation of eIF4G1. Formation of K63 and K33 Ub chain linkages, along with modification via the de-ubiquitinase (DUB) Ubp3, occur on an unknown substrate. Ubiquitination of the unknown substrate likely serves as a signal to trigger re-localization of eIF4G1 through the autophagy pathway. (Left panel) Like eIF4G1, Med13 requires Ubc4/Ubc5 for autophagic degradation. Preliminary data suggest Med13 may also require Cul3, though more studies would be required to confirm this and to investigate other potential E3 ligases which promote Med13 autophagy. Formation of K33 Ub chain linkages occur on either an unknown substrate or on Med13, and likely helps promote re-localization of Med13 to autophagy machinery. (Right panel) The sorting nexin heterodimer Snx4-Atg20 and autophagy-related protein Atg17 further mediate vacuolar proteolysis of eIF4G1 and Med13 by serving as a scaffold to the phagophore assembly site (PAS) at the vacuole. Model created with Canvas and BioRender.

Chapter 7

Summary and Conclusions

Summary of Findings

Protein Synthesis and Degradation Pathways Converge with the CKM and eIF4G1 to Respond Appropriately to Stress

This thesis has provided new insights into how transcription, translation, and protein degradation pathways are coordinated following cellular stress. Although much is known about each individual process, significant gaps exist in our knowledge of how these homeostasis-related programs are coordinated. In chapters 3 and 4, I revealed new crosstalk between transcriptional and translational control. These two pathways can converge through the Cdk8 Kinase Module (CKM) because the CKM serves a transcriptional function in controlling expression of translation machinery (**Figure 7.1**). In chapter 5, I also observed new links between ubiquitin and autophagy in controlling degradation of eIF4G1, an important translation initiation factor (TIF) involved in cap-dependent translation, following nitrogen starvation stress (**Figure 7.1**). Likewise in chapter 6, I revealed that Med13, a member of the CKM, requires ubiquitination for its autophagic degradation.

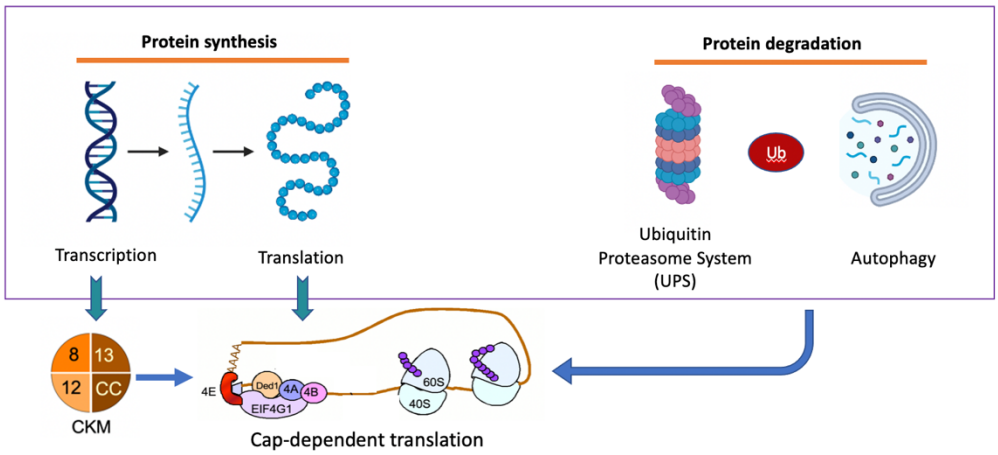

Figure 7.1. New crosstalk of protein synthesis and degradation pathways. Transcription and translation, two distinct pathways in protein synthesis, can converge through the Cdk8 Kinase Module (CKM). The CKM serves transcriptional functions in controlling expression of translation machinery. Ubiquitin and autophagy also converge to control degradation of eIF4G1, an important translation initiation factor (TIF) involved in cap-dependent translation, following nitrogen starvation stress.

New Transcriptional Role of the CKM in Regulating Translation-Associated Genes

In this thesis, I determined that the Cdk8 Kinase Module (CKM) positively regulates the expression of specific TIFs and RPs involved in translation, including the TIF eIF4G1 (Chapter 3), in physiological conditions. To our knowledge, this is the first description of the CKM in regulating translation-associated gene expression. These results build upon the model that the CKM serves a dual transcriptional role in both repressing stress response genes and positively regulating translation-related genes. This transcriptional role of the CKM is its primary role, a.k.a. "day job" (**Figure 7.2,** left panel**)**. We further observed that the CKM also controls cell fate following treatment with ribosome-targeting antibiotics, which further demonstrates that the CKM can respond to different cellular stresses that inhibit or alter protein synthesis (see Chapter 3) (**Figure 7.2,** top middle panel). Unlike following oxidative or starvation stress [7]**,** I observed that

disassembly of the CKM is not required for it to regulate genes that promote survival in response to treatment with specific ribosome-targeting antibiotics.

New Cytoplasmic Role of the CKM Member Med13 in Regulating P-Body Assembly Factor Edc3

The CKM is also well known to respond to different environmental stressors, including nitrogen starvation and oxidative stress. In oxidative stress, cyclin C serves a conserved cytoplasmic role in promoting mitochondrial fission to promote cell death, which can be referred to as its "night job" [124]. This model is consistent with my observation that cyclin C promotes mitochondrial fission in the presence of a ribosome-targeting antibiotic which also promotes ROS (see Chapter 3). We further outline a novel cytoplasmic "night job" of Med13 in promoting Edc3 to assemble into P-bodies before its autophagic degradation (Chapter 4) **(Figure 7.2,** lower right panel**)**. Edc3 is a conserved mRNA de-capping factor that is required for P-body assembly following various stresses including nitrogen starvation [276] [278]. These findings contribute to our understanding of how the CKM mediates both transcriptional and translational control following cellular stress, as well as the transcriptional and degradation mechanisms that control expression of eIF4G1. The outcome of these studies contributes to our understanding of the molecular pathways which become dysfunctional in many diseases including cancer and neurodegenerative disease [377].

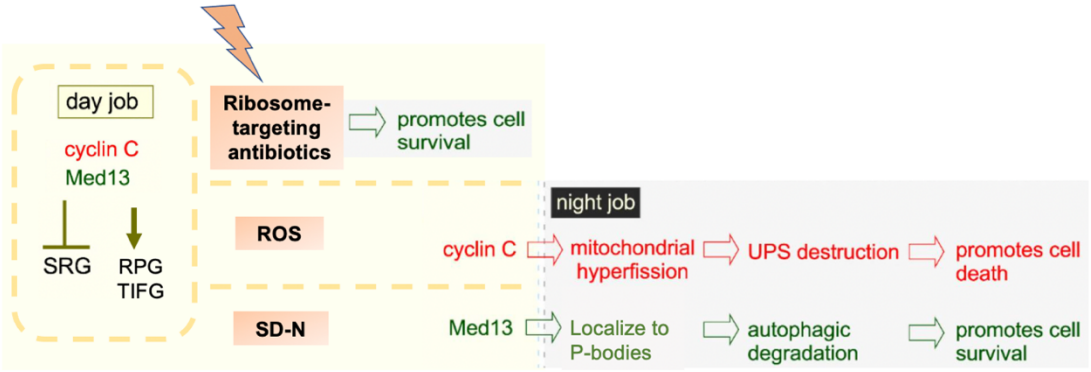

Figure 7.2. The Cdk8 Kinase Module (CKM) serves "day" and "night" roles in the cellular response to stress. In unstressed conditions, assembly of the yeast CKM at the mediator represses stress response genes (SRG) and promotes expression of specific ribosomal protein genes (RPG) and translation initiation factor genes (TIFG). This is known as its "day job". Assembly of the CKM serves a transcriptional role in promoting survival following treatment with several ribosome-targeting antibiotics which inhibit or alter protein synthesis. However, the exact transcriptional role requires investigation. One possible explanation is that the CKM promotes the upregulation of RP and TIF genes, and/or the CKM serves alternative transcriptional roles for promoting survival. Following reactive oxygen species (ROS) and nitrogen starvation (SD-N) stress, the CKM is disassembled, relieving repression of SRG (such as the gene *ATG8*) and promoting changes in RP and TIF mRNA expression. In oxidative stress, cyclin C serves a conserved cytoplasmic role in promoting mitochondrial fission which is important for eliciting cell death [124]. This secondary role can be referred to as its "night job". We further outline a novel cytoplasmic "night job" of Med13 in promoting degradation of Edc3, a P-body protein associated with translation regulation, following nitrogen starvation.

Conclusions

The CKM: A New Player in Coordinating Transcription with Translation Pathways

Transcription and translation are essential for protein synthesis and cellular processes including cell growth and survival. Regulated levels of transcription factors, ribosomal proteins (RPs) and translation initiation factors (TIFs) are also particularly important in environmental stress [378, 379] [380] [381] [382]. Imbalances in protein synthesis machinery are associated with conditions such as cancers, Alzheimer's Disease, heart defects, and intellectual disability [1-3]. However, the coordination between

transcription and translational control, especially under stress conditions, is exceedingly complex and not yet fully understood. Here, in Chapters 3 and 4, we demonstrate that the Cdk8 Kinase Module (CKM) is found at the crossroads of these processes.

The CKM, composed of cyclin C, Cdk8, and two structural proteins. Med12 and Med13, plays a crucial role in regulating the transcription of stress response genes (SRG) [7]. The CKM primarily suppresses SRG in yeast under normal conditions, while serving a dual function of activating and repressing these genes in mammalian cells [52] [53]. My research (outlined in Chapter 3) uncovered a novel role of the CKM in also maintaining constitutive expression of genes which encode proteins involved in translation under normal conditions in yeast. Among these include the 60S ribosomal protein (RP) Rpl3, as well as the TIFs Ded1 and eIF4G1. We found that the CKM indirectly promotes both the mRNA and protein expression of these RPs and TIFs through its Cdk8 kinase activity. Building upon the established model that the yeast CKM represses RNA Pol II-mediated gene transcription at the Mediator, one possible mechanism is that the CKM represses transcription of a repressor of these RP and TIF genes. Alternatively, this could be accomplished through Cdk8's known ability to directly phosphorylate and promote proteolysis of transcriptional repressors [194]. However, the control of each RP and TIF gene is complex, indicating that the CKM may influence their expression by phosphorylating multiple regulators of translation genes. More studies are needed to decipher the precise mechanisms by which the CKM controls RP and TIF genes.

Nevertheless, these new data demonstrate for the first time that the CKM can function at the crossroads of two protein synthesis pathways through its role in controlling translation machinery expression at the level of transcription. Importantly, these findings

further show that while transcription and translation are often considered separate processes, they are closely interconnected, and we are still discovering how they influence one another.

Stress Adaptation Requires Precise Changes in Ribosomal Protein And Translation Initiation Factor Expression

The CKM does not impact overall cell growth and translation rate in physiological conditions. However, the CKM control of specific RP and TIF genes is important because regulated RP and TIF expression is critical for adapting to stress [85] [383] [84] [384] [131]. Environmental signals which inhibit TORC1, for instance, cause inhibition of general protein synthesis to conserve energy and arrest cell growth [10, 11]. The inhibition of global translation largely depends on phosphorylation of a translation initiation factor eIF2α [12]. However, controlled gene and protein expression of specific translation-associated proteins are also important for fine-tuning the cellular response to stress [13, 14]. For example, recent studies demonstrated that mammalian Rpl3 is a critical regulator of mitohcondrial apoptosis and cell migration in nucleolar stress in mouse and HCT116 cells [378, 379]. In DNA damage or TORC1 inhibition stresses, the RNA helicase Ded1 regulates overall translation inhibition and cellular recovery [380], eIF4G1 levels control growth arrest and translation of stress-specific mRNAs [383], and both Ded1 and eIF4G1 promote stress granule formation to control mRNA function in adverse conditions [381]. Moreover, eIF4E binding sites are critical for formation of mRNA processing bodies (P-bodies), which are important for controlling translation and mRNA degradation in stress [385]. These suggest the possibility that the CKM regulates the expression of Rpl3, eIF4E,

eIF4G1, and Ded1 to prime the cell for an appropriate response to stress. Moreover, recent data in our lab demonstrated that this transcriptional role of the CKM in promoting expression of the evolutionarily conserved 60S RP Rpl3 occurs across different cell types, from yeast to mammalian cells (Friedson et al., 2024- *manuscript under revision*). This suggests the possibility that the CKM may promote Rpl3 expression for a similar cellular function across species.

The CKM Helps Control the Cellular Response to Stresses Which Inhibit or Alter Protein Synthesis

The CKM plays an important transcriptional role in promoting survival following starvation or stationary phase. These stresses both inhibit and fine-tune the translation machinery [10, 11]. Previous yeast competitive fitness screens demonstrate that compared to WT cells, CKM knockout mutants exhibit decreased competitive growth. This suggests a role of the CKM in promoting growth when resources are limited [252] [386]. My recent findings in yeast demonstrate that CKM mutants also exhibit heightened sensitivity to antibiotics (Chapter 3), highlighting that assembly of the CKM at the Mediator serves a critical transcriptional role in the cellular response to translation stress. However, more studies are required to determine how translation machinery and other potential processes regulated by the CKM, including SRG, could be contributing to how the CKM responds to translation stress induced by antibiotics.

The upregulation of translation machinery in cancer cells has led to the development of new chemotherapeutic strategies targeting ribosomes [81] [263]. In 2012, Homoharringtonine (HHT) received FDA approval for treating Chronic Myeloid Leukemia in patients resistant to tyrosine kinase inhibitors [387] [388]. Further data

collected by Dr. Stephen Willis in our lab demonstrate that loss of the CKM may enhance the effectiveness of HHT and other ribosome inhibitors. Cell lines lacking cyclin C or inhibited for Cdk8/19 function showed sensitivity to these drugs in both MEF and HCT116 cell lines (included in Friedson et al., 2024- *manuscript under revision*). These findings highlight dysregulation of the translational network upon CKM subunit loss, making the CKM an attractive druggable target for many diseases. Notably, altered expression of cyclin C, Med12, and Cdk8 has been implicated in various cancers [124]. Cyclin C has been shown to act as a tumor suppressor, while Cdk8 can act as an oncogene in specific cancers [389-391], suggesting that the CKM's roles in controlling cell survival are complex. Understanding the CKM's roles in controlling translation machinery and its response to inhibition can therefore improve treatments for these diseases.

Furthermore, when comparing the CKM's response to various translation inhibitors in yeast, it appears that its reaction is tailored to the specific mechanism of each inhibitor. For example, we observed that cyclin C facilitates mitochondrial fission and subsequent cell death in response to the translation inhibitor Paromomycin (Chapter 3), which is known to induce oxidative stress and disrupt mitochondrial membrane integrity [237]. Previously, our research indicated that cyclin C also induces stress-induced mitochondrial hyper-fission upon exposure to hydrogen peroxide, a direct oxidative stress inducer [124]. After oxidative stress induced by Paromomycin was alleviated with NAC, cyclin C's localization remained nuclear, suggesting that cyclin C's secondary response to Paromomycin likely involves intensified oxidative stress. This dual role of cyclin C illustrates that while it initially supports cell survival in the face of direct translation

inhibition stress, it can shift to induce cell death in the presence of oxidative stress or when mitochondrial translation is directly inhibited by compounds like Chloramphenicol.

The CKM Serves Both Nuclear and Cytoplasmic Roles With Translation-Associated Machinery Following Nitrogen Starvation Stress

Just like RPs and TIFs, the CKM also serves important multi-functional roles in stress. Upon sensing unfavorable environmental cues including nitrogen starvation and oxidative stress, the CKM disassembles to promote either a cell survival or death response [7]. It is well known that disassembly of the CKM in these stressors is critical for relieving the repression of stress responsive genes (SRG's) [46, 54]. My recent observations (see Chapter 4) suggest that the CKM also mediates efficient decrease in RP and TIF mRNA following nitrogen starvation, which demonstrates an additional role of CKM disassembly in the transcriptional response to stress. Moreover, our lab has previously demonstrated that the CKM also serves important secondary roles in the cytoplasm. Here in response to high levels of oxidative stress, cyclin C relocates to the mitochondria where it is required for stress-induced mitochondrial hyper-fission, and promotes regulated cell death [247]. In contrast, during survival cues triggered by nitrogen starvation, cyclin C is degraded within the nucleus [46]. This both protects the mitochondria from stress-induced fission and allows for the up-regulation of autophagy-related (ATG) genes that are required for cell survival. In addition, following nitrogen starvation, Med13 re-localizes to the cytoplasm, where it is assisted by the sorting nexin heterodimer Snx4-Atg20 to be degraded in the vacuole via a new cargo hitchhiking autophagy pathway [56].

As cyclin C has a cytoplasmic role following stress, we also investigated if the same were true for Med13. Studies outlined in Chapter 4 of this thesis, performed in

collaboration with two other graduate students, Dr. Sara Hanley and Dr. Stephen Willis, uncovered a cytoplasmic role for Med13 as well. In the cytoplasm, Med13 promotes the degradation and delivery of mRNA de-capping factor Edc3 into P-bodies. P-bodies are liquid condensates which are formed in stress to store or degrade non-translating mRNA-protein complexes [21], though how P-bodies are regulated in stress has not been well understood. Thus, our observation that Med13 helps degrade Edc3 fills a gap in knowledge of how P-body proteins are controlled in stress. These also demonstrate a cytoplasmic function of the CKM in orchestrating the control of mRNA and translation-associated proteins, in addition to its transcriptional role in controlling TIF and RP gene expression. This is important as we observed that the CKM facilitates cell cycle arrest and survival during periods of starvation or stationary phase (Hanley et al., *manuscript under revision*, 2024). These findings highlight that the CKM can enable cells to effectively respond to translation-inhibiting stressors by fine-tuning multiple aspects of mRNA expression and function.

Ubiquitin-Dependent Autophagic Degradation of Protein Synthesis Machinery Occurs in Nitrogen Starvation

When cells face adverse environmental conditions like nutrient deprivation, they must coordinate protein synthesis and degradation pathways to either promote survival or initiate programmed cell death, depending on the type and severity of the stress [6, 7]. For instance, during nitrogen starvation, cells adopt a pro-survival response by reducing general protein synthesis to conserve energy and halt cell growth [10, 11]. This inhibition of translation machinery involves the degradation of components such as ribosomal proteins and specific initiation factors [13, 14]. Despite overall translation repression under stress, cells must finely adjust translational machinery to synthesize stress-response

proteins (SRPs) crucial for survival [16-19]. Many of these SRPs are involved in autophagy, an upregulated catabolic process during adverse conditions like nitrogen starvation, which recycles proteins and organelles via vacuolar proteases [17, 22, 23].

The translation initiation factor (TIF) eIF4G1 acts as a scaffold to assemble other TIFs into the eIF4F complex, which recruits the 40S ribosome to mRNA under normal physiological conditions [307]. Thus, eIF4G1 plays a crucial role in the rate-limiting step of translation, controlling cap-dependent translation and cell growth. However, the detailed mechanisms underlying eIF4G1 autophagic degradation remained unclear. Moreover, ubiquitin and autophagy are more intricately linked than previously thought [303], but the comprehensive roles of Ub in selective autophagy pathways remains unclear. Here, we investigated the ubiquitin-dependent eIF4G1 autophagy mechanism (presented in Chapter 5), further illuminating the intricate relationship between protein synthesis and degradation pathways during nitrogen starvation stress.

In Chapter 5, we uncovered the molecular mechanisms driving ubiquitin-dependent autophagic degradation of the translation initiation factor eIF4G1 following nitrogen starvation. Our findings confirm previous insights that eIF4G1 undergoes autophagic degradation facilitated by the deubiquitinase Ubp3 after nitrogen starvation. We observed Atg17, Snx4, and its cofactor Atg20 mediate eIF4G1 targeting to vacuole-associated phagophores. Snx4 promotes selective autophagy of diverse protein substrates including Med13 [56, 117-119], suggesting that Snx4 also promotes degradation of eIF4G1 through a selective autophagy pathway. In addition, the involvement of the ubiquitin-interacting motif (UIM)-UIM-docking site (UDS) domain of Atg8 in eIF4G1 degradation supports a

selective autophagy model requiring a ubiquitin-binding receptor or adaptor. However, future studies are needed to determine which receptor it requires.

Furthermore, our study highlights ubiquitination's role in eIF4G1 autophagy, emphasizing the diversity of ubiquitin beyond targeting substrates to the proteasome. Ubiquitin chain linkages K33 and K63 are crucial for eIF4G1 autophagy, aligning with roles in protein trafficking and selective autophagy of cargo proteins [297, 302]. Cul3, known for its proteasomal functions [332], unexpectedly promotes eIF4G1 autophagy through neddylation-dependent activation, suggesting a new role for Cul3 in trafficking a substrate to autophagy machinery [334, 335]. Rsp5, a versatile E3 ligase, also contributes to eIF4G1 autophagy, though the precise function of Rsp5 is unclear due to the diverse roles of Rsp5 in various cellular pathways [340, 341].

Our studies show that eIF4G1 is not directly ubiquitinated following nitrogen starvation. This suggests a model in which another player in the pathway is being targeted by the PTM. A strong candidate is the unknown receptor protein. This receptor must contain a ubiquitin -interacting domain which in turn interacts with the UDS site in Atg8. Five candidate UIM-containing receptor proteins were identified in a Mass Spec screen. Further studies are needed to identify whether one of these UIM containing proteins is the receptor protein for eIF4G1 degradation, and whether it is the recipient protein of ubiquitination in this pathway.

We also observed that a similar ubiquitin-dependent autophagy pathway occurs for the transcription factor Med13 (see Chapter 6). Like eIF4G1, Med13 requires Ubc4/5, Cul3, and the K33 Ub chain linkages for Snx4-assisted autophagic degradation. As K33 Ub chains are associated with roles in protein trafficking, this suggests that ubiquitination

likely promotes re-localization of both Med13 and eIF4G1 to autophagy machinery, though more studies would be required to test this hypothesis. However, the different receptor protein and Atg8-binding domain requirements between eIF4G1 and Med13 suggest that they require unique mechanisms for ubiquitin-dependent autophagic degradation.

Our recent observation that Med13 normally positively regulates RP and TIF gene expression, including *EIF4G1* (see Chapter 3), suggests the possibility that this ubiquitin-dependent autophagy pathway targets Med13 to further repress RP and TIF levels following stress. Likewise, our newly discovered role of Med13 in promoting degradation of a P-body protein (see Chapter 4) further suggests a potential role of Ub in targeting Med13 to control P-body dynamics in nitrogen starvation. More studies are required to further elucidate the precise functions and mechanisms of ubiquitin in these pathways. Nevertheless, these data collectively demonstrate the crosstalk of ubiquitin and autophagy in mediating the degradation of important regulators of protein synthesis.

Understanding eIF4G1 Proteolysis for the Treatment or Prevention of Diseases

Given eIF4G1's conserved role in translation initiation and its involvement in stress responses like TORC1 inhibition [16, 131, 307], understanding eIF4G1's degradation pathway holds implications for understanding diseases linked to impaired proteostasis, such as cancer and neurodegenerative disorders. For instance, overexpression of mammalian EIF4G1 increases translation and promotes cancer cell proliferation and survival across multiple cancer types [81, 127, 128]. Mutations in serine residues of eIF4G1 are also associated with Parkinson's Disease [128, 312], while overexpression of eIF4G1 has been shown to clear toxic alpha-synuclein aggregates in yeast [309]. These

indicate that regulated eIF4G1 expression serves important functions in controlling cellular survival. Despite slight variations in functional domains, eIF4G1 functions are highly conserved from yeast to humans [370]. Uncovering eIF4G1's autophagic degradation pathway in yeast could thus provide insights into targets required for its proteolysis, offering potential therapeutic interventions. For example, pharmaceuticals targeting neddylation can modulate Cullin ligase complexes to inhibit cell growth in cancers [371]. Our finding that Cul3 regulates eIF4G1 autophagy also suggests avenues for testing stabilization of eIF4G1 expression in mammalian systems with Neddylation inhibitors and potentially reducing alpha-synuclein aggregation in neurodegenerative disorders.

References

1. Venturi, G. and L. Montanaro, *How Altered Ribosome Production Can Cause or Contribute to Human Disease: The Spectrum of Ribosomopathies.* Cells, 2020. **9**(10).

2. Scheper, G.C., M.S. van der Knaap, and C.G. Proud, *Translation matters: protein synthesis defects in inherited disease.* Nat Rev Genet, 2007. **8**(9): p. 711-23.

3. Cheng, J., et al., *The emerging roles of protein homeostasis-governing pathways in Alzheimer's disease.* Aging Cell, 2018. **17**(5): p. e12801.

4. Murphy, M.P. and H. LeVine, 3rd, *Alzheimer's disease and the amyloid-beta peptide.* J Alzheimers Dis, 2010. **19**(1): p. 311-23.

5. Williams, T.D. and A. Rousseau, *Translation regulation in response to stress.* Febs j, 2024.

6. Fulda, S., et al., *Cellular stress responses: cell survival and cell death.* Int J Cell Biol, 2010. **2010**: p. 214074.

7. Friedson, B. and K.F. Cooper, *Cdk8 Kinase Module: A Mediator of Life and Death Decisions in Times of Stress.* Microorganisms, 2021. **9**(10).

8. Foltman, M. and A. Sanchez-Diaz, *TOR Complex 1: Orchestrating Nutrient Signaling and Cell Cycle Progression.* Int J Mol Sci, 2023. **24**(21).

9. Gonzalez, S. and C. Rallis, *The TOR Signaling Pathway in Spatial and Temporal Control of Cell Size and Growth.* Front Cell Dev Biol, 2017. **5**: p. 61.

10. Conrad, M., et al., *Nutrient sensing and signaling in the yeast Saccharomyces cerevisiae.* FEMS Microbiol Rev, 2014. **38**(2): p. 254-99.

11. Rødkaer, S.V. and N.J. Faergeman, *Glucose- and nitrogen sensing and regulatory mechanisms in Saccharomyces cerevisiae.* FEMS Yeast Res, 2014. **14**(5): p. 683-96.

12. Wek, R.C., *Role of eIF2α Kinases in Translational Control and Adaptation to Cellular Stress.* Cold Spring Harb Perspect Biol, 2018. **10**(7).

13. Kelly, S.P. and D.M. Bedwell, *Both the autophagy and proteasomal pathways facilitate the Ubp3p-dependent depletion of a subset of translation and RNA turnover factors during nitrogen starvation in Saccharomyces cerevisiae.* Rna, 2015. **21**(5): p. 898-910.

14. Kraft, C., et al., *Mature ribosomes are selectively degraded upon starvation by an autophagy pathway requiring the Ubp3p/Bre5p ubiquitin protease.* Nat Cell Biol, 2008. **10**(5): p. 602-10.

15. Advani, V.M. and P. Ivanov, *Translational Control under Stress: Reshaping the Translatome.* Bioessays, 2019. **41**(5): p. e1900009.

16. Acevo-Rodríguez, P.S., et al., *Autophagy Regulation by the Translation Machinery and Its Implications in Cancer.* Front Oncol, 2020. **10**: p. 322.

17. Goldsmith, J., et al., *Ribosome profiling reveals a functional role for autophagy in mRNA translational control.* Commun Biol, 2020. **3**(1): p. 388.

18. Liu, X., et al., *Dhh1 promotes autophagy-related protein translation during nitrogen starvation.* PLoS Biol, 2019. **17**(4): p. e3000219.

19. Lubas, M., et al., *eIF5A is required for autophagy by mediating ATG3 translation.* EMBO Rep, 2018. **19**(6).

20. Brangwynne, C.P., et al., *Germline P granules are liquid droplets that localize by controlled dissolution/condensation.* Science, 2009. **324**(5935): p. 1729-32.

21. Luo, Y., Z. Na, and S.A. Slavoff, *P-Bodies: Composition, Properties, and Functions.* Biochemistry, 2018. **57**(17): p. 2424-2431.

22. Dobrenel, T., et al., *TOR Signaling and Nutrient Sensing.* Annu Rev Plant Biol, 2016. **67**: p. 261-85.

23. Onodera, J. and Y. Ohsumi, *Autophagy is required for maintenance of amino acid levels and protein synthesis under nitrogen starvation.* J Biol Chem, 2005. **280**(36): p. 31582-6.

24. Fleming, A., et al., *The different autophagy degradation pathways and neurodegeneration.* Neuron, 2022. **110**(6): p. 935-966.

25. Madeo, F., et al., *Oxygen stress: a regulator of apoptosis in yeast.* J Cell Biol, 1999. **145**(4): p. 757-67.

26. Perrone, G.G., S.X. Tan, and I.W. Dawes, *Reactive oxygen species and yeast apoptosis.* Biochim Biophys Acta, 2008. **1783**(7): p. 1354-68.

27. Ghosh, A. and N. Shcherbik, *Effects of Oxidative Stress on Protein Translation: Implications for Cardiovascular Diseases.* Int J Mol Sci, 2020. **21**(8).

28. Guaragnella, N., et al., *The role of mitochondria in yeast programmed cell death.* Front Oncol, 2012. **2**: p. 70.

29. Tait, S.W. and D.R. Green, *Mitochondrial regulation of cell death.* Cold Spring Harb Perspect Biol, 2013. **5**(9).

30. Struhl, K., *Fundamentally different logic of gene regulation in eukaryotes and prokaryotes.* Cell, 1999. **98**(1): p. 1-4.

31. Spitz, F. and E.E. Furlong, *Transcription factors: from enhancer binding to developmental control.* Nat Rev Genet, 2012. **13**(9): p. 613-26.

32. Bourbon, H.M., *Comparative genomics supports a deep evolutionary origin for the large, four-module transcriptional mediator complex.* Nucleic Acids Res, 2008. **36**(12): p. 3993-4008.

33. Nagulapalli, M., et al., *Evolution of disorder in Mediator complex and its functional relevance.* Nucleic Acids Res, 2016. **44**(4): p. 1591-612.

34. Malik, S., et al., *Structural and functional organization of TRAP220, the TRAP/mediator subunit that is targeted by nuclear receptors.* Mol Cell Biol, 2004. **24**(18): p. 8244-54.

35. Taatjes, D.J. and R. Tjian, *Structure and function of CRSP/Med2; a promoter-selective transcriptional coactivator complex.* Mol Cell, 2004. **14**(5): p. 675-83.

36. Jeronimo, C. and F. Robert, *The Mediator Complex: At the Nexus of RNA Polymerase II Transcription.* Trends Cell Biol, 2017. **27**(10): p. 765-783.

37. Jeronimo, C., et al., *Tail and Kinase Modules Differently Regulate Core Mediator Recruitment and Function In Vivo.* Mol Cell, 2016. **64**(3): p. 455-466.

38. Petrenko, N., et al., *Evidence that Mediator is essential for Pol II transcription, but is not a required component of the preinitiation complex in vivo.* Elife, 2017. **6**.

39. Elmlund, H., et al., *The cyclin-dependent kinase 8 module sterically blocks Mediator interactions with RNA polymerase II.* Proc Natl Acad Sci U S A, 2006. **103**(43): p. 15788-93.

40. Willis, S.D., et al., *Cyclin C-Cdk8 Kinase Phosphorylation of Rim15 Prevents the Aberrant Activation of Stress Response Genes.* Front Cell Dev Biol, 2022. **10**: p. 867257.

41. Osman, S., et al., *The Cdk8 kinase module regulates interaction of the mediator complex with RNA polymerase II.* J Biol Chem, 2021. **296**: p. 100734.

42. Nemet, J., et al., *The two faces of Cdk8, a positive/negative regulator of transcription.* Biochimie, 2014. **97**: p. 22-7.

43. van de Peppel, J., et al., *Mediator expression profiling epistasis reveals a signal transduction pathway with antagonistic submodules and highly specific downstream targets.* Mol Cell, 2005. **19**(4): p. 511-22.

44. Ansari, S.A. and R.H. Morse, *Mechanisms of Mediator complex action in transcriptional activation.* Cell Mol Life Sci, 2013. **70**(15): p. 2743-56.

45. Cooper, K.F., et al., *Stress and developmental regulation of the yeast C-type cyclin Ume3p (Srb11p/Ssn8p).* EMBO J, 1997. **16**(15): p. 4665-75.

46. Willis, S.D., et al., *Ubiquitin-proteasome-mediated cyclin C degradation promotes cell survival following nitrogen starvation.* Mol Biol Cell, 2020. **31**(10): p. 1015-1031.

47. Strich, R., M.R. Slater, and R.E. Esposito, *Identification of negative regulatory genes that govern the expression of early meiotic genes in yeast.* Proc. Natl. Acad. Sci. USA, 1989. **86**: p. 10018-10022.

48. Ansari, S.A., Q. He, and R.H. Morse, *Mediator complex association with constitutively transcribed genes in yeast.* Proc Natl Acad Sci U S A, 2009. **106**(39): p. 16734-9.

49. Hirst, M., et al., *GAL4 is regulated by the RNA polymerase II holoenzyme-associated cyclin-dependent protein kinase SRB10/CDK8.* Mol Cell, 1999. **3**(5): p. 673-8.

50. Vincent, O., et al., *Interaction of the Srb10 kinase with Sip4, a transcriptional activator of gluconeogenic genes in Saccharomyces cerevisiae.* Mol Cell Biol, 2001. **21**(17): p. 5790-6.

51. Sadowski, I., et al., *GAL4 is phosphorylated as a consequence of transcriptional activation.* Proc Natl Acad Sci U S A, 1991. **88**(23): p. 10510-4.

52. Li, Y.-C., et al., *Structure and noncanonical Cdk8 activation mechanism within an Argonaute-containing Mediator kinase module.* Science Advances, 2021. **7**(3): p. eabd4484.

53. Stieg, D.C., et al., *Cyclin C Regulated Oxidative Stress Responsive Transcriptome in Mus musculus Embryonic Fibroblasts.* G3 (Bethesda), 2019. **9**(6): p. 1901-1908.

54. Cooper, K.F., et al., *Oxidative-stress-induced nuclear to cytoplasmic relocalization is required for Not4-dependent cyclin C destruction.* J Cell Sci, 2012. **125**(Pt 4): p. 1015-26.

55. Delorme-Axford, E. and D.J. Klionsky, *Transcriptional and post-transcriptional regulation of autophagy in the yeast Saccharomyces cerevisiae.* J Biol Chem, 2018. **293**(15): p. 5396-5403.

56. Hanley, S.E., S.D. Willis, and K.F. Cooper, *Snx4-assisted vacuolar targeting of transcription factors defines a new autophagy pathway for controlling ATG expression.* Autophagy, 2021: p. 1-19.

57. Murray, A.W., *Recycling the cell cycle: cyclins revisited.* Cell, 2004. **116**(2): p. 221-34.

58. Morgan, D.O., *Cyclin-dependent kinases: engines, clocks, and microprocessors.* Annu Rev Cell Dev Biol, 1997. **13**: p. 261-91.

59. Wood, D.J. and J.A. Endicott, *Structural insights into the functional diversity of the CDK-cyclin family.* Open Biol, 2018. **8**(9).

60. Fisher, R.P., *The CDK Network: Linking Cycles of Cell Division and Gene Expression.* Genes Cancer, 2012. **3**(11-12): p. 731-8.

61. Lim, S. and P. Kaldis, *Cdks, cyclins and CKIs: roles beyond cell cycle regulation.* Development, 2013. **140**(15): p. 3079-93.

62. Galbraith, M.D., H. Bender, and J.M. Espinosa, *Therapeutic targeting of transcriptional cyclin-dependent kinases.* Transcription, 2019. **10**(2): p. 118-136.

63. Anshabo, A.T., et al., *CDK9: A Comprehensive Review of Its Biology, and Its Role as a Potential Target for Anti-Cancer Agents.* Front Oncol, 2021. **11**: p. 678559.

64. Dannappel, M.V., et al., *Molecular and in vivo Functions of the CDK8 and CDK19 Kinase Modules.* Front Cell Dev Biol, 2019. **6**: p. 171.

65. Constantin, T.A., et al., *Transcription associated cyclin-dependent kinases as therapeutic targets for prostate cancer.* Oncogene, 2022. **41**(24): p. 3303-3315.

66. Sonenberg, N. and A.G. Hinnebusch, *Regulation of translation initiation in eukaryotes: mechanisms and biological targets.* Cell, 2009. **136**(4): p. 731-45.

67. Hilliker, A., et al., *The DEAD-box protein Ded1 modulates translation by the formation and resolution of an eIF4F-mRNA complex.* Mol Cell, 2011. **43**(6): p. 962-72.

68. Gupta, N., J.R. Lorsch, and A.G. Hinnebusch, *Yeast Ded1 promotes 48S translation pre-initiation complex assembly in an mRNA-specific and eIF4F-dependent manner.* Elife, 2018. **7**.

69. Berset, C., et al., *RNA-binding activity of translation initiation factor eIF4G1 from Saccharomyces cerevisiae.* Rna, 2003. **9**(7): p. 871-80.

70. Jackson, R.J., C.U. Hellen, and T.V. Pestova, *The mechanism of eukaryotic translation initiation and principles of its regulation.* Nat Rev Mol Cell Biol, 2010. **11**(2): p. 113-27.

71. Iost, I., M. Dreyfus, and P. Linder, *Ded1p, a DEAD-box protein required for translation initiation in Saccharomyces cerevisiae, is an RNA helicase.* J Biol Chem, 1999. **274**(25): p. 17677-83.

72. Strunk, B.S. and K. Karbstein, *Powering through ribosome assembly.* Rna, 2009. **15**(12): p. 2083-104.

73. Mélèse, T. and Z. Xue, *The nucleolus: an organelle formed by the act of building a ribosome.* Curr Opin Cell Biol, 1995. **7**(3): p. 319-24.

74. Petibon, C., et al., *Regulation of ribosomal protein genes: An ordered anarchy.* Wiley Interdiscip Rev RNA, 2021. **12**(3): p. e1632.

75. Mittal, N., et al., *The Gcn4 transcription factor reduces protein synthesis capacity and extends yeast lifespan.* Nat Commun, 2017. **8**(1): p. 457.

76. Moehle, C.M. and A.G. Hinnebusch, *Association of RAP1 binding sites with stringent control of ribosomal protein gene transcription in Saccharomyces cerevisiae.* Mol Cell Biol, 1991. **11**(5): p. 2723-35.

77. Reja, R., et al., *Molecular mechanisms of ribosomal protein gene coregulation.* Genes Dev, 2015. **29**(18): p. 1942-54.

78. Magazinnik, T., et al., *Interplay between GCN2 and GCN4 expression, translation elongation factor 1 mutations and translational fidelity in yeast.* Nucleic Acids Res, 2005. **33**(14): p. 4584-92.

79. Joo, Y.J., et al., *Gcn4p-mediated transcriptional repression of ribosomal protein genes under amino-acid starvation.* Embo j, 2011. **30**(5): p. 859-72.

80. Kim, S.J. and R. Strich, *Rpl22 is required for IME1 mRNA translation and meiotic induction in S. cerevisiae.* Cell Div, 2016. **11**: p. 10.

81. Silvera, D., et al., *Essential role for eIF4GI overexpression in the pathogenesis of inflammatory breast cancer.* Nat Cell Biol, 2009. **11**(7): p. 903-8.

82. Pellegrino, S., et al., *Inhibition of the Eukaryotic 80S Ribosome as a Potential Anticancer Therapy: A Structural Perspective.* Cancers (Basel), 2021. **13**(17).

83. Haghighat, A. and N. Sonenberg, *eIF4G dramatically enhances the binding of eIF4E to the mRNA 5'-cap structure.* J Biol Chem, 1997. **272**(35): p. 21677-80.

84. Gilbert, W.V., et al., *Cap-independent translation is required for starvation-induced differentiation in yeast.* Science, 2007. **317**(5842): p. 1224-7.

85. Aryanpur, P.P., et al., *The DEAD-box RNA helicase Ded1 has a role in the translational response to TORC1 inhibition.* Mol Biol Cell, 2019. **30**(17): p. 2171-2184.

86. Marques-Ramos, A., et al., *Cap-independent translation ensures mTOR expression and function upon protein synthesis inhibition.* Rna, 2017. **23**(11): p. 1712-1728.

87. Pickart, C.M., *Mechanisms underlying ubiquitination.* Annu Rev Biochem, 2001. **70**: p. 503-33.

88. Ye, Y. and M. Rape, *Building ubiquitin chains: E2 enzymes at work.* Nat Rev Mol Cell Biol, 2009. **10**(11): p. 755-64.

89. Finley, D., et al., *The ubiquitin-proteasome system of Saccharomyces cerevisiae.* Genetics, 2012. **192**(2): p. 319-60.

90. Lecker, S.H., A.L. Goldberg, and W.E. Mitch, *Protein degradation by the ubiquitin-proteasome pathway in normal and disease states.* J Am Soc Nephrol, 2006. **17**(7): p. 1807-19.

91. Snyder, N.A. and G.M. Silva, *Deubiquitinating enzymes (DUBs): Regulation, homeostasis, and oxidative stress response.* J Biol Chem, 2021. **297**(3): p. 101077.

92. Randles, L. and K.J. Walters, *Ubiquitin and its binding domains.* Front Biosci (Landmark Ed), 2012. **17**(6): p. 2140-57.

93. Komander, D., *The emerging complexity of protein ubiquitination.* Biochem Soc Trans, 2009. **37**(Pt 5): p. 937-53.

94. Schauber, C., et al., *Rad23 links DNA repair to the ubiquitin/proteasome pathway.* Nature, 1998. **391**: p. 715-718.

95. Hartmann-Petersen, R., M. Seeger, and C. Gordon, *Transferring substrates to the 26S proteasome.* Trends Biochem Sci, 2003. **28**(1): p. 26-31.

96. Shi, Y., et al., *Rpn1 provides adjacent receptor sites for substrate binding and deubiquitination by the proteasome.* Science, 2016. **351**(6275).

97. Tanaka, K., *The proteasome: overview of structure and functions.* Proc Jpn Acad Ser B Phys Biol Sci, 2009. **85**(1): p. 12-36.

98. Khaminets, A., C. Behl, and I. Dikic, *Ubiquitin-Dependent And Independent Signals In Selective Autophagy.* Trends Cell Biol, 2016. **26**(1): p. 6-16.

99. Dikic, I., S. Wakatsuki, and K.J. Walters, *Ubiquitin-binding domains - from structures to functions.* Nat Rev Mol Cell Biol, 2009. **10**(10): p. 659-71.

100. Grumati, P. and I. Dikic, *Ubiquitin signaling and autophagy.* J Biol Chem, 2018. **293**(15): p. 5404-5413.

101. Takeshige, K., et al., *Autophagy in yeast demonstrated with proteinase-deficient mutants and conditions for its induction.* J Cell Biol, 1992. **119**(2): p. 301-11.

102. Klionsky, D.J., H. Nelson, and N. Nelson, *Compartment acidification is required for efficient sorting of proteins to the vacuole in Saccharomyces cerevisiae.* J Biol Chem, 1992. **267**(5): p. 3416-22.

103. Lynch-Day, M.A. and D.J. Klionsky, *The Cvt pathway as a model for selective autophagy.* FEBS Lett, 2010. **584**(7): p. 1359-66.

104. Lei, Y., et al., *How Cells Deal with the Fluctuating Environment: Autophagy Regulation under Stress in Yeast and Mammalian Systems.* Antioxidants (Basel), 2022. **11**(2).

105. Wen, X. and D.J. Klionsky, *An overview of macroautophagy in yeast.* J Mol Biol, 2016. **428**(9 Pt A): p. 1681-99.

106. Suzuki, K., et al., *Hierarchy of Atg proteins in pre-autophagosomal structure organization.* Genes Cells, 2007. **12**(2): p. 209-18.

107. Chan, S.N. and B.L. Tang, *Location and membrane sources for autophagosome formation - from ER-mitochondria contact sites to Golgi-endosome-derived carriers.* Mol Membr Biol, 2013. **30**(8): p. 394-402.

108. Reggiori, F. and D.J. Klionsky, *Autophagic processes in yeast: mechanism, machinery and regulation.* Genetics, 2013. **194**(2): p. 341-61.

109. Orenstein, S.J. and A.M. Cuervo, *Chaperone-mediated autophagy: molecular mechanisms and physiological relevance.* Semin Cell Dev Biol, 2010. **21**(7): p. 719-26.

110. Vargas, J.N.S., et al., *The mechanisms and roles of selective autophagy in mammals.* Nat Rev Mol Cell Biol, 2023. **24**(3): p. 167-185.

111. Kaushik, S. and A.M. Cuervo, *The coming of age of chaperone-mediated autophagy.* Nat Rev Mol Cell Biol, 2018. **19**(6): p. 365-381.

112. Noda, T., *Regulation of Autophagy through TORC1 and mTORC1.* Biomolecules, 2017. **7**(3).

113. Klionsky, D.J. and P. Codogno, *The mechanism and physiological function of macroautophagy.* J Innate Immun, 2013. **5**(5): p. 427-33.

114. Suzuki, K., *Selective autophagy in budding yeast.* Cell Death Differ, 2013. **20**(1): p. 43-8.

115. Farre, J.C. and S. Subramani, *Mechanistic insights into selective autophagy pathways: lessons from yeast.* Nat Rev Mol Cell Biol, 2016. **17**(9): p. 537-52.

116. Hanley, S.E. and K.F. Cooper, *Sorting Nexins in Protein Homeostasis.* Cells, 2020. **10**(1).

117. Nemec, A.A., et al., *Autophagic clearance of proteasomes in yeast requires the conserved sorting nexin Snx4.* J Biol Chem, 2017. **292**(52): p. 21466-21480.

118. Nice, D.C., et al., *Cooperative binding of the cytoplasm to vacuole targeting pathway proteins, Cvt13 and Cvt20, to phosphatidylinositol 3-phosphate at the pre-autophagosomal structure is required for selective autophagy.* J Biol Chem, 2002. **277**(33): p. 30198-207.

119. Okamoto, K., N. Kondo-Okamoto, and Y. Ohsumi, *Mitochondria-anchored receptor Atg32 mediates degradation of mitochondria via selective autophagy.* Dev Cell, 2009. **17**(1): p. 87-97.

120. Ohsumi, Y., *Historical landmarks of autophagy research.* Cell Res, 2014. **24**(1): p. 9-23.

121. Takeda, E., et al., *Receptor-mediated cargo hitchhiking on bulk autophagy.* Embo j, 2024. **43**(15): p. 3116-3140.

122. Stieg, D.C., et al., *A complex molecular switch directs stress-induced cyclin C nuclear release through SCF(Grr1)-mediated degradation of Med13.* Mol Biol Cell, 2018. **29**(3): p. 363-375.

123. Wang, K., et al., *Cyclin C mediates stress-induced mitochondrial fission and apoptosis.* Mol Biol Cell, 2015. **26**(6): p. 1030-43.

124. Jezek, J., et al., *Cyclin C: The Story of a Non-Cycling Cyclin.* Biology (Basel), 2019. **8**(1).

125. Jiao, L., et al., *Ribosome biogenesis in disease: new players and therapeutic targets.* Signal Transduct Target Ther, 2023. **8**(1): p. 15.

126. Chu, J., et al., *Translation Initiation Factors: Reprogramming Protein Synthesis in Cancer.* Trends Cell Biol, 2016. **26**(12): p. 918-933.

127. Jaiswal, P.K., et al., *Eukaryotic Translation Initiation Factor 4 Gamma 1 (EIF4G1): a target for cancer therapeutic intervention?* Cancer Cell Int, 2019. **19**: p. 224.

128. Liu, R.H., et al., *Eukaryotic translation initiation factor EIF4G1 p.Ser637Cys mutation in a family with Parkinson's disease with antecedent essential tremor.* Exp Ther Med, 2024. **27**(5): p. 206.

129. Kim, S.H., et al., *The mRNA translation initiation factor eIF4G1 controls mitochondrial oxidative phosphorylation, axonal morphogenesis, and memory.* Proc Natl Acad Sci U S A, 2023. **120**(25): p. e2300008120.

130. Gonatopoulos-Pournatzis, T., et al., *Autism-Misregulated eIF4G Microexons Control Synaptic Translation and Higher Order Cognitive Functions.* Mol Cell, 2020. **77**(6): p. 1176-1192.e16.

131. Ramírez-Valle, F., et al., *eIF4GI links nutrient sensing by mTOR to cell proliferation and inhibition of autophagy.* J Cell Biol, 2008. **181**(2): p. 293-307.

132. Berset, C., H. Trachsel, and M. Altmann, *The TOR (target of rapamycin) signal transduction pathway regulates the stability of translation initiation factor eIF4G in the yeast Saccharomyces cerevisiae.* Proceedings of the National Academy of Sciences, 1998. **95**(8): p. 4264-4269.

133. Chen, R.-H., Y.-H. Chen, and T.-Y. Huang, *Ubiquitin-mediated regulation of autophagy.* Journal of Biomedical Science, 2019. **26**(1): p. 80.

134. Berk, A.J., *Yin and yang of mediator function revealed by human mutants.* Proc Natl Acad Sci U S A, 2012. **109**(48): p. 19519-20.

135. Jezek, J., et al., *Mitochondrial translocation of cyclin C stimulates intrinsic apoptosis through Bax recruitment.* EMBO Rep, 2019. **20**(9): p. e47425.

136. Philip, S., et al., *Cyclin-Dependent Kinase 8: A New Hope in Targeted Cancer Therapy?* J Med Chem, 2018. **61**(12): p. 5073-5092.

137. Clark, A.D., M. Oldenbroek, and T.G. Boyer, *Mediator kinase module and human tumorigenesis.* Crit Rev Biochem Mol Biol, 2015. **50**(5): p. 393-426.

138. Ronne, H. and R. Rothstein, *Mitotic sectored colonies: evidence of heteroduplex DNA formation during direct repeat recombination.* Proc Natl Acad Sci U S A, 1988. **85**(8): p. 2696-700.

139. Janke, C., et al., *A versatile toolbox for PCR-based tagging of yeast genes: new fluorescent proteins, more markers and promoter substitution cassettes.* Yeast, 2004. **21**(11): p. 947-62.

140. Sikorski, R.S. and P. Hieter, *A system of shuttle vectors and yeast host strains designed for efficient manipulation of DNA in Saccharomyces cerevisiae.* Genet., 1989. **122**: p. 19-27.

141. Chang, Y. and W.K. Huh, *Ksp1-dependent phosphorylation of eIF4G modulates post-transcriptional regulation of specific mRNAs under glucose deprivation conditions.* Nucleic Acids Res, 2018. **46**(6): p. 3047-3060.

142. Spence, J., et al., *A ubiquitin mutant with specific defects in DNA repair and multiubiquitination.* Mol Cell Biol, 1995. **15**(3): p. 1265-73.

143. Le Boulch, M., et al., *Sensitive detection of protein ubiquitylation using a protein fragment complementation assay.* J Cell Sci, 2020. **133**(12).

144. Brothers, M. and J. Rine, *Mutations in the PCNA DNA Polymerase Clamp of Saccharomyces cerevisiae Reveal Complexities of the Cell Cycle and Ploidy on Heterochromatin Assembly.* Genetics, 2019. **213**(2): p. 449-463.

145. Shcherbik, N., S. Kumar, and D.S. Haines, *Substrate proteolysis is inhibited by dominant-negative Nedd4 and Rsp5 mutants harboring alterations in WW domain 1.* J Cell Sci, 2002. **115**(Pt 5): p. 1041-8.

146. Gadal, O., et al., *Nuclear export of 60s ribosomal subunits depends on Xpo1p and requires a nuclear export sequence-containing factor, Nmd3p, that associates with the large subunit protein Rpl10p.* Mol Cell Biol, 2001. **21**(10): p. 3405-15.

147. Milkereit, P., et al., *A Noc complex specifically involved in the formation and nuclear export of ribosomal 40 S subunits.* J Biol Chem, 2003. **278**(6): p. 4072-81.

148. Journo, D., A. Mor, and H. Abeliovich, *Aup1-mediated regulation of Rtg3 during mitophagy.* J Biol Chem, 2009. **284**(51): p. 35885-95.

149. Hanley, S.E., et al., *Ksp1 is an autophagic receptor protein for the Snx4-assisted autophagy of Ssn2/Med13.* Autophagy, 2024. **20**(2): p. 397-415.

150. Livak, K.J. and T.D. Schmittgen, *Analysis of relative gene expression data using real-time quantitative PCR and the 2(-Delta Delta C(T)) Method.* Methods, 2001. **25**(4): p. 402-8.

151. Wal, M. and B.F. Pugh, *Genome-wide mapping of nucleosome positions in yeast using high-resolution MNase ChIP-Seq.* Methods Enzymol, 2012. **513**: p. 233-50.

152. Willis, S.D., et al., *Snf1 cooperates with the CWI MAPK pathway to mediate the degradation of Med13 following oxidative stress.* Microb Cell, 2018. **5**(8): p. 357-370.

153. Shedlovskiy, D., N. Shcherbik, and D.G. Pestov, *One-step hot formamide extraction of RNA from Saccharomyces cerevisiae.* RNA Biol, 2017. **14**(12): p. 1722-1726.

154. Mansour, F.H. and D.G. Pestov, *Separation of long RNA by agarose-formaldehyde gel electrophoresis.* Anal Biochem, 2013. **441**(1): p. 18-20.

155. Pestov, D.G., Y.R. Lapik, and L.F. Lau, *Assays for ribosomal RNA processing and ribosome assembly.* Curr Protoc Cell Biol, 2008. **Chapter 22**: p. Unit 22.11.

156. Shcherbik, N., et al., *Distinct types of translation termination generate substrates for ribosome-associated quality control.* Nucleic Acids Res, 2016. **44**(14): p. 6840-52.

157. Allen, B.L. and D.J. Taatjes, *The Mediator complex: a central integrator of transcription.* Nat Rev Mol Cell Biol, 2015. **16**(3): p. 155-66.

158. Fant, C.B. and D.J. Taatjes, *Regulatory functions of the Mediator kinases CDK8 and CDK19.* Transcription, 2019. **10**(2): p. 76-90.

159. Knuesel, M.T., et al., *The human CDK8 subcomplex is a histone kinase that requires Med12 for activity and can function independently of mediator.* Mol Cell Biol, 2009. **29**(3): p. 650-61.

160. Holstege, F.C., et al., *Dissecting the regulatory circuitry of a eukaryotic genome.* Cell, 1998. **95**(5): p. 717-28.

161. Anandhakumar, J., et al., *Evidence for Multiple Mediator Complexes in Yeast Independently Recruited by Activated Heat Shock Factor.* Mol Cell Biol, 2016. **36**(14): p. 1943-60.

162. Tsai, K.L., et al., *A conserved Mediator-CDK8 kinase module association regulates Mediator-RNA polymerase II interaction.* Nat Struct Mol Biol, 2013. **20**(5): p. 611-9.

163. Li, Y.C., et al., *Structure and noncanonical Cdk8 activation mechanism within an Argonaute-containing Mediator kinase module.* Sci Adv, 2021. **7**(3).

164. Soutourina, J., *Transcription regulation by the Mediator complex.* Nat Rev Mol Cell Biol, 2018. **19**(4): p. 262-274.

165. Daniels, D.L., et al., *Mutual Exclusivity of MED12/MED12L, MED13/13L, and CDK8/19Paralogs Revealed within the CDK-Mediator Kinase Module.* Journal of Proteomics & Bioinformatics, 2013. **2013**: p. 1-7.

166. Donner, A.J., et al., *CDK8 is a positive regulator of transcriptional elongation within the serum response network.* Nat Struct Mol Biol, 2010. **17**(2): p. 194-201.

167. Galbraith, M.D., et al., *HIF1A employs CDK8-mediator to stimulate RNAPII elongation in response to hypoxia.* Cell, 2013. **153**(6): p. 1327-39.

168. Richter, W.F., et al., *The Mediator complex as a master regulator of transcription by RNA polymerase II.* Nat Rev Mol Cell Biol, 2022. **23**(11): p. 732-749.

169. El Khattabi, L., et al., *A Pliable Mediator Acts as a Functional Rather Than an Architectural Bridge between Promoters and Enhancers.* Cell, 2019. **178**(5): p. 1145-1158.e20.

170. Rocha, P.P., et al., *Med12 is essential for early mouse development and for canonical Wnt and Wnt/PCP signaling.* Development, 2010. **137**(16): p. 2723-31.

171. Westerling, T., E. Kuuluvainen, and T.P. Makela, *Cdk8 is essential for preimplantation mouse development.* Mol Cell Biol, 2007. **27**(17): p. 6177-82.

172. Petrenko, N., et al., *Mediator Undergoes a Compositional Change during Transcriptional Activation.* Mol Cell, 2016. **64**(3): p. 443-454.

173. Davis, M.A., et al., *The SCF-Fbw7 ubiquitin ligase degrades MED13 and MED13L and regulates CDK8 module association with Mediator.* Genes Dev, 2013. **27**(2): p. 151-6.

174. Mo, X., et al., *Ras induces mediator complex exchange on C/EBP beta.* Mol Cell, 2004. **13**(2): p. 241-50.

175. Pavri, R., et al., *PARP-1 determines specificity in a retinoid signaling pathway via direct modulation of mediator.* Mol Cell, 2005. **18**(1): p. 83-96.

176. Lambert, E., et al., *From structure to molecular condensates: emerging mechanisms for Mediator function.* FEBS J, 2023. **290**(2): p. 286-309.

177. Hengartner, C.J., et al., *Temporal regulation of RNA polymerase II by Srb10 and Kin28 cyclin-dependent kinases.* Mol Cell, 1998. **2**(1): p. 43-53.

178. Cooper, K.F. and R. Strich, *Functional analysis of the Ume3p/ Srb11p-RNA polymerase II holoenzyme interaction.* Gene Expr, 1999. **8**(1): p. 43-57.

179. Gonzalez, D., et al., *Suppression of Mediator is regulated by Cdk8-dependent Grr1 turnover of the Med3 coactivator.* Proc Natl Acad Sci U S A, 2014. **111**(7): p. 2500-5.

180. Fryer, C.J., J.B. White, and K.A. Jones, *Mastermind recruits CycC:CDK8 to phosphorylate the Notch ICD and coordinate activation with turnover.* Mol Cell, 2004. **16**(4): p. 509-20.

181. Alber, F., et al., *The molecular architecture of the nuclear pore complex.* Nature, 2007. **450**(7170): p. 695-701.

182. Adler, A.S., et al., *CDK8 maintains tumor dedifferentiation and embryonic stem cell pluripotency.* Cancer Res, 2012. **72**(8): p. 2129-39.

183. Bancerek, J., et al., *CDK8 kinase phosphorylates transcription factor STAT1 to selectively regulate the interferon response.* Immunity, 2013. **38**(2): p. 250-62.

184. Chen, M., et al., *CDK8/19 Mediator kinases potentiate induction of transcription by NFkappaB.* Proc Natl Acad Sci U S A, 2017. **114**(38): p. 10208-10213.

185. Hirst, K., et al., *The transcription factor, the Cdk, its cyclin and their regulator: directing the transcriptional response to a nutritional signal.* Embo j, 1994. **13**(22): p. 5410-20.

186. Lenssen, E., et al., *The Ccr4-not complex regulates Skn7 through Srb10 kinase.* Eukaryot Cell, 2007. **6**(12): p. 2251-9.

187. Steinparzer, I., et al., *Transcriptional Responses to IFN-γ Require Mediator Kinase-Dependent Pause Release and Mechanistically Distinct CDK8 and CDK19 Functions.* Molecular Cell, 2019. **76**(3): p. 485-499.e8.

188. Freitas, K.A., et al., *Enhanced T cell effector activity by targeting the Mediator kinase module.* Science, 2022. **378**(6620): p. eabn5647.

189. Chen, M., et al., *CDK8 and CDK19: positive regulators of signal-induced transcription and negative regulators of Mediator complex proteins.* Nucleic Acids Research, 2023. **51**(14): p. 7288-7313.

190. Alarcon, C., et al., *Nuclear CDKs drive Smad transcriptional activation and turnover in BMP and TGF-beta pathways.* Cell, 2009. **139**(4): p. 757-69.

191. Morris, E.J., et al., *E2F1 represses β-catenin transcription and is antagonized by both pRB and CDK8.* Nature, 2008. **455**(7212): p. 552-556.

192. Zhao, X., et al., *Regulation of lipogenesis by cyclin-dependent kinase 8-mediated control of SREBP-1.* J Clin Invest, 2012. **122**(7): p. 2417-27.

193. Kim, T.W., et al., *MED16 and MED23 of Mediator are coactivators of lipopolysaccharide- and heat-shock-induced transcriptional activators.* Proc Natl Acad Sci U S A, 2004. **101**(33): p. 12153-8.

194. Adegbola, A., et al., *Redefining the MED13L syndrome.* Eur J Hum Genet, 2015. **23**(10): p. 1308-17.

195. Poot, M., *Mutations in Mediator Complex Genes CDK8, MED12, MED13, and MEDL13 Mediate Overlapping Developmental Syndromes.* Mol Syndromol, 2020. **10**(5): p. 239-242.

196. Kuchin, S., P. Yeghiayan, and M. Carlson, *Cyclin-dependent protein kinase and cyclin homologs SSN3 and SSN8 contribute to transcriptional control in yeast.* Proc Natl Acad Sci U S A, 1995. **92**(9): p. 4006-10.

197. Cooper, K.F., M.J. Mallory, and R. Strich, *Oxidative stress-induced destruction of the yeast C-type cyclin Ume3p requires phosphatidylinositol-specific phospholipase C and the 26S proteasome.* Mol Cell Biol, 1999. **19**(5): p. 3338-48.

198. Wahi, M. and A.D. Johnson, *Identification of genes required for alpha 2 repression in Saccharomyces cerevisiae.* Genetics, 1995. **140**: p. 79-90.

199. Bjorklund, S. and C.M. Gustafsson, *The yeast Mediator complex and its regulation.* Trends Biochem Sci, 2005. **30**(5): p. 240-4.

200. Surosky, R.T., R. Strich, and R.E. Esposito, *The yeast UME5 gene regulates the stability of meiotic mRNAs in response to glucose.* Mol Cell Biol, 1994. **14**(5): p. 3446-58.

201. Cooper, K.F., et al., *Stress-induced nuclear-to-cytoplasmic translocation of cyclin C promotes mitochondrial fission in yeast.* Dev Cell, 2014. **28**(2): p. 161-73.

202. Hanley SE, W.S., Friedson, B Cooper KF, *Med13 is required for efficient P-body recruitment and autophagic degradation of Edc3 following nitrogen starvation.* Mol Cell Biol, 2024. **in revision**.

203. Hanley, S.E., S.D. Willis, and K.F. Cooper, *Snx4-assisted vacuolar targeting of transcription factors defines a new autophagy pathway for controlling ATG expression.* Autophagy, 2021. **17**(11): p. 3547-3565.

204. Shore, D. and B. Albert, *Ribosome biogenesis and the cellular energy economy.* Curr Biol, 2022. **32**(12): p. R611-r617.

205. Shcherbik, N. and D.G. Pestov, *Ubiquitin and ubiquitin-like proteins in the nucleolus: multitasking tools for a ribosome factory.* Genes Cancer, 2010. **1**(7): p. 681-689.

206. Black, J.J. and R. Green, *Saving ribosomal proteins for later.* Nature Cell Biology, 2023. **25**(11): p. 1568-1569.

207. Hirai, H. and K. Ohta, *Comparative Research: Regulatory Mechanisms of Ribosomal Gene Transcription in Saccharomyces cerevisiae and Schizosaccharomyces pombe.* Biomolecules, 2023. **13**(2).

208. Gomez-Herreros, F., et al., *The ribosome assembly gene network is controlled by the feedback regulation of transcription elongation.* Nucleic Acids Res, 2017. **45**(16): p. 9302-9318.

209. de la Cruz, J., et al., *Feedback regulation of ribosome assembly.* Curr Genet, 2018. **64**(2): p. 393-404.

210. Lascaris, R.F., W.H. Mager, and R.J. Planta, *DNA-binding requirements of the yeast protein Rap1p as selected in silico from ribosomal protein gene promoter sequences.* Bioinformatics, 1999. **15**(4): p. 267-77.

211. McNeil, J.B., et al., *The DNA-binding protein RAP1 is required for efficient transcriptional activation of the yeast PYK glycolytic gene.* Curr Genet, 1990. **18**(5): p. 405-12.

212. Wade, J.T., D.B. Hall, and K. Struhl, *The transcription factor Ifh1 is a key regulator of yeast ribosomal protein genes.* Nature, 2004. **432**(7020): p. 1054-1058.

213. Lieb, J.D., et al., *Promoter-specific binding of Rap1 revealed by genome-wide maps of protein-DNA association.* Nat Genet, 2001. **28**(4): p. 327-34.

214. Hinnebusch, A.G., *Translational regulation of yeast GCN4. A window on factors that control initiator-trna binding to the ribosome.* J Biol Chem, 1997. **272**(35): p. 21661-4.

215. Mittal, N., et al., *The Gcn4 transcription factor reduces protein synthesis capacity and extends yeast lifespan.* Nature Communications, 2017. **8**(1): p. 457.

216. Chi, Y., et al., *Negative regulation of Gcn4 and Msn2 transcription factors by Srb10 cyclin-dependent kinase.* Genes Dev, 2001. **15**(9): p. 1078-92.

217. Leppek, K., et al., *Combinatorial optimization of mRNA structure, stability, and translation for RNA-based therapeutics.* Nature Communications, 2022. **13**(1): p. 1536.

218. Bailey, T.B., et al., *Tup1 is critical for transcriptional repression in Quiescence in S. cerevisiae.* PLoS Genet, 2022. **18**(12): p. e1010559.

219. Zaman, Z., et al., *Interaction of a transcriptional repressor with the RNA polymerase II holoenzyme plays a crucial role in repression.* Proc Natl Acad Sci U S A, 2001. **98**(5): p. 2550-4.

220. Schuller, J. and N. Lehming, *The cyclin in the RNA polymerase holoenzyme is a target for the transcriptional repressor Tup1p in Saccharomyces cerevisiae.* J Mol Microbiol Biotechnol, 2003. **5**(4): p. 199-205.

221. Polymenis, M. and R. Aramayo, *Translate to divide: control of the cell cycle by protein synthesis.* Microb Cell, 2015. **2**(4): p. 94-104.

222. Steffen, K.K., et al., *Ribosome deficiency protects against ER stress in Saccharomyces cerevisiae.* Genetics, 2012. **191**(1): p. 107-18.

223. Rotenberg, M.O., M. Moritz, and J.L. Woolford, Jr., *Depletion of Saccharomyces cerevisiae ribosomal protein L16 causes a decrease in 60S ribosomal subunits and formation of half-mer polyribosomes.* Genes Dev, 1988. **2**(2): p. 160-72.

224. Rosado, I.V., D. Kressler, and J. de la Cruz, *Functional analysis of Saccharomyces cerevisiae ribosomal protein Rpl3p in ribosome synthesis.* Nucleic Acids Res, 2007. **35**(12): p. 4203-13.

225. Miluzio, A., et al., *Eukaryotic initiation factor 6 mediates a continuum between 60S ribosome biogenesis and translation.* EMBO Rep, 2009. **10**(5): p. 459-65.

226. Basu, U., et al., *The Saccharomyces cerevisiae TIF6 gene encoding translation initiation factor 6 is required for 60S ribosomal subunit biogenesis.* Mol Cell Biol, 2001. **21**(5): p. 1453-62.

227. Moore, J.B.t., et al., *Distinct ribosome maturation defects in yeast models of Diamond-Blackfan anemia and Shwachman-Diamond syndrome.* Haematologica, 2010. **95**(1): p. 57-64.

228. Dudley, A.M., et al., *A global view of pleiotropy and phenotypically derived gene function in yeast.* Mol Syst Biol, 2005. **1**: p. 2005 0001.

229. Bolger, T.A., et al., *The mRNA export factor Gle1 and inositol hexakisphosphate regulate distinct stages of translation.* Cell, 2008. **134**(4): p. 624-33.

230. Eustice, D.C. and J.M. Wilhelm, *Fidelity of the eukaryotic codon-anticodon interaction: interference by aminoglycoside antibiotics.* Biochemistry, 1984. **23**(7): p. 1462-7.

231. Borovinskaya, M.A., et al., *Structural basis for hygromycin B inhibition of protein biosynthesis.* RNA, 2008. **14**(8): p. 1590-9.

232. McGaha, S.M. and W.S. Champney, *Hygromycin B inhibition of protein synthesis and ribosome biogenesis in Escherichia coli.* Antimicrob Agents Chemother, 2007. **51**(2): p. 591-6.

233. Cabañas, M.J., D. Vázquez, and J. Modolell, *Dual interference of hygromycin B with ribosomal translocation and with aminoacyl-tRNA recognition.* Eur J Biochem, 1978. **87**(1): p. 21-7.

234. Brodersen, D.E., et al., *The structural basis for the action of the antibiotics tetracycline, pactamycin, and hygromycin B on the 30S ribosomal subunit.* Cell, 2000. **103**(7): p. 1143-54.

235. Abraham, A.K. and A. Pihl, *Effect of protein synthesis inhibitors on the fidelity of translation in eukaryotic systems.* Biochim Biophys Acta, 1983. **741**(2): p. 197-203.

236. Awad, D., et al., *Inhibiting eukaryotic ribosome biogenesis.* BMC Biol, 2019. **17**(1): p. 46.

237. Maarouf, M., et al., *In vivo interference of paromomycin with mitochondrial activity of Leishmania.* Exp Cell Res, 1997. **232**(2): p. 339-48.

238. Hirokawa, G., H. Kaji, and A. Kaji, *Inhibition of antiassociation activity of translation initiation factor 3 by paromomycin.* Antimicrob Agents Chemother, 2007. **51**(1): p. 175-80.

239. Li, C.H., et al., *Chloramphenicol causes mitochondrial stress, decreases ATP biosynthesis, induces matrix metalloproteinase-13 expression, and solid-tumor cell invasion.* Toxicol Sci, 2010. **116**(1): p. 140-50.

240. Jin, C., R. Strich, and K.F. Cooper, *Slt2p phosphorylation induces cyclin C nuclear-to-cytoplasmic translocation in response to oxidative stress.* Mol Biol Cell, 2014. **25**(8): p. 1396-407.

241. Khakhina, S., K.F. Cooper, and R. Strich, *Med13p prevents mitochondrial fission and programmed cell death in yeast through nuclear retention of cyclin C.* Mol Biol Cell, 2014. **25**(18): p. 2807-16.

242. Wang, X., et al., *Disruption of Rpn4-induced proteasome expression in Saccharomyces cerevisiae reduces cell viability under stressed conditions.* Genetics, 2008. **180**(4): p. 1945-53.

243. Kohanski, M.A., et al., *Mistranslation of membrane proteins and two-component system activation trigger antibiotic-mediated cell death.* Cell, 2008. **135**(4): p. 679-90.

244. Boehringer, J., et al., *Structural and functional characterization of Rpn12 identifies residues required for Rpn10 proteasome incorporation.* Biochem J, 2012. **448**(1): p. 55-65.

245. Kors, S., et al., *Regulation of Proteasome Activity by (Post-)transcriptional Mechanisms.* Front Mol Biosci, 2019. **6**: p. 48.

246. Chawla, B., et al., *Paromomycin affects translation and vesicle-mediated trafficking as revealed by proteomics of paromomycin -susceptible -resistant Leishmania donovani.* PLoS One, 2011. **6**(10): p. e26660.

247. Strich, R. and K. Cooper, *The dual role of cyclin C connects stress regulated gene expression to mitochondrial dynamics.* Microbial Cell, 2014. **1**(10): p. 318-324.

248. Badura, M., et al., *DNA damage and eIF4G1 in breast cancer cells reprogram translation for survival and DNA repair mRNAs.* Proc Natl Acad Sci U S A, 2012. **109**(46): p. 18767-72.

249. Park, E.H., et al., *Depletion of eIF4G from yeast cells narrows the range of translational efficiencies genome-wide.* BMC Genomics, 2011. **12**: p. 68.

250. Ramirez-Valle, F., et al., *eIF4GI links nutrient sensing by mTOR to cell proliferation and inhibition of autophagy.* J Cell Biol, 2008. **181**(2): p. 293-307.

251. Russo, A., et al., *rpL3 promotes the apoptosis of p53 mutated lung cancer cells by down-regulating CBS and NFkappaB upon 5-FU treatment.* Sci Rep, 2016. **6**: p. 38369.

252. Deutschbauer, A.M., et al., *Mechanisms of haploinsufficiency revealed by genome-wide profiling in yeast.* Genetics, 2005. **169**(4): p. 1915-25.

253. Brown, J.A., et al., *Global analysis of gene function in yeast by quantitative phenotypic profiling.* Mol Syst Biol, 2006. **2**: p. 2006 0001.

254. Dudley, A.M., et al., *A global view of pleiotropy and phenotypically derived gene function in yeast.* Mol Syst Biol, 2005. **1**: p. 2005.0001.

255. Fell, G.L., et al., *Identification of yeast genes involved in k homeostasis: loss of membrane traffic genes affects k uptake.* G3 (Bethesda), 2011. **1**(1): p. 43-56.

256. Hanna, J., D.S. Leggett, and D. Finley, *Ubiquitin depletion as a key mediator of toxicity by translational inhibitors.* Mol Cell Biol, 2003. **23**(24): p. 9251-61.

257. Joshi, K.K., et al., *A proteasome assembly defect in rpn3 mutants is associated with Rpn11 instability and increased sensitivity to stress.* J Mol Biol, 2011. **410**(3): p. 383-99.

258. Galbraith, M.D., et al., *CDK8 Kinase Activity Promotes Glycolysis.* Cell Rep, 2017. **21**(6): p. 1495-1506.

259. Pestova, T.V., et al., *Molecular mechanisms of translation initiation in eukaryotes.* Proc Natl Acad Sci U S A, 2001. **98**(13): p. 7029-36.

260. Jaiswal, P.K., et al., *Eukaryotic Translation Initiation Factor 4 Gamma 1 (eIF4G1) is upregulated during Prostate cancer progression and modulates cell growth and metastasis.* Sci Rep, 2018. **8**(1): p. 7459.

261. Jaiswal, P.K., et al., *Eukaryotic Translation Initiation Factor 4 Gamma 1 (EIF4G1): a target for cancer therapeutic intervention?* Cancer Cell International, 2019. **19**(1): p. 224.

262. Robichaud, N., et al., *Translational Control in Cancer.* Cold Spring Harb Perspect Biol, 2019. **11**(7).

263. Gilles, A., et al., *Targeting the Human 80S Ribosome in Cancer: From Structure to Function and Drug Design for Innovative Adjuvant Therapeutic Strategies.* Cells, 2020. **9**(3).

264. Roninson, I.B., et al., *Identifying Cancers Impacted by CDK8/19.* Cells, 2019. **8**(8).

265. Ross, Owen A., C. Cook, and L. Petrucelli, *Linking the VPS35 and EIF4G1 Pathways in Parkinson's Disease.* Neuron, 2015. **85**(1): p. 1-3.

266. Dhungel, N., et al., *Parkinson's Disease Genes VPS35 and EIF4G1 Interact Genetically and Converge on α-Synuclein.* Neuron, 2015. **85**(1): p. 76-87.

267. Kroschwald, S., et al., *Promiscuous interactions and protein disaggregases determine the material state of stress-inducible RNP granules.* Elife, 2015. **4**: p. e06807.

268. Sharif, H., et al., *Structural analysis of the yeast Dhh1-Pat1 complex reveals how Dhh1 engages Pat1, Edc3 and RNA in mutually exclusive interactions.* Nucleic Acids Res, 2013. **41**(17): p. 8377-90.

269. Riggs, C.L., et al., *Mammalian stress granules and P bodies at a glance.* J Cell Sci, 2020. **133**(16).

270. Saarikangas, J. and Y. Barral, *Protein aggregates are associated with replicative aging without compromising protein quality control.* Elife, 2015. **4**.

271. Law, M.J. and K. Ciccaglione, *Fine-Tuning of Histone H3 Lys4 Methylation During Pseudohyphal Differentiation by the CDK Submodule of RNA Polymerase II.* Genetics, 2015. **199**(2): p. 435-53.

272. Hirst, K., et al., *The transcription factor, the Cdk, its cyclin and their regulator: directing the transcriptional response to a nutritional signal.* EMBO, 1994. **13**: p. 5410-5420.

273. Larschan, E. and F. Winston, *The Saccharomyces cerevisiae Srb8-Srb11 complex functions with the SAGA complex during Gal4-activated transcription.* Mol Cell Biol, 2005. **25**(1): p. 114-23.

274. Mitchell, S.F., et al., *Global analysis of yeast mRNPs.* Nat Struct Mol Biol, 2013. **20**(1): p. 127-33.

275. Rao, B.S. and R. Parker, *Numerous interactions act redundantly to assemble a tunable size of P bodies in Saccharomyces cerevisiae.* Proc Natl Acad Sci U S A, 2017. **114**(45): p. E9569-e9578.

276. Decker, C.J., D. Teixeira, and R. Parker, *Edc3p and a glutamine/asparagine-rich domain of Lsm4p function in processing body assembly in Saccharomyces cerevisiae.* J Cell Biol, 2007. **179**(3): p. 437-49.

277. Fromm, S.A., et al., *The structural basis of Edc3- and Scd6-mediated activation of the Dcp1:Dcp2 mRNA decapping complex.* Embo j, 2012. **31**(2): p. 279-90.

278. Ling, S.H., et al., *Crystal structure of human Edc3 and its functional implications.* Mol Cell Biol, 2008. **28**(19): p. 5965-76.

279. Brengues, M. and R. Parker, *Accumulation of polyadenylated mRNA, Pab1p, eIF4E, and eIF4G with P-bodies in Saccharomyces cerevisiae.* Mol Biol Cell, 2007. **18**(7): p. 2592-602.

280. Hentze, M.W., *eIF4G: a multipurpose ribosome adapter?* Science, 1997. **275**(5299): p. 500-1.

281. Shintani, T. and D.J. Klionsky, *Cargo proteins facilitate the formation of transport vesicles in the cytoplasm to vacuole targeting pathway.* J Biol Chem, 2004. **279**(29): p. 29889-94.

282. Xing, W., et al., *A quantitative inventory of yeast P body proteins reveals principles of composition and specificity.* eLife, 2020. **9**: p. e56525.

283. Christiano, R., et al., *Global proteome turnover analyses of the Yeasts S. cerevisiae and S. pombe.* Cell Rep, 2014. **9**(5): p. 1959-1965.

284. Hu, Y. and F. Reggiori, *Molecular regulation of autophagosome formation.* Biochem Soc Trans, 2022. **50**(1): p. 55-69.

285. Buchan, J.R., et al., *Eukaryotic stress granules are cleared by autophagy and Cdc48/VCP function.* Cell, 2013. **153**(7): p. 1461-74.

286. Gray, J.V., et al., *"Sleeping beauty": quiescence in Saccharomyces cerevisiae.* Microbiol Mol Biol Rev, 2004. **68**(2): p. 187-206.

287. Desai, P. and R. Bandopadhyay, *Pathophysiological implications of RNP granules in frontotemporal dementia and ALS.* Neurochem Int, 2020. **140**: p. 104819.

288. Cebollero, E. and F. Reggiori, *Regulation of autophagy in yeast Saccharomyces cerevisiae.* Biochim Biophys Acta, 2009. **1793**(9): p. 1413-21.

289. Zientara-Rytter, K. and S. Subramani, *Mechanistic Insights into the Role of Atg11 in Selective Autophagy.* J Mol Biol, 2020. **432**(1): p. 104-122.

290. Nakatogawa, H., et al., *The autophagy-related protein kinase Atg1 interacts with the ubiquitin-like protein Atg8 via the Atg8 family interacting motif to facilitate autophagosome formation.* J Biol Chem, 2012. **287**(34): p. 28503-7.

291. Marshall, R.S., et al., *ATG8-Binding UIM Proteins Define a New Class of Autophagy Adaptors and Receptors.* Cell, 2019. **177**(3): p. 766-781 e24.

292. Lei, Y. and D.J. Klionsky, *UIM-UDS: a new interface between ATG8 and its interactors.* Cell Res, 2019. **29**(7): p. 507-508.

293. Johansen, T. and T. Lamark, *Selective Autophagy: ATG8 Family Proteins, LIR Motifs and Cargo Receptors.* J Mol Biol, 2020. **432**(1): p. 80-103.

294. Yin, Z., et al., *The Roles of Ubiquitin in Mediating Autophagy.* Cells, 2020. **9**(9).

295. Dittmar, G. and K.F. Winklhofer, *Linear Ubiquitin Chains: Cellular Functions and Strategies for Detection and Quantification.* Front Chem, 2019. **7**: p. 915.

296. Dósa, A. and T. Csizmadia, *The role of K63-linked polyubiquitin in several types of autophagy.* Biol Futur, 2022. **73**(2): p. 137-148.

297. Saeed, B., et al., *K63-linked ubiquitin chains are a global signal for endocytosis and contribute to selective autophagy in plants.* Curr Biol, 2023. **33**(7): p. 1337-1345.e5.

298. Richard, T.J.C., et al., *K63-linked ubiquitylation induces global sequestration of mitochondria.* Sci Rep, 2020. **10**(1): p. 22334.

299. Jin, S.M. and R.J. Youle, *PINK1- and Parkin-mediated mitophagy at a glance.* J Cell Sci, 2012. **125**(Pt 4): p. 795-9.

300. Shaid, S., et al., *Ubiquitination and selective autophagy.* Cell Death Differ, 2013. **20**(1): p. 21-30.

301. Yuan, W.C., et al., *K33-Linked Polyubiquitination of Coronin 7 by Cul3-KLHL20 Ubiquitin E3 Ligase Regulates Protein Trafficking.* Mol Cell, 2014. **54**(4): p. 586-600.

302. Tracz, M. and W. Bialek, *Beyond K48 and K63: non-canonical protein ubiquitination.* Cell Mol Biol Lett, 2021. **26**(1): p. 1.

303. Vainshtein, A. and P. Grumati, *Selective Autophagy by Close Encounters of the Ubiquitin Kind.* Cells, 2020. **9**(11).

304. Camougrand, N., et al., *The yeast mitophagy receptor Atg32 is ubiquitinated and degraded by the proteasome.* PLoS One, 2020. **15**(12): p. e0241576.

305. Marshall, R.S., et al., *ATG8-Binding UIM Proteins Define a New Class of Autophagy Adaptors and Receptors.* Cell, 2019. **177**(3): p. 766-781.e24.

306. Powers, T. and P. Walter, *Regulation of ribosome biogenesis by the rapamycin-sensitive TOR-signaling pathway in Saccharomyces cerevisiae.* Mol Biol Cell, 1999. **10**(4): p. 987-1000.

307. Goyer, C., et al., *TIF4631 and TIF4632: two yeast genes encoding the high-molecular-weight subunits of the cap-binding protein complex (eukaryotic initiation factor 4F) contain an RNA recognition motif-like sequence and carry out an essential function.* Mol Cell Biol, 1993. **13**(8): p. 4860-74.

308. Yang, Y. and Z. Wang, *IRES-mediated cap-independent translation, a path leading to hidden proteome.* Journal of Molecular Cell Biology, 2019. **11**(10): p. 911-919.

309. Dhungel, N., et al., *Parkinson's disease genes VPS35 and EIF4G1 interact genetically and converge on α-synuclein.* Neuron, 2015. **85**(1): p. 76-87.

310. Schmidt, M.F., et al., *Ubiquitin signalling in neurodegeneration: mechanisms and therapeutic opportunities.* Cell Death Differ, 2021. **28**(2): p. 570-590.

311. Cai, J., et al., *The role of ubiquitination and deubiquitination in the regulation of cell junctions.* Protein Cell, 2018. **9**(9): p. 754-769.

312. Chartier-Harlin, M.C., et al., *Translation initiator EIF4G1 mutations in familial Parkinson disease.* Am J Hum Genet, 2011. **89**(3): p. 398-406.

313. Tu, L., et al., *Over-expression of eukaryotic translation initiation factor 4 gamma 1 correlates with tumor progression and poor prognosis in nasopharyngeal carcinoma.* Mol Cancer, 2010. **9**: p. 78.

314. Ramos, P.C., et al., *Ump1p is required for proper maturation of the 20S proteasome and becomes its substrate upon completion of the assembly.* Cell, 1998. **92**(4): p. 489-99.

315. Torggler, R., D. Papinski, and C. Kraft, *Assays to Monitor Autophagy in Saccharomyces cerevisiae.* Cells, 2017. **6**(3).

316. Klionsky, D.J., et al., *Guidelines for the use and interpretation of assays for monitoring autophagy (3rd edition).* Autophagy, 2016. **12**(1): p. 1-222.

317. Matscheko, N., et al., *Atg11 tethers Atg9 vesicles to initiate selective autophagy.* PLoS Biol, 2019. **17**(7): p. e3000377.

318. Mao, K., et al., *The scaffold protein Atg11 recruits fission machinery to drive selective mitochondria degradation by autophagy.* Dev Cell, 2013. **26**(1): p. 9-18.

319. Hollenstein, D.M., et al., *Vac8 spatially confines autophagosome formation at the vacuole in S. cerevisiae.* J Cell Sci, 2019. **132**(22).

320. Hollenstein, D.M. and C. Kraft, *Autophagosomes are formed at a distinct cellular structure.* Curr Opin Cell Biol, 2020. **65**: p. 50-57.

321. Kanki, T., et al., *Atg32 is a mitochondrial protein that confers selectivity during mitophagy.* Dev Cell, 2009. **17**(1): p. 98-109.

322. Shpilka, T., et al., *Fatty acid synthase is preferentially degraded by autophagy upon nitrogen starvation in yeast.* Proc Natl Acad Sci U S A, 2015. **112**(5): p. 1434-9.

323. Popelka, H., et al., *Structure and function of yeast Atg20, a sorting nexin that facilitates autophagy induction.* Proc Natl Acad Sci U S A, 2017. **114**(47): p. E10112-E10121.

324. Beese, C.J., S.H. Brynjólfsdóttir, and L.B. Frankel, *Selective Autophagy of the Protein Homeostasis Machinery: Ribophagy, Proteaphagy and ER-Phagy.* Front Cell Dev Biol, 2019. **7**: p. 373.

325. Lu, K., I. Psakhye, and S. Jentsch, *Autophagic clearance of polyQ proteins mediated by ubiquitin-Atg8 adaptors of the conserved CUET protein family.* Cell, 2014. **158**(3): p. 549-63.

326. Marshall, R.S., F. McLoughlin, and R.D. Vierstra, *Autophagic Turnover of Inactive 26S Proteasomes in Yeast Is Directed by the Ubiquitin Receptor Cue5 and the Hsp42 Chaperone.* Cell Rep, 2016. **16**(6): p. 1717-32.

327. Mensah, T.N.A., A. Shroff, and T.Y. Nazarko, *Ubiquitin-binding autophagic receptors in yeast: Cue5 and beyond.* Autophagy, 2023. **19**(9): p. 2590-2594.

328. Werner-Washburne, M., et al., *Stationary phase in the yeast Saccharomyces cerevisiae.* Microbiol. Reviews, 1993. **57**: p. 383-401.

329. Seufert, W. and S. Jentsch, *Ubiquitin-conjugating enzymes UBC4 and UBC5 mediate selective degradation of short-lived and abnormal proteins.* EMBO J, 1990. **9**(2): p. 543-50.

330. Yang, Q., et al., *E3 ubiquitin ligases: styles, structures and functions.* Mol Biomed, 2021. **2**(1): p. 23.

331. Pintard, L., A. Willems, and M. Peter, *Cullin-based ubiquitin ligases: Cul3-BTB complexes join the family.* Embo j, 2004. **23**(8): p. 1681-7.

332. Petroski, M.D. and R.J. Deshaies, *Function and regulation of cullin-RING ubiquitin ligases.* Nat Rev Mol Cell Biol, 2005. **6**(1): p. 9-20.

333. Nguyen, H.C., W. Wang, and Y. Xiong, *Cullin-RING E3 Ubiquitin Ligases: Bridges to Destruction.* Subcell Biochem, 2017. **83**: p. 323-347.

334. Tateishi, K., et al., *The NEDD8 system is essential for cell cycle progression and morphogenetic pathway in mice.* J Cell Biol, 2001. **155**(4): p. 571-9.

335. Liakopoulos, D., et al., *A novel protein modification pathway related to the ubiquitin system.* Embo j, 1998. **17**(8): p. 2208-14.

336. Deshaies, R.J., E.D. Emberley, and A. Saha, *Control of cullin-ring ubiquitin ligase activity by nedd8.* Subcell Biochem, 2010. **54**: p. 41-56.

337. Willems, A.R., M. Schwab, and M. Tyers, *A hitchhiker's guide to the cullin ubiquitin ligases: SCF and its kin.* Biochim Biophys Acta, 2004. **1695**(1-3): p. 133-70.

338. Lammer, D., et al., *Modification of yeast Cdc53p by the ubiquitin-related protein rub1p affects function of the SCFCdc4 complex.* Genes Dev, 1998. **12**(7): p. 914-26.

339. Kraft, C. and M. Peter, *Is the Rsp5 ubiquitin ligase involved in the regulation of ribophagy?* Autophagy, 2008. **4**(6): p. 838-40.

340. Stoll, K.E., et al., *The essential Ubc4/Ubc5 function in yeast is HECT E3-dependent, and RING E3-dependent pathways require only monoubiquitin transfer by Ubc4.* J Biol Chem, 2011. **286**(17): p. 15165-70.

341. Hiraishi, H., et al., *A functional analysis of the yeast ubiquitin ligase Rsp5: the involvement of the ubiquitin-conjugating enzyme Ubc4 and poly-ubiquitination in ethanol-induced down-regulation of targeted proteins.* Biosci Biotechnol Biochem, 2009. **73**(10): p. 2268-73.

342. MacDonald, C., et al., *A Cycle of Ubiquitination Regulates Adaptor Function of the Nedd4-Family Ubiquitin Ligase Rsp5.* Curr Biol, 2020. **30**(3): p. 465-479.e5.

343. Galan, J. and R. Haguenauer-Tsapis, *Ubiquitin lys63 is involved in ubiquitination of a yeast plasma membrane protein.* Embo J, 1997. **16**(19): p. 5847-54.

344. Belgareh-Touzé, N., et al., *Versatile role of the yeast ubiquitin ligase Rsp5p in intracellular trafficking.* Biochem Soc Trans, 2008. **36**(Pt 5): p. 791-6.

345. Kaliszewski, P. and T. Zoładek, *The role of Rsp5 ubiquitin ligase in regulation of diverse processes in yeast cells.* Acta Biochim Pol, 2008. **55**(4): p. 649-62.

346. Shcherbik, N. and D.G. Pestov, *The ubiquitin ligase Rsp5 is required for ribosome stability in Saccharomyces cerevisiae.* Rna, 2011. **17**(8): p. 1422-8.

347. Wood, A., et al., *Bre1, an E3 ubiquitin ligase required for recruitment and substrate selection of Rad6 at a promoter.* Mol Cell, 2003. **11**(1): p. 267-74.

348. Zhuang, M., et al., *Structures of SPOP-substrate complexes: insights into molecular architectures of BTB-Cul3 ubiquitin ligases.* Mol Cell, 2009. **36**(1): p. 39-50.

349. Nguyen, L.K., W. Kolch, and B.N. Kholodenko, *When ubiquitination meets phosphorylation: a systems biology perspective of EGFR/MAPK signalling.* Cell Commun Signal, 2013. **11**: p. 52.

350. Miller, C.J. and B.E. Turk, *Homing in: Mechanisms of Substrate Targeting by Protein Kinases.* Trends Biochem Sci, 2018. **43**(5): p. 380-394.

351. Tuazon, P.T., W.C. Merrick, and J.A. Traugh, *Comparative analysis of phosphorylation of translational initiation and elongation factors by seven protein kinases.* J Biol Chem, 1989. **264**(5): p. 2773-7.

352. Raught, B., et al., *Serum-stimulated, rapamycin-sensitive phosphorylation sites in the eukaryotic translation initiation factor 4GI.* Embo j, 2000. **19**(3): p. 434-44.

353. Farré, J.C. and S. Subramani, *Mechanistic insights into selective autophagy pathways: lessons from yeast.* Nat Rev Mol Cell Biol, 2016. **17**(9): p. 537-52.

354. Mao, K., et al., *Two MAPK-signaling pathways are required for mitophagy in Saccharomyces cerevisiae.* J Cell Biol, 2011. **193**(4): p. 755-67.

355. Mao, K. and D.J. Klionsky, *MAPKs regulate mitophagy in Saccharomyces cerevisiae.* Autophagy, 2011. **7**(12): p. 1564-5.

356. Manjithaya, R., et al., *A yeast MAPK cascade regulates pexophagy but not other autophagy pathways.* J Cell Biol, 2010. **189**(2): p. 303-10.

357. Gwizdek, C., et al., *The mRNA nuclear export factor Hpr1 is regulated by Rsp5-mediated ubiquitylation.* J Biol Chem, 2005. **280**(14): p. 13401-5.

358. Rodrigo-Brenni, M.C. and D.O. Morgan, *Sequential E2s drive polyubiquitin chain assembly on APC targets.* Cell, 2007. **130**(1): p. 127-39.

359. Nibe, Y., et al., *Novel polyubiquitin imaging system, PolyUb-FC, reveals that K33-linked polyubiquitin is recruited by SQSTM1/p62.* Autophagy, 2018. **14**(2): p. 347-358.

360. Kovačević, I., et al., *The Cullin-3-Rbx1-KCTD10 complex controls endothelial barrier function via K63 ubiquitination of RhoB.* J Cell Biol, 2018. **217**(3): p. 1015-1032.

361. Lin, P., et al., *Current trends of high-risk gene Cul3 in neurodevelopmental disorders.* Front Psychiatry, 2023. **14**: p. 1215110.

362. Gao, N., et al., *Deficiency of Cullin 3, a Protein Encoded by a Schizophrenia and Autism Risk Gene, Impairs Behaviors by Enhancing the Excitability of Ventral Tegmental Area (VTA) DA Neurons.* J Neurosci, 2023. **43**(36): p. 6249-6267.

363. Dong, Z., et al., *CUL3 Deficiency Causes Social Deficits and Anxiety-like Behaviors by Impairing Excitation-Inhibition Balance through the Promotion of Cap-Dependent Translation.* Neuron, 2020. **105**(3): p. 475-490.e6.

364. Li, X., et al., *CUL3 (cullin 3)-mediated ubiquitination and degradation of BECN1 (beclin 1) inhibit autophagy and promote tumor progression.* Autophagy, 2021. **17**(12): p. 4323-4340.

365. Gupta, R., et al., *Ubiquitination screen using protein microarrays for comprehensive identification of Rsp5 substrates in yeast.* Mol Syst Biol, 2007. **3**: p. 116.

366. Belgareh-Touzé, N., L. Cavellini, and M.M. Cohen, *Ubiquitination of ERMES components by the E3 ligase Rsp5 is involved in mitophagy.* Autophagy, 2017. **13**(1): p. 114-132.

367. Marshall, R.S. and R.D. Vierstra, *A trio of ubiquitin ligases sequentially drives ubiquitylation and autophagic degradation of dysfunctional yeast proteasomes.* Cell Rep, 2022. **38**(11): p. 110535.

368. Ohtake, F., et al., *K63 ubiquitylation triggers proteasomal degradation by seeding branched ubiquitin chains.* Proc Natl Acad Sci U S A, 2018. **115**(7): p. E1401-e1408.

369. Gelperin, D., et al., *Loss of ypk1 function causes rapamycin sensitivity, inhibition of translation initiation and synthetic lethality in 14-3-3-deficient yeast.* Genetics, 2002. **161**(4): p. 1453-64.

370. Das, S. and B. Das, *eIF4G-an integrator of mRNA metabolism?* FEMS Yeast Res, 2016. **16**(7).

371. Fu, D.J. and T. Wang, *Targeting NEDD8-activating enzyme for cancer therapy: developments, clinical trials, challenges and future research directions.* J Hematol Oncol, 2023. **16**(1): p. 87.

372. Deol, K.K., S. Lorenz, and E.R. Strieter, *Enzymatic Logic of Ubiquitin Chain Assembly.* Front Physiol, 2019. **10**: p. 835.

373. Finley, D., et al., *Inhibition of proteolysis and cell cycle progression in a multiubiquitination-deficient yeast mutant.* Mol Cell Biol, 1994. **14**(8): p. 5501-9.

374. Dargemont, C. and B. Ossareh-Nazari, *Cdc48/p97, a key actor in the interplay between autophagy and ubiquitin/proteasome catabolic pathways.* Biochim Biophys Acta, 2012. **1823**(1): p. 138-44.

375. Bodnar, N.O. and T.A. Rapoport, *Molecular Mechanism of Substrate Processing by the Cdc48 ATPase Complex.* Cell, 2017. **169**(4): p. 722-735.e9.

376. Hubner, M. and M. Peter, *Cullin-3 and the endocytic system: New functions of ubiquitination for endosome maturation.* Cell Logist, 2012. **2**(3): p. 166-168.

377. Klaips, C.L., G.G. Jayaraj, and F.U. Hartl, *Pathways of cellular proteostasis in aging and disease.* J Cell Biol, 2018. **217**(1): p. 51-63.

378. Russo, A., et al., *Regulatory role of rpL3 in cell response to nucleolar stress induced by Act D in tumor cells lacking functional p53.* Cell Cycle, 2016. **15**(1): p. 41-51.

379. Esposito, D., et al., *Human rpL3 plays a crucial role in cell response to nucleolar stress induced by 5-FU and L-OHP.* Oncotarget, 2014. **5**(22): p. 11737-51.

380. Aryanpur, P.P., T.M. Mittelmeier, and T.A. Bolger, *The RNA Helicase Ded1 Regulates Translation and Granule Formation during Multiple Phases of Cellular Stress Responses.* Mol Cell Biol, 2022. **42**(1): p. e0024421.

381. Buchan, J.R. and R. Parker, *Eukaryotic stress granules: the ins and outs of translation.* Mol Cell, 2009. **36**(6): p. 932-41.

382. Estruch, F., *Stress-controlled transcription factors, stress-induced genes and stress tolerance in budding yeast.* FEMS Microbiol Rev, 2000. **24**(4): p. 469-86.

383. Badura, M., et al., *DNA damage and eIF4G1 in breast cancer cells reprogram translation for survival and DNA repair mRNAs.* Proceedings of the National Academy of Sciences, 2012. **109**(46): p. 18767.

384. Berset, C., H. Trachsel, and M. Altmann, *The TOR (target of rapamycin) signal transduction pathway regulates the stability of translation initiation factor eIF4G in the yeast Saccharomyces cerevisiae</em&gt.* Proceedings of the National Academy of Sciences, 1998. **95**(8): p. 4264.

385. Park, K., et al., *Roles of eIF4E-binding protein Caf20 in Ste12 translation and P-body formation in yeast.* J Microbiol, 2018. **56**(10): p. 744-747.

386. Brown, J.A., et al., *Global analysis of gene function in yeast by quantitative phenotypic profiling.* Mol Syst Biol, 2006. **2**: p. 2006.0001.

387. Tang, J.F., et al., *Homoharringtonine inhibits melanoma cells proliferation in vitro and vivo by inducing DNA damage, apoptosis, and G2/M cell cycle arrest.* Arch Biochem Biophys, 2021. **700**: p. 108774.

388. Lü, S. and J. Wang, *Homoharringtonine and omacetaxine for myeloid hematological malignancies.* J Hematol Oncol, 2014. **7**: p. 2.

389. Zhao, J., R. Ramos, and M. Demma, *CDK8 regulates E2F1 transcriptional activity through S375 phosphorylation.* Oncogene, 2013. **32**(30): p. 3520-30.

390. Broude, E.V., et al., *Expression of CDK8 and CDK8-interacting Genes as Potential Biomarkers in Breast Cancer.* Curr Cancer Drug Targets, 2015. **15**(8): p. 739-49.

391. Li, N., et al., *Cyclin C is a haploinsufficient tumour suppressor.* Nat Cell Biol, 2014. **16**(11): p. 1080-91.

392. Cooper, K.F., et al., *Ama1p is a meiosis-specific regulator of the anaphase promoting complex/cyclosome in yeast.* Proc Natl Acad Sci U S A, 2000. **97**(26): p. 14548-53.

393. Strässer, K. and E. Hurt, *Yra1p, a conserved nuclear RNA-binding protein, interacts directly with Mex67p and is required for mRNA export.* Embo j, 2000. **19**(3): p. 410-20.

394. Toth, E., et al., *Cpf1 nucleases demonstrate robust activity to induce DNA modification by exploiting homology directed repair pathways in mammalian cells.* Biol Direct, 2016. **11**: p. 46.

395. Jones, E.W., G.S. Zubenko, and R.R. Parker, *PEP4 gene function is required for expression of several vacuolar hydrolases in Saccharomyces cerevisiae.* Genetics, 1982. **102**(4): p. 665-77.

396. Krasley, E., et al., *Regulation of the oxidative stress response through Slt2p-dependent destruction of cyclin C in Saccharomyces cerevisiae.* Genetics, 2006. **172**(3): p. 1477-86.

397. Abeliovich, H., et al., *Chemical genetic analysis of Apg1 reveals a non-kinase role in the induction of autophagy.* Mol Biol Cell, 2003. **14**(2): p. 477-90.

Appendix A

Chapter 3 Supplemental Tables and Figures

Table A1

Yeast Strains Used in This Study.

Strain*	Genotype	Source
RSY10*		[47]
RSY391**	*cnc1::LEU2*	[45]
RSY1696*	*cnc1::KANMX4*	[392]
RSY1726*	*cdk8::KANMX4*	[392]
RSY2176*	*cdk8::NatNT2*	[40]
RSY2305**	*pep4::HIS3 prb1-Δ1.6R SSN2/MED13-mNeongreen::NatNT2*	[203]
RSY2316*	*rpn4::KANMX4*	This study
RSY2332*	*rpn4::KANMX4 cnc1::NatNT2*	This study
RSY2334*	*MED13-9MYC::HIS3*	This study
RSY2444*	*med13::HIS3*	[46]
RSY2452*	*rpn4::KANMX4 cdk8::NatNT2*	This study
RSY2689*	*Rps9a-GFP::HIS3*	This study
RSY2691*	*cdk8::KANMX4 Rps9a-GFP::HIS3*	This study

Note.*Genotype of all strains is *MAT**a** ade2 ade6 can1-10 his3-11, 15 leu2-3, 112 trp1-1 ura3-1* (W303).

Genotype is *MATa** his3-Δ200 can1 ura3-52 leu2Δ1 lys2-801 trp1-289* (BJ5459).

Table A2

Plasmids Used in This Study

Plasmid Name	Gene	Epitope Tag	Marker	Promoter	2μ/ CEN/ int	Reference
LEP752	*NUP49*	mCherry	*LEU2*	*ADH1*	CEN	[54]
Mito-TFP	*preSu9*	TFP	*HIS3*	*ADH1*	CEN	[46]
pKC337	*CNC1*	Myc	*TRP1*	*ADH1*	CEN	[45]
pSW205	*CNC1*	mCherry	*LEU2*	*ADH1*	CEN	This study
pUM511	*CDK8*	HA	*TRP1*	*ADH1*	CEN	[122]
pUM516	*CDK8*^{D290A}	HA	*TRP1*	*ADH1*	CEN	[122]
pUN100	*NOP1*	DSRed	*LEU2*		CEN	[393]
RPL25-eGFP	*RPL25*	GFP	*URA3*	*own*	CEN	[146]
RPS2-eGFP	*RPS2*	GFP	*URA3*	*own*	CEN	[147]

Note. *pSW496 and pSW497 were CRISPR plasmids containing guide RNAs to create cyclin deletion of exon 1 and 2, respectively. The guide RNAs were cloned into pTE4398 [394] under the U6 promoter. The vector also contained the Cas12a/Cpf1 coding region under the CMV promoter for one-step transfection.

Table A3

List of Transcription Factors which can Associate with RP and TIF Genes Regulated by the Yeast CKM

A

Significant	Insignificant
DED1	RAP1
RPL3	RPS20
TIF6	RPS9A
TIF4631	RPS24A
TIF4632	RPL25
	CDC33

B

TF	Documented	Potential
Tup1	6	0
Snf2	3	0
Cst6	1.5	0
Met28	1.2	0
Swi5	0	4.8
Hac1	0	2
Cup2	0	1.2
Hsf1	0	1.5
Ndt80	0	2
Xbp1	0	1.2
Abf1	0	2
Ace2	0	4.8
Leu3	0	2.4

Note. (A) A set of significantly regulated and unregulated genes in CKM mutants was created based on the results from RT-qPCR analysis in Figure 1. (B) Using YEASTRACT+, regulatory associations of yeast transcription factors were extracted for these two sets of genes. Associations were filtered using expression evidence in unstressed log-phase growth against the known *S. cerevisiae* transcription factor list. From this data, transcription factors which had less than 80% of the gene list map were filtered out. Enriched transcription factors that mapped to both of the gene sets were filtered out as redundant. The resulting transcription factors were then given an enrichment score (% genes associated from significant / % genes associated from insignificant). These are separated into documented interactions from the literature and potential interactions based on promoter sequence.

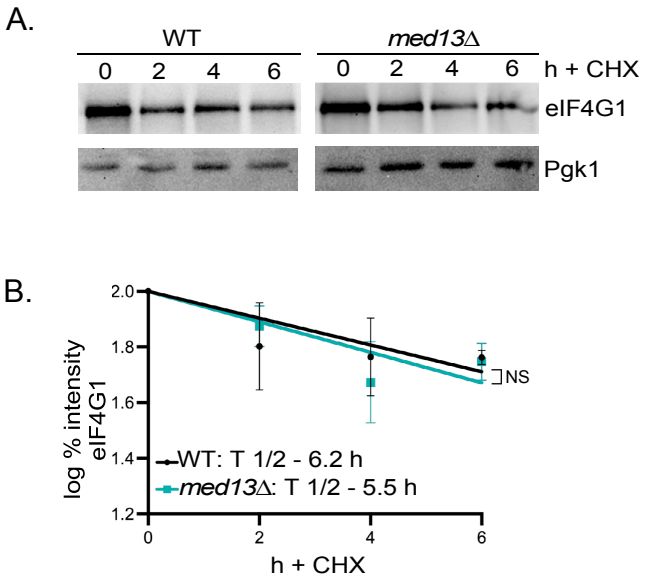

Figure A1. eIF4G1 cycloheximide chase assays. (A) Western blot analysis of extracts prepared from mid-log WT (RSY10) and *med13*Δ (RSY2444) cultures expressing endogenous eIF4G1 treated with 150 µg/ml Cycloheximide (CHX) in SD-complete medium for the indicated times. Pgk1 was used as a normalization control protein (B) Quantification of the results obtained in A to demonstrate degradation kinetics. The linear regression line indicates Log% (Log10) protein expression at 2 h, 4 h, and 6 h of CHX treatment relative to 0 h. Error bars indicate S.D., N = 3 of biologically independent experiments. NS, non significant.

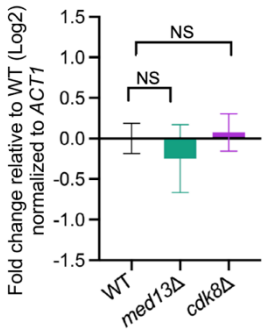

Figure A2. The CKM does not control the expression of *RAP1*. RT-qPCR analysis of the *RAP1* in WT (RSY10) and *med13*Δ (RSY2444) cells in unstressed conditions. ΔΔCt results for relative fold change (Log2) values using wild-type unstressed cells as a control. Transcript levels are given relative to the internal *ACT1* mRNA control. NS, not significant. For all RT-qPCR assays, the error bars indicate the SD from the mean of two technical replicates from three independent cultures (N=3).

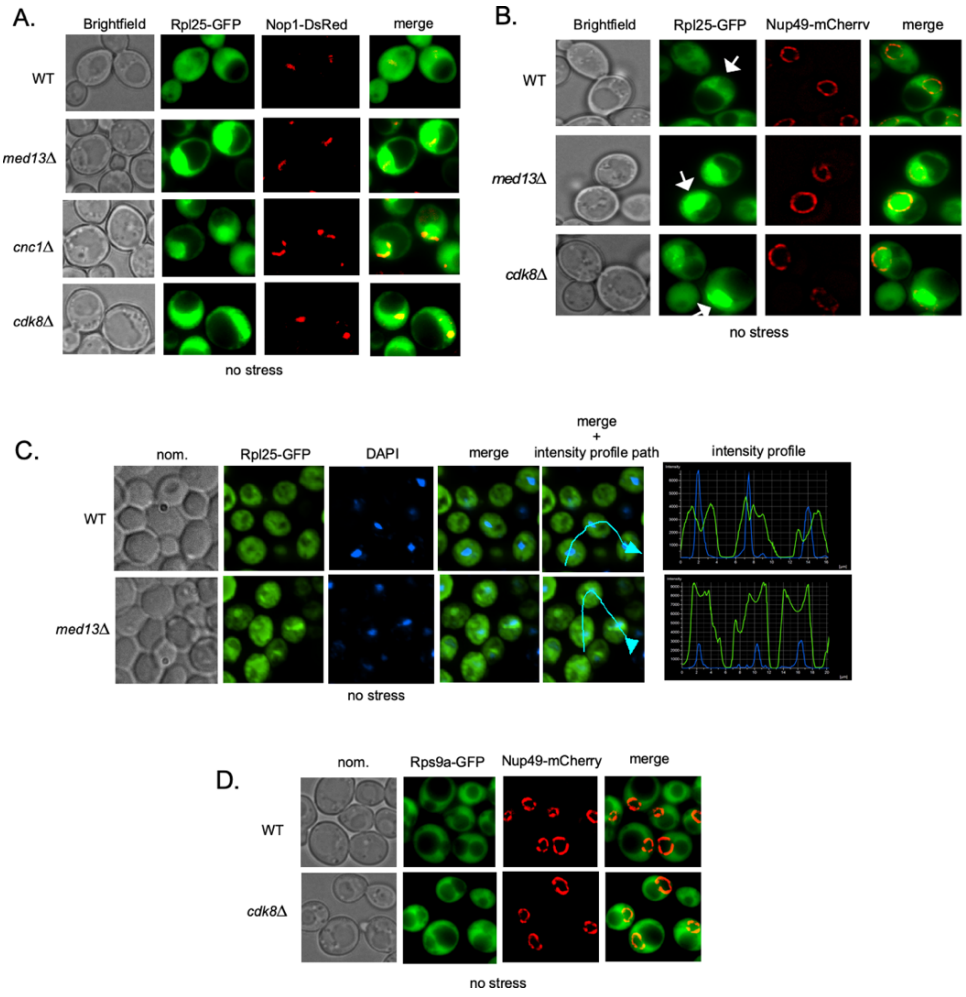

Figure A3. 60S ribosomal protein Rpl25 accumulates within the nucleolus in CKM mutants. (A) Fluorescence microscopy of Rpl25-GFP localization in WT (RSY10), *med13*Δ (RSY2444), and *cdk8*Δ (RSY2176) cells expressing the nucleolar marker Nop1-DsRed (plasmid name pUN100) and Rpl25-GFP plasmid in physiological conditions (SD selective medium). Representative single-plane images are shown using a Keyence microscope. Scale: 5 μm. (B) As in A, except cells are expressing Rpl25-GFP plasmid and the nuclear membrane marker Nup49-mCherry (plasmid name LEP752). (C) As in A, except indicated cells are expressing Rpl25-GFP and the nucleus is observed with a DAPI stain and visualized using a Nikon microscope. Right hand panel demonstrates fluorescence intensity profiles of Rpl25-GFP levels compared to DAPI (TFP) fluorescence intensities to compare accumulation of Rpl25-GFP within the nucleus. (D) As in A, except WT (RSY2689) and *cdk8*Δ (RSY2691) cells expressing endogenous Rps9a-GFP and the nuclear marker Nup49mCherry.

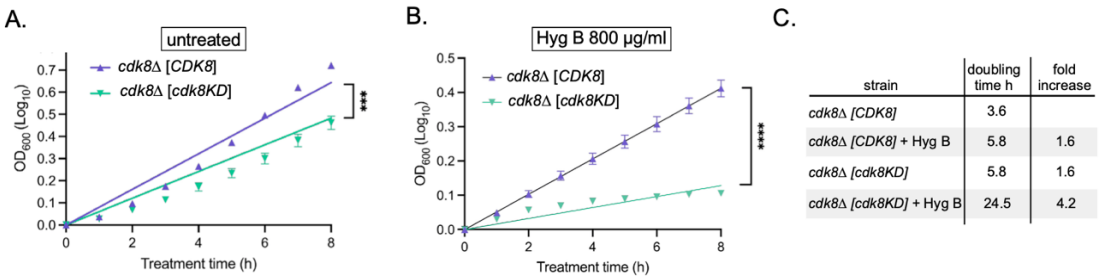

Figure A4. Cdk8 kinase activity is required for growth in Hyg B. Left-hand and middle panels: 1206 cell growth assays of cdk8Δ harboring either wild type [CDK8] or the kinase-dead (D290A) allele [cdk8KD]. Cells were grown in SD selective liquid medium with and without 800 µg/ml Hyg B. Error bars indicate S.D., N = 3 of biologically independent experiments. Right-hand panel: Summary of the doubling times of the strains shown with and without treatment with 800 µg/ml Hyg B. ***p ≤ 0.005, ****p ≤ 0.001.

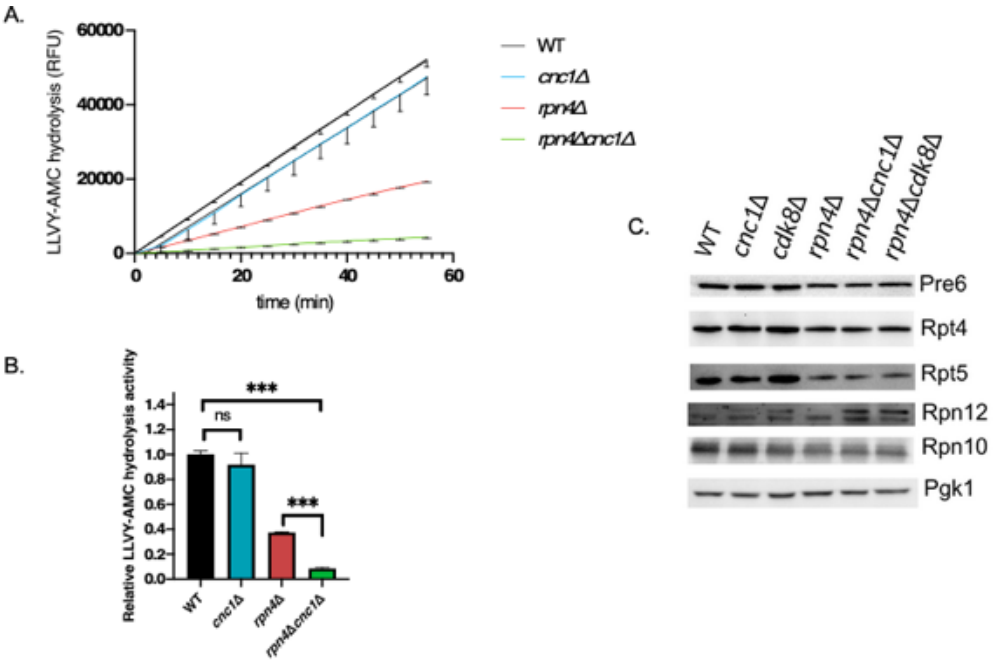

Figure A5. Cyclin C enhances proteasome activity through Rpn4 in yeast. (A) Relative fluorescence measurement of chymotrypsin-like proteasome activity in WT (RSY10) versus *cnc1Δ* (RSY391), *rpn4Δ* (RSY2316), *rpn4Δcnc1Δ* (RSY2332). All samples were incubated with SUC-LLVY-AMC fluorescent substrate with and without the proteasome inhibitor MG132 as a control. Measurements were taken at 5-minute intervals for 55 minutes. Increased LLVY-AMC hydrolysis correlates with increased proteasome activity.

(B) Quantification of SUC-LLVY-AMC hydrolysis in the mutant strains relative to WT at 55 minutes as described in A. Error bars indicate S.D., N=2 biologically independent experiments. (C) Western blot analysis of proteasome protein levels in WT (RSY10) versus *cnc1Δ* (RSY391)*, cdk8Δ* (RSY2176) *rpn4Δ* (RSY2316), *rpn4Δcnc1Δ* (RSY2332), and *rpn4Δcdk8Δ* (RSY2452) strains using antibodies against specific proteasome proteins in yeast.

Appendix B

Chapter 4 Supplemental Tables and Figures

Table B1

Yeast Strains Used in This Study.

Strain*	Genotype	Source
RSY10*	*MAT**a** ade2 ade6 can1-10 his3-11, 15 leu2-3, 112 trp1-1 ura3-1*	(Strich et al., 1989)
BJ5459**	*pep4::HIS3 prb1-Δ1.6R*	(Zubenko et al., 1983)
RSY2176*	*cdk8::NatNT2*	This study
RSY2305**	*pep4::HIS3 prb1-Δ1.6R SSN2/MED13-mNeonGreen::NatNT2*	(Hanley et al., 2021)
RSY2444*	*SSN2/MED13::HIS3*	(Hanley et al., 2021)
RSY2714*	*edc3::KanMX4 DCP2-GFP::HphNT1*	This study
RSY2902*	*MED13-Q/N-9-9MYC::NatNT2 DCP2-GFP::HphNT1*	This study

*Genotype of all stains is *MAT**a** ade2 ade6 can1-10 his3-11, 15 leu2-3, 112 trp1-1 ura3-1* (W303). **Genotype of all strains is *MAT**a** his3-Δ200 can1 ura3-52 leu2Δ1 lys2-801 trp1-289* (BJ5459). *** Genotype of both strains is *MAT**a** his3Δ1 leu2Δ0 lys2Δ0 met15Δ0 ura3Δ0.*

Table B2

Plasmids Used in This Study.

Plasmid Name	Gene	Epitope Tag	Marker	Promoter	2µ/ CEN/ int	Reference
pRP1574	*EDC3*	mCherry	*URA3*	Own	CEN	(Buchan et al., 2008)
pSW221	*VPH1*	mCherry	*URA3*	*ADH1*	CEN	(Willis et al., 2020)
pSW521	*EDC3*	GFP	*URA3*	Own	CEN	This study
pSW337	*ATG8*	GFP	*TRP1*	Own	CEN	(Hanley et al., 2021)
pSH36	$ATG8^{Y49A,L50A}$	GFP	*TRP1*	Own	CEN	(Hanley et al., 2023)
RPL25eGFP	*RPL25*	GFP	*URA3*	Own	CEN	(Gadal et al., 2001)
RPS2eGFP	*RPS2*	GFP	*URA3*	Own	CEN	(Milkereit et al., 2003)

Appendix C

Chapter 5 Supplemental Tables and Figures

Table C1

Yeast Strains Used in This Study.

Strain	Genotype	Source
RSY10*		[47]
RSY414/MHY414**		[329]
RSY415/MHY508**	*ubc4Δ1::HIS3 ubc5Δ1::LEU2*	[329]
RSY449/BJ5459***	*pep4::HIS3 prb1-Δ1.6R*	[395]
RSY1006	*slt2::HIS5+*	[396]
RSY1858*	*pdr5::KanMX4*	[241]
RSY2094*	*atg1::KanMX4*	[56]
RSY2104*	*atg17::KanMX4*	[56]
RSY2160*	*ump1::KanMX4*	[46]
RSY2196*	*dsk2::NATMX rad23::KANMX4 ddi1::HPHMX*	[46]
RSY2248*	*atg11::KanMX4*	[56]
RSY2272*	*snx4::HPHMX*	[56]
RSY2551*	*vam3::KanMX4*	[56]
RSY2559*	*atg19::HPHMX atg34::KanMX4*	[56]
RSY2266*	*ksp1::KanMX4*	[121, 149]
RSY2642*	*eIF4G1-GFP::KanMX*$^{\alpha}$	This study
RSY2653***	*pep4::^HIS3 prb1-Δ1.6R TIF4631/eIF4G1-GFP::KanMX*	This study
RSY2770/SUB280^{+}	ubi1-Δ1::TRP ubi1-Δ2::URA3 ubi3-Δub2 ubi4-Δ2::LEU2 [pUB39 Ub:URA] [pUB100:HIS3])	[373]
RSY2771^{+}	Identical to RSY2770/SUB280 except for UB K63R mutation	[373]
RSY2776^{+}	Identical to RSY2770/SUB280 except for UB K33R mutation	[373]
RSY2813*	*cul3::HPHMX*	This study
RSY2883****	*SmBiT-UBQ::LUE2*	[143]
RSY2885****	*TIF4631/eIF4G1-LgBiT/His::HPH*	[143]

RSY2890****	*Htb2-LgBiT::URA3*	[143]
RSY2892****	*eIF4G1/TIF4631- LgBiT/His::HPH SmBiT-UBQ::NAT*	[143]
RSY2897****	*Htb2-LgBiT::URA3 SmBiT-UBQ::LUE2*	[143]
RSY2898****	*Htb2-LgBiT::URA3 SmBiT-UBQ::LUE2 bre1::HPH*	[143]
RSY2911****	*eIF4G1/TIF4631- LgBiT/His::HPH SmBiT-UBQ::NAT pep4::KanMX*	This study
RSY2912****	*eIF4G1/TIF4631- LgBiT/His::HPH pep4::KanMX*	This study
RSY2945****	*eIF4G1/TIF4631- LgBiT/His::HPH pep4::HIS3 cul3::KanMX*	This study
RSY2909*	*eIF4G1/TIF4631-3xMYC::TRP1*	This study
RSY2913*	*rub1::NAT TIF4631/eIF4G1-5xMYC::HIS3*	This study
RSY2924*	*TIF4631/eIF4G1-5xMYC::HIS3*	This study
RSY2925*	*ubc5::NAT TIF4631/eIF4G1-5xMYC::HIS3*	This study
RSY2933*	*ubx5::KanMX4 TIF4631/eIF4G1-3xMYC::TRP1*	This study
RSY2934*	*atg20::KanMX4 TIF4631/eIF4G1-3xMYC::TRP1*	This study
RSY2935*	*ubp3::KanMX4 TIF4631/eIF4G1-3xMYC::TRP1*	This study
RSY2936*	*cue5::KanMX4 TIF4631/eIF4G1-3xMYC::TRP1*	This study
RSY2939*	*TIF4631/eIF4G1* ^{S24A} *-3xMYC:HIS3*	This study
RSY2948*	*atg8::KanMX4 TIF4631/eIF4G1-5xMYC::HIS3*	This study
RSY2955*	*TIF4631/eIF4G1*$^{(932\text{-}936\Delta)}$*-3xMYC::TRP1*^	This study

Note.

*Genotype is *MAT**a** ade2 ade6 can1-10 his3-11, 15 leu2-3, 112 trp1-1 ura3-1* (W303).
** Genotype is MATa his3Δ200 leu2,3-115 lys2-801 trp1-1 ura3-5
*** Genotype is *MAT***a** *his3-Δ200 can1 ura3-52 leu2Δ1 lys2-801 trp1-289* (BJ5459).
$^{+}$ Genotype is his3-Δ200 leu2-3,112 lys2-801 ura3-52 trp1-1
**** Genotype is MATa his3Δ1 leu2Δ0 met15Δ0 ura3Δ0 (BY4741)
$^{\alpha}$ The gene TIF4631 is the official yeast gene name which encodes the eIf4G1 protein. For clarity purposes, both TIF4631/eIF4G1 are indicated for the genotype names as needed).

^ CRISPR-mediated deletion of potential Cul3 binding site (amino acids 932-936) on eIF4G1 (to form strain RSY2955) was formed using the following primers (KCO indicates primer name):
<u>For PCR with Cas9/guide RNA:</u>
KCO 4454: gac ttt ATA TTT GTT GCG GTA GAA
KCO 4455: aaac ACT TCT ACC GCA ACA AAT AT aa

For PCR repair template:
KCO4456:
CAAAGAAATAGCCAAAGGGCTCCTCCTCCAAAGGAAGAACCAGCaGCtGCAA
CAAATATG
KCO4457:
TTACTCTTCGTCATCACTTTCTCCCATTAATGCACTGAACATATTTGTTGCaGCt
GCTG
For PCR of eIF4G1 from new CRISPR gDNA: KCO3493 and KCO3495
For sequencing new strain with mutated eIF4G1: KCO3463

Table C2

Plasmids Used in This Study.

Plasmid Name	Gene	Epitope Tag	Marker	Promoter	2μ/ CEN/ int	Reference
HB0535**	*TIF4631/eIF4G1*	5xMYC	*HIS3*		CEN	[141]
HB0536**	*TIF4631/eIF4G1*^{S24A}	5xMYC	*HIS3*		CEN	[141]
pJR3428*	*Cas9 guide RNA*		*URA3*	GAL1	2μ	[144]
pRsp5Δcis	*RSP5*$^{WW1\Delta}$	HA	*URA3*	Own	CEN	[145]
pSH36	*ATG8*^{Y49A,L50A}	GFP	*TRP1*	ADH1	CEN	[149]
pSW221	*VPH1*	mCherry	*URA3*			[46]
pSW337	*ATG8*	GFP	*TRP1*	Own	CEN	[397]
pSW557	*ATG8*^{I76A,F77A,I78A}	GFP	*TRP1*	Own	CEN	This study
pSW591	*TIF4631/eIF4G1*	MYC	*TRP1*	ADH1	2μ	This study
RPL25-eGFP	*RPL25*	GFP	*URA3*	Own	CEN	[146]
RPS2-eGFP	*RPS2*	GFP	*URA3*	Own	CEN	[147]

Note. *pJR3428 is a CRISPR plasmid containing guide RNAs digested with BSMBI. Was used to create strain RSY2955.

**HB0535 are HB0536 are integrating plasmids cut with PstI.

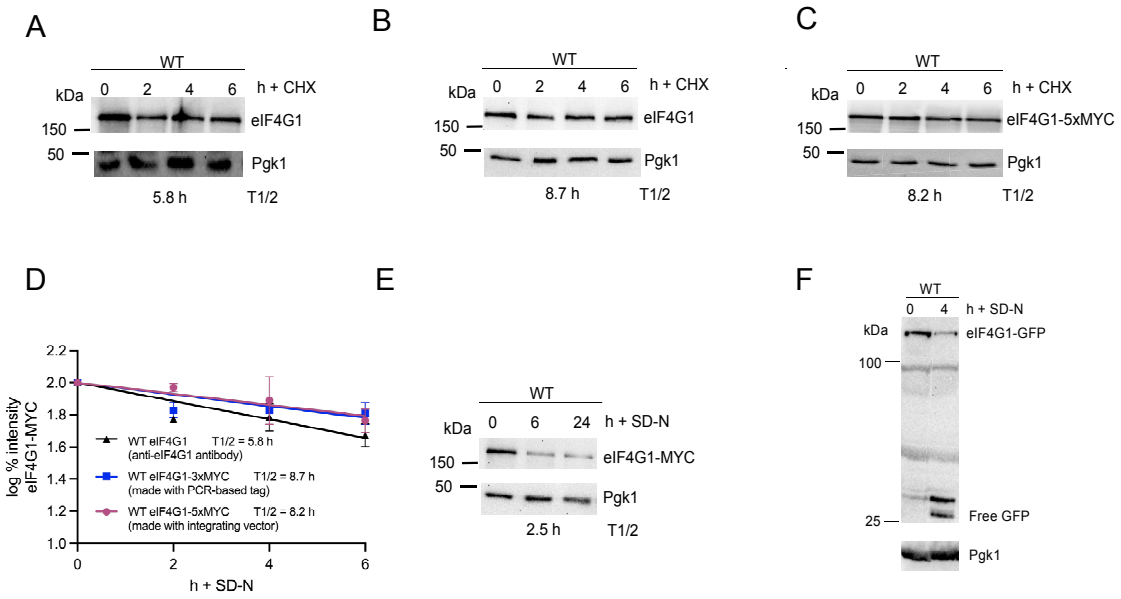

Figure C1. eIF4G1 is actively turned over via vacuolar proteolysis following nitrogen starvation. (A) Western blot analysis of extracts prepared from WT (RSY10) cells at mid-log in SD complete medium then treated with 150 µg/ml Cycloheximide (CHX) for the indicated times. eIF4G1 was visualized using an anti-eIF4G1 antibody. Pgk1 was used a normalization control protein. (B) As in A, except extracts were prepared from WT (RSY2909) cells expressing endogenous eIF4G1-3xMYC. (C) As in A, except extracts were prepared from WT (RSY2924) cells expressing endogenous eIF4G1-5xMYC, which was made with the yeast integrating vector HB0535. (D) Quantification of the results obtained in A-C to demonstrate degradation kinetics. The linear regression line indicates Log% (Log10) protein expression at 2 h, 4 h, and 6 h of SD-N relative to 0 h. T1/2 indicates half-life of protein and error bars indicate S.D., N = 3 of biologically independent experiments. (E) As in A-B, except extracts were prepared from WT (RSY2909) cells expressing endogenous eIF4G1-3xMYC at mid-log in SD complete medium then resuspended in SD-N medium for the indicated times. (F) Western blot analysis of eIF4G1-GFP cleavage assays in WT (RSY2642) cells at 4 h following nitrogen starvation. Free GFP indicates vacuolar proteolysis of full length eIF4G1-GFP. Pgk1 was used a normalization control protein.

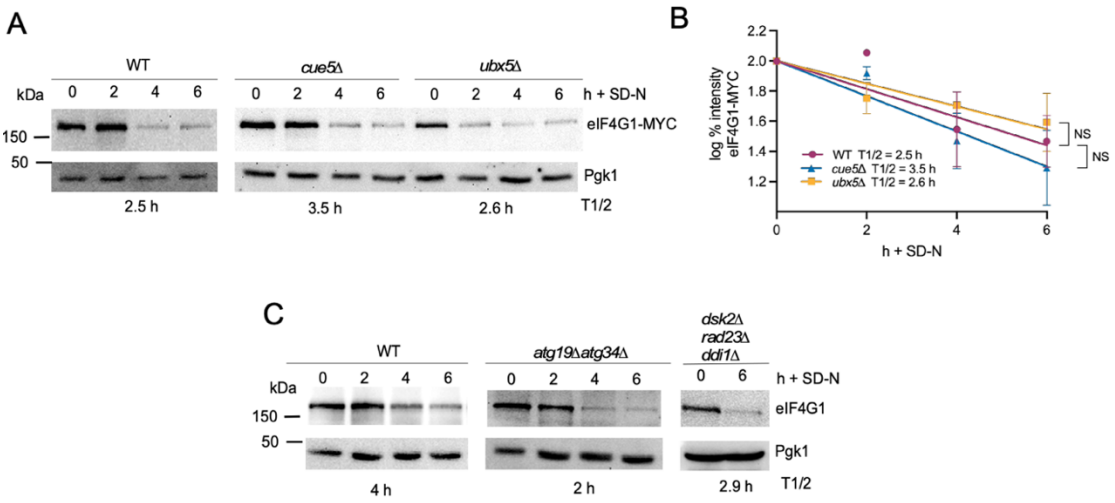

Figure C2. Analysis of receptor-mediated autophagic degradation of eIF4G1 following nitrogen starvation. (A) Western blot analysis of extracts prepared from mid-log WT (RSY2909), *cue5*Δ (RSY2936), and *ubx5*Δ (RSY2933) cells expressing endogenous eIF4G1-3xMYC resuspended in SD-N medium for the indicated times. Pgk1 was used a normalization control protein. (B) Quantification of the results obtained in A to demonstrate degradation kinetics. The linear regression line indicates Log% (Log10) protein expression at 2 h, 4 h, and 6 h of SD-N relative to 0 h. T1/2 indicates half-life of protein and error bars indicate S.D., N = at least 2 of biologically independent experiments. (C) As in A, except extracts were prepared from WT (RSY10), *atg19*Δ*atg34*Δ (RSY2559), and *dsk2*Δ*rad23*Δ*ddi1*Δ (RSY2196) cells. Endogenous eIF4G1 was examined using anti-eIF4G1 antibody.

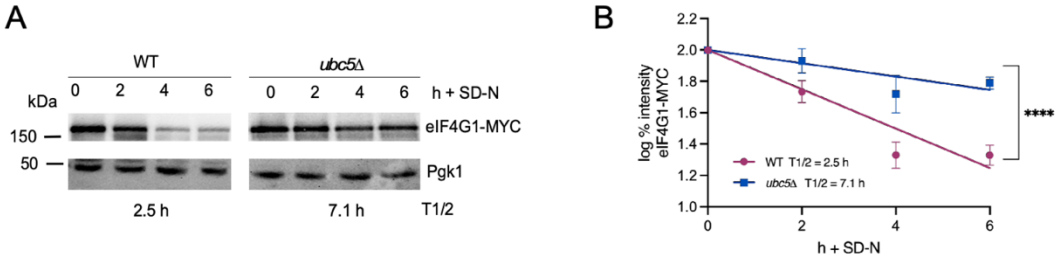

Figure C3. Ubc5 can work independently of paralog Ubc4 to promote eIF4G1 degradation following nitrogen starvation. (A) Western blot analysis of extracts prepared from mid-log WT (RSY2924) and *ubc5*Δ (RSY2925) cells expressing endogenous eIF4G1-5xMYC were resuspended in SD-N medium for the indicated times. Pgk1 was used a normalization control protein. (B) Quantification of the results obtained in A to demonstrate degradation kinetics. The linear regression line indicates Log% (Log10) protein expression at 2 h, 4 h, and 6 h of SD-N relative to 0 h. T1/2 indicates half-life of protein and error bars indicate S.D., N = 3 of biologically independent experiments.

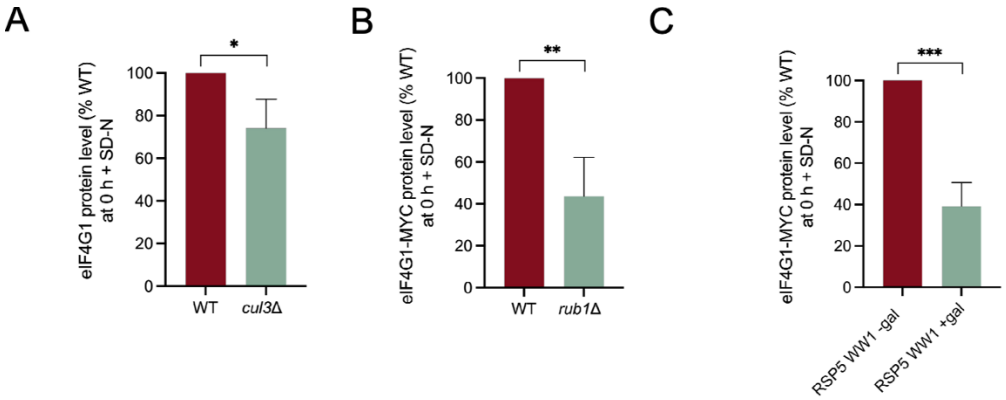

Figure C4. eIF4G1 requires both Cul3 and Rsp5 ubiquitin ligases to maintain protein expression in physiological conditions. (A) Quantification analysis of western blots described in Figure 4A-B. Endogenous eIF4G1 protein levels at t=0 h + SD-N in *cul3*Δ (RSY2813) mutants were compared as % expression relative to WT (RSY10). Error bars indicate S.D., N = 3 of biologically independent experiments. (B) As in A, except endogenous eIF4G1-3xMYC protein levels t= 0 h SD-N in *rub1*Δ (RSY2913) were quantified relative to WT from western blots described in Figure 4C-D. (C) As in A-B, except endogenous eIF4G1-5xMYC protein levels t= 0 h SD-N were quantified from western blots described in Figure 4E-F.

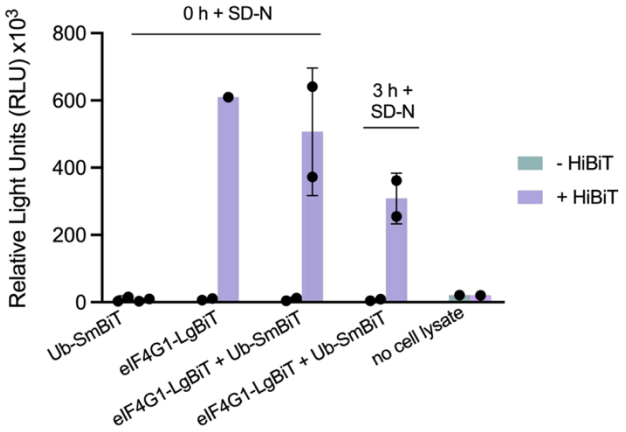

Figure C5. Ubiquitination does not occur directly on eIF4G1. NuBiCA assay to detect ubiquitinated eIF4G1-LgBiT/His using a luminescence plate reader. LgBiT/His-tagged eIF4G1 of the indicated strains (RSY2911, RSY2912, and RSY2883) were grown to mid-log (~6×10^6 cells), and 100 µg of whole cell lysate was loaded onto a 96-well plate for each sample. To observe the NanoBiT signal (which can detect binding of Ub-SmBiT with eIF4G1-LgBiT), all samples were incubated with the NanoLuc substrate furimazine (NanoBiT) in luciferase assay buffer for a total volume of 200µl. To control the amount of eIF4G1-LgBiT for each sample, samples were incubated with or without the HiBiT peptide, which tightly interacts with LgBiT to produce a luminescent signal. Samples without cell lysate, or without either eIF4G1-LgBiT or Ub-SmBiT, were used as a negative control. S.D., N=2 of biologically independent experiments.

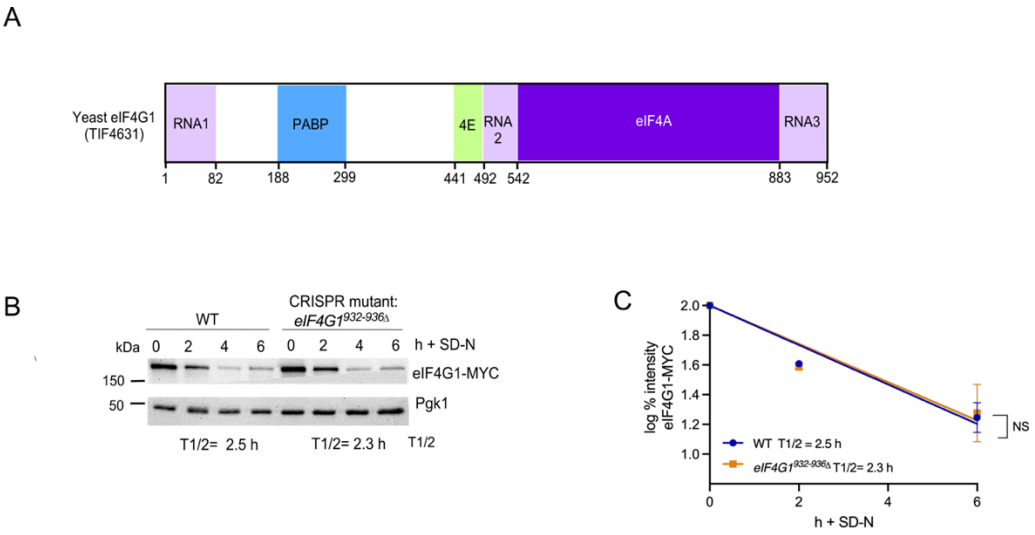

Figure C6. eIF4G1 does not require direct binding with Cul3 for degradation following nitrogen starvation. (A) Binding domains and residues on yeast eIF4G1 (gene name TIF4631). PABP indicates binding domain for Poly(A)-binding protein; 4E indicates eIF4E. (B) Western blot analysis of extracts prepared from mid-log WT (RSY2909) and eIF4G1$^{932\text{-}936\Delta}$ (RSY2955) mutants constructed with CRISPR method and resuspended in SD-N medium for the indicated times. eIF4G1 was endogenously tagged with 3xMYC and Pgk1 was used a normalization control protein. (C) Quantification of the results obtained in B to demonstrate degradation kinetics. The linear regression line indicates Log% (Log10) protein expression at 2 h, 4 h, and 6 h of SD-N relative to 0 h. T1/2 indicates half-life of protein and error bars indicate S.D., N = N of biologically independent experiments.

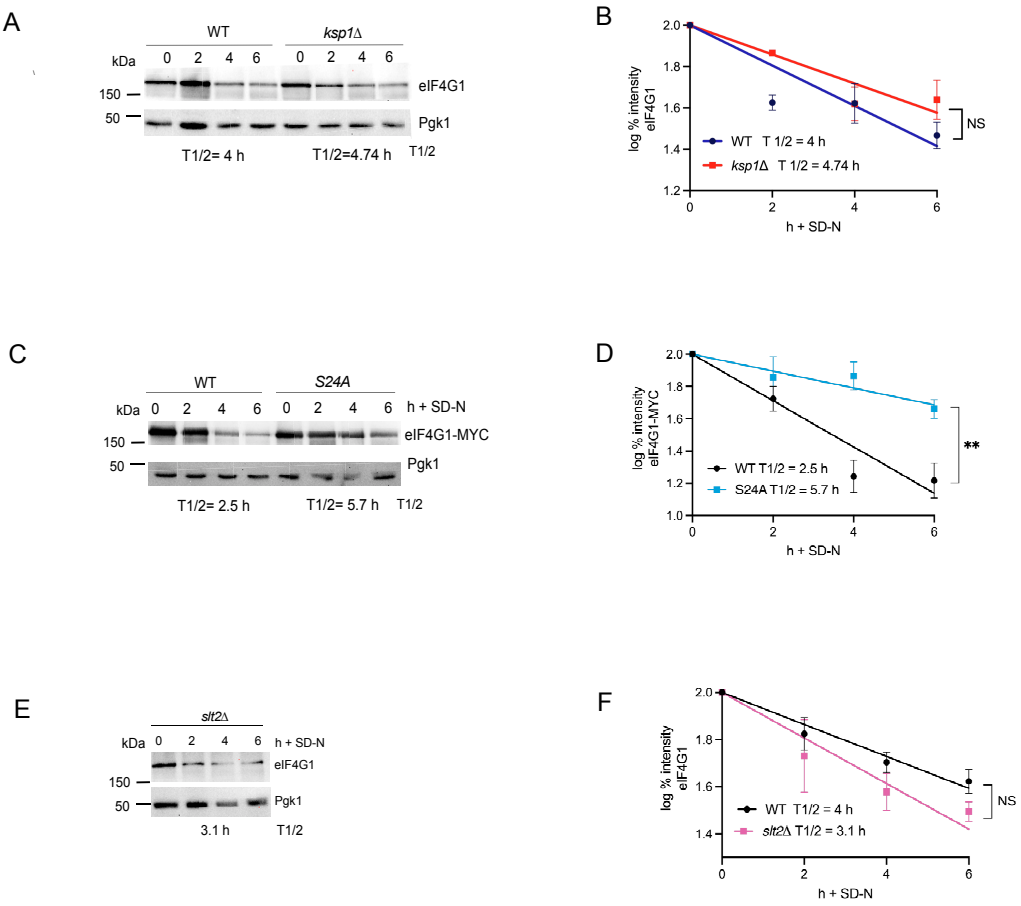

Figure C7. Ksp1 and Slt2 are not required for eIF4G1 autophagic degradation following nitrogen starvation. (A) Western blot analysis of extracts prepared from mid-log WT (RSY10) cells and *ksp1*Δ (RSY2266) mutants resuspended in SD-N medium for the indicated times. Endogenous eIF4G1 was examined using anti-eIF4G1 antibody and Pgk1 was used a normalization control protein. (B) Quantification of the results obtained in A to demonstrate degradation kinetics. The linear regression line indicates Log% (Log10) protein expression at 2 h, 4 h, and 6 h of SD-N relative to 0 h. T1/2 indicates half-life of protein and error bars indicate S.D., N = 2 of biologically independent experiments. (C-D) As in A-B, except western blot analysis of extracts prepared from mid-log WT (RSY2924) cells and eIF4G1^{S24A} (RSY2939) mutants. eIF4G1 was endogenously tagged with 5xMYC and Pgk1 was used a normalization control protein. Error bars indicate S.D., N = 3 of biologically independent experiments. (E-F) As in A-B, except western blot analysis of extracts prepared from mid-log WT (RSY10) and *slt2*Δ (RSY1006) cells. Endogenous eIF4G1 was examined using anti-eIF4G1 antibody and Pgk1 was used a normalization control protein. Error bars indicate S.D., N = 3 of biologically independent experiments.

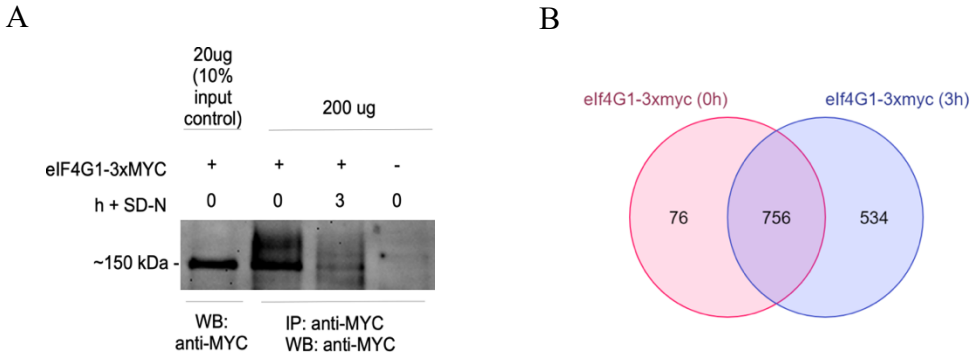

Figure C8. Mass spectrometry analysis of eIF4G1-MYC before and after nitrogen starvation. **(**A)Verification of immunoprecipitated eIF4G1-3XMYC for Mass Spectrometry analysis. Extracts were prepared from mid-log WT (RSY2909) cells expressing endogenously tagged eIF4G1-3xMYC and resuspended in SD-N medium for 3h SD-N. eIF4G1-3xMYC was immunoprecipitated with anti-MYC antibodies and the western blot was incubated with anti-MYC antibodies. Input of whole cell lysate was used to detect eIF4G1-3xMYC without immunoprecipitation as a positive control, and immunoprecipitation of WT (RSY10) cells without endogenously tagged eIF4G1 (last lane) was used as a negative control. (B) Venn diagram between mass spectrometry proteins from the eIf4G1-3xmyc(0h) and eIf4G1-3xmyc(3h) samples (diagram created by LifeSensors). A total of 756 proteins detected were common between the two samples, 76 unique proteins were found in eIf4G1-3xmyc(0h), and 534 unique proteins were found in eIf4G1-3xmyc(3h).

Appendix D

Chapter 6 Supplemental Tables and Figures

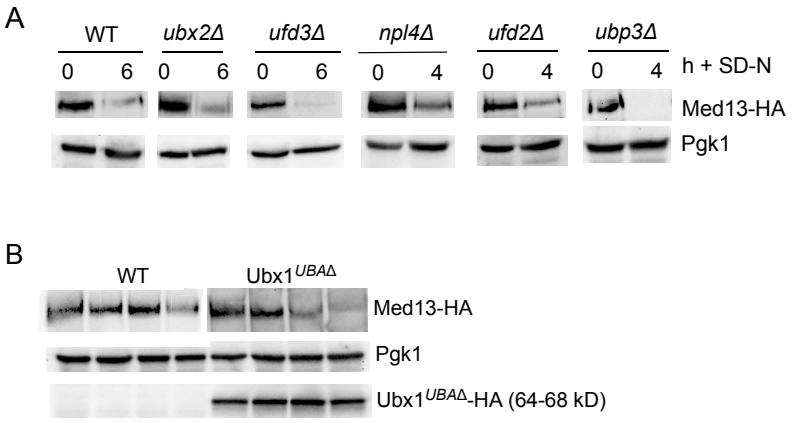

Figure D1. Med13 does not require several ubiquitin-binding cofactors which interact with the CDC48 complex. (A) Western blot analysis of extracts prepared from WT (RSY703), *ubx2*Δ, *ufd3*Δ*, npl4*Δ*, ufd2*Δ*,* and *upb3*Δ mutants from the BY4742 Res Gen knockout collection. Cells were grown to mid-log then resuspended in SD-N medium for the indicated times. Med13-HA was observed using an overexpression plasmid (PKC801) and Pgk1 was used a normalization control protein. (B) As in A, except Med13-HA levels were observed in WT (RSY703) cells containing an empty vector control and *ubx1*Δ cells (RSY2718) expressing a plasmid of Ubx1 without its ubiquitin-associating domain (Ubx1$^{UBA\Delta}$). The Ubx1$^{UBA\Delta}$ mutant prevents ubiquitin-associating ability of Ubx1. The Ubx1$^{UBA\Delta}$ -HA plasmid is induced with 100 μm copper sulfate and can be visualized with anti-HA antibodies upon induction.

Appendix E

List of Abbreviations

AIM – Atg8 Interacting Motif
ATG – Autophagy-Related Genes
Cdk – Cyclin Dependent Kinase
ChIP – Chromatin Immunoprecipitation
CHX – Cycloheximide
CKM – Cdk8 Kinase Module
CMA – Chaperone-Mediated Autophagy
DUB – Deubiquitinating enzyme
Hyg B – Hygromycin B
IDR – Intrinsically Disordered Region
IRES – Internal Ribosome Entry Site
K33 / K63 – Lysine 33 / Lysine 63 Ubiquitin Chain Linkage
LDS - LIR/AIM Docking Site
LLPS – Liquid-Liquid Phase Separation
TF – Transcription Factor
TIF – Translation Initiation Factor
MAPK – Mitogen-Activated Protein Kinase
MOMP – Mitochondrial Outer Membrane Potential
NAC – N-Acetyl Cysteine (an antioxidant)
NS – Not Significant
PAS – Phagophore Assembly Site
P-bodies – Processing Bodies
PTM – Post-translational Modification
RBP – RNA Binding Protein
RNP – Ribonucleoprotein
RCD – Regulated Cell Death
RING – Really Interesting New Gene Type E3 Ligase
RNP – Ribonucleoprotein
ROS – Reactive Oxygen Species
RP – Ribosomal protein
SD – Synthetic Defined Medium containing nitrogen and 2% glucose
SD-N – Nitrogen starved medium
SRG – Stress Response Gene
SRP – Stress Response Protein
TORC1 – Target of Rapamycin Complex 1
Ub – Ubiquitin
UDS – Ubiquitin Interacting Motif-Docking Site
UIM – Ubiquitin Interacting Motif
UPS – Ubiquitin Proteasome System
URS – Upstream Regulatory Sequence
UTR – Untranslated Region
WT – Wild Type

Appendix F

Attributes

Results and experiments were carried out by Brittany Friedson unless otherwise noted below.

Chapter 1

Figure 4 and Figure 9 models, as well as a large portion of the text, are adapted from review article written by Dr. Katrina Cooper and Brittany Friedson [7]. Structure of the yeast CKM determined by cryo-EM and mass spectrometry was reproduced with permission from Li et al (2021) Scientific Advances. PMID: 33390853 [52].

Chapter 3

Gratitude to Dr. Natalia Shcherbik at Rowan-Virtua School of Translational and Biomedical Engineering and Sciences for helping to carry out sucrose density centrifugation and northern blot analyses. Alicia Campbell at Rowan-Virtua School of Translational and Biomedical Engineering and Sciences kindly helped carry out ChIP analyses. Figures of transcription and translation models were created by Dr. Katrina Cooper Rowan-Virtua School of Translational and Biomedical Engineering and Sciences. Dr. Stephen Willis carried out YEASTRACT analysis and all mammalian cell experiments referenced in the text. Thank you to Dr. Kiran Madura (Rutgers University) for providing the resources and protocol for proteasome activity assays, to P. Rajyaguru (The Indian Institute of Science) for antibodies to eIF4G1 as well as T. Bolger (University of Georgia) for antibodies to Ded1. Gratitude to Dr. Randy Strich, Dr. Stephen Willis, Dr. Katrina Cooper, Dr. Natalia Shcherbik, Dr. Brian Weiser, Dr. Kiran Madura, and Dr. Dimitri Pestov for providing ideas for experiments and conclusions demonstrated in this chapter.

Chapter 4

This chapter contributes to a project implemented by Dr. Sara Hanley (reference: SH Hanley 2023 Rowan Thesis). Dr. Sara Hanley at Rowan-Virtua School of Translational and Biomedical Engineering and Sciences carried out fluorescence microscopy of WT cells shown in Figure 1A and Y2H analyses in Figure 2. Dr. Katrina Cooper at Rowan-Virtua School of Translational and Biomedical Engineering and Sciences carried out CoIP and Y2H in Figure 2 and fluorescence microscopy in Figure 3A, as well as western blot analyses detecting Xrn1 degradation. Dr. Stephen Willis carried out western blot analyses in Figure 1E and in the *med13Δ* mutant cells in 4A. Both Dr. Sara Hanley and Dr. Katrina Cooper created the final model and wrote the original text partially adapted into this chapter. Additional gratitude to Dr. Stephen Willis, Dr. Sara Hanley, and Dr. Katrina Cooper for their ideas for this project.

Chapter 5

LifeSensors company kindly carried out Mass Spec analyses of eIF4G1. Gratitude to the Dr. Daniel Finley (Harvard Medical School) for providing strains of ubiquitin chain mutants, and to Dr. Won-Ki Huh (Seoul National University) for providing eIF4G1 plasmids. Thank you to Dr. Michael Law (Stockton University) for providing the resources and protocol for the yeast CRISPR/Cas9 method. Additional gratitude to Dr. Katrina Cooper, Dr. Randy Strich, Dr. Natalia Shcherbik, Dr. Brian Weiser, and Dr. Kiran Madura for providing ideas for experiments and conclusions demonstrated in this chapter.

Chapter 6

Gratitude to Ayesha Gurnani, a medical student at Rowan SOM, for helping to carry out Ub chain mutant assays of Med13 stability.